Industria Textilă

ISSN 1222–5347

3/2023

ISI rated journal, included in the ISI Master Journal List of the Institute of Science Information, Philadelphia, USA, starting with vol. 58, no. 1/2007, with impact factor 1.4 and AIS 0.110 in 2022.

The journal is indexed by CrossRef, starting with no. 1/2017 having the title DOI: https://doi.org/10.35530/IT.

Edited in 6 issues per year, indexed and abstracted in:
Science Citation Index Expanded (SCIE), Materials Science Citation Index®, Journal Citation Reports/Science Edition, World Textile Abstracts, Chemical Abstracts, VINITI, Scopus, Toga FIZ technik, EBSCO, ProQuest Central, Crossref
Edited with the Romanian Ministry of Research, Innovation and Digitalization support

Scientific reviewers for the papers published in this number:

EDITORIAL STAFF

INDUSTRIA TEXTILA journal, edited by INCDTP BUCHAREST, implements and respects Regulation 2016/679/EU on the protection of individuals with regard to the processing of personal data and on the free movement of such data ("RGPD"). For information, please visit the Personal Data Processing Protection Policy link or e-mail to DPO **rpd@incdtp.ro**

Aknowledged in Romania, in the Engineering sciences domain, by the National Council of the Scientific Research from the Higher Education (CNCSIS), in group A
Journal edited in colaboration with **Editura AGIR**, 118 Calea Victoriei, sector 1, Bucharest, tel./fax: 021-316.89.92; 021-316.89.93; e-mail: editura@agir.ro, www.edituraagir.ro

Textile industry and coronavirus – the impact of the pandemic on sales performance: a case study of Inditex

DOI: 10.35530/IT.074.03.202237

IVANA RAĐENOVIĆ
DANICA LEČIĆ-CVETKOVIĆ
TEODORA RAJKOVIĆ
NENAD ANIČIĆ

ABSTRACT – REZUMAT

Textile industry and coronavirus – the impact of the pandemic on sales performance: a case study of Inditex

The global coronavirus pandemic has caused major problems in the business of companies in the textile and fashion industry all over the world. This pandemic contributed to the development and increasing application of e-business. It also caused increased development of online sales for many companies to meet customer demands in uncertain market conditions. The main objective of the paper is to present the potentiality of the application of a defined set of key performance indicators (KPIs) for measuring and comparative analysis of sales performance in the year due pandemic (2020) and the year before the pandemic (2019). KPIs were defined based on the parameters that were the most exposed to changes during the emergence of a coronavirus disease. The analysis is conducted on the example of one of the leading companies in the textile and fashion industry, Inditex. Based on the results, it can be concluded that despite a significant reduction in total sales in 2020, Inditex managed to achieve a high sales success rate, although the sales target achievement rate was lower compared to the previous year. According to a unique business model based on a global, flexible, digitally integrated, and sustainable online platform, Inditex had a big increase in online sales, which had a key role in the year of the pandemic when 640 retail stores were closed.

Keywords: *textile and fashion industry, sales, key performance indicators, coronavirus pandemic, Inditex*

Industria textilă și coronavirusul – impactul pandemiei asupra performanței vânzărilor: un studiu de caz al companiei Inditex

Pandemia globală de coronavirus a cauzat probleme majore în afacerile companiilor din industria textilă și a modei din întreaga lume. Această pandemie a contribuit la dezvoltarea și creșterea aplicării e-business-ului. De asemenea, a determinat o dezvoltare în creștere a vânzărilor online pentru multe companii, pentru a satisface cerințele clienților în condițiile unei piețe incerte. Obiectivul principal al lucrării este de a prezenta potențialul aplicării unui set definit de indicatori cheie de performanță (KPI) pentru măsurarea și analiza comparativă a performanței vânzărilor în anul afectat de pandemie (2020) și anul anterior pandemiei (2019). KPI-urile au fost definițe pe baza parametrilor care au fost cei mai expuși schimbărilor în timpul apariției bolii cauzate de coronavirus. Analiza este realizată pe exemplul uneia dintre companiile lider din industria textilă și a modei, Inditex. Pe baza rezultatelor, se poate concluziona că, în ciuda unei reduceri semnificative a vânzărilor totale în 2020, Inditex a reușit să atingă o rată ridicată a vânzărilor, deși rata de realizare a țintei de vânzări a fost mai mică comparativ cu anul precedent. Conform unui model de afaceri unic bazat pe o platformă online globală, flexibilă, integrată digital și sustenabilă, Inditex a înregistrat o creștere mare a vânzărilor online, care a avut un rol cheie în anul pandemiei, atunci când 640 de magazine de vânzare cu amănuntul au fost închise.

Cuvinte-cheie: *industria textilă și a modei, vânzări, indicatori cheie de performanță, pandemie de coronavirus, Inditex*

INTRODUCTION

The emergence of a coronavirus disease called COVID-19 in early 2020 has further affected the business results of many participants in supply chains, in already uncertain market conditions. Many companies have faced various challenges due to the occurrence of prescribed epidemiological measures, restrictions, border closures, and temporary bans on the movements of the population. Textile and fashion companies endured great consequences during the coronavirus pandemic. Fashion retailers had to comply with the prescribed epidemiological measures that led to mass closures of retail stores. Faced with large losses and seized stocks of goods, to survive in the new crisis, companies from the textile and fashion industry have found a solution in the digitalization and application of electronic business (e-business). Because of that, this industry had a large digital transformation in the year of the pandemic, with a further tendency to develop and apply digitalization as a pivotal asset of the business in the future. Digital transformation is especially noticed in online sales, as many brands and retailers have begun to adopt digital solutions and improve their e-business, applying various tools to meet customer demands in uncertain market conditions. Adopting online marketing tools should be reflected in the company's marketing performance and implicitly in their financial performance, including reputation, market share, number of clients, and customer loyalty [1]. The rapid spread of COVID-19 has indeed changed the interaction between businesses and customers because many businesses started to feel a drastic drop in sales or even no customers at all. After all, customers have started activities in their homes [2]. Due to the closure of stationary retail stores, online shopping has become the only means for consumers to satisfy their consumption needs [3]. The same authors state that e-commerce has been predominant during the COVID-19 pandemic, and retailers have put much effort into building, improving, and promoting their online stores. E-commerce is becoming an increasingly bigger component of all business models, and sales management needs to adjust to this form of selling which is very different from the standard sales practices of the past [4]. COVID-19 brought the importance of digital to evidence because most of the stores were closed and fashion brands had to bet everything on social media and e-commerce [5]. By creating special advantages for online shopping, virtual cabins, and presentations, fashion brands have managed to attract customers who may not have previously bought clothes and fashion accessories online. An advantage of online stores is that all products are described through text, with photos, multimedia files, and links that lead to additional information about products [6]. The online shopping market in the fashion industry had a rapid increase during the COVID-19 epidemic [7] where e-commerce and online sales have achieved unprecedented growth. The application of modern technologies provided customers with a unique shopping experience while respecting all prescribed measures and protecting health and safety. It is interesting to note that while e-commerce was already a consolidated pillar of fashion shopping, it recently started to evolve to achieve through AR (Augmented Reality) and VR (Virtual Reality) what customers could before find in physical stores: interesting experiences and sensory stimuli [5].

Sales management is one of the key aspects of managing the entire business of the company. Successful sales management becomes an extension of any company's supply chain as it creates the sale and the connection to the end-user [4]. Firms employing a comprehensive sales enablement function are making dramatic changes in their sales operations and transforming most aspects of sales management [8]. Business based on managing the performance of the company is one of the most modern ways to improve business and gain a competitive advantage.

Business analysis based on the application of key performance indicators (KPIs) has proven to be one of the key phases of crisis management, such as the global pandemic. Considering the unprecedented growth of e-commerce and online sales within the textile and fashion industry during the pandemic, and given the fact that there is not a large number of scientific papers dealing with this topic in this industry, KPIs for sales management have been defined in this paper. The defined KPIs were applied for a comparative analysis of sales performance in the year due to the pandemic and the year before, on the example of a leading company in the textile and fashion industry, Inditex. This company applies online sales since 2007 [9], which gained importance in the year of the pandemic because of the restrictions such as the closure of retail stores and shopping moles.

The paper is structured into six chapters, as follows. After the introduction, the second chapter describes some of the most important impacts of the coronavirus pandemic on the textile and fashion industry and its sales processes. The third chapter describes the basic concepts related to performance, performance indicators, and KPIs. The fourth chapter presents a set of defined KPIs in sales management. The fifth chapter presents the results of the application of previously defined KPIs, as a tool for comparative analysis of Inditex sales performance in the year of the pandemic (2020) and the year before (2019), as well as a detailed discussion of the results. The conclusions are presented in the sixth chapter.

THE IMPACT OF THE CORONAVIRUS PANDEMIC ON THE TEXTILE AND FASHION INDUSTRY

The textile industry presents an important branch of the processing industry and is significant for the economy of a country [10]. It presents one of the biggest, oldest, and most commercialized industries in the world [11]. The textile and apparel industry plays a substantial part in the industrial progress of nations as it offers tools to actualize economic stability [12]. It is under constant pressure caused by customers' changing preferences and the need to deliver products and services at an ever-increasing pace [13]. Negative impacts of the pandemic on the business of the textile and fashion industry are cessation of production, a decrease in demand, and closing of retail. With the quarantine, the production of fashion was slowed down by the absence of workers in production sites [5]. Due to public health concerns and social distancing measures, within days, governments around the world demanded the closure of non-essential retail, including fashion which led to retailers pivoting to online sales, began fundraising for local and international charities, and developing plans to support employees [14]. One of the main reasons for decreased demand in the fashion market was restrictions such as closing borders and curfews. The closure of retail stores due to prescribed epidemiological measures has led to a large reduction in physical sales and large losses, in the form of seized stocks of goods in retail stores and warehouses. Also, one of the promotional strategies of online sales during the pandemic conditions was related to lowering the prices of fashion items that are most often worn around the house, such as sweatsuits, sweatshirts, leggings, pyjamas, etc. Businesses had to respond on multiple fronts at once: at the same time that they work to protect their workers' safety, they must also safeguard their operational viability, now increasingly under strain from a historic supply chain shock [15]. Decreases and increases in demand for certain products, lack of supply, inventory management problems, and productivity drops have disrupted the planning and supply chain management in many fashion companies. Epidemic outbreaks are special cases of supply chain risk which are specifically characterized by long-term disruption, the spread of disruption, and high uncertainty [16]. The coronavirus is impacting both upstream and downstream flows of material in the supply chain, where the major disruptions of the global economy are a function of events that are indeed part of the natural evolution of supply chains [17]. To manage supply chains in crises, such as a pandemic, it is necessary to have real-time information-based decision-making and collection of relevant data, to integrate planning activities at the level of the entire supply chain. By applying the Internet and Information and Communication Technologies (ICT), business transactions can be executed in a much faster, easier, and cheaper way. While the coronavirus pandemic had a negative impact on business, it contributed to the development and increasing application of e-business. Compared to 2020, in 2021 there was more than a 20% increase in the application of e-commerce worldwide [18].

Inditex (*Industria de Diseno Textil*) is one of the leading companies in the fast fashion market. Founded in 1963, it began as a small family business producing women's clothing. Since then, the company has constantly grown and developed, while in the last few years, it has experienced the peak of its business as a leader in the fashion industry in the production of men's and women's clothing and fashion accessories. Today, the company sells its products in 216 markets around the world through an online platform and has over 6,654 retail stores in 96 countries [19]. The company owns eight world-renowned fashion brands: Zara, Zara Home, Stradivarius, Bershka, Pull & Bear, Massimo Dutti, Oysho, and Uterqüe [19]. Today's fashion marketplace is highly competitive and the constant need to "refresh" product ranges means that there is an inevitable move by many retailers to extend the number of "seasons", i.e. the frequency with which the entire merchandise within a store is changed [20]. Also, it implies variations in the design of fashion pieces, as well as a faster reaction to changes in trends and customer requirements. At Inditex Company, the year 2020 was marked by the coronavirus pandemic and the main priorities were the protection and preservation of the health of customers, suppliers, and all employees. The biggest challenge was the restrictions on the closure of retail stores. Although the business was conducted in very unstable and difficult conditions, Inditex still managed to achieve good business results thanks to the total integration of retail facilities with online platforms. Strengthening this integration made it possible to receive one million orders in one day on the online platform for the first time in the second quarter of 2020. During the first seven months of the pandemic (from February to August 2020), Inditex brands achieved close to 3 billion online visits, while their social network profiles reached 190 million followers – which was a record [21]. The continuous development of the IT platform (*IOP – Inditex Open Platform*) and the application of an integrated inventory management system (*SINT – Single Inventory Integration*) had a key role in meeting the demand increase.

PERFORMANCES, PERFORMANCE INDICATORS, AND KEY PERFORMANCE INDICATORS

The term performance is today often applied in various areas of management to determine the efficiency and effectiveness of business and business processes. The performance presents a variable of a certain object in the managed subsystem [22]. Performance measurement is a process of quantification and assessment of the degree of goal achievement at the level of organizational units, employees, and processes [23]. To ensure the achievement of the company objectives, it is necessary to monitor and measure the performance of all business activities and apply appropriate improvements in situations where it is noticed that the performance values are not in line with the aimed values and business objectives. Harrington states that "measurements are the key. If you cannot measure it, you cannot control it. If you cannot control it, you cannot manage it. If you cannot manage it, you cannot improve it" [24]. A performance indicator presents a variable that indicates the effectiveness and/or efficiency of a process, system, or part of a system compared to a benchmark. It improves internal communication (among employees) and external communication (among the organization and customers/stakeholders) [25]. KPIs can be defined as "a way for an organization to measure its success or otherwise in reaching its defined goals or objectives" [26]. Also, they are "a quantitative value that can be scaled and used for purposes of comparison" [27]. KPIs are those indicators that focus on the aspects of organizational performance that are most critical to the current and future success of the company [28]. They present a measure that assesses how an organization executes its strategic vision [29]. Many papers presented the topic of the application of KPIs in the textile industry. By increasing awareness of environmental protection and harsh global competition, Lai, Hsu, and Chen divided KPIs into three different groups in the supply chain: supplier, central factory, and customer [30]. Hossain, Sarker, and Khan analysed Water Key Performance Indicator (KPI) to determine annual textile effluents and project wastewater volume [31]. Charkha and Jaju suggested an innovative Supply Chain Performance Measurement (SCPM) framework for the textile industry considering specific performance measures and focusing on the production process of the textile industry [32]. Ishaq Bhatti, Awan, and Razaq stated: "The textile industry is one of three industries that focus more on delivery reliability and customer satisfaction" [33]. These authors measured the performance in terms of quality cost, flexibility financial, safety, time, employees satisfaction, customer satisfaction, delivery reliability, and social performance indicators that have a positive significant impact on the overall organization's performance. Erbaşi divided performance indicators for textile production firms into five groups: production indicators, marketing indicators, finance indicators, human resources indicators, and management indicators [34]. Burkhanov and Tursunov analyzed the relevance of the topic of developing indicators for ensuring financial security for textile enterprises increased especially during the COVID-19 pandemic [35]. Santos performed a financial analysis to evaluate how firms in the textile industry in France have been tackling the challenges of the recent crisis caused by the COVID-19 virus and evaluate their economic sustainability [36]. Although there are a high number of papers related to performance measurement, unfortunately, no papers are revealing the possibilities of KPIs application for measuring sales performance during the coronavirus pandemic in the textile and fashion industry. This paper aims to fill that gap in the literature in that field.

PERFORMANCE INDICATORS FOR SALES MANAGEMENT IN THE FASHION INDUSTRY COMPANY

This chapter presents a set of defined KPIs in sales management, as a tool for measuring sales performance, to comparatively analyse sales results in the pandemic year with the previous year. These KPIs can be also applied to improve the sales process, overall business results and maintain a competitive advantage in the market.

KPI 1 – Sales Growth (SG) presents a performance indicator in sales management that provides information on the increase in total sales in the observed period compared to the previous period. The calculation formula of the KPI SG is presented in equation 1 and the aimed value of this KPI is ≥ 10%:

$$SG = \frac{AS_t - AS_{t-1}}{AS_{t-1}} \cdot 100\ (\%) \qquad (1)$$

where AS_t is the value of achieved sales in the observed period t [€], and AS_{t-1} – value of achieved sales in the previous period t–1 [€].

KPI 2 – Online Sales Growth (OSG) presents a performance indicator in sales management that provides information on the increase in online sales in the observed period compared to the previous period. The calculation formula of the KPI OSG is presented in equation 2 and the aimed value of this KPI is ≥ 20%:

$$OSG = \frac{OS_t - OS_{t-1}}{OS_{t-1}} \cdot 100\ (\%) \qquad (2)$$

where OS_t is the value of achieved online sales in the observed period t in €, OS_{t-1} – value of achieved online sales in the previous period t–1 in €.

KPI 3 – Sales Success Rate (SSR) presents a performance indicator in sales management that provides information on the percentage of customers that a company has succeeded to sell its products in relation to the number of contacts made with customers. The calculation formula of the KPI SSR is presented in equation 3 and the aimed value of this KPI is to be as high as possible (maximum 100%).

$$SSR = \frac{RS}{MC} \cdot 100\ (\%) \qquad (3)$$

where RS is the number of customers with whom sales are realized [1], MC – number of customers with whom contacts were made [1].

KPI 4 – Sales Target Achievement Rate (STAR) is a performance indicator in sales management that compares the value of total achieved sales with the value of planned sales for the same observed period. The calculation formula of the KPI STAR is presented in equation 4 and the aimed value of this KPI is ≥ 100%:

$$STAR = \frac{AS}{PS} \cdot 100\ (\%) \qquad (4)$$

where AS is the value of total achieved sales in the observed period t in €, and PS – value of planned sales for the observed period t in €.

KPI 5 – Number of New Stores (NNS) presents a performance indicator in sales management that provides information on the number of newly opened stores in the observed period. The calculation formula of the KPI NNS is presented in equation 5 and the aimed value of this KPI is ≥ 0 [1].

$$BNP = NS_2 - NS_1 \qquad (5)$$

where NS_1 is the number of stores at the beginning of the observed period t, and NS_2 – number of stores at the end of the observed period t.

KPI 6 – Regional Sales (RGS_x) presents a performance indicator in sales management that provides information on the percentage share of regional sales in total sales. The calculation formula of the KPI RGS_x is presented in equation 6 and the aimed value of this KPI is to be as high as possible (maximum 100%).

$$RGS_x = \frac{AS_x}{TAS} \cdot 100\ (\%) \qquad (6)$$

where AS_x is the value of achieved sales within the observed region x in €, and TAS – value of total achieved sales in €.

RESULTS AND DISCUSSION

Given that 2020 was marked by the coronavirus pandemic, it was expected that the pandemic would affect the sales results of companies in all industries, including the sales results of Inditex, one of the leading companies in the fashion industry. A comparative analysis of Inditex's sales results was conducted by applying defined KPIs in the year before the pandemic (2019) and the year of the pandemic (2020). Data on business results for the year 2019 are

Table 1

VALUES OF KPIs IN INDITEX SALES MANAGEMENT FOR YEARS 2019 AND 2020				
KPI		Aimed value	Before the pandemic (2019)	The year of the pandemic (2020)
1	SG (%)	≥ 10	8.2	– 27.9
2	OSG (%)	≥ 20	23	69.2
3	SSR (%)	≈ 100	95	90
4	STAR (%)	≥ 100	108.2	72.1
5	NNS	≥ 0	– 21	– 640
6	RGS_{Spain} (%)	≈ 100	15.7	14.6
6	RGS_{Europe} (%)	≈ 100	46	48.7
6	RGS_{USA} (%)	≈ 100	15.8	13.5
6	$RGS_{Asia\ and\ the\ rest}$ (%)	≈ 100	22.5	23.2

Note: Calculations of authors based on the annual reports for years 2019 and 2020 from Inditex Company.

observed from the annual report of Inditex and refer to sales data for the period from 2015 to 2019 [37]. Data on business results for the year 2020 are observed from Inditex's annual report for the year 2020 [38]. Table 1 shows the values of observed KPIs of Inditex sales for the years 2019 and 2020, while the detailed analysis of obtained values is given below.

KPI 1 – SALES GROWTH (SG)

The aimed value of KPI SG is at least 10%. Based on the obtained value of KPI SG in 2019 (8.2%), the sales of Inditex in 2019 are less than the aimed value by 1.8%. Based on the obtained value of KPI SG for 2020 (–27.9 [%]), the sales of Inditex in 2020 decreased significantly, by 36.1 [%] compared to 2019.

KPI 2 – ONLINE SALES GROWTH (OSG)

The aimed value of KPI OSG is at least 20%. Based on the obtained value of KPI OSG in 2019 (23%), the online sales of Inditex in 2019 are higher by 3% than the aimed value. The obtained value of KPI OSG for 2020 is 69.2%. It can be concluded that the increase in online sales of Inditex in 2020 is significantly higher compared to the previous year, by 46.2%, and compared to aimed value by 49.2%. Since Inditex has been selling its products online since 2007 [9], it is very important to monitor the growth of online sales. In 2020, the number of active users of Inditex online applications reached 132 million, and the number of online visits increased by 50%, up to 5.3 billion [39].

KPI 3 – SALES SUCCESS RATE (SSR)

The aimed value of the KPI SSR is to be as high as possible, i.e. approximately 100%. Considering the obtained value of the KPI SSR for 2019 of 95%, it can be concluded that this value was at a satisfactory level. The obtained value of this indicator for 2020 is 90%. It is decreased by 5% compared to 2019, and lower by 10% than the aimed value.

KPI 4 – SALES TARGET ACHIEVEMENT RATE (STAR)

The aimed value of the KPI STAR is to be greater than or equal to 100%. Given that the value obtained for 2019 for the KPI STAR was 108.2%, the sales target in 2019 was exceeded by 8.2%. For 2020, the value of KPI STAR is 72.1%, and it can be concluded that the sales target was not achieved in 2020, by 27.9%. This indicates that in 2020 sales were lower by 36.1%, compared to the previous year.

KPI 5 – NUMBER OF NEW STORES (NNS)

The aimed value of the KPI NNS is to be greater than or equal to 0. In 2019, the value of KPI NNS is –21, which means that 21 Inditex stores were closed in 2019. That is significantly less than the aimed value. But, in 2020, the value of KPI NNS is –640, which indicates that in that year 640 Inditex stores were closed, for 621 stores more than in 2019. The value of this KPI presents the most negative impact of the coronavirus pandemic on Inditex's business.

KPI 6 – REGIONAL SALES (RGS_x)

The aimed value of KPI RGS_x is to be as high as possible, i.e. approximately 100%. The values of this KPI need to be calculated for each region (*x*) separately: Spain, Europe without Spain, USA, and Asia and the rest of the world. In 2019, the value of this KPI for the Spanish region is 15.7%, for the region of Europe without Spain 46%, for the USA region 15.8%, and for the region of Asia and the rest of the world 22.5%. In 2020, the value of this KPI for the Spanish region is 14.6%, for the region of Europe without Spain is 48.7%, for the USA region is 13.5%, and for the region of Asia and the rest of the world is 23.2%. Based on these values, it can be concluded that the highest percentage share in the total Inditex sales in 2019 and 2020 has the region of Europe without Spain. Also, it can be noticed that for all observed periods, more than 60% of the total sales of Inditex are sales in the regions of Europe and Spain.

Based on the previous comparative analysis of values presented in table 1, it can finally be concluded that the coronavirus pandemic significantly affected the sales results of the Inditex Company. There was a significant reduction in total sales (KPI SG) of Inditex Company in 2020, by 36.1% compared to the year before the pandemic, 2019. Also, it can be noticed that online sales (KPI OSG) in 2020 increased more than two times compared to the increase in online sales in 2019, by 46.2%. Regarding the sales success rate (KPI SSR), the value of this indicator for 2020 decreased by 5% compared to 2019, although this value is still high (90%). The rate of achieved sales target (KPI STAR) for 2020 is slightly higher than 70%, and it can be concluded that the sales target was not achieved by about 30%. Another important result of this analysis is that the events during 2020 led to the closure of 640 retail stores of Inditex

(KPI NNS). It greatly impacted the reduction in total sales, primarily physical sales in retail stores. A comparative analysis for the observed two years of regional sales yielded similar values for each of the observed regions, and the highest percentage of Inditex sales in both years, 2019 and 2020, are regions of Europe and Spain, with a total of over 60%.

Results of the application of KPIs in sales management in Inditex Company show the need for improvements in sales after the crisis caused by the coronavirus pandemic and the continuous advancement of sales activities in the future. Accordingly, some recommendations for the Inditex Company, as well as for any textile and fashion companies for the improvement of sales performance that could be implemented are:

- The transition from traditional to online sales (mostly or completely) and adaptation of business to online sales;
- Application of KPIs for evaluation and continuous monitoring of the achievement of the company's targeted sales goals;
- Implementation of an additional set of new KPIs or composite indicators in sales management to improve sales processes and performances;
- Introduce new KPIs in analysing online purchasing, which could generate new ideas and innovations in products, services and projects;
- Maintaining the fashion market with a constant offer of new collections;
- Frequent use of social media and social networks for promotions, as well as better adapted Internet sites and mobile phone applications for online shopping;
- Development and implementation of a model that recommends available and/or newly released products based on previous customers' browsing behaviour and purchases, i.e. customer profiling and mix-and-match product recommendations.

CONCLUSIONS

This paper presents the possibility of applying KPIs for the analysis of sales results of companies in the field of textile and fashion industry. A set of six KPIs has been identified, and mathematical calculations and aimed values were presented. These KPIs were applied as a tool for comparative analysis of the sales results of Inditex, one of the market leaders in the textile and fashion industries. Based on the results of the comparative analysis, conclusive considerations follow. Despite a significant reduction in total sales in 2020, Inditex Company managed to achieve a high sales success rate of 90%, although the sales target achievement rate decreased by nearly 40%, compared to the previous year. According to the unique business model of the company, and based on a global, flexible, digitally integrated, and sustainable online platform, there was a big increase in online sales of nearly 46.2%. It had a key role in the year when 640 physical retail stores were closed.

Results of the analysis presented in this paper indicated that improvements in sales in Inditex company after the crisis caused by the coronavirus pandemic need to be conducted. Also, some recommendations/future directions of action for the analysed company, but also the companies in the textile and fashion industry, are presented.

The first direction of future research of the authors of this paper is to apply the defined set of six KPIs to several other companies in the textile and fashion industry. Based on that, a comparative analysis of the sales performance of these companies would be conducted. The second direction of future research would be to apply defined KPIs to a group of companies from other industries. Based on that would be performed a comparative analysis of the sales performance of these companies from different industries, be to obtain data on the pandemic impact on other industries.

REFERENCES

[1] Orzan, M.C., Burlacu, S., Florescu, M.S., Orzan, O.A., Macovei, O.I., *The effects of online marketing on financial performance in the textile industry*, In: Industria Textila, 2020, 71, 3, 288–293, http://doi.org/10.35530/IT.071.03.1826

[2] Wulandari, N.L.P.T., Darma, G.S., *Textile industry issue in pandemic of COVID-19*, In: PalArch's Journal of Archaeology of Egypt/Egyptology, 2020, 17, 7, 8064–8074

[3] Koch, J., Frommeyer, B., Schewe, G., *Online shopping motives during the COVID-19 pandemic – lessons from the crisis*, In: Sustainability, 2020, 12, 24, 10247, http://doi.org/10.3390/su122410247

[4] Cook, T.A., *Mastering Global Business Development and Sales Management,* CRC Press, 2020

[5] Silvestri, B., *The Future of Fashion: How the Quest for Digitization and the Use of Artificial Intelligence and Extended Reality Will Reshape the Fashion Industry After COVID-19*, In: ZoneModa Journal, 2020, 10, 2, 61–73, http://doi.org/10.6092/issn.2611-0563/11803

[6] Rahman, M.A., Islam, M.A., Esha, B.H., Sultana, N., Chakravorty, S., *Consumer buying behavior towards online shopping: An empirical study on Dhaka city, Bangladesh*, In: Cogent Business & Management, 2018, 5, 1, 1514940, http://doi.org/10.1080/23311975.2018.1514940

[7] Sumarliah, E., Usmanova, K., Mousa, K., Indriya, I., *E-commerce in the fashion business: the roles of the COVID-19 situational factors, hedonic and utilitarian motives on consumers' intention to purchase online,* In: International Journal of Fashion Design, Technology and Education, 2021, 1–11, http://doi.org/10.1080/17543266.2021.1958926

[8] Ingram, T.N., LaForge, R.W., Avila, R.A., Schwepker, C.H., Williams, M.R., *Sales management: Analysis and decision making*, Routledge, 2019
[9] Inditex, *Annex III. Markets and concepts with online sales*, n.d., Available at: http://static.inditex.com/annual_report_2016/en/annual-accounts/consolidated-directors-report/annex-iii-markets-and-concepts-with-online-sales.php [Accessed February 2022]
[10] Miletic, S., Stanojević, Š.Z., Jovanović, I., Radivojevic, M., Conić, V., *AHP analysis of organizational culture in textile companies in Serbia*, In: Industria Textila, 2020, 2, 124–131, http://doi.org/10.35530/IT.071.02.1588
[11] Karabasevic, D., Radanov, P., Stanujkic, D., Popovic, G., Predic, B., *Going green: strategic evaluation of green ICT adoption in the textile industry by using bipolar fuzzy MULTIMOORA method*, In: Industria Textila, 2021, 72, 1, 3–10, http://doi.org/10.35530/IT.072.01.1841
[12] Hussain, H. I., Haseeb, M., Kot, S., Jermsittiparsert, K., *Non-linear impact of textile and clothing manufacturing on economic growth: The case of top-Asian economies,* In: Fibres & Textiles in Eastern Europe, 2020, 5, 143, 27–36, http://doi.org/10.5604/01.3001.0014.2381
[13] Warwas, I., Podgórniak-Krzykacz, A., Przywojska, J., Kozar, Ł., *Going Green and Socially Responsible – Textile Industry in Transition to Sustainability and a Circular Economy,* In: Fibres & Textiles in Eastern Europe, 2021, 3, 147, 8–18, http://doi.org/10.5604/01.3001.0014.7782
[14] Brydges, T., Hanlon, M., *Garment worker rights and the fashion industry's response to COVID-19,* In: Dialogues in Human geography, 2020, 10, 2, 195–198, http://doi.org/10.1177/2043820620933851
[15] Alicke, K., Azcue, X., Barriball, E., *Operations Practice: Supply-Chain Recovery in Corona Virus Times – Plan for Now and the Future*, McKinsey & Company, 2020
[16] Utami, P., Ali, J., Salleh, M.S., *Supply Chains In Indonesia Facing Virus Corona (COVID-19): Models Innovation And Obstacles Faced*, In: Bina Bangsa International Journal of Business and Management, 2021, 1, 1, 1–12, http://doi.org/10.46306/bbijbm.v1i1.1
[17] Handfield, R.B., Graham, G., Burns, L., *Corona virus, tariffs, trade wars and supply chain evolutionary design*, In: International Journal of Operations & Production Management, 2020, 40, 10, 1649–1660, http://doi.org/10.1108/IJOPM-03-2020-0171
[18] McKinsey & Company, *State of Fashion 2022: An uneven recovery and new frontiers*, 2021, Available at: https://www.mckinsey.com/industries/retail/our-insights/state-of-fashion# [Accessed May 2021]
[19] Inditex, *Who we are*, Available at: https://www.inditex.com/en/about-us/who-we-are [Accessed March 2021]
[20] Christopher, M., Lowson, R., Peck, H., *Creating agile supply chains in the fashion industry,* In: International Journal of Retail & Distribution Management, 2004, 32, 8, 367–376, http://doi.org/10.1108/09590550410546188
[21] Inditex, *Inditex returns to profitability and generates €734 million net cash in the second quarter,* 2020, Available at: https://www.inditex.com/en/article?articleId=653527&title=Inditex+returns+to+profitability+and+generates+%E2%82%AC734+million+net+cash+in+the+second+ quarter [Accessed May 2021]
[22] Atanasov, N., *Model za izbor adekvatnog skupa indikatora performansi u upravljanju proizvodnjom,* Doctoral dissertation, Belgrade: Faculty of Organizational Sciences, 2016
[23] Neely, A., *Business Performance Measurement: Theory and Practice,* Cambridge: Cambridge University Press, 2002
[24] Harrington, H.J., *Business Process Improvement: The Breakthrough Strategy for Total Quality, Productivity, and Competitiveness*, New York: McGraw-Hill Inc., 1991
[25] Franceschini, F., Galetto, M., Maisano, D., *Designing performance measurement systems: theory and practice of key performance indicators,* Springer, 2018
[26] Durchslag, A., Reuters, T., *Effective Operations and Performance Management,* London: Bloomsbury Information Ltd., 2010
[27] Simons, R., *Performance Measurement & Control Systems for Implementing Strategy*, Pearson Education Limited, 2014
[28] Parmenter, D., *Key Performance Indicators: Developing, Implementing, and Using Winning KPIs*, Fourth edition, New Jersey: John Wiley & Sons, Inc., 2020
[29] Adriansyah, A.K., Ridwan, A.Y., *Developing Sales Management Sustainability Monitoring based on ERP System,* In: 6th International Conference on Interactive Digital Media (ICIDM), 2020, 1–5, http://doi.org/10.1109/ICIDM51048.2020.9339672
[30] Lai, R.S., Hsu, L.L., Chen, J.C., *Green supply chain management systems: A case study in the textile industry*, In: Human systems management, 2012, 31, 2, 111–121, http://doi.org/10.3233/HSM-2012-0765
[31] Hossain, L., Sarker, S.K., Khan, M.S., *Evaluation of present and future wastewater impacts of textile dyeing industries in Bangladesh*, In: Environmental Development, 2018, 26, 23–33, http://doi.org/10.1016/j.envdev.2018.03.005
[32] Charkha, P.G., Jaju, S.B., *Designing innovative framework for supply chain performance measurement in textile industry,* In: International Journal of Logistics Systems and Management 1, 2014, 18, 2, 216–230
[33] Ishaq Bhatti, M., Awan, H.M., Razaq, Z., *The key performance indicators (KPIs) and their impact on overall organizational performance*, In: Quality & Quantity, 2014, 48, 6, 3127–3143, http://doi.org/10.1007/s11135-013-9945-y
[34] Erbaşi, A., *Use of Analytic Hierarchy Process Method in Determination of Performance Indicators: The Case of Turkish Textile Industry*, In: Journal of Textile & Apparel/Tekstil ve Konfeksiyon, 2012, 22, 3

[35] Burkhanov, A., Tursunov, B.O., *Main indicators of textile enterprises' financial security assessment*, In: Vlakna a Textil, 2020, 27, 3, 35–40
[36] Santos, E., *How does the pandemic has affected the economic sustainability of Textile industry in France?*, In: The 21st International Scientific Conference Globalization and its Socio-Economic Consequences 2021, 2021, 129, 09017, http://doi.org/10.1051/shsconf/202112909017
[37] Inditex, *Annual Report 2019,* 2020, Available at: https://www.inditex.com/documents/10279/645708/2019+Inditex+Annual+Report.pdf/25aa68e3-d7b2-bc1d-3dab-571c0b4a0151 [Accessed March 2021]
[38] Inditex, *Annual Report 2020 Results*, 2021, Available at: https://www.inditex.com/documents/10279/664163/2020+Inditex+Annual+Report.pdf/cb184fcc-d1d5-a691-1ee3-8e46871615ab [Accessed October 2021]
[39] Inditex, *FY2020 Results,* 2021, Available at: https://www.inditex.com/documents/10279/648111/Full+year+2020+Results_v2.pdf/e622f911-a0ee-1103-2b64-0c12829833b5 [Accessed October 2021]

Authors:

IVANA RAĐENOVIĆ, DANICA LEČIĆ-CVETKOVIĆ, TEODORA RAJKOVIĆ, NENAD ANIČIĆ

University of Belgrade, Faculty of Organizational Sciences, Jove Ilića 154, 11010, Belgrade, Serbia
e-mail: ivanaradjenovic3@gmail.com, danica.lecic-cvetkovic@fon.bg.ac.rs, nenad.anicic@fon.bg.ac.rs

Corresponding author:

TEODORA RAJKOVIĆ
e-mail: teodora.rajkovic@fon.bg.ac.rs

Investigation of the changes in reflective properties of reflective tapes due to various effects

DOI: 10.35530/IT.074.03.202259

OKSAN ORAL
ESRA DIRGAR
NILGUN OZDIL

ABSTRACT – REZUMAT

Investigation of the changes in reflective properties of reflective tapes due to various effects

Mankind's need to protect itself from various dangers, cold, heat and other natural phenomena have survived from the first days of its existence to the present day. Materials with high visibility have also been developed primarily with the need for protection. These materials are widely used on bicycle wheels, road signs and traffic signs in daily life. Materials used in various textile products such as activewear, sportswear, children's clothing, accessories, hats, uniforms, foot and armbands, and backpacks make life easier by providing safety for the people who walk with their pets, as well as road workers, traffic policemen, firefighters, pedestrians and bicycle riders people who do sports and walking at night due to their busy life.

Many of the traffic accidents occurring today are due to the inability to notice individuals moving on the side of the road. In conditions where the lighting is not sufficient, the reflective feature of the clothes worn will allow people to be noticed more easily. Reflective tapes are used to add reflective properties to clothes. However, these tapes may lose their reflective properties as a result of the various effects they are exposed to. A performance loss that may occur in reflective tape properties due to these effects will put the wearer's life at risk. For this reason, in this study, the changes in the reflective properties of retroreflective tapes after various effects were investigated.

Keywords: *retroreflectivity, reflective tapes, safety clothing, high visibility, knitted fabric, woven fabric*

Investigarea modificărilor proprietăților reflectorizante ale benzilor reflectorizante din cauza diferitelor efecte ale acestora

Nevoia omenirii de a se proteja de diverse pericole, frig, căldură și alte fenomene naturale a supraviețuit din primele zile ale existenței sale până în zilele noastre. Materialele cu vizibilitate ridicată au fost, de asemenea, dezvoltate în primul rând din necesitatea de protecție. Aceste materiale sunt utilizate pe scară largă în viața de zi cu zi pe roțile de biciclete, semnele rutiere și semnele de circulație. Materialele utilizate în diverse produse textile precum îmbrăcămintea activă, îmbrăcămintea sport, îmbrăcămintea pentru copii, accesoriile, pălăriile, uniformele, benzile pentru picioare și brațe, rucsacurile, ușurează viața, oferind siguranță persoanelor care se plimbă cu animalele de companie, precum și lucrătorilor rutieri, polițiștilor rutieri, pompierilor, pietonilor și bicicliștilor, persoanelor care fac sport și se plimbă noaptea din cauza vieții aglomerate.

Multe dintre accidentele de circulație care au loc astăzi sunt cauzate de incapacitatea de a observa persoanele care se deplasează pe marginea drumului. În conditiile în care iluminarea nu este suficientă, caracteristica reflectorizantă a articolelor purtate va permite persoanalor să fie mai ușor observate. Benzile reflectorizante sunt folosite pentru a adăuga proprietăți reflectorizante articolelor de îmbrăcăminte. Totuși, aceste benzi își pot pierde proprietățile reflectorizante ca urmare a diferitelor efecte la care sunt expuse. O pierdere de performanță care poate apărea în proprietățile benzii reflectorizante din cauza acestor efecte va pune viața purtătorului în pericol. Din acest motiv, în acest studiu au fost investigate modificările proprietăților reflectorizante ale benzilor retroreflectorizante după diferite tratamente.

Cuvinte-cheie: *retroreflectivitate, benzi reflectorizante, îmbrăcăminte de siguranță, vizibilitate ridicată, tricot, țesătură*

INTRODUCTION

The need of human beings to protect themselves from various dangers, cold, heat and other natural events has remained up-to-date since the first days of its existence. High-visibility materials were also developed primarily out of the need for protection.

Most of the traffic accidents occurring today are due to the low visibility of individuals moving on the roadside [1]. The human eye perceives large and contrasting objects and objects with brightness and mobility more easily. Therefore, high-visibility clothing helps drivers see individuals moving along the road earlier. While reflective clothing protects the wearer from risks, they do not eliminate the risk but will optimize visibility and significantly reduce the risk of accidents [1]. The safety of people who are at risk of being hit by vehicles can be increased by the use of high-visibility clothing with appropriate features and designs.

According to the statement made by the General Directorate of Security Traffic Services Presidency on life safety in traffic, it was stated that in the accidents that occurred in 2014, 22.7% of the pedestrians were involved in an accident at night and the most important reason for these accidents was that the pedestrians were not noticed by the drivers. In this context, it was stated that it would be beneficial for traffic safety to use reflective clothing and accessories (such as bags, and hats) that will increase the visibility of pedestrians and especially child pedestrians at night and make them easier to be noticed by drivers [2].

When the statistical data are examined, it has been recorded that 413 pedestrians lost their lives in the accident and 10,620 people were injured during the dark hours of the day between 2011 and 2013 in Turkey. As can be seen from these data, hundreds of people lose their lives and thousands are injured by the effect of not being visible enough in dark environments [3].

The best solution to prevent accidents is to make the pedestrian as visible as possible. This goal can be achieved if pedestrians wear clothing made of retroreflective materials [4].

High-visibility garments are generally used in hazardous work environments with poor light, bad weather or heavy traffic to increase visibility and ensure user safety [5].

In this study, the reflective tapes and the changes in the reflection properties of the tapes after various effects were investigated.

Usage areas of high-visibility clothing

High visibility in workwear is very important. Work clothes are clothes worn to prevent the risk of exposure to harmful substances and bad environmental conditions, to protect them from this risk and/or to reduce this risk [6]. These garments are within the scope of protective clothing and they are used by various professional groups such as road workers, traffic police, firefighters, pedestrians and cyclists, warehouse operators, park operators, forestry workers, railroad workers, emergency response personnel, law enforcement officers, parking attendants, road construction workers and roadside assistance personnel.

Today, due to the workload, many people have the opportunity to do sports in the evenings. High visibility is even more important in the dark, in heavy traffic or bad weather conditions. Today, there are many reflective clothing and accessories (bags, hats, wristbands, belts, etc.) produced in this field. In addition, high-visibility clothing is used in athletes' clothing and shoes, children's clothing, pedestrian clothing, hats, gloves or backpacks, and pet clothing because working people walk their pets in the evening [7].

It is thought that high-visibility clothing helps to be aware of children who are in traffic and use their bicycles to go to school. Today, there are many accessories with this feature such as wristbands, umbrellas, belts, gloves, covers for bicycle saddles, shoes, etc.

Methods of giving high visibility to clothing

High-visibility clothing can be a textile product in the form of vests, trousers or overalls. High-visibility clothing optimizes visibility in low-light and dark environments, especially in autumn and winter.

High visibility feature can be given to textile products in 3 ways:

- Reflective materials: this glow when exposed to light.
- Fluorescent materials: it appears as a red-orange colour all day long.
- Photoluminescent materials: these materials store energy by absorbing daylight or artificial light and give a green-yellow colour in the dark [8].

Fluorescent material takes some of the invisible ultraviolet light from sunlight and sends it back to the viewer as more visible light, thanks to special pigments. Reflective and fluorescent materials emit light when exposed to light emitted from any external source [9]. The reflective (reflective) material in the high-visibility clothing makes it easier for pedestrians to be detected by oncoming vehicle drivers, especially when pedestrians are on the move [10].

Photoluminescent materials, such as textile dyes and printing dyes, can be applied to textile products in the form of fibre, yarn and fabric with techniques such as dye printing, coating and lamination. However, the application of photoluminescent materials to any textile surface with these methods increases the hardness of the product and especially affects the comfort of clothing [9]

Features of reflective (retroreflective) tapes

Retroreflective material reflects light in the direction of the light source, for example, making pedestrian visibility brighter and more visible at night than non-reflective materials [11].

Reflective tapes usually consist of small glass beads or prismatic elements encased in a transparent film. The most commonly used type is tapes created by bead technology. Microscopic glass beads of different diameters are dispersed over the surface of a substrate layer, usually a textile material. These beads adhere to the substrate with an adhesive layer. The performance of the tape is determined by several factors; Bead sizes, how spherical the beads are, the distribution of the beads on the surface, and the depth at which they are embedded in the adhesive layer are all factors that affect tape performance. The durability of a tape depends not only on how well the individual beads are held on the tape but also on the flexibility of the adhesive layer and the strength of the substrate material [12].

Another type of retroreflective (reflective) tape often used in high-visibility personal protective equipment consists of micro prismatic structures. This type of material is embossed with many reflectors shaped like cube corners. These can be arranged in different directions to provide different retroreflective properties. Each micro prismatic shape works by reflecting light from three sides of its structure.

Use of reflective (retroreflective) tape in clothing

Reflective tapes are used to increase the wearer's visibility to others, especially in the dark, and are often sewn or affixed. The tape alerts other people of the person's presence by reflecting light. The tape is generally applied on work clothes, overalls, vests and jackets in various ways, such as vertical, horizontal or cross (X) [13].

The properties of high-visibility clothing and reflective materials were investigated by various researchers.

In their study, Uonarosa and Ayer conducted a daytime field study to investigate the effects of clothing colour, amount of reflective material, driver age and season on the perceived distance of pedestrians by drivers, and the distances at which pedestrians were first detected were recorded. The results showed that the amount of reflective material and the season significantly affect the distance at which pedestrians are perceived by drivers [14].

In this study, Sayer and Mefford conducted a natural field survey to evaluate the effects of clothing colour, amount of reflective material, pedestrian arm movement, traffic density and driver age on the daytime appearance of personal safety clothing. The study showed that high-visibility clothing features increase pedestrian visibility in both day and night conditions [15].

Costello and Wogalter, measured whether people were willing to pay more for clothing with reflective materials compared to clothing without reflective materials, and concluded that they were willing to pay more for reflective materials in clothing [6].

Wood et al. determined the drivers' ability to detect pedestrians at night in their study. Results show that driver age, clothing form, headlights and glare significantly affect performance [5].

Fekety et al. investigated the visibility benefits of adding electroluminescent (EL) panels to pedestrian clothing containing retroreflective materials. Studies have shown that pedestrians are not visible enough to drivers at night and that retroreflective materials can increase pedestrian visibility [16].

Akgün et al. stated in their study that the colour perception of the fabric affects the colour and reflectance (reflection) properties of the yarns in the fabric structure [17].

In conditions where the lighting is not sufficient, especially the insufficient retroreflective properties of the workwear puts the employee's life in danger. It is desired that the visibility features of workwear are sufficient to meet the expectations not only when they are used for the first time, but also after washing and long periods of use. A performance loss that may occur in the properties of reflective tapes due to use and mechanical effects may endanger the life of the wearer [18].

This study was conducted to reveal the changes in the reflection properties of reflective tapes under different conditions.

MATERIAL AND METHODS

In the research, 100% polyester, neon yellow coloured, interlock knitted fabric and woven fabric, which are two types of fabrics that are widely used in the production of high-visibility clothing, were used. As a reflective tape, 2 different types of reflective tapes were used, one of which is stitched to the fabric and the other is adhered to the fabric (figure 1).

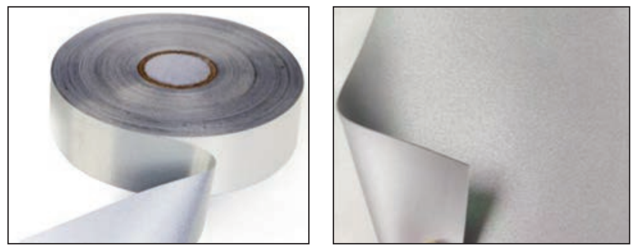

a *b*

Fig. 1. The reflective tape joined by:
a – stitching; *b* – self-adhesive reflective tape

The tape to be joined by stitching was sewn with 100% polyester sewing thread with 4 stitches per cm. The self-adhesive reflective tape was adhered to the fabric in an industrial iron under operating conditions and the film layer on it was removed after cooling.

To investigate the reflective performance of the fabrics, first of all, the reflection values of the bands were measured. Then, tests such as abrasion, stretching, washing, and UV ageing were applied to the tapes in their current state and when they were sewn or adhered to fabrics, and then the change in the reflection performance of the tapes was evaluated.

All materials were conditioned for 24 hours at 20°C±2 temperature and 65±5% relative humidity under standard atmospheric conditions before the test.

Weight: It is the weight in grams of one square meter of fabric. The fabrics' weight was made with five test samples according to the TS 251 standard. The fabrics were cut with a 100 cm^2 weight template and weighed on a precision scale (figure 2, *a*).

Retroreflective performance determination: Measurement of the retroreflective performance of the reflective tapes used, individually and sewn or glued to the fabric, was made with the retroreflectometer in

a *b* *c* *d* *e* *f*

Fig. 2. Images of: *a* – precision scale; *b* – delta retrosign retroreflectometre; *c* – Martindale abrasion tester (James Heal); *d* – flexing tester; *e* – UV ageing test chamber; *f* – knitted fabric stretch recovery tester

figure 2, *b*. In the measurement, retroreflectivity coefficient "R", 90° rotation angle, 12' observation angle and 5° entry angle were used.

While measuring, the device is placed on the retroreflective marking surface so that only the desired region is in the measuring area of the device. After the first measurement was taken, the retroreflectometer was shifted to other parts of the reflective fabric and measurements were continued.

Abrasion

Abrasion is the deformation that occurs as a result of any material rubbing against another surface. This test was carried out to check whether the reflection properties of the tapes have changed in high-visibility clothing due to abrasion.

The abrasion test was carried out according to ISO 12947-2 (9 kPa pressure, 5000 cycles) using the Martindale abrasion tester (figure 2, *c*) and standard wool fabric was used as the abrasive material. The reflection performances of the worn samples were tested.

Washing

Test samples were washed according to EN ISO 6330-2000 Method 2A. After washing, the reflective performances of the samples were tested.

Flexing: Flexural tests of the samples were carried out according to EN ISO 7854 Method A. The reflective performance of the samples was measured after 7500 cycles. The device on which the test is performed is shown in figure 2, *d*. immediately followed by, 20 hours at –30±2°C).

UV ageing

UV ageing was done according to EN ISO 4892 and the samples were kept in the UV ageing test chamber (figure 2, *e*) for 50, 100, 150 and 300 hours (max. 35 watts/cm^2) and then their reflective performances were measured.

Elongation

To see the effect of the woven tapes used on the elongation of the knitted fabric, an elongation test was carried out on knitted fabrics according to TS 10985. Three specimens were tested for each fabric sample. The samples were prepared separately from knitted without tape, with sewn tape and with adhesive tape. Three specimens were tested for each fabric sample.

RESULTS AND DISCUSSIONS

Findings of fabric properties

Table 1 shows the properties of the fabrics used in the study.

Table 1

CHARACTERISTICS OF THE FABRICS USED IN THE STUDY

Fabric type	Material	Yarn count	Weight (g/m²)
Knitted fabric	100% Polyester	70 denier	100.48
Woven fabric	100% Polyester	70 denier	88.30

Findings regarding the determination of retroreflective performances

The retroreflective performance values of the reflective tapes used individually and as sewn or adhered to the fabric and after various effects are shown in table 2 and the graph of these values is shown in figure 3.

From the data obtained, it is seen that the retroreflective performance of the adhesive tape is lower than the performance of the sewn tape. It is also seen that the reflection performance of the tapes decreases when they are sewn or adhered to the fabric.

It is understood from the measurement results that there is not much decrease in the reflective performance of the samples after washing.

When the reflective performances of the samples were examined after the abrasion, it was observed that the reflective performance of the samples decreased between 18–22%. Among these samples, it is seen that the decrease in reflection performance is the most in the samples with woven tape.

When the reflection performances of the samples are examined after stretching, it is seen that the reflection performance of the samples decreases between 5–12%. The decrease in retroreflective performance after various effects in reflective tapes also reduces the service life of these garments.

Findings for the determination of retroreflective performances after UV ageing

The samples were kept in a UV cabinet for 50, 100, 150 and 300 hours. It was observed that there was

Table 2

RETROREFLECTIVE VALUES OF THE SAMPLES AFTER WASHING, ABRASION AND FLEXING

Samples	Retroreflectivity (cd/lx.m^2)	Retroreflectivity after washing (cd/lx.m^2)	Retroreflectivity after abrasion (cd/lx.m^2)	Retroreflectivity after flexing (cd/lx.m^2)
Self-adhesive reflective tape	310	297.6	251.3	272
Inadhesive reflective tape	405	394.6	317	387.75
Knitted fabric with sewn tape	378.25	402	322	366
Knitted fabric with adhesive tape	289.75	288.3	237	278
Woven fabric with sewn tape	397	399.25	335.33	377.33
Woven fabric with adhesive tape	307	286.75	244	279

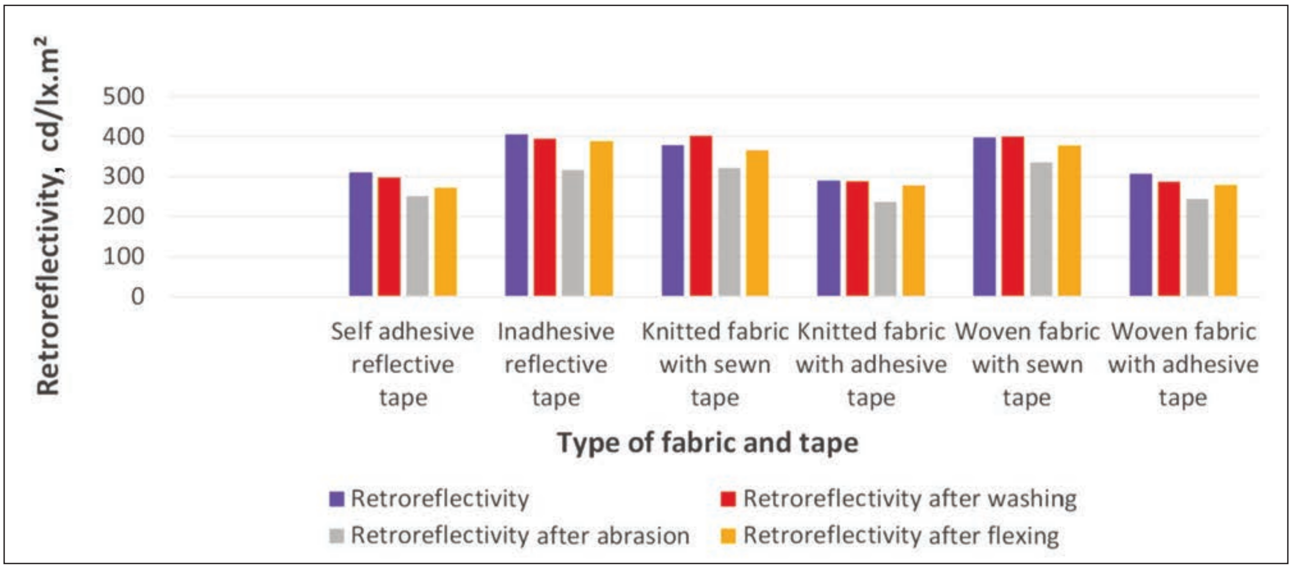

Fig. 3. Retroreflective performances of samples after various effects

no change in the measured retroreflective values of the samples at the end of each waiting period.

Findings of elasticity values of samples

As can be seen in table 3 and figure 4, the elongation amount of the knitted fabric is very high. Woven reflective tape is used in both knitted and woven fabrics in the market. In this study, the elasticity test was applied only to knitted fabric samples and knitted fabric samples to which tape was attached since it is thought that the woven tape will restrict the stretching of the knitted fabric. As a result, it appears that sewing or glueing the reflective tape limits the elongation of the knitted fabric.

Table 3

ELASTICITY VALUES OF THE SAMPLES

Sample	Elongation rate (%)
Knitted fabric	30.7
Knitted fabric with sewn tape	0.77
Knitted fabric with adhesive tape	1.53

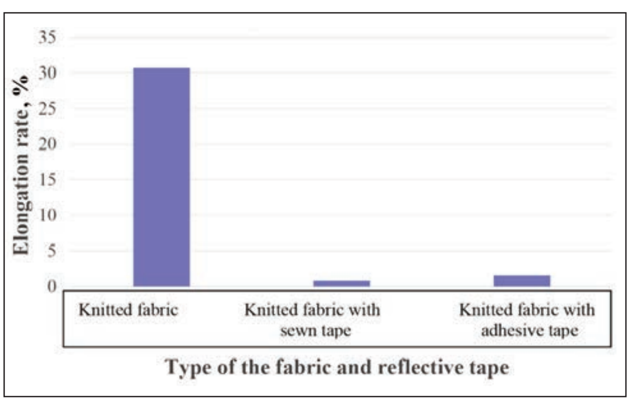

Fig. 4. Elongation values of samples

CONCLUSION

The importance of high-visibility clothing and textiles is increasing day by day. While these clothes were used for protection at the beginning, they have started to be used in many areas from wedding dresses to clothes worn in performing arts, to decoration products. The materials used in the production of these products, when left under the sun or any artificial light for a certain period, give light that can be seen clearly in the dark and provide visibility. Although the glow produced by these materials gradually decreases after a while, when left in the sun or artificial light source, it can store the light again and give light in the dark.

High-visibility clothing is classified as visually striking personal protective clothing to reduce the risk of death or injury in traffic accidents. The fact that the traffic is more intense day by day leads to congestion and therefore to greater risks. Especially at night and during harsh weather conditions, the risks increase even more. Wearing high-visibility clothing can also reduce or prevent these risks.

In this study, the change in the high visibility of the high-visibility samples created with different fabrics and different tape types was evaluated after various effects.

When the samples were examined, it was seen that the retroreflective value of the non-adhesive tape was higher than the retroreflective value of the self-adhesive tape. After the washing process, the reflective value of both tapes decreased by 3–4%, and after the rubbing process, it was seen to decrease by approximately 20%.

It has been observed that when the tapes are sewn or glued onto knitted or woven fabric, their retroreflective values are reduced by 6–7%. However, after the washing process, it was observed that the reflective value of the tape stitched to both knitted and woven fabrics increased by 5–6%. It was observed that the reflective value of the tape adhered to both knitted and woven fabrics decreased after washing.

While the reflective values of the tapes sewn or adhered to the knitted fabric decreased by 15–26% after abrasion, the reflective value of the tapes sewn or adhered to the woven fabric decreased by 19–20%. This difference is due to the flexibility of knitted fabrics.

It was observed that there was not much change in the reflective performance values of the samples after washing and ageing in the UV ageing test chamber for 300 hours.

When the elasticity value of the knitted fabric is examined, it is seen that the woven reflective tapes restrict the movement of the person and reduce comfort, which is one of the most important features especially in protective clothing. Therefore, the production of reflective tapes with a more flexible structure produced with the knitting technique should be considered to increase the comfort of clothing.

The decrease in retroreflective performance after various effects in reflective tapes reduces the protective feature of the garment, thus reducing its useful life.

ACKNOWLEDGEMENT

This study was supported by Ege University Scientific Research Projects Coordination Unit. Project Number: 2017/BMYO/002.

REFERENCES

[1] Bartkowiak, G., *Protective clothing – Reflective clothing*, 2012
[2] *Can güvenliğiniz için gece reflektif kıyafetler giyin*, Available at: http://www.memurlar.net/haber/537179/ [Acceseed on April 18, 2022]
[3] *Altınok'tan Reflektif Uyarı*, Available at: https://www.bartin.info/asayis/altinoktan-reflektif-uyari-h10788.html [Acceseed on April 18, 2022]
[4] Muttart, J.W., *Effects of Retroreflective Material Upon Pedestrian Identification at Night*, In: Accident Reconstruction Journal, 2000, 1–12
[5] Wood, J.M., Tyrrell. R.A., *Carberry T.P., Limitations in Drivers' Ability to Recognize Pedestrians at Night*, In: Human Factors: The Journal of the Human Factors and Ergonomics Society, 2005, 47, 3, 644–653
[6] Costello, T.M., Wogalter, M.S., *Reflective Trim on Clothing: Desirability Indicated by Purchase Preferenc*e, In: Proceedıngs of the Human Factors and Ergonomics Society 51st Annual Meeting, 2007, 1119–1123
[7] Dirgar, E., Çiçek, R., *Yüksek Görünürlüğe Sahip Giysilerin ve Tekstillerin İncelenmesi*, Uluslararası Geleneksel Sanatlar Sempozyumu, Trabzon, 2017
[8] Güney Unlü, F., *Koruyucu Giysilerde İç Konfor Şartlarının İncelenmesi*, Yayınlanmamış Yüksek Lisans Tezi, Isparta, 118 sayfa, 2008
[9] Yılmaz, D., Güder, G., Tikidaş, T., *Karanlıkta Görünürlüğe Sahip Tekstil Ürünlerinin Üretimi*, In: Turkchem Magazin Dergisi, 2013
[10] Coşkun, E., Oğulata, R.T., *Akıllı Tekstiller ve Genel Özellikleri*, In: Çukurova Üniversitesi Fen Bilimleri Enstitüsü Dergisi, 2008, 18, 3, 100–109
[11] Cassidy, P.E., Brooks, B.E., Anderson, N.J., *Size isn't everything: The effects of size and brightness of retroreflective materials on nighttimeconspicuity*, In: Proceedings of the Human Factors and Ergonomics Society 49th Annual Meeting, 2005, 1931–1934
[12] Gamble, M., *Clothing for Conspicuity*, In: The Journal of Employee Protection, 2018
[13] Minahan, P., *Use of retro-reflective tape on work clothing*, In: Mines safety bulletin no. 50, 2004
[14] Uonarosa, M.A., Ayer, J.A., *Seasonal Variations In Conspicuity of High-Visibility Garments*, 2007
[15] Sayer, J.R., Mefford, M.L., *The roles of garment design and scene complexity in the daytime conspicuity of high-visibility safety apparel*, 2005.
[16] Fekety, D.K., Edewaard, D.E., Stafford Sewall, A.A., Tyrrell, R.A., *Electroluminescent Materials Can Further Enhance the Nighttime Conspicuity of Pedestrians Wearing Retroreflective Materials*, 2016
[17] Akgün, M., Alpay, H.R., Becerir, B., *Kumaş Yapısal Parametreleri ile Reflektans Değerleri Arasındaki İlişkilerin Değerlendirilmesi,* Uludağ Üniversitesi Mühendislik-Mimarlık Fakültesi Dergisi, 2012, 17
[18] Temel, E., Mengüç, G.S., Bozdoğan, F., *Çeşitli Etkiler Sonrası Retroreflektif Özelliklerin Değişimi*, XIII. Uluslararası İzmir Tekstil ve Hazır Giyim Sempozyumu, 2014
[19] Ozdil, N., *Kumaşlarda Fiziksel Kalite Kontrol Yöntemleri*, Ege Üniversitesi Tekstil ve Konfeksiyon Araştırma-Uygulama Merkezi Yayını, 2016, 21

Authors:

OKSAN ORAL[1], ESRA DIRGAR[1], NILGUN OZDIL[2]

[1]Ege University, Emel Akın Vocational Training School, Bornova, 35100, Izmir, Turkey
e-mail: esra.dirgar@ege.edu.tr

[2]Ege University, Engineering Faculty, Textile Engineering Department, Bornova, 35100, Izmir, Turkey
e-mail: nilgun.ozdil@ege.edu.tr

Corresponding author:

OKSAN ORAL
e-mail:oksan.kansoy@ege.edu.tr

Evaluation of copper electrodes for biomedical monitoring systems

DOI: 10.35530/IT.074.03.202298

RALUCA MARIA AILENI
CRISTINA STROE
IUKSEL RASIT

ABSTRACT – REZUMAT

Evaluation of copper electrodes for biomedical monitoring systems

This paper presents several aspects of in vivo biocompatibility tests using the animal model, considering conductive electrodes based on cotton fabric and a conductive paste-based polymeric matrix with copper microparticles that offer the potential to be used in medical devices. Additionally, this work presents a potential application of the electrodes for temperature sensors using the Arduino development board. In addition, after performing in vivo tests, analysis of the primary irritation scores, animal irritation scores, and cumulative irritation index showed that the electrodes resulted in a negligible measurement of perceived skin irritation.

Keywords: *textile, electrodes, conductive, biocompatibility testing, in vivo*

Evaluarea electrozilor din cupru pentru sisteme de monitorizare biomedicală

Această lucrare prezintă aspecte ale testelor de biocompatibilitate în vivo utilizând modelul animal, luând în considerare electrozii conductivi din țesătură din bumbac și pastă conductivă pe bază de matrice polimerică cu microparticule de cupru cu potențial de a fi utilizați în dispozitive medicale. În plus, această lucrare prezintă o aplicație a electrozilor pentru senzorii de temperatură utilizând o placă de dezvoltare Arduino. În continuare, după efectuarea testelor în vivo, analiza scorurilor de Iritație Primară, Iritaţie de Animal și Indexului Cumulat de Iritaţie a arătat că electrozii au provocat un răspuns iritativ neglijabil la nivelul pielii.

Cuvinte-cheie: *textil, electrozi, conductiv, teste de biocompatibilitate, in vivo*

INTRODUCTION

Biomaterials and medical devices represent an extraordinarily diverse and heterogeneous group [1]. The use of these products entails direct or indirect contact with the body; commercial availability requires testing of their safety. The safety assessment of medical devices establishes the risk of adverse health reactions in case of their normal or abnormal use [2, 3]. Since these adverse reactions may occur following exposure to these materials, preclinical testing of the toxic potential of the materials or their components is required [4]. Since January 1995, medical devices used in practice in the EU must have been evaluated in terms of safety according to Directive 93/42 EEC [5, 6]. This directive aims to establish a single European market that ensures that both patients and users are protected against exposure to additional risks.

Currently, the safety of medical devices is established through toxicological studies [7] and other studies recommended in SR EN ISO 10993-1:2021 – Biological evaluation of medical devices [8], SR EN ISO 10993-10:2014 [9] and SR EN ISO 10993-23: 2021 [10].

Recent research has investigated the biocompatibility of copper in combination with other metals. For example, Cu–Au core-shell nanowire electrodes for electrophysiological monitoring (electromyogram, electrocardiogram sensors) [11] were tested using artificial perspiration and cell culture. However, copper nanowires have the disadvantage of oxidation and lack biological compatibility. In addition, electrode-based Cu–Au core-shell nanowires [11], polypyrrole and Cu(II) metal-organic nanocomposites [12], copper–ruthenium composites [13], and CuO electrodes [14] present desirable biocompatibility (*in vitro* and *in vivo*) without generating inflammatory responses [12]. According to some studies, the limitations of flexible sensors include inadequate biocompatibility, even for noninvasive products that only come into contact with human skin [15]. Even if conductive inks based on metal or carbon nanotubes (CNTs) were to be intensively studied, these inks have raised concerns regarding their possibly harmful effect on health and their manufacture is expensive. Thus, metallic reactive inks (e.g., Ag) are more attractive due to their excellent electrical conductivity and biocompatibility [16].

EXPERIMENTAL PART

Biocompatibility testing of conductive/insulating materials used to make medical monitoring devices was carried through *in vivo* tests because these products (namely, electrode materials) involve direct or indirect contact with the body and require safety testing before becoming available for commercial use. The safety assessment of medical devices establishes the risk of adverse health reactions in case of their normal or abnormal use. As these adverse reactions may occur following exposure to such electrode materials, preclinical testing of the toxic potential of the materials or their components is required according to directive 93/42 EEC.

Here, the biocompatibility of electrode materials (namely, electroconductive textile materials with a surface resistance of 10^3 Ω) was evaluated using two reference materials (P_1 – textile material treated by alkaline boiling-bleaching, and P_2 – raw textile material treated in plasma with O_2 to obtain a hydrophilic surface). In addition, the textile electrode material was functionalized by depositing conductive pastes comprising a polymeric matrix (polyvinyl alcohol) and copper (Cu) microparticles after treatment in RF oxygen plasma (P_3). Table 1 shows images of the electrode materials. The biocompatibility assessment was carried out by testing skin irritation according to the SR EN ISO 10993-10:2014/SR EN ISO 10993-23:2021 standard (Biological evaluation of medical devices. Part 23: Tests for irritation).

Figure 1 shows electron microscopy images (magnitude 60x) of the fabric surface for samples P_1 (untreated – figure 1, *a*), P_2 (raw fabric → O_2 plasma RF treatment, using an RF generator in kHz and power P = 100 W – figure 1, *b*), P_3 (treatment by alkaline boiling-bleaching and deposition of conductive paste based on PVA and Cu – figure 1, *c*).

For biocompatibility testing, three rabbits (male New Zealand albino rabbits) weighing between 3400 and 4600 g were used for each test sample, as provided by the Bio base of the Cantacuzino Institute, Băneasa Station.

The samples were cut into 2×3 cm samples and were used after impregnation with physiological serum. They were then covered with an additional dressing and immobilized with semiocclusive adhesive tape for a minimum of 4 hours. Over the control areas, the electrode samples were applied and impregnated with physiological serum, with control over the exact dimensions and duration of exposure. After 4 hours, the test sample (and blank) were removed, and the exposed areas were washed with distilled water.

Two examiners observed the animals to monitor the reactions of their exposed skin, in an environment with natural lighting. The exposed areas of the test sample and control were examined at 1, 24, 48 and 72 hours after the first exposure. The experimental room temperature was 20±1°C, and the relative humidity was 50–60%. Lighting was artificial, with alternating 12-hour spans of light/darkness.

Due to the possibility of irritation reactions, the study was initiated by exposing each test sample to a single animal (A_i). For this test, the samples (electrode material) were cut into 2×3 cm samples and used after impregnation with physiological serum. To fix a sample on animal skin, it was covered with an additional dressing and immobilized with semiocclusive adhesive tape for a minimum of 4 hours (figure 2). Initially, the control samples P_1 and P_2 impregnated with physiological serum were applied for 4 hours, and after 4 hours, the test sample and control were removed. Then, the exposed areas were washed with distilled water. Examination of the exposed areas, test sample and control was carried out 1, 24, 48, and 72 hours after the first exposure.

Since no reactions indicated that the test sample induced irritation, the study continued with two more exposures performed as follows. After the 72-hour observation interval following the first exposure, two additional 4-hour exposures were made in two successive applications. The above procedure was repeated on two more animals. Three skin exposures were made for the test/control sample on three animals each. Approximately one hour after removing the semiocclusive bandages, skin reactions were recorded. After exposure and removal of the dressing, the observations were repeated at intervals of 24, 48, and 72 hours. Skin observations were made before the second additional exposure and after 24, 48, and 72 hours. After three exposures and monitoring of the skin reactions, the Primary Irritation Score was determined according to the types of skin reactions and their applicable quantification (table 1, table 2). The Irritation Score per Animal (SIA) is obtained by summing the Primary Irritation Score (SIP) of each moment of observation divided by the number of observations. The cumulative irritation index (CII) was obtained by dividing the sum of irritation scores per animal by the number of animals (table 3).

Thus, for sample P_3, the exposure areas after the first and second applications are presented in table 4. Table 5 shows the images obtained after the first application upon examining the exposed areas at 1, 24, and 48 hours after the first application. Table 6 shows the images obtained after the second application. According to the Primary Irritation scores, the Animal Irritation Scores and the Cumulative Irritation Index for samples P_1, P_2, and P_3 all were determined to be in the Negligible response category.

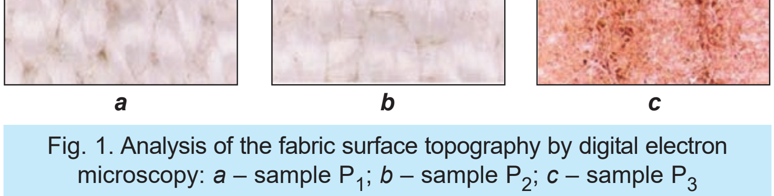

a *b* *c*

Fig. 1. Analysis of the fabric surface topography by digital electron microscopy: *a* – sample P_1; *b* – sample P_2; *c* – sample P_3

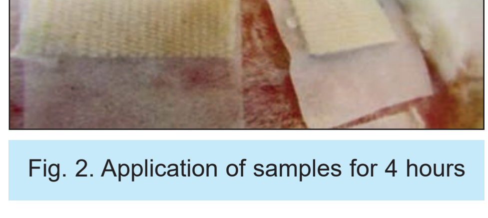

Fig. 2. Application of samples for 4 hours

Table 1

TYPES OF SKIN REACTIONS AND THEIR QUANTIFICATION	
Reactions	**Primary irritation score**
Erythema and eschar	-
No erythema	0
Weak erythema (barely perceptible)	1
Perceptible erythema	2
Moderate erythema	3
Intense erythema (with a tendency to eschar formation)	4
Edema	-
No edema	0
Slight edema (barely perceptible)	1
Perceptible edema	2
Moderate edema	3
Intense edema (more than 1 mm – extended outside the contact area)	4
Maximum possible irritation score	8

Table 2

IRRITANT RESPONSE CATEGORIES	
Average	**Response category**
0 to 0.4	Negligible
0.5 to 1.9	Weak
2 to 4.9	Moderate
5 to 8	Severe
0 to 0.4	Response category

RESULTS AND DISCUSSION

For all samples (P_1–P_3), the Animal Irritation Score (SIA) and Primary Irritation Score (SIP) were 0. In addition, the cumulative irritation index for test samples P_1 (control sample obtained through classical methods for hydrophilization (boiling-bleaching)) and P_2 (control sample obtained by hydrophilization using RF plasma oxygen) was 0 (table 5). Thus, according to table 2, the scores reflect a Negligible response. Following this biocompatibility evaluation, we concluded

Table 3

SCORES OBTAINED FOR SINGLE AND REPEATED APPLICATION OF ELECTRODE MATERIALS											
	Single application				**Repeated application**						
SIP	1	2	3	4	5	6	7	8	9	10	Total
Exposure	-		I			II			III		-
Hours	1	24	48	72	24	48	72	24	48	72	-
Samples P_1 and P_2											
A1	0	0	0	0	0	0	0	0	0	0	0
A2	0	0	0	0	0	0	0	0	0	0	0
A3	0	0	0	0	0	0	0	0	0	0	0
Sample P_3											
A1	0	0	0	0	0	0	0	0	0	0	0
A2	0	0	0	0	0	0	0	0	0	0	0
A3	0	0	0	0	0	0	0	0	0	0	0

Table 4

EXAMINATION OF EXPOSED AREAS AFTER THE FIRST AND SECOND APPLICATION			
Examination of exposed areas after the first application			
	1 h after the first application	24 h after the first application	48 h after the first application
P_3	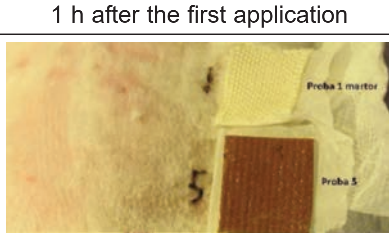	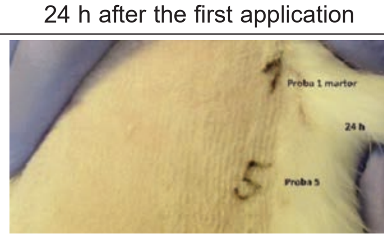	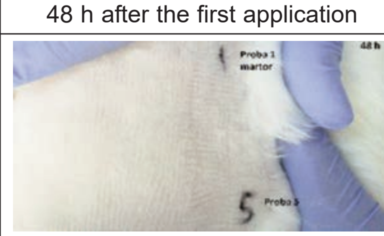
Examination of exposed areas after the second application			
P_3		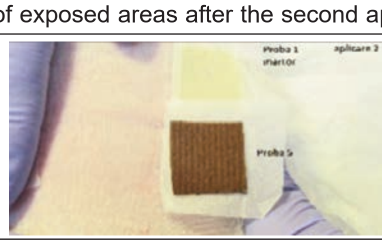	

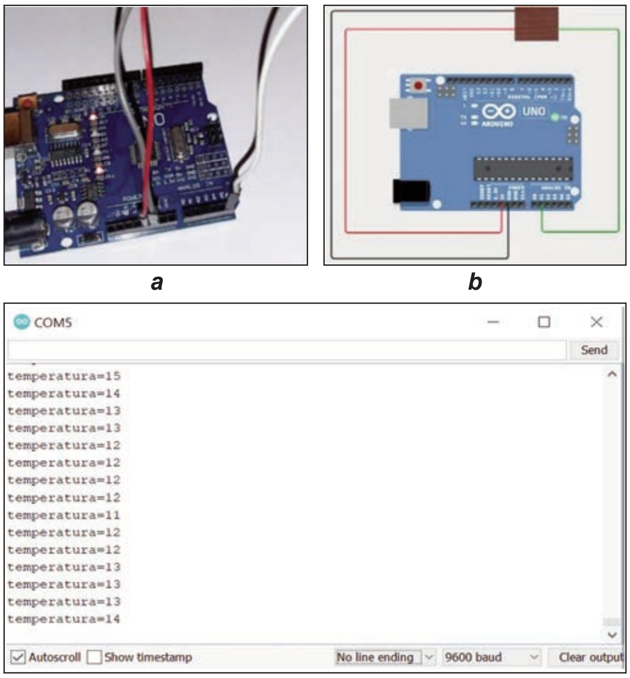

a *b* *c*

Fig. 3. Demonstrative model based on flexible Cu electrode (P_3) for temperature monitoring: *a* – development board Arduino connection to analogue pins; *b* – simulation of the temperature monitoring using P_3 electrode; *c* – reading data from analogue pins on the Arduino (sample P_3)

that material P_3 can be used as an electrode material to realize physiological monitoring systems. The P3 material was implemented in a demonstrative model using an Arduino development board (figure 3, *a*) to highlight the change in electrical resistance depending on the temperature and verify the potential application of sample P_3 in temperature monitoring systems. Conductive connectors (figure 3, *a*), flexible textile electrodes made of electrode materials (P_3 – figure 3, *b*) and support materials (P_1 or P_2) were used as shown.

The discrete values for temperature were read each 0.8 seconds, corresponding to a sampling frequency of 1.25 Hz:

$$f = \frac{1}{T} \qquad (1)$$

where f in Hz represents the frequency and T in s represents the time.

CONCLUSIONS

In conclusion, our electrode material based on a polymer matrix and copper microparticles can be used in sensor-based systems as electrical resistance monitors to measure the variation temperature-dependent electrical resistance of a surface and thus determine the temperature of that body. Biocompatibility tests to evaluate skin irritation were carried out *in vivo* using an animal model, and analysis of the primary irritation, animal irritation and cumulative irritation index scores for samples P_1, P_2 and P_3 indicated a negligible irritant response. In the future, the commercial use of these materials in biomedical monitoring systems will involve supplementary investigations, such as preclinical testing of the toxic potential of the materials or their components, which is required according to the MDD 93/42 EEC (Medical Device Directive) because biomedical monitoring devices fall into class I devices for noninvasive measurement. Our demonstrative model based on the Arduino development board highlighted that it is possible to record temperature variation using our electrode materials based on textile materials covered with a conductive paste based on Cu microparticles.

ACKNOWLEDGEMENTS

The research presented in this paper was prepared in the INCDTP laboratories. Funds support this work from MCID, National Project ″Electroconductive composite textile materials based on 3D polymer matrices for sensor systems monitoring and attenuating electromagnetic waves (3D ELECTROTEX)”, Grant Agreement PN 19 17 01 01.

Table 5

SCORES OBTAINED FOR SINGLE AND REPEATED APPLICATION OF ELECTRODE MATERIALS

	Primary Irritation Score (SIP)										Animal Irritation Score (SIA) $SIA = \sum_{i=1}^{10} SIP$	Cumulative Irritation Index (CII) $CII = \sum_{i=1}^{3} \frac{SIA}{3}$
	Single application				Repeat application							
SIP	1	2	3	4	5	6	7	8	9	10	-	
Exposure		I			II			III			-	
hours	1	24	48	72	24	48	72	24	48	72	-	
	Samples P_1 and P_2											
A1	0	0	0	0	0	0	0	0	0	0	0	
A2	0	0	0	0	0	0	0	0	0	0	0	0
A3	0	0	0	0	0	0	0	0	0	0	0	
	Sample P_3											
A1	0	0	0	0	0	0	0	0	0	0	0	
A2	0	0	0	0	0	0	0	0	0	0	0	0
A3	0	0	0	0	0	0	0	0	0	0	0	

REFERENCES

[1] Bollen, L.S., Svendsen, O., *Regulatory guidelines for biocompatibility safety testing, Medical Plastic and Biomaterials*, 1997, 4, 16–20

[2] Fischbach, F.T., Dunning, M.B., *A manual of laboratory and diagnostic tests*, Lippincott Williams & Wilkins, 2009

[3] Gliklich, R.E., Dreyer, N.A., Leavy, M.B. eds., *Registries for evaluating patient outcomes: a user's guide,* 2014

[4] Ettlinger, R., Lächelt, U., Gref, R., Horcajada, P., Lammers, T., Serre, C., Couvreur, P., Morris, R.E., Wuttke, S., *Toxicity of metal-organic framework nanoparticles: from essential analyses to potential applications*, In: Chemical Society Reviews, 2022

[5] Mason, S., *European regulation of medical devices. The textbook of pharmaceutical medicine*, 2013, 418–434

[6] The directive, C., *93/42/EEC of 14 June 1993 concerning medical devices*, 1993

[7] Myers, D.K., Goldberg, A.M., Poth, A., Wolf, M.F., Carraway, J., McKim, J., Coleman, K.P., Hutchinson, R., Brown, R., Krug, H.F., Bahinski, A., *From in vivo to in vitro: The medical device testing paradigm shift*, In: ALTEX-Alternatives to animal experimentation, 2017, 4, 34, 479–500

[8] SR EN ISO 10993-1:2021 – *Biological evaluation of medical devices*, Available at: www.en-standard.eu/bs-en-iso-10993-1-2020-biological-evaluation-of-medical-devices-evaluation-and-testing-within-a-risk-management-process [Accessed 24 May 2022]

[9] SR EN ISO 10993-10:2014 – *Biological evaluation of medical devices – Part 10: Tests for irritation and skin sensitization*, Available at: www.en-standard.eu/din-en-iso-10993-10-biological-evaluation-of-medical-devices-part-10-tests-for-irritation-and-skin-sensitization-iso-10993-10-2010 [Accessed 21 May 2022]

[10] ISO 10993-23:2021, *Biological evaluation of medical devices – Part 23: Tests for irritation*, Available at: www.iso.org/standard/74151.html [Accessed 24 April 2022]

[11] Kim, D., Bang, J., Won, P., Kim, Y., Jung, J., Lee, J., Kwon, J., Lee, H., Hong, S., Jeon, N.L., Han, S., *Biocompatible Cost-Effective Electrophysiological Monitoring with Oxidation-Free Cu–Au Core–Shell Nanowire*, In: Advanced Materials Technologies, 2020, 5, 12, 2000661

[12] Neisi, Z., Ansari-Asl, Z., Jafarinejad-Farsangi, S., Tarzi, M.E., Sedaghat, T., Nobakht, V., *Synthesis, characterization and biocompatibility of polypyrrole/Cu (II) metal-organic framework nanocomposites*, In: Colloids and Surfaces B: Biointerfaces, 2019, 178, 365–376

[13] Stupin, D.D., Abelit, A.A., Mereshchenko, A.S., Panov, M.S., Ryazantsev, M.N., *Copper–Ruthenium Composite as Perspective Material for Bioelectrodes: Laser-Assisted Synthesis, Biocompatibility Study, and an Impedance-Based Cellular Biosensor as Proof of Concept*, In: Biosensors, 2022, 7, 12, 527

[14] Shinde, S.K., Kim, D.Y., Ghodake, G.S., Maile, N.C., Kadam, A.A., Lee, D.S., Rath, M.C., Fulari, V.J., *Morphological enhancement to CuO nanostructures by electron beam irradiation for biocompatibility and electrochemical performance*, In: Ultrasonics sonochemistry, 2018, 40, 314–322

[15] Xie, L., Zhang, Z., Wu, Q., Gao, Z., Mi, G., Wang, R., Sun, H.B., Zhao, Y., Du, Y., *Intelligent wearable devices based on nanomaterials and nanostructures for healthcare*, In: Nanoscale, 2023

[16] Gusta, R.K., Nguyen, T.A., *Smart multifunctional nano-inks*, Elsevier, 2023

Authors:

RALUCA MARIA AILENI[1], IUKSEL RASIT[2], CRISTINA STROE[1]

[1]National Research and Development Institute for Textiles and Leather,
Lucretiu Patrascanu 16, 030508 Bucharest, Romania

[2]National Institute for Chemical-Pharmaceutical Research and Development – ICCF,
Calea Vitan 112, Bucharest, Romania

Corresponding author:

RALUCA MARIA AILENI
e-mail: raluca.aileni@incdtp.ro

The elasticity distribution of under-band based on pressure comfort and breast support performance for seamless sports bras

DOI: 10.35530/IT.074.03.202244

XIAOFANG LIU
XIAOFEN JI
YUXIU YAN
QI ZHOU

ABSTRACT – REZUMAT

The elasticity distribution of under-band based on pressure comfort and breast support performance for seamless sports bras

Seamless knitted sports bra is becoming popular for its high performance in tactility and pressure comfort, however, it also encounters the problem of insufficient support. To improve the support performance, it is always knitted with strong elastic material in a reduced size than the body dimension, which will generate much pressure on the body, leading to discomfort. As the pressure distribution may affect the pressure comfort and support performance of the sports bra, this study aimed to explore novel information in optimizing the pressure comfort and support performance by applying elasticity distribution. 4 sports bras with different elasticity distribution on the under-band were developed to compare with the one without elasticity distribution, and 12 healthy women were involved as subjects. The pressure distribution and pressure comfort sensations both in static and dynamic conditions, and the reduction of breast displacement (RBD) of 5 sports bras were measured and analysed by ANOVA analysis. The results indicated that the pressure distribution, the pressure comfort and RBD were effectively changed by elasticity distribution. Bra D with a high Young's modulus on the side area of the under-band was ideal and typical both in pressure comfort and RBD.

Keywords: *seamless knitted, sports bra, under-band, elasticity distribution, pressure comfort, breast support*

Distribuția elasticității benzii de susținere pe baza confortului și performanței de susținere pentru sutiene sport fără cusături

Sutienul sport tricotat fără cusături devine popular pentru performanța sa ridicată în tactilitate și confort la presiune, însă, cu toate acestea, se confruntă și cu problema suportului insuficient. Pentru a îmbunătăți performanța de susținere, acesta este întotdeauna tricotat cu material foarte elastic, într-o dimensiune mai redusă decât dimensiunea corpului, ceea ce va genera presiune ridicată asupra corpului, ducând la disconfort. Deoarece distribuția presiunii poate afecta confortul la presiune și performanța de susținere a sutienului sport, acest studiu și-a propus să exploreze informații noi în optimizarea confortului la presiune și a performanței de susținere prin aplicarea distribuției elasticității. Au fost dezvoltate 4 sutiene sport cu distribuție diferită a elasticității benzii de susținere pentru a fi comparate cu cele fără distribuție a elasticității, iar 12 persoane de sex feminin au fost implicate ca subiecți. Distribuția presiunii și senzațiile de confort la presiune atât în condiții statice, cât și dinamice, precum și reducerea deplasării sânilor (RBD) a celor 5 sutiene sport au fost măsurate și evaluate prin analiza ANOVA. Rezultatele au indicat că distribuția presiunii, confortul la presiune și RBD au fost modificate efectiv de distribuția elasticității. Sutienul D cu un modul Young ridicat pe zona laterală a benzii de susținere a fost ideal, atât în ceea ce privește confortul la presiune, cât și RBD.

Cuvinte-cheie: *tricotat fără cusături, sutien sport, bandă de susținere, distribuția elasticității, confort la presiune, susținerea sânilor*

INTRODUCTION

Due to the limited anatomical support, women's breasts will move relative to the chest wall when they participate in physical activities [1]. Therefore, sports bra, which was proven to be effective at reducing breast movement and exercise-related breast pain, has been advocated for exercising females [1]. Because of its high performance in tactility and pressure comfort, a seamless knitted sports bra is becoming popular. However, it also encounters some problems such as sizing, compression of the breasts, and especially insufficient support [2]. As a primary supporting part for breasts, the under-band of a seamless sports bra is often made with a strong elastic material in a reduced size than body dimension rather than cutting and combination of different fabrics in the under-band of a traditional bra. When it extends to adapt to body dimension during wearing, the fabric's tensile behaviour stores strain energy in the fabric, leading to the application of pressure on the skin [3]. If too loose, it will slide up and down the torso, and decrease the breast support performance during exercise [4]. If too tight, it will cause serious skin traces, result in uncomfortable feeling, or even heart, lung and bowel function injury for the wearer [5]. As a result, there is a contradiction between pressure comfort and support function for the under-band of a seamless sports bra. Most studies, however, only focused on pressure comfort or support function of the under-band [4, 6, 7], and there was limited research on how to optimize these two factors.

According to previous research, pressure comfort is not only affected by the value of pressure but also by the distribution of pressure. Due to the differences between pressure comfort thresholds (PCT), i.e., a feeling boundary between comfort and discomfort, between different body parts [8], the change in pressure distribution may cause a change in pressure comfort. It has been reported in some research about other garments that appropriate pressure distribution would improve subjective pressure comfort responses. For example, compression shaping pants with graduated pressure distribution could promote blood microcirculation of lower limbs and enhance wearing comfort [9]. However, the pressure distribution of the under-band has yet to be studied.

Elasticity distribution, i.e., applying fabrics with different Young's modulus in different areas, is a commonly used way to change pressure distribution. The pressure exerted on the body depends on the fabric tension and radius of the body curvature [3, 10]. As the radius of body curvature is a constant for a certain person, the pressure distribution could be changed by the fabric tension. With the same elongation, changes in Young's modulus will generate different levels of fabric tension and contact pressure to the body [11]. For seamless knitted fabric, elasticity distribution can be achieved by knitting with different structures, loop length or percentages of firm and soft yarns in different regions [2, 9, 12]. 4D garments fabricated by careful control of the percentages of firm and soft yarns could change the pressure distribution, and reduce uncomfortable pressure and unwanted sliding caused by body motion [12]. However, the effect of elasticity distribution of under-band on the pressure distribution, pressure comfort and the support performance of seamless sports bras has yet to be investigated.

This study aimed to explore the effect of elasticity distribution of under-band on the pressure distribution, pressure comfort and the support performance of seamless knitted sports bra, and search for appropriate elasticity distribution of the under-band which could improve the support performance without decreasing the pressure comfort of the seamless sports bra. Therefore, 5 seamless knitted sports bras with under-bands of different elasticity distribution were designed. The objective pressure, psychological pressure comfort sensations and the reduction of breast displacement (RBD) of these 5 bras were measured and compared. RBD is defined as the displacement percentage change (breast displacement without a bra minus breast displacement with a bra, divided by breast displacement without a bra), and is considered to be a unique evaluation standard of the supporting performance for sports bras [7]. It is hoped that the result could provide novel information in optimizing both the pressure comfort and breast support performance of sports bras to benefit exercising women.

METHODOLOGY

Participants

Following institutional ethical approval, 12 healthy, pre-menopausal and recreationally active women, who undertook 30 min of exercise more than twice a week were recruited for the experiment. And to minimize the potential between-participant effect in pressure comfort and breast displacement, all participants were chosen to be professionally fit to wear a 75B bra size [13]. The 3D body scanner ($(TC)^2$, US) was used to measure the subjects, and the mean and standard deviation (SD) of their anthropometric measurements were shown in table 1. The procedures of the experiment were carefully explained to all subjects before they signed the informed consent to participate. All participants had not experienced surgical procedures to the breasts or gone through pregnancy or breastfeeding and were not in their menstrual cycle. Participants were wearing the same type of sports pants and sports shoes and randomly wore one of these five bras (bras only on their upper body).

Table 1

ANTHROPOMETRIC MEASUREMENTS OF THE SUBJECTS

Anthropometric measurements	Mean	Std. D
Age	21.35	0.33
Weight (kg)	49.43	0.25
Height (cm)	159.76	0.93
BMI	19.37	0.31
Bust girth (cm)	87.17	1.12
Under-bust girth (cm)	75.42	0.77
Bust height (cm)	114.15	0.20
Under-bust height (cm)	108.13	0.27
Bust point width (cm)	20.07	0.12
Length from the front neck point to bust point (cm)	20.17	0.11
Vertical arc length from bust point to under-bust (cm)	7.59	0.04
Width of the breast (cm)	15.19	0.25
Height of the breast (cm)	6.03	0.14
Arc length of the outer side of the breast (cm)	10.30	0.18
Arc length of the inner side of the breast (cm)	8.20	0.14

Experiment samples

The experiment samples are 5 seamless knitted compression sports bras, with fibre contents of 53% Polyester, 33% Polyamide, and 14% Spandex for all parts. They were knitted by a seamless knitting machine (Santoni SM8-Top2, Italian) with 14" 28G 1248 Ndl, in the air-conditioned university workshop with the standard atmospheric condition (temperature: 23±1 °C; relative humidity: 65±3%). The sports bras were knitted with two yarns, polyester filament (100D) and nylon /spandex core-spun yarn (20/30 D).

The unit yarn feeding tension was set at 0.050 cN/dtex. Except for the only difference in the knitting structures, the yarns type, linear density, length, width, style and elongation of the under-band were kept the same, and other parts of the sports bras (such as straps, cups, back panels, etc.) were identical to each other, with the same size of 75 B according to the participants' anthropometric measurements (as shown in table 1).

4 points on the under-band were selected as the basis for elastic distribution: the centre front point, the point directly below the nipple, the intersection point of the under-band and side seam, the intersection point of the under-bust line and scapular line (points 1, 2, 3, and 4 in figure 1). These 4 points were selected based on the pressure measuring points proposed by Rong Zheng and the differences in the radius of body curvature which may affect the pressure distribution [2].

The under-band of these 5 sports bras were the same in length (60 cm) and width (2.5 cm).

2 popular knitting structures for under-band (Rib stitch 1×1 for structure I, and Rib stitch 2×2 for structure II) with different Young's modulus was used for elasticity distribution. The under-band of Bra A was knitted with structure I, the under-band of the other 4 sports bras was knitted with structure II 5 cm long in the area centred on these 4 points respectively, and structure I in the other areas (figure 2). Since the friction coefficients of these two structures were different (table 2), which might affect the mechanical properties of the under-band, a layer of fabric with the same width and length and low Young' modulus was sewed to the inner surface of the under-band to minimize the difference in friction coefficients for experiment purpose. And a strap with the inner fabric sewed to structure I and structure II were used for the tensile test, respectively. As the under-band mainly stretched in the course direction, and the radius of the curvature of the body in the wale direction is large, only Young's modulus in the course direction was measured.

The tensile test was carried out with a tensile tester (Instron, USA), the density was tested with an electronic balance (XingYun, China), and the thickness was tested with a fabric thickness tester (FangYuan, China). The friction coefficient of the fabric was measured on a device modified after the tensile tester, based on the research of Lo et al. [14], the results were shown in table 2.

Experiment protocol

A parallel, randomized blinded design wear trial was carried out in a room with a temperature of 20±3°C and a relative humidity of 65±5%. The experiment protocols comprised 3 parts:

Part 1: *Objective pressure test*

The objective pressure test (both in static and dynamic conditions) method developed by Coltman et al. [15] was adopted and modified. A 5-minute duration was chosen to minimize participants' burden, although women usually exercise in sports bras for a much longer time. The pressure was measured by a custom-designed calibrated pressure sensor

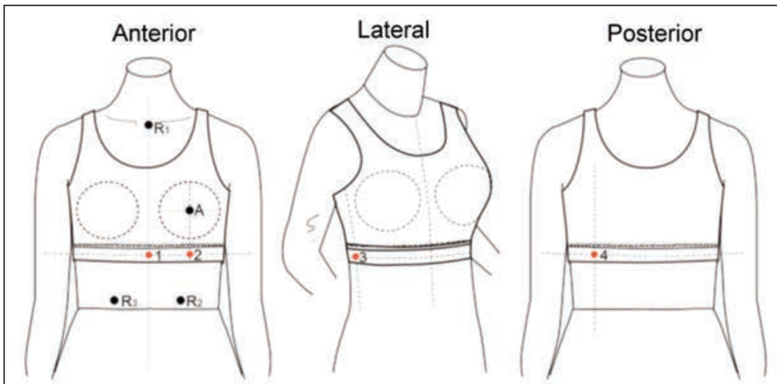

Measuring point		Location
Pressure	1	The center front point
	2	The point directly below the nipple
	3	Intersection point of under-band and side seam
	4	Intersection point of under-band and scapular line
Breast movement	A	The nipple point
	R_1	Suprasternal notch
	R_2	left anteroinferior aspect of the 10th ribs
	R_3	right anteroinferior aspect of the 10th ribs

Fig. 1. Position of pressure sensors and reflective markers

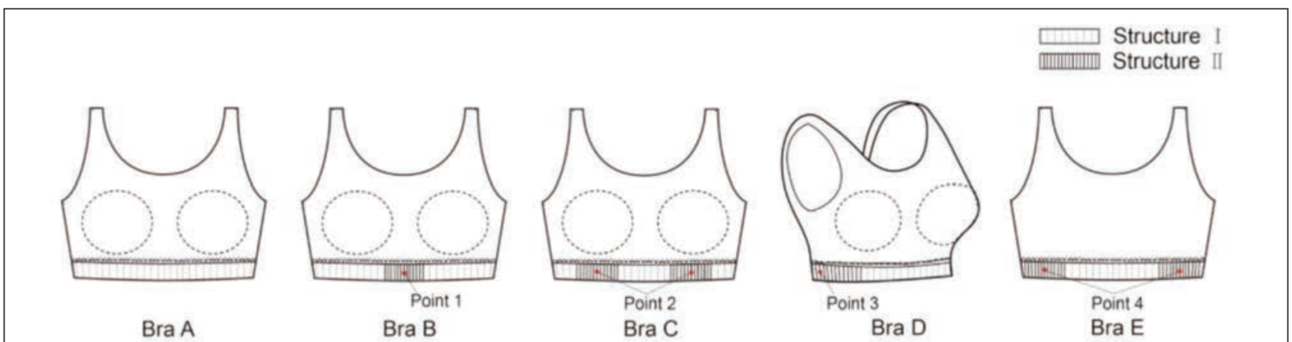

Fig. 2. Experimental samples

Table 2

DETAILS OF TWO KNITTING STRUCURES USED IN THE UNDER-BAND							
Knitting structure	**Fabric content**	**Knitting stitch**	**Thickness (mm)**	**Density (g/m^2)**	**Young's modulus (mPa)**	**Friction coefficient**	**Schematic structure**
I	53% polyester, 33% polyamide, and 14% spandex	Rib stitch 1×1	0.83	369.11	1.57	0.56	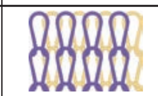
II	53% polyester, 33% polyamide, and 14% spandex	Rib stitch 2×2	1.23	429.21	2.01	0.68	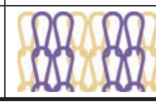

(Novel, Germany). Participants ran in each sports bra condition for 5 minutes, and the static pressure was collected when participants sat and stood motionlessly in a controlled posture before running for 10 seconds respectively in both postures. The dynamic peak pressure was measured when participants were running on the treadmill at the speed of 7.5 km/h for 6 consecutive 10 seconds (the third minute). The test was repeated 3 times, and the average static pressure was taken as the average of the two 10-second periods in standing and sitting posture three times, while the dynamic peak pressure was taken as the average of the peak pressure in six 10-second periods three times.

Part 2: *Subjective pressure comfort test*

The Under-band pressure comfort was measured by questioning the wearers about their subjective compressive feelings to these 4 measuring points and the whole under-band in static (standing and sitting) and dynamic (running) conditions, using a compressive feeling scale (rated 1 to 5), whereby 1, 2, 3, 4, 5 represented compressive feelings from extremely weak (most comfortable) to extremely strong (least comfortable) respectively. The compressive feelings in static and dynamic conditions were tested right after the pressure in two conditions has been collected, and the test was also repeated 3 times.

Part 3: *Breast movement test*

The movement of the breast when wearing 5 bras and when naked was captured by the motion capture system (Qualisys, Sweden) during running. 1 retro-reflective marker was positioned on the nipple (or on the bra cup over the nipple), another 3 were positioned on the suprasternal notch, the left and right anteroinferior aspect of the 10^{th} ribs as the trunk reference as shown in figure 1 (points A and R_1, R_2, R_3), to record the movement of breasts with or without bras in three directions (x as anterior-posterior, y as medial-lateral, and z as vertical direction) [16].

Similarly, the displacement was measured when participants were running on the treadmill for 6 consecutive 10 seconds (the third minute of running). The displacement of the breast (maximum displacement minus minimum displacement in a gait cycle) when naked and when wearing 5 sports bras and the RBD (breast displacement without bra minus breast displacement with a bra, divided by breast displacement without bra) of 5 sports bras were calculated.

Statistical analysis

The data were statistically analysed using SPSS version 25.0. The pressure of 4 points, the RBD and the subjective compressive feelings were analysed by repeated-measures analysis of variance (ANOVA). Upon detection of a significant difference in the ANOVA test, a post hoc test was performed to examine the pairwise comparison. The significance level was set at $P < 0.05$, and $P < 0.001$ (a very significant difference) was also marked. Effect sizes were calculated using partial eta squared ($\eta^2_{partial}$), and it was defined as a small effect when $\eta^2_{partial} > 0.01$, a medium effect when $\eta^2_{partial} > 0.06$, and a large effect when $\eta^2_{partial} > 0.14$, according to Cohen (1988).

RESULTS AND DISCUSSION

Pressure distribution

Repeated-measures analysis of ANOVA showed that there were significant pressure differences in sports bras ($P < 0.001$, $F = 52.875$, $\eta^2_{partial} = 0.794$ for static condition, and $P < 0.001$, $F = 69.634$, $\eta^2_{partial} = 0.835$ for dynamic condition), measuring point ($P < 0.001$, $F = 2631.069$, $\eta^2_{partial} = 0.980$ for static condition, and $P < 0.001$, $F = 2914.062$, $\eta^2_{partial} = 0.981$ for dynamic condition), and sports bras by measuring point interaction effect ($P < 0.001$, $F = 44.881$, $\eta^2_{partial} = 0.765$ for static condition, and $P < 0.001$, $F = 60.403$, $\eta^2_{partial} = 0.815$ for dynamic condition). The results revealed that the elasticity distribution significantly affected the pressure distribution of the under-bands of these 5 seamless sports bras both in static and dynamic conditions, and the effect varied with bras and measuring points. The dynamic peak pressure showed a much similar distribution to the static pressure except a little higher value at all 4 points (up to 0.20 kPa at point 3 of Bra D), as shown in figure 3. The pressure differences between these two conditions (static and dynamic) were much smaller than other parts of sports bras, such as a strap, which was reported to be 5.1 kPa [15]. This might be attributed to the lower deformation in the under-band than other parts during exercise.

When Compared to Bra A (without elasticity distribution), the pressure of the other 4 sports bras increased not only at the centre point of section II (the section knitted with structure II) but also at other

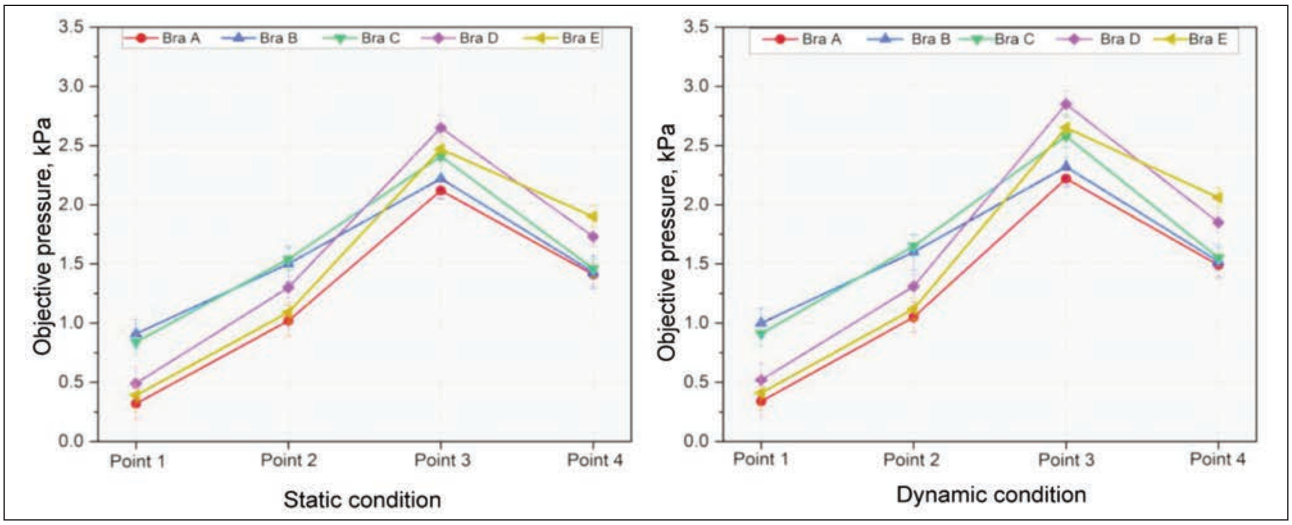

Fig. 3. The pressure distribution of 5 seamless sports bras

Table 3

THE PRESSURE INCREMENTS OF 4 SPORTS BRAS COMPARED TO BRA A									
Sports Bra		**Static pressure increments (kPa)**				**Dynamic peak pressure increments (kPa)**			
		Measuring point				**Measuring point**			
		1	**2**	**3**	**4**	**1**	**2**	**3**	**4**
B	Mean	**0.59**	0.48	0.10	0.02	**0.66**	0.55	0.10	0.03
	Std. D	0.07	0.11	0.13	0.09	0.09	0.10	0.11	0.15
C	Mean	0.52	**0.52**	0.29	0.05	0.57	**0.60**	0.36	0.06
	Std. D	0.06	0.07	0.15	0.03	0.05	0.09	0.13	0.08
D	Mean	0.17	0.28	**0.53**	0.32	0.08	0.26	**0.63**	0.36
	Std. D	0.12	0.04	0.06	0.03	0.09	0.05	0.07	0.06
E	Mean	0.07	0.07	0.35	**0.49**	0.07	0.07	0.43	**0.57**
	Std. D	0.09	0.13	0.08	0.04	0.12	0.10	0.05	0.06

Note: The data underlined: the pressure increments of the centre point of section II (the section knitted with structure II) on the under-band for 4 seamless sports bras with elasticity distribution, compared to Bra A (without elasticity distribution).

measuring points in both conditions. And the pressure increment seemed to be related to the distance from the measuring point to the centre point of section II. The centre point often showed a larger pressure increment, while the point far away from it showed a smaller pressure increment, as shown in table 3. For example, the largest pressure increments of Bra B occurred at point 1, followed by points 2, 3 and 4, in both conditions. This might have been because a high-modulus section would make the section nearby stretch more, resulting in larger elongation and thus higher pressure, which was also observed in previous studies [12].

Pressure comfort

The elasticity distribution also significantly affected the compressive feelings of the under-band both in static and dynamic conditions. The result of repeated-measures analysis of ANOVA showed significant differences in sports bra ($P < 0.001$, $F = 51.650$, $\eta^2_{partial} = 0.790$ for static condition, and $P < 0.001$, $F = 72.877$, $\eta^2_{partial} = 0.841$ for dynamic condition), measuring point ($P < 0.001$, $F = 2307.771$, $\eta^2_{partial} = 0.977$ for static condition, and $P < 0.001$, $F = 2768.904$, $\eta^2_{partial} = 0.982$ for dynamic condition), and sports bra by measuring point interaction effect ($P < 0.001$, $F = 38.484$, $\eta^2_{partial} = 0.737$ for static condition, and $P < 0.001$, $F = 58.350$, $\eta^2_{partial} = 0.809$ for dynamic condition). The dynamic compressive feelings showed a little higher score than static compressive feelings at all 4 points, however, the differences between these 5 sports bras were similar to the static condition, as shown in figure 4.

Bra A, D, and E performed satisfactorily in comfort performance, which showed low compressive feelings at all 4 points (ranging from 1.65~2.23 for static condition, and 1.85~2.43 for dynamic condition). Bra B and C exhibited low compressive feelings at points 3 and 4 (ranging from 1.87~1.98 for static condition, and 2.07~2.25 for dynamic condition), but high compressive feelings at points 1 and 2 (up to 4.01 for static condition and 4.21 for dynamic condition at point 2

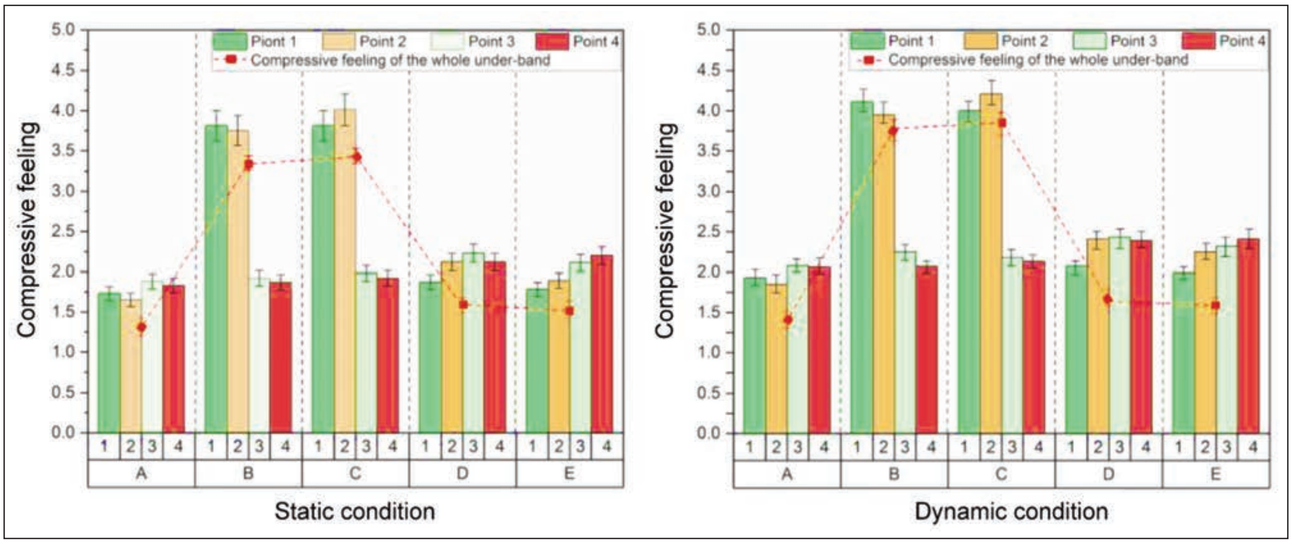

Fig. 4. The compressive feelings of 5 seamless sports bras

of Bra C), significantly higher than that of Bra A, D, and E (P<0.001).

Compared with the pressure distribution, although Bra B and C showed much lower pressure at points 1 and 2 than at point 3 (figure 3), the compressive feelings of points 1 and 2 were much higher than at point 3. The results indicated a much lower PCT at points 1 and 2 which was also observed in previous research [17]. Therefore, Bra B and C which mainly increased pressure at points 1 and 2, tended to make the pressure of these two points higher than PCT, resulting in pressure discomfort.

The compressive feelings of the whole under-band of these 5 sports bras showed consistent results, and there was also a significant difference between sports bras ($F = 42.167$, $P < 0.001$, $\eta^2_{partial} = 0.754$ for static condition, and $F = 38.218$, $P < 0.001$, $\eta^2_{partial} = 0.735$ for dynamic condition). Bra B and C which exerted significantly higher compressive feelings at points 1 and 2, also showed significantly higher compressive feelings of the whole under-band, than Bra A, D, and E ($P < 0.001$).

Reduction of breast displacement (RBD)

Significant differences in bra ($F = 268.924$, $P < 0.001$, $\eta^2_{partial} = 0.951$), direction ($F = 2516.400$, $P < 0.001$, $\eta^2_{partial} = 0.979$), and bra by direction interaction effect ($F = 10.287$, $P < 0.001$, $\eta^2_{partial} = 0.428$) in RBD was detected. It indicated that there were significant differences in RBD between these 5 sports bras and the differences varied with directions. Bra B, C and D performed significantly better than Bra A and E in all three directions ($P < 0.001$) while there was no significant difference between Bra A and E.

Moreover, Bra B, C and D showed different RBD performances in different directions, of which Bra C performed best in all three directions. Bra C showed a significantly higher RBD than Bra D in direction X ($P < 0.05$) and Y ($P < 0.001$), and a significantly higher RBD than Bra B in direction Z ($P < 0.05$). Bra B performed significantly better than Bra D in the direction Y ($P < 0.001$).

The results indicated that the elasticity distribution of Bra B, C and D could significantly improve RBD in all 3 directions. During running, breast displacement mainly occurs in the vertical direction. In the process of the breast's upward (or downward) movement, the points surrounding the breast (such as points 1, 2 and 3) may receive a large pulling force (or impact), making it no longer in firm contact with the sternum, or result in the sliding of under-bands which were often reported in previous researches [4, 7, 18]. The pressure increments in these 3 points increased the friction between the under-band and the skin, attached the bra firmly to the trunk and reduced the occurrence of sliding, which subsequently led to a better performance in RBD.

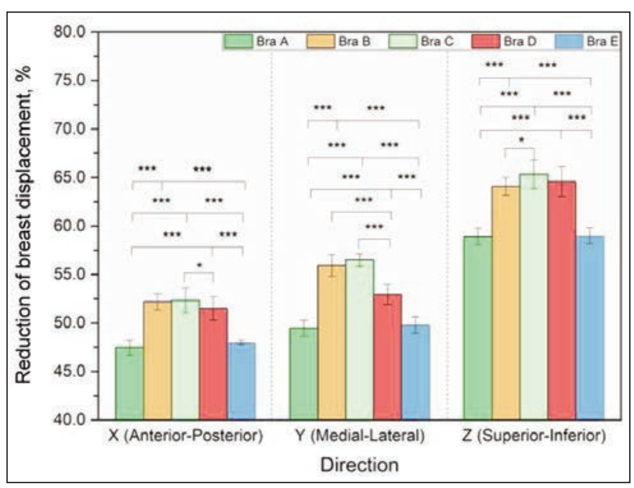

Fig. 5. RBD of 5 seamless sports bras in 3 directions

CONCLUSION

This study provided novel information in optimizing the pressure comfort and support performance for seamless knitted sports bras, by applying elasticity distribution in the under-band. The results showed that elasticity distribution significantly affected the pressure distribution, compressive feelings and RBD of the seamless sports bras, in both static and dynamic conditions ($P < 0.001$).

No matter where the fabric structure with high Young's modulus was used in the under-band, the pressure increased at each point. And the pressure increment appeared to be related to the distance from the high-modulus section to the measuring point, for both conditions. Compared to Bra A, the elasticity distribution of Bra B, C and D mainly increased the pressure at points around the breasts (points 1, 2 and 3), significantly improving the support performance ($P < 0.001$). However, Bra B and C also showed significantly higher compressive feelings for points 1 and 2, and the whole under-band ($P < 0.001$). Bra E mainly increased the pressure at points 4 and 3 and showed no significant difference in compressive feelings or support performance with Bra A. Comprehensively, Bra D was ideal and typical, which significantly improved the support performance ($P < 0.001$) without increasing compressive feelings. Therefore, it is suggested that applying a high-modulus structure (e.g., Rib stitch 2×2) around the intersection point of the under-band and side seam (Point 3), and a low-modulus structure (e.g., Rib stitch 1×1) in another area, to improve the breast support performance without decreasing pressure comfort. Moreover, the friction coefficient should also be taken into consideration, as the decrease of friction coefficient may lead to lower friction of the points around the breasts, resulting in the decrease of RBD. To minimize the influence of friction coefficient ($\mu_{II} > \mu_{I}$), we sewed a layer of the same fabric to the inner surface of the under-band for experiment purposes only. Without this layer, the friction of Bra B, C and D at the points around the breast would be even higher, which might result in an even better performance in RBD. However, some structures may decrease the friction coefficient, which may contribute to the decrease of RBD, future studies should also pay attention to the effect of elasticity distribution on friction.

As this study is a new attempt to optimize the pressure comfort and RBD of the seamless sports bra by applying elasticity distribution in the under-band, only 2 fabric structures and 4 measuring points were chosen. Future work may involve more different measuring points, yarn type, linear density, knitting structures, elongations, sizes and so on, as these factors may also affect the pressure comfort and breast support performance of seamless sports bras. Furthermore, a large-scale experiment with stratified depth randomization will be needed for future research to benefit more exercising women of different ages, body mass, and breast size.

REFERENCES

[1] Scurr, J.C., White, J.L., Hedger, W., *Supported and unsupported breast displacement in three dimensions across treadmill activity levels*, In: Journal of Sports Sciences, 2011, 29, 1, 55–61, http://doi:10.1080/02640414.2010.521944

[2] Zheng, R., Yu, W., Fan, J., *Pressure evaluation of 3D seamless knitted bras and conventional wired bras*, In: Fibers and Polymers, 2009, 10, 1, 124–131, http://doi:10.1007/s12221-009-0124-7

[3] Maleki, M.S., Mahmoudnia, S., Mousazadegan, F., *Influence of weft knitted fabrics tensile characteristics and garment size on the body movement comfort*, In: Indian Journal of Fibre & Textile Research, 2020, 45, 3, 352–358

[4] McGhee, D.E., Steele, J.R., *Biomechanics of Breast Support for Active Women*, In: Exercise and Sport Sciences Reviews, 2020, 48, 3, 99–109, http://doi:10.1249/JES.0000000000000221

[5] Macintyre, L., Baird, M., *Pressure garments for use in the treatment of hypertrophic scars – an evaluation of current construction techniques in NHS hospitals*, In: Burns, 2005, 31, 1, 11–14, http://doi:10.1016/j.burns.2004.08.007

[6] Liu, C., Miao, F.-X., Dong, X.-Y., Xu, B., *Enhancing pressure comfort of a bra's under-band*, In: Textile Research Journal, 2017, 88, 19, 2250–2257, http://doi:10.1177/0040517517720496

[7] Zhou, J., Yu, W., Ng, S.-p., *Identifying effective design features of commercial sports bras*, In: Textile Research Journal, 2012, 83, 14, 1500–1513, http://doi:10.1177/0040517512464289

[8] Wang, Y., Liu, Y., Luo, S., Chen, C., Jin, L. *The Pressure Comfort Sensation of Female's Body Parts Caused by Compression Garment*, In: Advances in Human Factors in Wearable Technologies and Game Design, Advances in Intelligent Systems and Computing, 2018, 94–104

[9] Li, H., Wang, Y., Chen, Z., *Evaluation on the pressure distribution and body-shaping effectivity of graduated compression shaping pants*, In: International Journal of Clothing Science and Technology, 2020, 33, 2, 153–162, http://doi:10.1108/ijcst-02-2020-0018

[10] Lu, M., Qiu, J., Wang, G., Dai, X., *Mechanical analysis of breast–bra interaction for sports bra design*, In: Materials Today Communications, 2016, 6, 28–36, http://doi:10.1016/j.mtcomm.2015.11.005

[11] Sun, Y., Yick, K.-l., Cai, Y., Yu, W., Chen, L., Lau, N., Zhang, S., *Finite Element Analysis on Contact Pressure and 3D Breast Deformation for Application in Women's Bras*, In: Fibers and Polymers, 2021, 22, 10, 2910–2921, http://doi:10.1007/s12221-021-0878-0

[12] Liu, Z., Han, X., Zhang, Y., Chen, X., Lai, Y.-K., Doubrovski, E.L., Whiting, E., Wang, C.C.L., *Knitting 4D garments with elasticity controlled for body motion*, In: ACM Transactions on Graphics, 2021, 40, 4, 1–16, http://doi:10.1145/3450626.3459868

[13] McGhee, D.E., Stetle, J.R., *How do respiratory state and measurement method affect bra size calculations?*, In: British Journal of Sports Medicine, 2006, 40, 970–974

[14] Lo, W.T., Yick, K.L., Ng, S.P., Yip, J., *New methods for evaluating physical and thermal comfort properties of orthotic materials used in insoles for patients with diabetes*, In: Journal of Rehabilitation Research and Development, 2014, 51, 2, 311–324, http://doi:10.1682/JRRD.2013.01.0012

[15] Coltman, C.E., McGhee, D.E., Steele, J.R., *Bra strap orientations and designs to minimise bra strap discomfort and pressure during sport and exercise in women with large breasts*, In: Sports Medicine-Open, 2015, 1, 1, 21, http://doi:10.1186/s40798-015-0014-z

[16] Scurr, J.C., White, J.L., Hedger, W., *The effect of breast support on the kinematics of the breast during the running gait cycle*, In: Journal of Sports Sciences, 2010, 28, 10, 1103–1109, http://doi:10.1080/02640414.2010.497542

[17] Park, S., Kim, N., Hong, K., Lee, Y., *Clothing Pressure, Blood Flow, and Subjective Sensations of Women in Their 50s and 60s When Wearing a Commercial Yoga Bra Top*, In: Journal of the Korean Society of Clothing and Textiles, 2021, 45, 4, 586–597, http://doi:10.5850/jksct.2021.45.4.586

[18] McGhee, D.E., Steele, J.R., *Breast elevation and compression decrease exercise-induced breast discomfort*, In: Medicine and Science in Sports and Exercise, 2010, 42, 7, 1333–1338, http://doi:10.1249/MSS.0b013e3181ca7fd8

Authors:

XIAOFANG LIU[1], XIAOFEN JI[1], YUXIU YAN[1], QI ZHOU[2]

[1]Zhejiang Sci-Tech University, College of Textile Science and Engineering (International Institute of Silk),
No. 928, 2nd Street, Hangzhou 310018, Zhejiang Province, China
e-mail: fongfonghz@163.com

[2]Jiujiang University, College of Art, No.551, Qianjin East Road,
2nd Street, Jiujiang 332005, Jiangxi Province, China

Corresponding author:

XIAOFEN JI
e-mail: xiaofenji@zstu.edu.cn

Consuming perception analysis of the yoga wear using fuzzy AHP model

DOI: 10.35530/IT.074.03.202285

HAO TANG
WENJUAN LI
SHUANG LIU
YAN HONG
CHUAN JIANG

ABSTRACT – REZUMAT

Consuming perception analysis of the yoga wear using fuzzy AHP model

In this paper, we propose to analyse the consumer perception of yoga wear and then improve its design based on the demand-driven design principle. For this purpose, we break down the problem into three levels: Goal Level (development of the new yoga wear), Requirement Level, and Design Solution Level (garment design solutions corresponding to the requirements of the Requirement Level). For the requirement level, we take into account the FEA (functional, expressive and aesthetic) factors for the consumer perception analysis. Due to the hierarchical characteristics of the analysis, we propose a fuzzy AHP (analytic hierarchy process) approach for the related data analysis. By using the AHP model, we can analyse requirements alongside their solutions in design alongside their respective weights. 50 evaluators (yogis) and 20 designers took part in the experiments. Similar design solutions and performance evaluation of the solutions were defined through consumer research and subjective evaluation experiments with standard procedures. We hope that this paper will guide the analysis and development of yoga wear design.

Keywords: *FEA considerations, yoga wear design, fuzzy AHP, perception analysis, conceptual model*

Analiza percepției consumatorilor asupra echipamentului pentru yoga folosind modelul fuzzy AHP

În această lucrare, ne propunem să analizăm percepția consumatorului asupra echipamentului pentru yoga și apoi să îmbunătățim designul acestuia pe baza principiului de design bazat pe cerere. În acest scop, împărțim problema în trei niveluri: Nivelul obiectivului (dezvoltarea noului echipament de yoga), Nivelul cerințelor și Nivelul soluției de proiectare (soluții de proiectare a articolelor de îmbrăcăminte corespunzătoare cerințelor Nivelului cerințelor). Pentru nivelul cerințelor, luăm în considerare factorii FEA (funcționali, expresivi și estetici) pentru analiza percepției consumatorului. Datorită caracteristicilor ierarhice ale analizei, propunem o abordare fuzzy AHP (proces de ierarhie analitică) pentru analiza datelor aferente. Utilizând modelul AHP, suntem capabili să analizăm cerințele împreună cu soluțiile lor în proiectare, alături de problemele respective. La experimente au participat 50 de evaluatori (yoghini) și 20 de designeri. Soluții similare de proiectare și evaluarea performanței soluțiilor au fost definite prin cercetarea consumatorilor și experimente de evaluare subiectivă cu proceduri standard. Speranța noastră este că această lucrare va ghida analiza și dezvoltarea designului de echipament pentru yoga.

Cuvinte-cheie*: considerații FEA, designul echipamentului pentru yoga, fuzzy AHP, analiza percepției, model conceptual*

INTRODUCTION

With the increasing working pressure, people are increasingly suffering from sub-health problems. The popularity of Yoga has greatly increased, making it one of the world's most popular exercises. As a healthy and harmonious exercise [1], it meets the needs of people in the pursuit of a healthy and active lifestyle. With the emerging popularity of yoga excise, the demands for yoga-related products such as yoga wear have increased [2]. Yoga leads to the excise of physical stability and balance, mental calmness and concentration. The postures involved in the Yoga excise are various and most of them involve the stretching of muscles and the movement of joints in different parts of the body [3–5]. Therefore, Yoga wear is normally designed to be extremely fitting to avoid extra fabrics that will affect the human body movement during the excise. Except for the considerations of the human body movement, as Yoga belongs to the fitness exercise, the comfort, flexibility, moisture absorption and breathability of Yoga wear are particularly important in the development of yoga wear [6]. However, according to previous fashion market scanning, the existing yoga wear that is supplied in the market is not widely accepted. The main problems are that the fabric of these products is with poor moisture absorption and breathability, and poor flexibility and ease of shifting during yoga practice.

This study focuses on the improvement of the design of yoga wear, solving the problems that exist in it and investigating the consuming perception analysis of yoga wear. For this purpose, we use the demand-driven design principle to break down the problem into three levels: Goal Level (development of the new yoga wear), Requirement Level, and Design Solution Level (solutions on this level will correspond to the requirements ascertained in the previous level). Firstly, a questionnaire was used to investigate the basic information and consumer behaviour of the Yoga wear user. Then, consumer requirements for yoga wear are analysed. The FEA (functional, expressive, and aesthetic) model by Lamb and Kallal is applied as a conceptual framework for designing garments with specific needs [7]. This gives an approach to solving problems to distinguish functional and fashionable design processes for a given garment. This is an efficient way to assess the needs of the wearer while still incorporating FEA factors [8]. As the proposed analysis process is in a hierarchical structure. Therefore, the AHP model is used for the data analysis. The AHP (analytic hierarchy process) model is a classic model with a hierarchical structure [9]. However, the AHP model relies too much on expert subjective judgments in data analysis, and the data is too subjective. Therefore, fuzzy logic is used for the quantification of the related data. Using fuzzy logic, the subjectivity of the data is overcome so that all data can be quantified by the AHP model [10].

In this study, consumer perception analysis of yoga wear and user needs for the yoga wear design are studied. Using AHP as a model, we propose a conceptual model to break down into different levels the problem of design purpose. To analyse consumer needs, we take FEA principles into account. Thus, the method proposed provides a quantitative approach to the problem of fashion design with special needs. Then, we can apply the result of this research model to heighten the efficacy of the collaborative design process involving both designers and consumers [11].

The remainder of the paper is organized as follows: 2nd section is a literature review of concepts which are closely related to the subject of this article, i.e., the FEA and fuzzy AHP models. 3rd section presents the proposed model. 4th section shows an experiment to obtain the concept for the design of yoga wear. 5th section is a discussion of the research results, and 6th section is the conclusion.

LITERATURE REVIEW FOR RELATED CONCEPTS

There are two models used in this paper: The AHP model and the FEA model.

FEA model

The FEA model is a conceptual framework for designing need-specific garments that combines functional, expressive and aesthetic factors to effectively assess user needs. One key problem in the process of garment design is the analysis of user needs [12]. As explained in the Introduction, the FEA model created by Lamb and Kallal [13] was made to determine the requirements and desires of the user [13]. The FEA framework is seen to have certain usefulness for various projects. For example, Watkins came up with a design process which can give greater weight to user needs by using their model [14]. Bye and Hakala developed ankle braces designed and sized especially for women which showed how important it is to know the needs of the wearer [15]. Cristiano Ciappei and Christian Simoni used the FEA model to better shoe production by identifying key success factors ingrained in the process of developing new products [16].

The current theory of the application of the FEA model says that despite the problem having been defined by the client at the inception of the process, the design step of the analysis should still be followed by the designers to determine the problem from the client's perspective. In this process, we can focus on product factors about the requirements of the consumer.

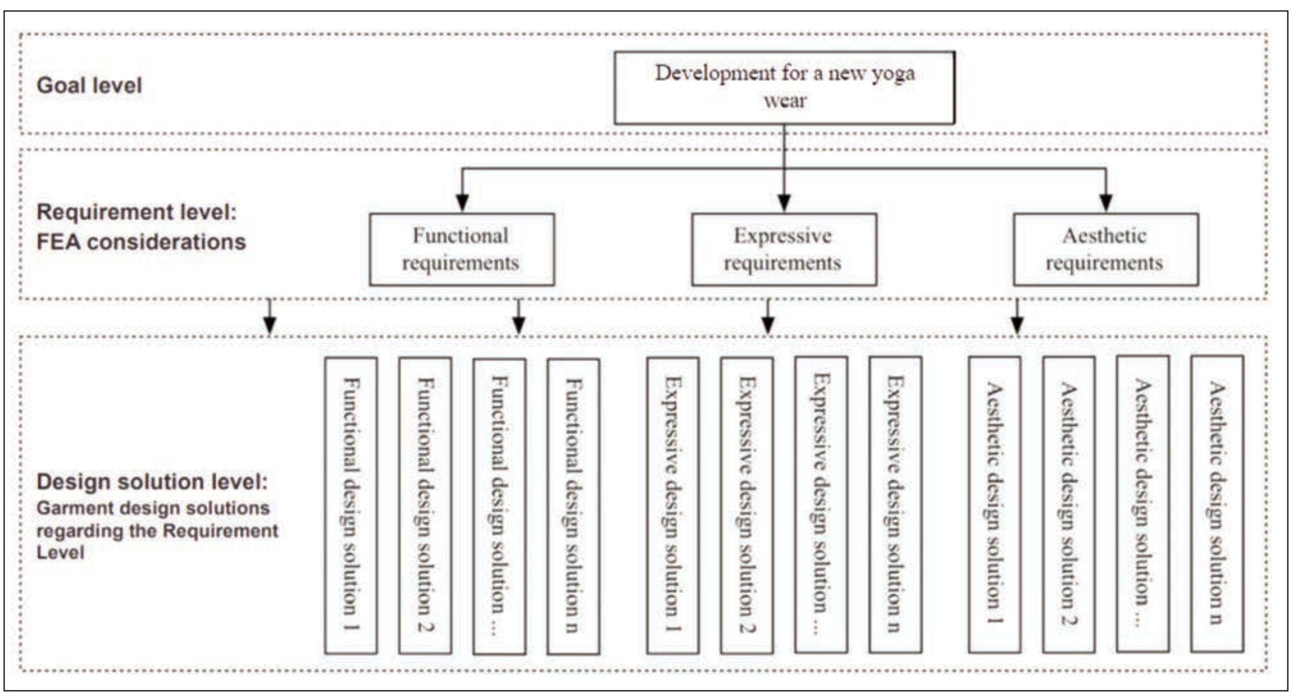

Fig. 1. Proposal of the conceptual model, combining FEA and Fuzzy AHP models

Fuzzy AHP model

AHP (analytic hierarchy process), developed by Saaty, is a structured technique for organizing and analysing complex decisions, which has particular applications in group decision-making [17]. It deals with the determination of the relative importance of a set of activities in a multi-criteria decision problem. Rather than attempting to give one precise answer, AHP aids developers in reaching one which suits their goal based on their view of the problem. It gives a comprehensive and easy-to-understand framework for making choices to solve problems, representing and quantifying its elements, as they relate to the project objectives, and evaluating alternative solutions [18]. AHP users divide the problem at hand into a set of simpler sub-problems, which can be dealt with independently.

AHP renders the possibility of incorporating choices based on abstract qualitative criteria as well as tangible quantitative criteria. The AHP follows three principles: first, the structure of the model, second, the comparison of alternative solutions (elements of the lower level) and criteria (elements of the upper level), and third, the synthesis of the priorities. AHP is commonly used in literature to solve various decision-making problems of a complex nature [2, 19].

In this research, we rely solely upon data derived from the subjective evaluation of experts and are therefore riddled with uncertainty. Fuzzy logic is an approach that deals with uncertain data and imprecise knowledge [20]. A fuzzy set is introduced to AHP to process the uncertainty in the decision-making process [21]. Fuzzy AHP has proven to be a very useful methodology for multiple-criteria decision-making in fuzzy environments and has found substantial applications in recent years [22].

The proposed conceptual model

The conceptual model for consuming perception analysis proposed combines the FEA model and the Fuzzy AHP model. Figure 1 presents the framework of the proposed model. There are three steps to using the model proposed:

(1) Fifty yogis will be invited to participate in the study's target consumer research. The study will investigate their basic information as well as their consumption habits and the discomfort of yoga wear during practice.

(2) A group of designers will be invited to generate a set of garment design solutions regarding the FEA considerations. Taking each part of FEA individually, some design ideas will be created. For example, regarding the "functional requirements", we can have a solution related to this idea such as "Selection of fabric with breathable properties".

(3) Identify the relative weight of the components of the requirement level. The yogis who are taking part in this research will act as evaluators to perform this step. Each yogi will use a linguistic rating scale to compare the relative importance of each set of two components in the requirement phase. For example, the evaluator could compare the importance of "Functional requirements" with "Expressive requirements" saying that one is "more important" than the other.

(4) Identify the relative weight of the design solutions of each component of the design solution level. The same designers taking part in step 2 will use the same method to complete this step. Thus, after all the steps are finished, we can identify the structure and components of the proposed model and the relative weights of each level's components can be examined. Since the data derived from these evaluation steps are subjective, we are dealing with uncertainty; therefore, fuzzy set theory is applied to the evaluation data. Among the most commonly used fuzzy numbers are the Triangular Fuzzy Numbers (TFNs) which are utilized in this article. After quantifying the precise terms of the linguistic rating scale proposed (figure 2) into TFNs, the data from the evaluation step is likewise collected and quantified into TFNs, and an aggregation procedure is performed in a comparison matrix. Then, fuzzy operations are used to process this comparison matrix. Relative weight values of the components of the AHP model can be obtained. After

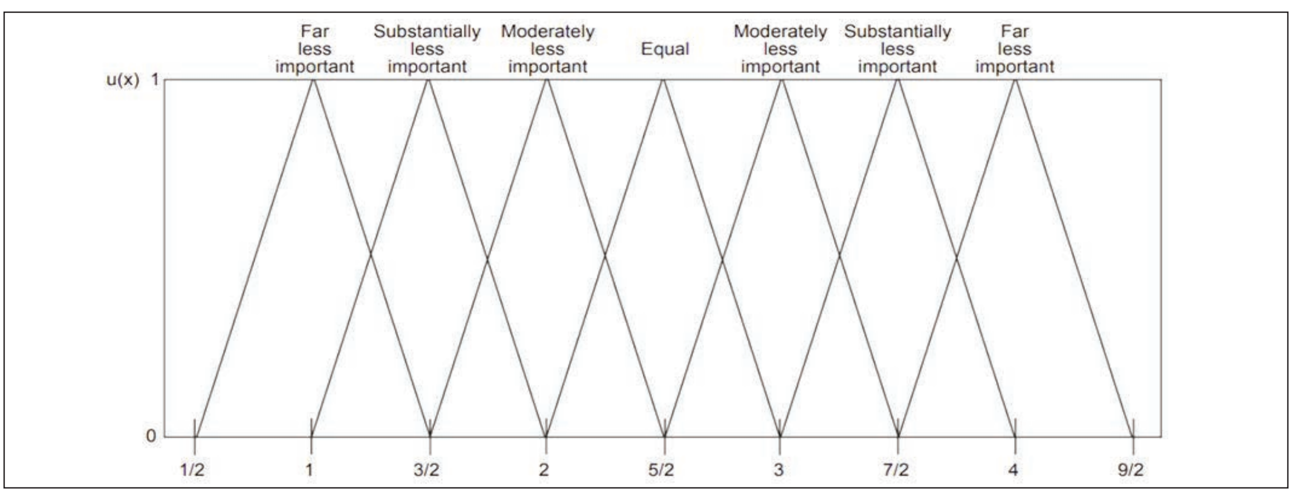

Fig. 2. Linguistic rating scale used in this study

performing this procedure, we can say that the higher the value for relative weight, the better the design solution.

EXPERIMENT AND RESULT

Subjects

To perform the procedure, we select 20 designers and 50 evaluators. We will regard these two groups of people as the subjects of our study. Designers will identify the design solutions for the model proposed by reading FEA considerations, while evaluators will cooperate with the investigation on target consumers and be responsible for the access of the components of the AHP model. For this article, the designers are chosen from yoga wear fashion brands. They should meet the following three requirements:
(1) he/she has at least 5 years of experience working in yoga wear;
(2) he/she is aware of the physical, mental, emotional, and social characteristics of yoga wear consumers;
(3) he/she has a lot of experience in garment design solutions for yoga wear.
50 members are working as evaluators in this study. They have experienced yogis. On average, they buy at least three pieces of yoga wear per year. Before the start of the study, they are made aware of the research purpose of this study, and they willingly decide to take part.

Experiment I: Yoga wear consumer insight

Experiment I is divided into three main parts. The first part investigated the basic information of the target consumers such as gender, age and education. The second part investigated the consumer's habits and the third part investigated their preferences for yoga wear, the discomfort of yoga wear during practice and their expectations for yoga wear.
(1) The results show that 72% of yogis are women; Over 43% of yogis are between 30 and 49 years old; 38% are above 50 years of age; 19% are aged 18–29. Overall, the popularity of yoga is high, with a larger proportion of people aged 30 to 49 and above 50. Consumers of yoga wear over 50 years old said they do not like yoga wear with too bright colours and high skin exposure. At the same time, the problem of fat accumulation caused by older age makes those over the 50s prefer yoga wear that is loose and has a body-modifying function. Most yogis have higher education, 93% of them have a bachelor's degree or above.
(2) On average, 50% of yogis buy 3–5 pieces of yoga wear per year, and 26% buy 6–10 pieces of yoga wear per year. 53% spend an average of RMB 500–1000 per year on yoga wear, and 21% spend RMB 1000–2000.
(3) As yoga grows in popularity, people are moving away from the traditional grey yoga wear, softer colours such as pale pink, light blue and beige are gaining popularity [23]. The result shows that 60% of consumers prefer to buy yoga wear in Morandi colours, 47% prefer black and white yoga wear and 38% prefer brightly coloured yoga wear, while yoga wear with line designs or prints is less popular than plain yoga wear. Simple designs, soft colours and yoga wear suitable for all ages are more in line with market demand, considering the high popularity of yoga and the wide age coverage of yogis.
(4) The results show that there are four main problems with yoga wear. 64% of participants said that yoga wear is not breathable and the fabric sticks to the skin after sweating; 62% said that yoga wear is easy to shift and slip off; 43% felt uncomfortable due to the excessive pressure of yoga wear; and 45% said that yoga wear is easily deformed after washing.

Experiment II: Identification of design solutions based on FEA considerations

Experiment II comprises the 20 designers acting as an evaluation panel. They use the considerations in the FEA framework to identify design solutions. The experiment is comprised of two parts: (1) the creation of design solutions and their definitions, and (2) the selection and evaluation of these design solutions.
Experiment II began with a training session, where the designers were informed that searching for appropriate design solutions is the purpose of the experiment. This was followed by a time of brainstorming. Each of the panellists was able to use open sources (books, the internet, literature etc.) throughout this process to gather ideas about design solutions for yoga wear. After the brainstorming process, each trained member of the evaluation panel came up with a plethora of design solution ideas taking the form of words/short sentences. Then these ideas were combined and regarded by each person taking part in the panel. A "round table" discussion among all the participants was carried out to vote on all the words/short sentences. The panellists followed two key principles to guide the selection: (1) Redundant words/sentences were to be avoided, and (2) all of the solutions should be represented among the chosen words. Between each step, the results were announced to everyone on the panel, and could only be used if they were unanimously approved. Finally, the completed list of ideas for design solutions was created, as given in table 1.

Experiment III: Identification of relationships between FEA considerations

Experiment III is performed by the 50 yogis invited to identify the relationship between FEA considerations. Every one of the yogis is asked to compare two FEA principles about their relevance. During this phase of fuzzy processing, the evaluator's e_l (l = 1, 2, …, m, m = 20) use the linguistic weight set L_k, L_k = {Far more important, more important, a little more important, moderate, a little less important, less important, far less important} (k = 1, 2, 3, …, 6, 7), to evaluate the relative importance of the FEA considerations.
For example, the evaluator e_l is given this prompt: "Compared with C1 (Functional requirements), what is the importance level of C2 (Expressive requirements)?"

Table 1

DESIGN SOLUTIONS BASED ON FEA CONSIDERATIONS FOR YOGA WEAR	
Design solutions	**Definition of design solutions**
S1: Good moisture absorption and breathability, lightweight and quick drying	Make sure sweat can be absorbed and evaporated quickly to avoid the discomfort caused by overweight yoga wear
S2: High resilience and flexibility	Make sure the yoga wear fits snugly and won't shift during practice
S3: Antibacterial and anti-odour	Inhibits the growth of bacteria in fabrics
S4: Soft and skin-friendly with comfortable clothing pressure	Soft yoga wear fabric for high contact comfort and pressure comfort
S5: Body sculpting function	Yoga wear can provide body-shaping effects such as hip lifting, waist tightening and leg slimming
S6: Environmental and sustainable	The fabrics and production processes are in line with the concept of sustainability
S7: Reflecting brand values	Yoga wear with a brand logo or feature that reflects the brand values
S8: Colour and pattern	The colour or print of the yoga wear makes the practitioner relaxed and in a happy mood
S9: Various neckline designs	A variety of necklines were applied such as high neck, halter, wide boat neck, etc
S10: Splitting and splicing designs	Cuts or partly see-through fabrics were used to show some part of the wearer's body
S11: Breast support with adjustable lacing	Make sure the woman's breasts are supported steadily during practice and the lacing can be adjusted as required
S12: Removable knee cushions	Protecting the knees when practising knee-straining yoga poses
S13: High-waist yoga pants	Provides more coverage and stability during some yoga poses compared to low-rise yoga pant
S14: Tight yoga wear	Make sure the yoga wear won't hinder movement and block the view
S15: Proper body coverage	Make sure the yoga wear is not so revealing as to cause psychological discomfort to the wearer

To answer this question, the evaluator e_l may choose a linguistic term from L_k.

The outcomes of this part of the experiment will be recorded as linguistic evaluation results, being uncertain and not concrete; therefore, fuzzy set theory is used to quantify the data and continue further processing.

Fuzzy set tools were developed by Lotfi A. Zadeh and Dieter Klaua [24]. Classically, according to set theory, a given element has a binary relationship to being included as a set member; that is, the element is either in the set, or it is not in the set. However, the fuzzy set theory allows for a gradient of set inclusion in which membership is described as a function which is valued along the real unit interval [0, 1] [25–27]. These fuzzy sets can be seen as a generalization of classic sets because the functions indicating membership in classical sets are simply unique cases where they only take values 0 or 1. Fuzzy set theory is applicable in many situations especially regarding sensory or subjective evaluation because of the high levels of ease with which this theory can handle uncertain data, such as linguistics and clustering [14, 17, 19].

Using this theory of fuzzy sets, the verbal cues given to each evaluator can be made on a scale L_k and can thus be given concrete values and turned into Triangular Fuzzy Numbers (TFNs). A Triangular Fuzzy Number (TFN), M, is described with tuples formalism as $M = (l/m, m/u)$ or $M = (l, m, u)$. the letters l, m and u, respectively, give the smallest, most likely, and largest values that can describe a funny event. TFNs have linear representations to each side so their membership function is given by:

$$u_M(x) = \begin{cases} 0, & x \in [-\infty, l] \\ \dfrac{x-l}{m-l}, & x \in [l, m] \\ \dfrac{x-m}{m-u}, & x \in [m, u] \\ 0, & x \in [u, +\infty] \end{cases} \quad (1)$$

If $M_1 = (l_1, m_1, u_1)$ and $M_2 = (l_2, m_2, u_2)$ are two TFNs, the operation laws between them are given by:

$$M_1 + M_2 = (l_1 + l_2, m_1 + m_2, u_1 + u_2) \quad (2)$$

$$M_1 * M_2 = (l_1 * l_2, m_1 * m_2, u_1 * u_2) \quad (3)$$

$$t * M_1 = (t * l_1, t * m_1, t * u_1) \quad (4)$$

$$(l_1, m_1, u_1)^{-1} = (1/u_1, 1/m_1, 1/l_1) \quad (5)$$

Using TFNs, we can give concrete values to the linguistic scores which we receive from evaluators. Table 2 shows the proposed quantified TFNs.

Based on the operation rules given by equations 3, 4 and 5, the evaluation scores given by each evaluator e_l can be aggregated as $\{a_{ijh} \mid i = 1,\ldots,7, j = 1,\ldots,7, h = 1,\ldots,m\}$, where a_{ijh} represents the number of evaluators who chooses one certain degree. Therefore,

Table 2

LINGUISTIC TERMS OF THE LINGUISTIC RATING SCALE PROPOSED AND THEIR RELATED TFN	
Linguistic term	**Related TFN**
Far more important	(0.84,1,1)
More important	(0.67,0.84,1)
A little more important	(0.5,0.67,0.84)
Moderate	(0.34,0.5,0.67)
A little less important	(0.17,0.34,0.5)
Less important	(0,0.17,0.34)
Far less important	(0,0,0.17)

$$a_{ij} = (\frac{1}{m} \sum_j^1 a_{ijh}\, t_1, \frac{1}{m} \sum_j^1 a_{ijh}\, t_2, \frac{1}{m} \sum_j^1 a_{ijh}\, t_3) \quad (6)$$

where, t_1, t_2 and t_3 correspond to the value of the triangular fuzzy numbers, and take their values from table 2. Table 3 presents the aggregated evaluation matrix of the relations between different FEA considerations.

The evaluation matrix is processed using extent analysis. It is assumed that the evaluators' values processed by the extent analysis are:

$$M_{E_i}^1, M_{E_i}^2, M_{E_i}^3, ..., M_{E_i}^m, \quad i = 1, 2,..., n$$

where, (i = 1, 2,…, n) are all TFNs. The value of fuzzy synthetic extent concerning the *i-th* object is defined as:

$$S_i = \sum_{j=1}^m M_{E_i}^j \odot \left[\sum_{i=1}^n \sum_{j=1}^m M_{E_i}^j\right]^{-1} \quad (7)$$

Let $A = (a_{ij})_{n\times m}$ be a fuzzy analytical matrix, where $(a_{ij}) = (l_{ij}, m_{ij}, u_{ij})$ are defined by the calculated values:

$$l_{ij} = \frac{1}{u_{ij}};\ m_{ij} = \frac{1}{m_{ij}};\ u_{ij} = \frac{1}{l_{ij}}.$$

If $M_1 = (l_1, m_1, u_1)$ and $M_2 = (l_2, m_2, u_2)$ are two triangular fuzzy numbers, the degree of possibility of $M_2 = (l_2, m_2, u_2)$ $M_1 = (l_1, m_1, u_1)$ is defined-by:

$$V(M_2 \geq M_1) = SUP_{y\geq x}\,[min\ \mu_{M_1}(x), \mu_{M_2}(y)] \quad (8)$$

and can be expressed as follows:

$$V(M_2 \geq M_1) = hgt(M_1 \cap M_2)$$

$$\mu_{M_1}(d) = \begin{cases} 1 & \text{if } m_2 \geq m_1 \\ 0 & \text{if } l_1 \geq u_2 \\ \dfrac{l_2 - u_1}{(m_2 - u_2) - (m_1 - l_1)} & \text{otherwise} \end{cases} \quad (9)$$

Figure 3 illustrates equation 9, where 'd' is the ordinate of the highest intersection point between μ_{M_1} and μ_{M_2}. To compare M_1 and M_2, we need both the values of $V(M_2 \geq M_1)$ and $V(M_1 \geq M_2)$. The degree possibility for a convex fuzzy number to be greater than the k convex fuzzy M_i (i = 1, 2, …, k) numbers can be defined as:

$$V(M \geq M_1, M_2,..., M_k) =$$
$$= V[(M \geq M_1 \text{ and } M \geq M_2 \text{ and ... } M \geq M_k) =$$
$$= min\ V(M \geq M_i)], \quad i = 1,2,3,..., k \quad (10)$$

Assuming that $d(A_i) = min\ V(S_i \geq S_k)$ *for* k = 1, 2,…, n; $k \neq i$, then the weight vector will be given by

$$W' = [d'(A_1), d'(A_2),..., d'(A_n)]^T \quad (11)$$

where, A_i and i = 1, 2,…, and n denotes the i-th element and n the number of elements, respectively.

A fuzzy number is a convex, normalized fuzzy set $\widetilde{A \subseteq R}$ whose membership function is at least segmentally continuous and has the functional value $\mu_{\tilde{A}}(x) = 1$ precisely on the element. Using the classical normalization operation, the normalised weight vectors are obtained as follows:

$$W = [d(A_1), d(A_2),..., d(A_n)]^T \quad (12)$$

where W is a non-fuzzy number.

The Euclidean distance for two TFNs $M_1 = (l_1, m_1, u_1)$ and $M_2 = (l_2, m_2, u_2)$ can be calculated as Equation 13 and the importance of S_1 can be calculated as equation 14.

$$d = \sqrt{(l_1 - l_2)^2 + (m_1 - m_2)^2 + (u_1 - u_2)^2} \quad (13)$$

$$s = \frac{1}{1+d} \quad (14)$$

The aggregated evaluation data in table 3 can be processed using equations 7–12. First, by applying equation 2, we can calculate the fuzzy number as shown below

$$R_{R_1} = \sum_{j=1}^3 a_{1j} =$$
$$= (0.340, 0.500, 0.570) \oplus (0.532, 0.695, 0.818) \oplus$$
$$\oplus (0.514, 0.681, 0.800) = (1.386, 1.876, 2.288)$$

Similarly,

$$R_{R_2} = \sum_{j=1}^3 a_{2j} =$$
$$= (0.186, 0.311, 0.475) \oplus (0.340, 0.500, 0.670) \oplus$$
$$\oplus (0.253, 0.376, 0.542) = (0.779, 1.187, 1.687)$$

$$R_{R_3} = \sum_{j=1}^3 a_{3j} = (1.007, 1.457, 1.914)$$

Table 3

A SCALE OF JUDGMENT OF FORECAST ACCURACY			
Requirements	**C1: Functional requirements**	**C2: Expressive requirements**	**C3: Aesthetic requirements**
C_1: Functional requirements	(0.340,0.500,0.670)	(0.532,0.695,0.818)	(0.514,0.681,0.800)
C_2: Expressive requirements	(0.186,0.311,0.475)	(0.340,0.500,0.670)	(0.253,0.376,0.542)
C_3: Aesthetic requirements	(0.203,0.326,0.493)	(0.464,0.631,0.751)	(0.340,0.500,0.670)

Using equation 7:

$$\widetilde{S_1} = R_{R_1} \odot [R_{R_1} \oplus R_{R_2} \oplus R_{R_3}]^{-1} =$$
$$= (1.386, 1.876, 2.288) \odot (\frac{1}{5.889}, \frac{1}{4.52}, \frac{1}{3.172}) =$$
$$= (0.235, 0.415, 0.721)$$

Similarly,

$\widetilde{S_2} = (0.132, 0.263, 0.532)$, $\widetilde{S_3} = (0.171, 0.322, 0.603)$

Using equation 9:

$$V = (\widetilde{S_1} \geq \widetilde{S_2}) = 1 \quad V = (\widetilde{S_2} \geq \widetilde{S_1}) = 0.472$$
$$V = (\widetilde{S_1} \geq \widetilde{S_3}) = 1 \quad V = (\widetilde{S_3} \geq \widetilde{S_1}) = 0.615$$
$$V = (\widetilde{S_2} \geq \widetilde{S_3}) = 0.676 \quad V = (\widetilde{S_3} \geq \widetilde{S_2}) = 1$$

Thus, according to equation 10, numerical values of the evaluation criteria were obtained as:

$$d(R_1) = V(\widetilde{S_1} \geq \widetilde{S_2}, \widetilde{S_3}) = min\{1,1\} = 1$$
$$d(R_2) = V(\widetilde{S_2} \geq \widetilde{S_1}, \widetilde{S_3}) = min\{0.472, 0.676\} = 0.472$$
$$d(R_3) = V(\widetilde{S_3} \geq \widetilde{S_1}, \widetilde{S_2}) = min\{0.615, 1\} = 0.615$$

Then, according to equation 11, the ordering vector W'_R of C_1, C_2, and C_3 was obtained as $W'_R = (1, 0.472, 0.615)$. Using classical normalization operations (equation 12), the normalized weight vector W_R can be defined as $W_R = (0.479, 0.226, 0.295)$

Therefore, it can be seen that *Functional* is more important than *Expressive* and *Aesthetic.* The results in table 4 show that Functional is the most important in $S_1, S_2, S_3, S_{11}, S_{12}, S_{14}$. Expressive is the most important in $S_4, S_6, S_7, S_{10}, S_{15}$ and Aesthetic is the most important in S_5, S_8, S_9, S_{13}.

Experiment IIII: Evaluation of design solutions

Experiment IIII is created to gain insight into the perspective of the yogis on the design solutions which were made during the third experiment. This will be done by having the yogis evaluate each design solution according to FEA criteria. The linguistic weight set M_p, M_p = {*Extremely important, important, a little important, moderate, a little unimportant, not important, extremely unimportant*} (p = 1, 2, 3,…, 6, 7) is applied in the process of deciding the relevance of each design solution.

For example, evaluator e_l was given this question: "Regarding C_1 *(Functional requirements)*, what is the importance level of S_1 *(Good moisture absorption and breathability, lightweight and quick-drying)*?" As a response, the evaluator e_l must pick a linguistic term from M_p. Following this guide, every design solution can be measured against the various FEA criteria (table 4).

Characteristics of the design solutions can be seen in table 4, presenting aggregated evaluation data, weighted evaluation data, and the overall performance score based on the weighted evaluation data. Based on table 4, S_8*: Colour and pattern* has the lowest unweighted overall performance score, which is (0.607, 0.772, 0.891), and S_1: *Good moisture absorption and breathability, lightweight and quick drying* has the highest weighted overall performance score, which is (0.679, 0.843, 0.946). Therefore, designers of yoga wear should focus on the moisture absorption and breathability of the garment as well as its quick-drying properties. Also, consider other design solutions depending on the actual situation.

To compare different design solutions, the weighted overall performance scores (table 4) of each element are compared. As previously mentioned, the lowest overall score is held by the element which is labelled S_8*: Colour and pattern* (0.607, 0.772, 0.891).

Therefore, S8 can be used as a baseline from which to compare all of the other elements' performance scores, using distance as the calculated value. The greater distance belongs to those elements which have the best performance scores.

We can view these fuzzy distances as being Euclidean in nature. Since we are using a TFN to represent the overall performance scores, we propose a method of measurement where the distance between any two TFNs can be calculated using Euclidean distances. In the following, the distance between all the aggregated TFNs is measured to the "worst" condition (S_8*: Colour and pattern* (0.607, 0.772, 0.891)). The Euclidean distance for two TFNs $M_1 = (l_1, m_1, u_1)$ and $M_2 = (l_2, m_2, u_2)$ can be calculated as equation 13 [26].

For example, to analyse the overall performance of S_1, its overall performance score (0.679, 0.843, 0.946) is compared with that of S_8 (0.607, 0.772, 0.891) using equation 13, and the importance of S_1 can be calculated as equation 14 [26].

We can formulate the distances by applying this procedure to each aggregated TFN and normalizing the results. This is shown in figure 3. Then we analyse the data by completing the aforementioned comparison method. The larger the distance, the more important the design solution was found to be in the eyes of the evaluators.

From figure 3, it can be seen that the trend of design solutions according to different FEA considerations is the following, from the highest distance score to the lowest: S_1*: Good moisture absorption and breathability, lightweight and quick drying* (0.066), S_{11}*: Breast support with adjustable lacing* (0.063), S_{15}*: Proper body coverage* (0.063), S_{13}*: High-waist yoga pants* (0.058), S_5*: Body sculpting function* (0.051), S_4*: Soft and skin-friendly with comfortable clothing pressure* (0.047), S_3*: Antibacterial and anti-odour* (0.047), S_{14}*: Tight yoga wear* (0.041), S_2*: High resilience and flexibility* (0.041), S_9*: Various neckline designs* (0.027), S_{12}*: Removable knee cushions* (0.026), S_6*: Environmental and sustainable* (0.022), S_7*: Reflecting brand values* (0.015), S_{10}*: Splitting and splicing designs* (0.009), and S_8*: Colour and pattern,* having a score of (0.000), which serves as the comparison value. The larger the score distances, the more important the design solutions are. The most significant design

Table 4

AGGREGATED EVALUATION DATA, WEIGHTED AGGREGATED EVALUATION DATA OF THE DESIGN SOLUTIONS BASED ON FEA CONSIDERATIONS, AND THEIR OVERALL PERFORMANCE SCORES

Design solutions	Aggregated valuation data regarding FEA considerations separately	Weighted aggregated evaluation data regarding FEA considerations separately	Overall performance score based on weighted evaluation data
S1: Good moisture absorption and breathability, lightweight and quick drying	F:(0.692, 0.858, 0.962)	F:(0.332, 0.411, 0.461)	(0.679, 0.843, 0.946)
	E:(0.656, 0.819, 0.924)	E:(0.148, 0.185, 0.209)	
	A:(0.674, 0.837, 0.937)	A:(0.199, 0.247, 0.276)	
S2: High resilience and flexibility	F:(0.667, 0.833, 0.931)	F:(0.320, 0.399, 0.446)	(0.653, 0.817, 0.919)
	E:(0.627, 0.787, 0.906)	E:(0.142, 0.178, 0.205)	
	A:(0.649, 0.815, 0.910)	A:(0.191, 0.240, 0.268)	
S3: Antibacterial and anti-odour	F:(0.670, 0.833, 0.945)	F:(0.321, 0.399, 0.453)	(0.658, 0.820, 0.931)
	E:(0.653, 0.814, 0.910)	E:(0.148, 0.184, 0.206)	
	A:(0.639, 0.805, 0.923)	A:(0.189, 0.237, 0.272)	
S4: Soft and skin-friendly with comfortable clothing pressure	F:(0.649, 0.816, 0.924)	F:(0.311, 0.391, 0.442)	(0.657, 0.823, 0.930)
	E:(0.674, 0.837, 0.937)	E:(0.152, 0.189, 0.212)	
	A:(0.656, 0.823, 0.934)	A:(0.194, 0.243, 0.276)	
S5: Body sculpting function	F:(0.653, 0.819, 0.930)	F:(0.313, 0.392, 0.446)	(0.658, 0.824, 0.940)
	E:(0.646, 0.812, 0.927)	E:(0.146, 0.184, 0.210)	
	A:(0.674, 0.841, 0.962)	A:(0.199, 0.248, 0.284)	
S6: Environmental and sustainable	F:(0.627, 0.795, 0.917)	F:(0.301, 0.381, 0.439)	(0.629, 0.796, 0.912)
	E:(0.678, 0.843, 0.945)	E:(0.153, 0.191, 0.214)	
	A:(0.592, 0.758, 0.879)	A:(0.175, 0.224, 0.259)	
S7: Reflecting brand values	F:(0.621, 0.787, 0.902)	F:(0.297, 0.377, 0.432)	(0.623, 0.788, 0.904)
	E:(0.653, 0.819, 0.924)	E:(0.148, 0.185, 0.209)	
	A:(0.603, 0.766, 0.892)	A:(0.178, 0.226, 0.263)	
S8: Colour and pattern	F:(0.596, 0.762, 0.878)	F:(0.285, 0.365, 0.421)	(0.607, 0.772, 0.891)
	E:(0.610, 0.773, 0.892)	E:(0.138, 0.175, 0.202)	
	A:(0.624, 0.787, 0.910)	A:(0.184, 0.232, 0.268)	
S9: Various neckline designs	F:(0.600, 0.762, 0.881)	F:(0.287, 0.365, 0.422)	(0.637, 0.801, 0.913)
	E:(0.649, 0.812, 0.931)	E:(0.147, 0.184, 0.210)	
	A:(0.689, 0.854, 0.951)	A:(0.203, 0.252, 0.281)	
S10: Splitting and splicing designs	F:(0.589, 0.751, 0.878)	F:(0.282, 0.360, 0.421)	(0.616, 0.780, 0.900)
	E:(0.664, 0.829, 0.934)	E:(0.150, 0.187, 0.211)	
	A:(0.624, 0.790, 0.910)	A:(0.184, 0.233, 0.268)	
S11: Breast support with adjustable lacing	F:(0.688, 0.854, 0.952)	F:(0.330, 0.409, 0.456)	(0.673, 0.840, 0.944)
	E:(0.674, 0.840, 0.941)	E:(0.152, 0.190, 0.213)	
	A:(0.649, 0.816, 0.931)	A:(0.191, 0.241, 0.275)	
S12: Removable knee cushions	F:(0.663, 0.830, 0.941)	F:(0.318, 0.397, 0.451)	(0.635, 0.799, 0.915)
	E:(0.607, 0.773, 0.892)	E:(0.137, 0.175, 0.202)	
	A:(0.610, 0.769, 0.889)	A:(0.180, 0.227, 0.262)	
S13: High-waist yoga pants	F:(0.667, 0.834, 0.956)	F:(0.319, 0.399, 0.458)	(0.665, 0.831, 0.948)
	E:(0.649, 0.815, 0.927)	E:(0.147, 0.184, 0.210)	
	A:(0.674, 0.840, 0.948)	A:(0.199, 0.248, 0.280)	
S14: Tight yoga wear	F:(0.656, 0.823, 0.934)	F:(0.314, 0.394, 0.448)	(0.649, 0.814, 0.931)
	E:(0.649, 0.815, 0.927)	E:(0.147, 0.184, 0.210)	
	A:(0.638, 0.801, 0.924)	A:(0.188, 0.236, 0.273)	
S15: Proper body coverage	F:(0.670, 0.836, 0.935)	F:(0.321, 0.401, 0.448)	(0.675, 0.841, 0.940)
	E:(0.671, 0.837, 0.945)	E:(0.152, 0.189, 0.214)	
	A:(0.686, 0.851, 0.944)	A:(0.202, 0.251, 0.278)	

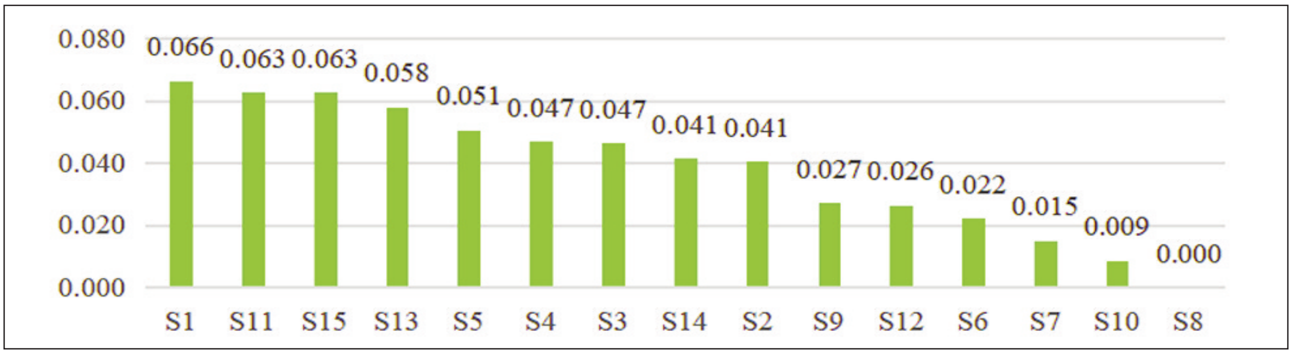

Fig. 3. Normalised distance values of design solutions compared to the distance of the lowest overall performance score of S8 Colour and pattern

solutions in order from the most to the least important are as follows: S_1, S_{11}, S_{15}, S_{13}, S_5, S_4, S_{14}, S_2, S_9, S_{12}, S_6, S_7, S_{10}, S_8, referring to figure 3.

Figure 4 shows that, S_1: *Good moisture absorption and breathability, lightweight and quick drying*, S_{11}: *Breast support with adjustable lacing*, S_{15}: *Proper body coverage*, S_{13}: *High-waist yoga pants* are the most important of all the design solutions and their distance difference is so small that they can be seen as equally important. The second most important is S_5: *Body sculpting function*, S_4: *Soft and skin-friendly with comfortable clothing pressure*, S_3: *Antibacterial and anti-odour*, S_{14}: *Tight yoga wear*, and S_2: *High resilience and flexibility,* these five design solutions can also be seen as equally important. The least important are S_9: *Various neckline designs*, S_{12}: *Removable knee cushions, S6: Environmental and sustainable*, S_7: *Reflecting brand values*, S_{10}: *Splitting and splicing designs,* and S_8: *Colour and pattern.*

CONCLUSIONS

In this perception study of yoga wear, a conceptual fuzzy AHP model is applied to analyse FEA considerations to find the best possible design solutions. There are four subsequent steps in this model, giving four experiments, including the Yoga wear consumer insight, the generation of garment design solutions regarding garment considerations, here applying FEA. This is followed by an evaluation of the relative weight of each of the three requirements, and finally of each of the components of the requirement level. This algorithm can be duplicated and easily applied to any area of fashion. Due to user involvement, here the yogis, the result of the experiment takes into consideration the needs of the user. The experimental results show that the solution design and evaluation based on the FEA model are very reasonable and comprehensive. This model can be used as an analytical way to incorporate the consumer in the process of garment design. Nevertheless, more design solutions can be integrated into the model, as well as different users such as the senior yogis. Therefore, as a proposal for future work, model integration in the area of open source is favoured. This platform can be used to integrate more users and update design solutions according to trends, thereby renewing design solutions continuously.

ACKNOWLEDGEMENTS

This research was funded by the National Natural Science Foundation of China (Grant Number: 61906129), the China Association for Science and Technology Youth Support Talent Project (Grant Number: 2021-298), and the Hong Kong Polytechnic University GBA Startup Postdoc Programme 2022 (Grant Number: SP-22-13).

REFERENCES

[1] Gilbert, C., *Yoga and breathing,* In: Journal of Bodywork and movement therapies, 1999, 3, 1, 44–54

[2] Kim, J.G., *Effects of chronic yoga activity on physical fitness and mental health of old people for 12weeks*, In: Journal of Coaching Development, 2013, 15, 3, 161–168

[3] Kim, M.J., Kim, Y.J., Lee, E.H., et al., *Effects of the yoga participation on intima-media thickness and blood flow variables in menopause women*, In: 운동사대회, 2008, 699–699

[4] Park, J.G., Lim, R.H., *An effect of the 12 weeks the hatha yoga program for female physical fitness*, In: The Korean Journal of physical education, 2004, 43, 6, 959–966

[5] Tew, G.A., Howsam, J., Hardy, M., Bissell, L., *Adapted yoga to improve physical function and health-related quality of life in physically-inactive older adults: a randomised controlled pilot trial,* In: BMC GERIATRICS, 2017, 17, 131

[6] Pu, L., Hong, Y., Mu, H., *Conceptual Fuzzy AHP Model for Perception Analysis of a Children's Raincoat,* In: Fibres & Textiles in Eastern Europe, 2020

[7] Hong, Y., Curteza, A., Zeng, X., Bruniaux, P., Chen, Y., *Sensory Evaluation Based Fuzzy AHP Approach for Material Selection in Customized Garment Design and Development Process,* In: Book of Abstracts, 2016a Iasi. IOP Publishing, 1–8

[8] Pu, L.Z., Wagner, M., Abtew, M., Hong, Y., Wang, P.G., *Raincoat design for children for age group 7–8 years: A design development case study*, In: Industria Textilă, 2018, 69, 5, 394–399, http://doi.org/10.35530/IT.069.05.1471

[9] Kim, J.Y., *A research on the actual condition of yogawear and consumer's preference of yogawear*, In: Fashion & Textile Research Journal, 2008, 10, 2, 147–154
[10] Ben Hassen, M., Halim, M.T., Abualsauod, E., Othman, A., *Quality yarn index using AHP and Fuzzy method,* In: Industria Textila, 2020, 71, 5, 487–491, http://doi.org/10.35530/IT.071.05.1699
[11] Hong, Y., Bruniaux, P., Zeng, X., Liu, K., Curteza, A., Chen, Y., *Visual-Simulation-Based Personalized Garment Block Design Method for Physically Disabled People with Scoliosis (PDPS)*, In: Autex Research Journal, 2018, 18, 1, 35–45
[12] Lamb, J.M., Kallal, M.J., *A Conceptual Framework for Apparel Design,* In: Clothing and Textiles Research Journal, 1992, 10, 42–47
[13] Watkins, S.M., *Using the Design Process to Teach Functional Apparel Design*, In: Clothing and Textiles Research Journal, 1988, 7, 10–14
[14] Bye, E., Hakala, L., *Sailing Apparel For Women: A Design Development Case Study*, In: Clothing and Textiles Research Journal, 2005, 23, 45–55
[15] Ciappei, C., Simoni, C., *Drivers of New Product Success in the Italian Sport Shoe Cluster of Montebelluna*, In: Journal of Fashion Marketing and Management, 2005, 9, 1, 20–42
[16] Chang, D.Y., *Applications of the Extent Analysis Method on Fuzzy AHP,* In: European Journal of Operational Research, 1996, 95, 649–655
[17] Chamodrakas, I., Batis, D., Martakos, D., *Supplier Selection In Electronic Marketplaces Using Satisficing And Fuzzy AHP,* In: Expert Systems with Applications, 2010, 37, 1, 490–498
[18] Hong, Y., Zeng, X., Bruniaux, P., Curteza, A., Chen, Y., *Movement Analysis and Ergonomic Garment Opening Design of Garment Block Patterns for Physically Disabled People with Scoliosis Using Fuzzy Logic,* In: International Conference on Applied Human Factors and Ergonomics, Springer, 2017, 303–314
[19] Hong, Y., Zeng, X., Bruniaux, P., Liu, K., *Interactive Virtual Try-On Based Three-Dimensional Garment Block Design for Disabled People of Scoliosis Type*, In: Textile Research Journal, 2017, 87, 1261–1274
[20] Hong, Y., Zeng, X., Bruniaux, P., *Knowledge Acquisition and Modeling of Garment Product Development*, In: Uncertainty Modelling in Knowledge Engineering and Decision Making: Proceedings of the 12th International FLINS Conference (FLINS 2016), Roubaix. World Scientific, 2016, 438–444
[21] Hong, Y., Bruniaux, P., Zeng, X., Curteza, A., Liu, K., *Design and Evaluation of Personalized Garment Block Design Method for Atypical Morphology Using the Knowledge-Supported Virtual Simulation Method*, In: Textile Research Journal, 2017, 88, 15, https://doi.org/10.1177/0040517517708537
[22] Liu, X., Zeng, X., Xu, Y., Koehl, L., *A Fuzzy Model Of Customer Satisfaction Index In E-Commerce,* In: Mathematics and Computers in Simulation, 2008, 77, 512–521
[23] Wang, Y.T., Huang, G., Duke, G., et al., *Tai Chi, yoga, and qigong as mind-body exercises*, In: Evidence-Based Complementary and Alternative Medicine, 2017
[24] Zeng, X., Ding, Y., Koehl, L., *A 2-Tuple Fuzzy Linguistic Model for Sensory Fabric Hand Evaluation*, 2004
[25] Ruan, D., Zeng, X., *Intelligent Sensory Evaluation: Methodologies and Applications*, Springer Science & Business Media, 2013
[26] Saaty, T.L., *Exploring the interface between hierarchies, multiple objectives and fuzzy sets*, In: Fuzzy Sets and Systems, 1978, 1, 1, 57–68
[27] Cao, J., *Fuzzy Comprehensive Evaluation of Subjective Evaluation of Cotton Fabric Hand Feel*, In: Journal of Textile Research, 2003,24, 1, 27–29

Authors:

HAO TANG[1], WENJUAN LI[1], SHUANG LIU[1], YAN HONG[2], CHUAN JIANG[3]

[1]Physical Education Department, Wuxi Taihu University, 214063, Wuxi, China
e-mail: tangh1@wxu.edu.cn, liwj@wxu.edu.cn, lius@wxu.edu.cn

[2]College of Textile and Clothing Engineering, Soochow University, Suzhou 215021, China

[3]China National Textile and Apparel Council, Beijing 100020, China

Corresponding authors:

YAN HONG
e-mail: hongyan@suda.edu.cn
CHUAN JIANG
e-mail: texhr@cntac.org.cn

Slit tear resistance of leather used in upholstery manufacturing

DOI: 10.35530/IT.074.03.202275

MARIANA COSTEA
ARINA SEUL
AURA MIHAI

ABSTRACT – REZUMAT

Slit tear resistance of leather used in upholstery manufacturing

The paper presents experimental research on the slit tear resistance of leather used for producing upholstery. A finite element analysis is done by simulating the product's behaviour, considering different factors and parameters, and materials are classified according to the normal stress results. The maximum force exerted during the tearing of the specimen has been observed at the SATRA tensile testing machine, with STM 466ST attachment and digital software control. The load at break, the extension at break, Young's Modulus, and the load-distance graphs were registered and the medium values were calculated. The Taguchi method based on orthogonal arrays was used to maximize the material characteristics significant for this type of analysis.

Keywords: *leather for upholstery, slit tear test, Taguchi method, finite element analysis*

Rezistența la sfâșiere a pieilor utilizate la fabricarea tapițeriilor

Lucrarea prezintă cercetări experimentale privind rezistența la sfâșiere a pieilor folosite pentru producerea tapițeriilor. O analiză cu elemente finite a fost făcută prin simularea comportamentului produsului luând în considerare mai mulți factori și parametri, materialele fiind clasificate în funcție de rezultatele tensiunii axiale. A fost observată forța maximă exercitată în timpul ruperii specimenului, folosind aparatul de testare la tracțiune SATRA, cu atașament STM 466ST și control digital prin software. A fost înregistrată forța la rupere, alungirea la rupere, modulul lui Young, precum și graficele încărcare-distanță și au fost calculate valorile medii. A fost utilizată metoda Taguchi bazată pe rețele ortogonale pentru a maximiza caracteristicile materialelor semnificative pentru acest tip de analiză.

Cuvinte-cheie: *piei pentru tapițerii, testul pentru sfâșiere, metoda Taguchi, analiza elementelor finite*

INTRODUCTION

Leather is still one of the most popular types of materials used to make upholstery products. It is a material with multiple uses in daily life due to its properties: vapour permeability, mechanical strength, air permeability, flexibility, and softness [1]. The processed leather must be of good quality, with as few surface defects as possible, and, after tanning, it has to be soft, supple, plastic, evenly painted, without stains, and must not discolour under the action of light [2]. The leather samples selected for the present research are hides types, finished on the exterior, with the natural outer, corrected, and respectively reinforced.

Leather hides contain water, protein, fatty materials and some minerals. The most important for leather making is protein, which consists of several types. The main ones are collagen and keratin. The approximate composition of a leather hide is 64% water, 33% protein (structural proteins: 0.3% elastin, 29% collagen, 2% keratin; 1.7% non-structural protein), 2% fats, 0.5% mineral salt, 0.5 other substances (pigments etc.) [3].

Because in everyday use, bags, backpacks, keys, various gadgets, accessories, and so on are placed on the upholstery pieces, which adds to the actual sitting on it, all this can tear the product. Testing slit tear resistance is very important in choosing materials and determining the final cost of products. The most important physical and chemical properties that material should have (table 1): excellent strength-on-weight ratio, very good tear resistance, and high resistance to environmental degradation [4, 5].

METHOD

Finite Element Analysis (FEA) is a complex numerical method used in various fields to simulate the behaviour of virtual products considering many factors and parameters.

Among the possible simulations can be reproduced the physical-mechanical tests, such as uniaxial and multiaxial tensile test [6, 7], last forming test [8, 9], crack of leather, stitch resistance [10], tear strength [11, 12] and others, necessary for evaluating the physical and mechanical parameters of the materials, including leather, synthetic leather, textiles, used in the upholstery industry.

A 3D design of the sample is done in Delcam PowerShape software. The application chosen to simulate the slit tear resistance on the leather specimen is ANSYS R17.2- Static Structural module. The following working procedure was adopted:

- Import and edit 3D geometry;

Table 1

PHYSICAL AND CHEMICAL PROPERTIES Of DIFFERENT MATERIALS

No.	Test description	Method	Specification		
			cow-hides	goat-hides	pig-hides
1	Water content/ volatile matter (%)	DIN EN ISO 4684	8–15	12–16	12–16
2	pH value	DIN EN ISO 4045	3.5	3.5–4	4
3	Chrome oxide concentration	DIN 5398-2	≤0.1	≤0.1	≤0.1
4	Fat content (%)	DIN EN ISO 4048	7–12	7–12	7–12
5	Tensile strength (N)	DIN EN ISO 3376	≥120	Min. 80	Min. 80
6	Percentage extension (%)	DIN EN ISO 3376	40–60	35–60	35–60
7	Stitch tear resistance (N)	DIN EN ISO 23910	≥80	≥60	≥60
8	Water vapour permeability (mg/cm^2)	DIN EN ISO 14268	≥1.0	2.5	2.5
9	Colour fastness to perspiration of the grain side	DIN EN ISO 105-E04	≥4–5	≥4–5	≥4–5
10	Resistance to water	Water dripped onto the back side rear side, dry at room temperature	Water dripped onto the back side may not result in a colour change or leave traces on the upper side after having dried (at ambient temperature)		
11	FOLDING TEST (72 hrs, at 80°C)	Folding 5 cm wide leather strip (grain side to grain side) and loading the fold with a weight of 2 kg.	No cracks shall be allowed to occur in the finish layer. check with a (6 times) magnifying glass		
12	Adhesive strength of finishing - dry	DIN EN ISO 11644	≥4	≥4	≥4
13	Adhesive strength of finishing - wet	DIN EN ISO 11644	≥1.2	≥1.2	≥1.5
14	Material and substances	PN-1004	Material according to pn-1004. the use of PCP is prohibited, the remaining quantity (e.g. contamination) must be less than 1 mg/kg		
15	Burning behaviour (flammability) (mm/min)	FMVSS 302 / PTL 8501	<100	<100	<100

- Establishing material properties;
- Setting analysis conditions (mesh, contacts, restrictions, loads);
- Setting the parameters to evaluate;
- Solving the model;
- Analysing the results.

Geometry and material properties play an important role in the virtual simulation of the mechanical test. As indicated by the “Standard Test Method for Slit Tear Resistance of Leather, ASTM D 2212”, the leather rectangular specimen has a length of 51 mm and a width of 25.4 mm with a slot in the middle with a side of 20 mm and another one of 5 mm. To the rectangular specimen, was assigned the properties of cow-hides, namely Young's modulus determined experimentally, as presented in table 1. The material is considered to be homogeneous and isotropic. 2 rectangular clamps were inserted on either side of the slot, as presented in figure 1.

A bonded contact with a 0.15 mm trim was established between the clamps and the leather specimen. Also, a standard mechanical dropped mesh with 49500 nodes and 35859 elements was created.

As shown in the standard, while the lower clamp is fixed, the upper clamp moves until the material breaks. Based on these specifications, the model has loaded the ANSYS Static Structural module.

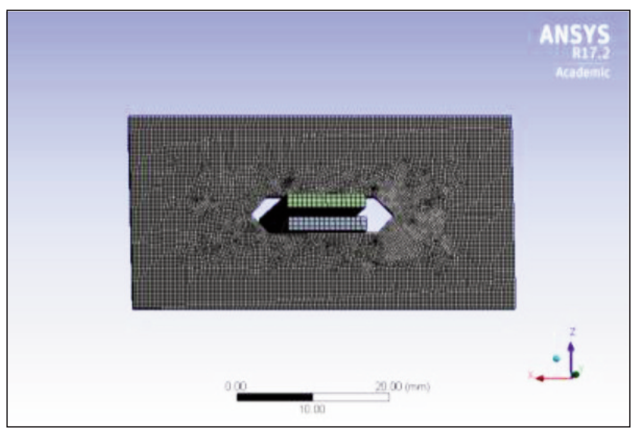

Fig. 1. 3D model for the slit tearing test

RESULTS AND DISCUSSIONS

The Taguchi method was used to determine the experimental plans (Design of Experiments – DOE). The method developed by Genichi Taguchi combines statistical methods with engineering techniques, to improve the quality of manufactured goods, manufacturing processes, or experimental testing.

The method of experimental plans allows rigorous organization of experiments, taking into account a well-defined objective. Through this method, a considerable decrease in the number of experimental attempts is obtained.

3 types of materials were used: cow-hides (1), goat-hides (2), pig-hides (3), with 3 types of thicknesses: 1.5 mm (X), 1.3 mm (Y), 1.1 mm (Z), and 3 different types of finishings: natural (A), corrected (B), reinforced (C).

Using the application Minitab v.16, a matrix of experiments consisting of 9 experimental plans was obtained, as seen in the table below (table 2).

Table 2

MATRIX OF EXPERIMENTS			
Material type	**Thickness**	**Cover**	**Experiment**
1	X	A	P1
1	Y	B	P2
1	Z	C	P3
2	X	B	P4
2	Y	C	P5
2	Z	A	P6
3	X	C	P7
3	Y	A	P8
3	Z	B	P9

Using Ansys, the normal stress (MPa) was evaluated for each experiment, being the stress produced by the perpendicular action of the force acting on the area of the specimen during the double-edged slit tearing test [13].

The formula to calculate average normal stress is force per unit area [14]:

$$\tau = \frac{F}{A} \tag{1}$$

where τ is the normal stress, and F – the force applied. In this case, it is used the maximum force for optimal material combination and A – the cross-sectional area of material with an area perpendicular to the applied force vector.

The simulation (figure 2) shows the distribution of normal stress along with the slot.

In table 3, the experiments are ordered according to the results, from the best to the lowest values

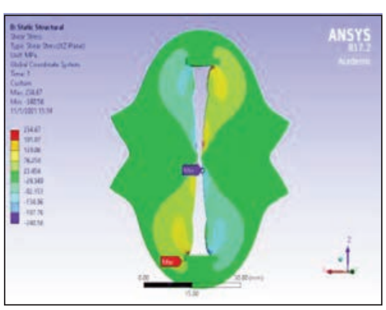

Fig. 2. Normal stress distribution analysis during slit tearing test

Table 3

TABLE OF EXPERIMENTS, ANSYS STATIC STRUCTURAL MODULE	
Experiment	**Normal stress (MPa)**
P1	120.040
P2	107.860
P3	78.124
P8	46.743
P9	45.878
P7	44.536
P4	43.402
P6	32.306
P5	33.260

obtained for the Normal Stress evaluated using FEA. The results of Normal Stress (MPa) show that the optimum material is **P1.**

MODEL VALIDATION

The reliability of Finite Element Analysis was validated by performing physical tests.

The tests were carried out according to the "Standard Test Method for Slit Tear Resistance of Leather, ASTM D 2212". Other 3 standards were used as reference documents ASTM D 1610 Practice for Conditioning Leather and Leather; Products for Testing; D 1813 Test Method for Measuring Thickness of Leather Test Specimens, D 2209 Test Method for Tensile Strength of Leather.

According to ASTM D 2212, slit tear resistance is the load required to tear the cross-sectional thickness of the leather at a slit cut through the leather by a die or a sharp knife.

This test method is designed to measure the load required to tear leather at a slit cut perpendicular to its surface. It is of particular value in estimating the durability of leather to withstand tearing stresses encountered in the manufacture of upholstered products.

Equipment – SATRA STM 466ST Tensile testing machine attachment.

The specimen dimensions were 25.4 by 51 mm, cut with the long dimension either parallel or perpendicular to the backbone. The specimen cut with the slit tear had a slot of 11 mm long by 4.8 mm wide.

There were used 9 types of leather. All specimens were conditioned as prescribed in ASTM D 1610.

The testing has been done at a loading speed of 100 mm/min ± 20 mm/minute, in conformity with the norm SR EN ISO 3377-2:2016 [15].

After testing the slit tear resistance (figure 3) for the nine types of leather at break, the software of the tensile machine SATRA STM 466ST has registered for each experimental type the load-distance graphics as well as the maximum force at break in N, the load at break in N, the first peak in N, the averages of peaks and troughs in N, the break extension in %, Young's Modulus in N/mm^2. For each experimental plan,


Fig. 3. Slit tear test on SATRA STM 466ST

three slit tests were performed. For an adequate illustration of the characteristics registered at the tensile testing machine STM466, there have been used the medium values correspond to each experimental type (table 4).

Figure 4, *a, b*, and c shows the load-distance graphs for the tested materials tested with SATRA-STM 466 ST apparatus, for three experiments, P3, P5, P9.

The best result for the maximum force was registered for the **P1 experiment**, followed by P2 and P3. These results validate the results obtained previously with FEA.

EVALUATION OF MATERIALS USING THE TAGUCHI METHOD

The experimental matrix contains three input variables, all at three levels, as presented in table 5. The choice of the signal factors was required so that the considered process can conclude the expected performance and have the smallest sensitivity to

Table 4

RESULTS OF SLIT TEAR TEST ON SATRA STM 466ST

Experiment	Cycle	Average of peaks and troughs (N)	Break extension (mm)	The first peak (N)	Load at break (N)	Maximum force (N)	Young's modulus, (N/mm^2)
P1	Mean	121.82	49.78	135.87	104.03	142.37	14.55
	Std Dev	2.53	5.19	17.13	13.15	11.59	1.34
	Max	123.47	55.2	154.7	116.5	154.7	14.92
	Min	118.91	44.85	121.2	90.3	131.7	14.24
P2	Mean	116.99	52.47	137.57	88.9	142.30	40.24
	Std Dev	13.47	3.71	5.56	18.47	8.06	5.45
	Max	132.47	56.67	143.8	109.7	149.5	46.53
	Min	107.92	49.67	133.1	74.4	133.6	36.87
P3	Mean	95.38	44.54	105.87	84.87	114.73	26.19
	Std Dev	9.43	1.64	14.94	21.76	10.97	3.12
	Max	105.47	45.5	122	107	124.9	29.12
	Min	86.79	42.65	92.5	63.5	103.1	22.91
P4	Mean	50.19	44.21	49.67	48.57	55.2	14.93
	Std Dev	0.56	0.63	3	1.63	0.53	0.72
	Max	50.56	44.9	52.7	50.4	55.6	15.7
	Min	49.54	43.67	46.7	47.3	54.6	14.28
P5	Mean	25.5	51.92	26.67	22.07	30.63	10.83
	Std Dev	2.46	1.35	0.15	1.1	3.96	1.37
	Max	27.07	52.85	26.8	22.8	34.4	12.32
	Min	22.66	50.38	26.5	20.8	26.5	9.62
P6	Mean	47.03	53.92	51.57	38.67	53	11.15
	Std Dev	2.32	5.75	3.52	2.84	2.71	0.86
	Max	49.67	58.03	55.6	41.9	55.6	12.1
	Min	45.31	47.35	49.1	36.6	50.2	10.43
P7	Mean	50.51	47.22	55.97	47.6	60.43	15.38
	Std Dev	2.42	1.49	7.6	6.7	3.07	1.47
	Max	53.27	48.3	63.7	54.7	63.7	16.45
	Min	48.75	45.53	48.5	41.4	57.6	13.71
P8	Mean	90.86	48.08	91.83	80.83	103.5	36.16
	Std Dev	5.55	5.56	9.19	5.53	3.47	2.61
	Max	94.83	52.67	102	86	105.7	38.55
	Min	84.52	41.9	84.1	75	99.5	33.37
P9	Mean	60.61	44.67	65.67	56.83	72.6	15.67
	Std Dev	7.03	1.92	14.09	7.25	14.17	3.45
	Max	65.88	46.5	81.4	62.9	85.9	19.21
	Min	52.64	42.67	54.2	48.8	57.7	12.32

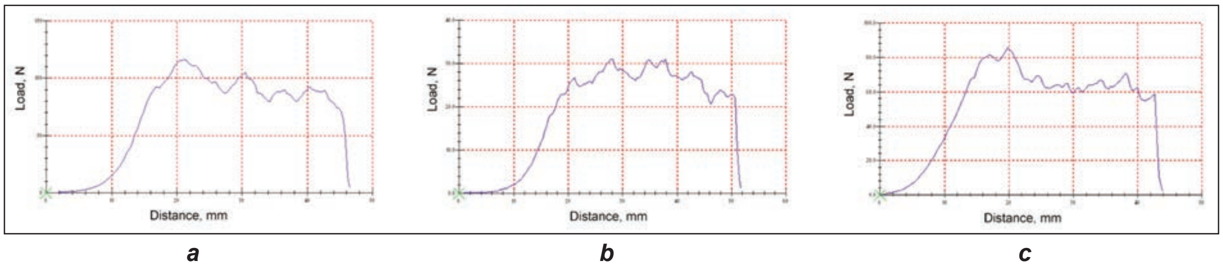

Fig. 4. Load-distance graph: *a* – P3 experiment; *b* – P5 experiment; *c* – P9 experiment

Table 5

SIGNAL FACTORS			
Levels	**Material type**	**Thickness (mm)**	**Finishing type**
1	Cow-hides	1.5	Natural
2	Goat-hides	1.3	Corrected
3	Pig-hides	1.1	Reinforced

noises. The current study targeted the influence of signal parameters on the slit tear resistance of leather for upholstery.

The first three columns of table 6, noted A, B, and C represent the signal factors (material, thickness, and finishing), while the following two, noted N1 and N2 are the noise factors (maximum force and first peak force).

The S/N ratio (signal-to-noise) is a technique used in engineering and science that correlates the signal parameters to the noise parameters (table 7). The aim of applying this technique is to obtain the most advantageous solution of signal parameters that influence the structure so that the S/N ratio is maximized [16, 17]. Also, the standard variation, the mean values, and the coefficients of variation are calculated. The results obtained after the statistical analysis for the S/N ratio are graphically represented in figure 5. To determine the accuracy of the Taguchi model that was given, a normal probability plot was drawn (figure 6). It can be noted that the distribution of the

Table 6

RESULTS OF DOE-TAGUCHI, *L*9 ARRAY									
Experiment	**A**	**B**	**C**	**N1-Maximum force**	**N2-First peak**	**SNRA1**	**STDE1**	**MEAN1**	**CV1**
P1	1	1	1	142.37	135.87	42.8607	4.59619	139.120	0.0330376
P2	1	2	2	142.30	137.57	42.9148	3.34462	139.935	0.0239012
P3	1	3	3	114.73	105.87	40.8305	6.26497	110.300	0.0567993
P4	2	1	2	55.20	49.67	34.3562	3.91030	52.435	0.0745742
P5	2	2	3	30.63	26.67	29.0802	2.80014	28.650	0.0977362
P6	2	3	1	53.00	51.57	34.3651	1.01116	52.285	0.0193394
P7	3	1	3	60.43	55.97	35.2793	3.15370	58.200	0.0541872
P8	3	2	1	103.50	91.83	39.7482	8.25194	97.665	0.0844923
P9	3	3	2	72.60	65.67	36.7612	4.90025	69.135	0.0708794

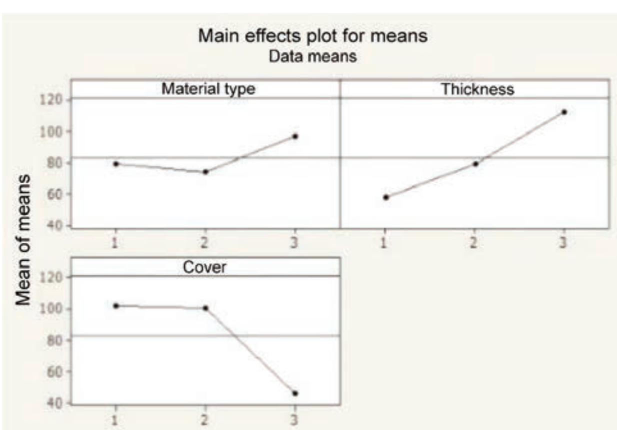

Fig. 5. Main effects plot for means

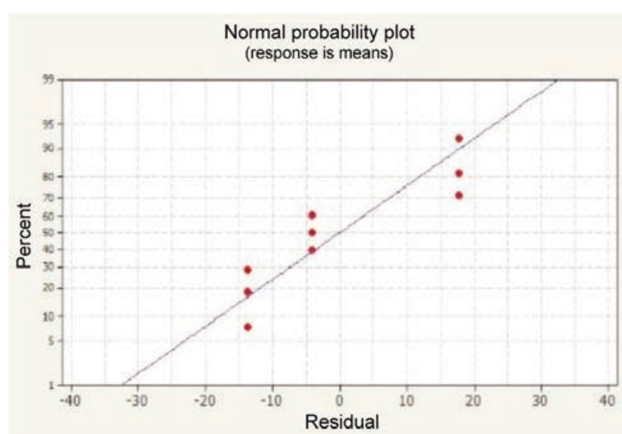

Fig. 6. Normal probability plot for means

residual values reported to the median is close to normal.
The classification of influence level, presented in table 6, is maximum influence – the A factor *A* (material type), followed by finishing, and minimum influence – the B factor (thickness).
The S/N ratio is calculated for every factor level association. The formula for the larger-is-better S/N ratio is:

$$\frac{S}{N} = -10\log\left[\sqrt{y^2}(1 + 3s^2 \times \sqrt{y^2})\right] \qquad (2)$$

where *S* is the standard deviation, *y* – nominal value, *s* – an average of determined values and *N* – number of runs.

Table 7

RESPONSE TABLE FOR SIGNAL-TO-NOISE RATIOS LARGER IS BETTER			
Level	**A**	**B**	**C**
1	42.20	37.50	38.99
2	32.60	37.25	38.01
3	37.26	37.32	35.06
Delta	9.60	0.25	3.93
Rank	1	3	2

The best association of signal parameters to obtain the higher value for the S/N ratio is A1B1C1*,* representing cow-hides, 1.5 mm thickness, and natural cover (table 7) representing the **P1 experiment.**

CONCLUSIONS

The following conclusions were formed:

- A finite element analysis resulted in normal stress values that offered the possibility of ranking the experiments. FEA is a technique used successfully in many fields, and as this article demonstrates, it can also be used successfully in the field of upholstery production to simulate the behaviour of materials considering many factors and parameters.
- To determine the experimental plans for the rigorous organization of experiments, taking into account a well-defined objective the Taguchi method was used. Through this method, a considerable decrease in the number of experimental attempts is obtained.
- The accuracy of the results obtained by Finite Element Analysis was validated by performing physical tests. Slit tear resistance of leather was performed using SATRA STM 466ST equipment to evaluate the durability of leather encountered in the manufacture of upholstered products, for the nine types of leather at break. There were registered load-distance graphics, as well as the maximum force at break, the load at break, the first peak, the averages of peaks and troughs, the break extension, and Young's Modulus.
- Signal-to-noise ratio from the Taguchi technique was used to obtain the most advantageous solution of parameters that influence the material. By classification of influence level, the best results have been obtained for cow-hides, 1.5 mm thickness, and natural cover.

ACKNOWLEDGEMENTS

The paper was supported by the “Language guide for footwear and leather industry” project, number 2020-1-TR01-KA202-092689, co-funded by the Erasmus+ Programme of the European Union.

REFERENCES

[1] Alexe, C.A., Gaidau, C., Stanca, M., Radu, A., Stroe, M., Baibarac, M., Mateescu, G., Mateescu, A., Stanculescu, I.R., *Multifunctional leather surfaces coated with nanocomposites through conventional and unconventional methods*, In: Materials Today: Proceedings, 2021, ISSN 2214-7853, https://doi.org/10.1016/j.matpr.2021.09.377

[2] Ionescu, C., Costea, M., *Leather and leather substitutes upholstery (In Romanian)*, Performantica Publishing House, 2016, ISBN 978-606-685-486-3

[3] Pruneanu, M., Bucișcanu, I., Maier, V., Toma, S., *Recycling of chamois leather waste into valuable products with potential applications in the field of technical textiles,* In: 7th International Symposium Technical Textiles - Present & Future, Iasi, Romania, 2021, 179–186, https://doi.org/10.2478/9788366675735-030179

[4] Brooke, L., Wakefield, D.S., Bown, A., *The development history of inflated lifting body form LTA vehicle hulls*. In: Proceedings in 7th International Airship Convention, Friedrichshafen, 2008, 1–6

[5] Bharathi, D., Alagirusamy, R., Joshi, M., et al., *Central Slit Tearing Behaviour of Thermoplastic Polyurethane-Coated High-Strength Fabrics,* In: Trans. Indian Natl. Acad. Eng., 2020, 5, 779–787, https://doi.org/10.1007/s41403-020-00183-x

[6] Tsukada, T., Akihiro, M., *Finite element analysis of compressible anisotropic materials with dispersed fiber orientation,* In: The Proceedings of Mechanical Engineering Congress, Japan, 2020, J23403, https://doi.org/10.1299/jsmemecj.2020.J2340

[7] Zubauskienė, D., *Upholstery materials behavior evaluation method* (Doctoral dissertation, Kauno Technologijos Universitetas, 2018, Available at: https://en.ktu.edu/events/upholstery-materials-behavior-evaluation-method/ [Accessed on May 2022]

[8] Rupérez, M.J., Giner, E., Monserrat, C., Montiel, E., *Simulation of the behavior of the calfskin used as shoe upper material in footwear CAD,* In: Computer-Aided Design, 2012, 44, 12, 1205–1216*,* https://doi.org/10.1016/j.cad.2012.06.009

[9] Lin, J., Hayhurst, D.R., Howard, I.C., Reedman, D.C., *Modelling of the performance of leather in a uni-axial shoe-last simulator,* In: The Journal of Strain Analysis for Engineering Design, 1992, 27, 4, 187–196, https://doi.org/10.1243/03093247v274187

[10] Jankauskaite, V., Strazdiene, E., Laukaitiene, A., *Stress distribution in polymeric film laminated leather under biaxial loading,* In: Proceedings of the Estonian Academy of Sciences, 2006, 55, 111–124

[11] Min, H., *Study of Two Models for Tearing Resistance Assessment Using Essential work of Fracture Method*, Master's Degree Thesis, 2008, Available at: https://www.diva-portal.org/smash/get/diva2:832493/FULLTEXT01.pdf [Accessed on May 2022]

[12] Wang, P., Ma, Q., Sun, B., Gu, B., *Finite element modeling of woven fabric tearing damage,* In: Textile Research Journal, 2011, 81, 12, 1273–1286, https://doi.org/10.1177/0040517510397578

[13] Rice, J.R., Mechanics of solids. Physics, Britannica, Available at: https://www.britannica.com/science/mechanics-of-solids#ref611497 [Accessed on May 2022]

[14] Hibbeler, R.C., *Mechanics of Materials,* New Jersey USA: Pearson Education, 2004, 32, ISBN 0-13-191345-X

[15] SR EN ISO 3377-2:2016, *Leather – Physical and mechanical tests. Determination of tear load. Part 2: Double edge tear*

[16] Pamuk, G., Ceken, F., *Comparison of the mechanical behavior spacer knit cotton and flax fabric reinforced composites,* In: Industria Textilă, 2013, 64, 1, 3–7

[17] Ionesi, S.D., Fangueiro, R., Ciobanu, L., Dumitraș, C., Ursache, M., Dulgheriu, I., *Evaluation of impact behaviour of composite materials using Taguchi method*, In: Industria Textila, 2014, 65, 3, 152–157, ISSN 1453-5424

Authors:

MARIANA COSTEA, ARINA SEUL, AURA MIHAI

"Gheorghe Asachi" Technical University of Iasi, Faculty of Industrial Design and Business Management,
D. Mangeron, 29, 70050, Iasi, Romania
e-mail: mariana.costea@academic.tuiasi.ro, aura.mihai@academic.tuiasi.ro

Corresponding author:

ARINA SEUL
e-mail: arina.seul@academic.tuiasi.ro

The mathematical study of compression behaviours of silicone rubber composites reinforced by warp-knitted spacer fabrics

DOI: 10.35530/IT.074.03.2022138

ZHOU ZI-XIANG CHEN SI

ABSTRACT – REZUMAT

The mathematical study of compression behaviours of silicone rubber composites reinforced by warp-knitted spacer fabrics

To synthetically investigate the compressive mechanism of warp knitted spacer fabric reinforced silicone rubber matrix composite (SRWSF) under 20% deformation, a compression meso-mechanics theoretical model was established in this paper. The silicone rubber was processed as isotropic material according to the nonlinear constitutive equation, the spacer yarn was assumed as a continuous uniform element. The compression meso-mechanics theoretical model consists of the mechanical model of silicone rubber and the compression model of warp knitted spacer fabric (WSF), based on the Euler-Bernoulli beam theory and the Spence Invariant constitutive model theory. To verify the feasibility of the compression meso-mechanics theoretical model of SRWSF, the compression test of SRWSF was carried out. The simulated compression stress-strain curve was compared with the results of the experiment. The result shows that the compression theoretical model has a high agreement with the experimental result under 20% strain, as compared with the Polynomial fitting curve. This phenomenon indicates that the compression theoretical model established in this study can reasonably simulate the actual compression behaviours within 20% deformation for SRWSF. Moreover, the theoretical model can help understand the compression mechanism of SRWSF and optimise the designing of silicone-rubber-matrix composite reinforced by WSF for cushioning applications.

Keywords: *warp-knitted spacer fabric, silicone-rubber matrix, compression meso-mechanics model, Euler-Bernoulli beam, Spence Invariant theory*

Studiul matematic al comportamentelor de compresie ale compozitelor din cauciuc siliconic armate cu distanțiere tricotate din urzeală

Pentru a investiga sintetic mecanismul de compresie al compozitului cu matrice de cauciuc siliconic armat cu distanțiere tricotate din urzeală (SRWSF) sub o deformare de 20%, în această lucrare a fost stabilit un model teoretic al mezomecanicii de compresie. Cauciucul siliconic a fost prelucrat ca material izotrop conform ecuației constitutive neliniare, firul distanțier a fost presupus ca un element uniform continuu. Modelul teoretic al mezomecanicii de compresie constă dintr-un modelul mecanic al cauciucului siliconic și modelul de compresie al distanțierului tricotat din urzeală (WSF), bazat pe teoria fasciculului Euler-Bernoulli și teoria modelului constitutiv Spence Invariant. Pentru a verifica fezabilitatea modelului teoretic al mezomecanicii de compresie SRWSF, a fost efectuat testul de compresie SRWSF. Curba simulată de tensiune-deformare sub compresie a fost comparată cu rezultatele experimentului. Rezultatul arată că modelul teoretic de compresie are un grad de conformitate ridicat cu rezultatul experimental sub deformare de 20%, în comparație cu curba de potrivire polinomială. Acest fenomen indică faptul că modelul teoretic de compresie stabilit în acest studiu poate simula în mod rezonabil comportamentele reale de compresie cu o deformare de 20% pentru SRWSF. Mai mult, modelul teoretic poate fi util pentru înțelegerea mecanismului de compresie al SRWSF și optimizarea proiectării compozitului silicon-cauciuc-matrice armat cu WSF pentru aplicații de amortizare.

Cuvinte-cheie*: distanțier tricotat din urzeală, matrice de cauciuc siliconic, model al mezomecanicii de compresie, fascicul Euler-Bernoulli, Teoria Spence Invariant*

INTRODUCTION

Recently, textile fabrics are commonly used as alternative low-cost reinforcement for cushioning applications, due to their special properties like specific modulus, low density and customized development function [1]. However, the fibres are not to be used as the particular structure for the textile, only the knitted fabrics, the woven fabrics and the nonwoven fabrics are used as the unique structure for composites. Warp-knitted spacer fabrics are one of the novel textile materials. Warp-knitted spacer fabrics (WSF) are composed of two separate layers connected by spacer yarns. From this unique construction, the greater ability of compression anti-deformation and rebound elasticity are exhibited for WSF compared with the other textiles. All of these advantages make the warp-knitted spacer fabric have more potential to be used as reinforcement for structural applications.

There have been many types of research on the mechanical features of composites reinforced by WSF [2–8]. In practical engineering, the most concerned problem is to establish a theoretical model to predict composite mechanical properties, rather than only rely on the experiment results. Chen [9, 10] set up a compression meso-mechanics theoretical model of polyurethane-based warp-knitted spacer fabric composite, based on the Winkler elastic foundation beam theory and structure parameters of composite. The compression theoretical model can effectively simulate the actual compressive behaviours of composite. The theoretical model of warp-knitted spacer fabric reinforced syntactic foam was established by Zhi [11], according to the Eshelby-Mori-Tanaka equivalent inclusion method. The theoretical model was suitable for the variation tendency of the compression for samples. The Kelvin-Voigt model was utilized by Mashi [12], and the result showed that 97.7 per cent accuracy existed between the model and the result of the low-velocity impact experiment. It can be concluded from their studies that the processing of the mechanical evolution of composite can be efficiently simulated by the theoretical model. The theoretical model plays an important role and can guide optimizing the designing of composite.

However, in the published study, the mechanical behaviours of silicone-rubber-matrix composite reinforced by warp-knitted spacer fabric were researched only in the experimental phase [13, 14]. The mechanism of silicone-rubber matrix composites reinforced by warp-knitted spacer fabric on the compression behaviours has not been studied, which limits the SRWSF's applications. Therefore, to understand the compression mechanism of SRWSF for achieving governable preparation of SRWSF. It is necessary to analyse the compression processing of SRWSF from a meso-mechanics angle. In this study, two samples of the composite material were prepared with the same processing, and the compression test was conducted on the samples. A compression meso-mechanics theoretical model for SRWSF was established, based on the Euler-Bernoulli beam theory and Spence Invariant constitutive theory. Moreover, the structure parameters of each part of the composite were involved in the model. Additionally, the polynomial curve of the compression experiment of SRWSF was fitted, based on the results of a compressive test of SRWSF. The theoretical model was compared with the polynomial curve and compression experiment of SRWSF to verify the feasibility of the compression meso-mechanics theoretical model of SRWSF. The resulting compression meso-mechanics theoretical model, which was first established in this study, allows for analysing and predicting the compression behaviours of silicone rubber composites reinforced by warp-knitted spacer fabric.

MATERIALS AND METHOD

Material

In this study, the PET monofilament of 0.16 mm in diameter was used as the spacer yarn for warp-knitted spacer fabric. The hexagonal mesh was involved for the surface layer of sample 1. The rhombic mesh was involved for the surface layer of sample 2. The fabric surface was composed of polyester monofilament and the density of polyester is equal to 1.4 g/cm^3. The silicone rubber matrix was made of silicone rubber A and B according to the ratio of 1:1, at room temperature. Then, the warp-knitted spacer fabric was filled with silicone rubber by hand lay-up processing at room temperature for 8 hours. Next, the specimen was placed at room temperature for 24 hours, after vulcanizing. Finally, the composite was generated, which was tested in this study. The production process of composites is shown in figure 1.

The parameters of composites were measured from the two ends and the middle position with a measuring tool whose minimum indexing value is not more than 0.05 mm, along the length and width direction of the sample, and then the average values were computed from the measured parameters. Finally, the chain notations for composites are listed in table 1.

Method

The WSF was characterized for the compression property based on the Chinese standard GB/T 24442.1-2009 (Textile – Determination of compression property – Part 1: Constant method) by using the SHIMADZU Universal testing machine, at a load speed of 4 mm/min in an environment of 23°C and 65% relative humidity. The silicone rubber mechanical experiment was carried out according to the Chinese standard GB/T 528-2009 (Rubber, vulcanized or thermoplastic – Determination of tensile stress-strain properties) by using a SHIMADZU

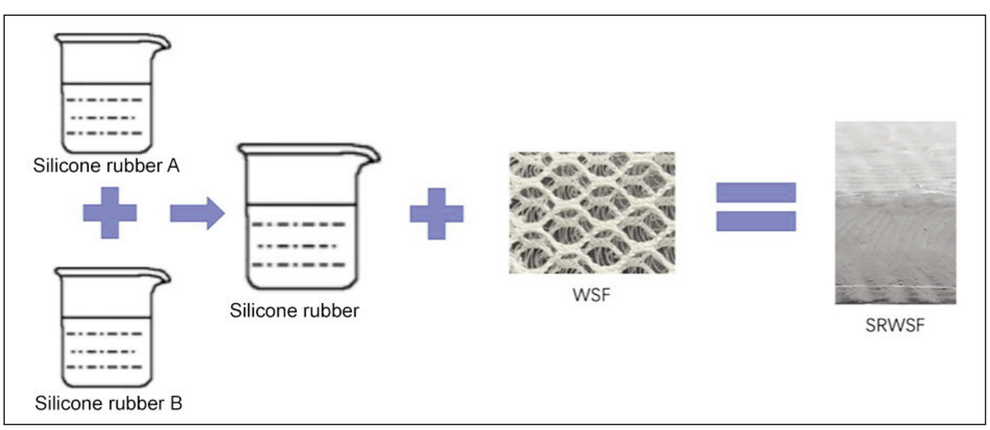

Fig. 1. The production process of composites

Table 1

THE PARAMETERS OF COMPOSITES									
Parameters	**Length (mm)**	**Width (mm)**	**Thickness (mm)**	**Spacer yarn volume fraction (%)**	**Composite elastic modulus (MPa)**	**Spacer yarn elastic modulus (MPa)**	**Spacer yarn Poisson's ratio**	**Silicone rubber elastic modulus (MPa)**	**Silicone rubber Poisson's ratio**
Sample 1	101.03	49.82	33.12	2.17	0.44	3200	0.22	0.1609	0.47
Sample 2	100.51	49.30	32.97	2.17	0.44	3200	0.22	0.1609	0.47

Table 2

THE VALUE OF THE WSF COMPRESSION EXPERIMENT			
Stress (MPa)	**Strain (%)**	**Stress (MPa)**	**Strain (%)**
0	0	0.02878	19.3929
0.00534	2.7377	0.03015	22.1689
0.01021	5.5140	0.03078	24.9449
0.01523	8.2896	0.03098	27.7209
0.01953	11.0652	0.03069	30.4964
0.02335	13.8412	0.03044	33.2725
0.02648	16.6174	-	-

Table 3

THE VALUE OF SILICONE RUBBER COMPRESSION EXPERIMENT			
Stress (MPa)	**Strain (%)**	**Stress (MPa)**	**Strain (%)**
0	0	1.01397	351.8063
0.14827	48.0562	1.20246	402.4314
0.21235	98.6812	1.36455	453.0562
0.33674	149.3062	1.62213	503.6811
0.45862	199.9314	0.00880	554.3063
0.65966	250.5562	0.02890	604.9313
0.80415	301.1812	-	-

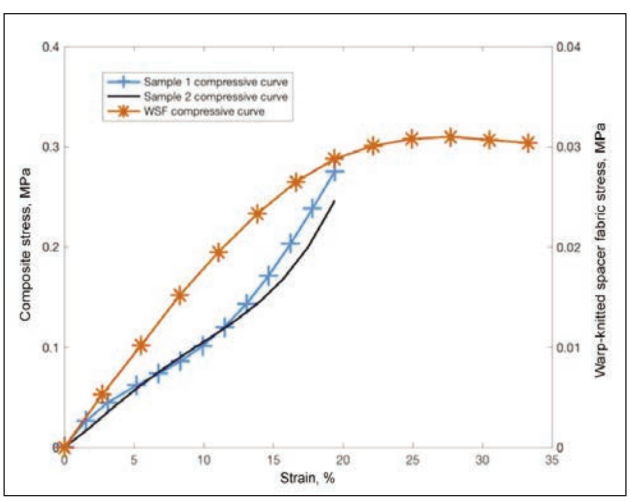

Fig. 2. The stress-strain curve of the compressive experiment

Table 4

THE VALUE OF THE SRWSF COMPRESSION EXPERIMENT			
Stress (MPa)	**Strain (%)**	**Stress (MPa)**	**Strain (%)**
Sample 1			
0	0	0.11008	11.5033
0.01064	1.5564	0.13253	13.0830
0.02945	3.1362	0.16103	14.6624
0.06076	5.1844	0.18959	16.2423
0.08691	6.7642	0.21944	17.8220
0.09661	8.3439	0.25127	19.4016
0.10839	9.9234	-	-
Sample 2			
0	0	0.11222	12.2436
0.01377	1.7529	0.14345	13.9921
0.03468	3.5015	0.17394	15.7405
0.06022	5.2501	0.20604	17.4891
0.08739	6.9985	0.24055	19.2376
0.09638	8.7470	0.24392	19.4015
0.11121	10.4952	-	-

Universal testing machine, at a load speed of 450 mm/min in an environment of 23°C and 65% relative humidity. The SRWSFs were characterized for compression properties based on the Chinese standard GB/T 8171-2008 (Test method for mechanical shock fragility rating of products using packaging cushioning materials) by using the SHIMADZU Universal testing machine, at a load speed of 9 mm/min in an environment of 23°C and 65% relative humidity. The parameters of the compressive experiment of WSF, as shown in table 2. The parameters of the mechanical experiment of silicone rubber, as shown in table 3. The parameters of the compressive experiment of SRWSF, as shown in table 4.
The stress-strain curve of the compressive experiment of SRWSF and WSF is shown in figure 2.

Compression meso-mechanics theoretical modelling

As we know, the composite was composed of reinforcement and matrix materials. The external load was mainly absorbed by the reinforcement materials during the compression processing. Furthermore, the deformation degree of the matrix was limited by reinforcement, due to the elastic modulus of reinforcement being greater than the elastic modulus of the matrix. On the other hand, the load was dispersed by the matrix materials, meanwhile, the reinforcement can be protected with matrix materials.

In this study, the warp-knitted spacer fabric was used as reinforcement which contained the spacer yarns and the fabric layers. The spacer yarns were regarded as a fixed hinge according to the connection method between the spacer yarns and the fabric layers. The shearing stress from the contact of spacer yarns and fabric layers can be ignored due to the small diameter of the spacer monofilament. The fabric layers have a slight deformation during the compression test, resulting in the stress being mainly absorbed by the spacer yarns. It is assumed that the cross-section of spacer yarns is evenly distributed along the axial direction, thus, the spacer yarns can be processed as a continuous homogeneous element. The strength of spacer yarns and silicone rubber are distinct. The silicone rubber has a lower elastic modulus and thermoplastic feature, leading to the result that it can be mixed with the spacer yarns well before vulcanization. The spacer yarns obtain a remarkable agreement deformation with silicone rubber. Meanwhile, the regular support of the side wall for the spacer yarns can be provided from silicone rubber, due to the excellent deformation ability of silicone rubber. Moreover, satisfactory synchronization was exhibited between the spacer yarns and silicone rubber. Thus, the produced composites can be processed as the Euler-Bernoulli beam, which means the shear force between spacer yarns and silicone rubber can be ignored during the compression processing [15]. In this study, the analysis of the deformation of spacer yarns was mainly considered in the compression processing of composites. According to the previous research [16], the geometric model of the axis of spacer yarns was established based on the trajectory of the guide bar used in the warp knitting machine, the schematic diagram of the compression deformation state for WSF, as shown in figure 3. As supposed in figure 3, in the initial configuration, the yarn direction was defined by a unit vector field a_0 and it had position vector $\underline{X}$ with components X_R, and the length of yarn is L. In the deformed configuration, the yarn direction may be described by a unit vector field a_i, and the deformed configuration has position vector $\underline{x}$ with coordinates x_i, while the length of yarn is l. The stretch ratio λ can be shown in equation 1:

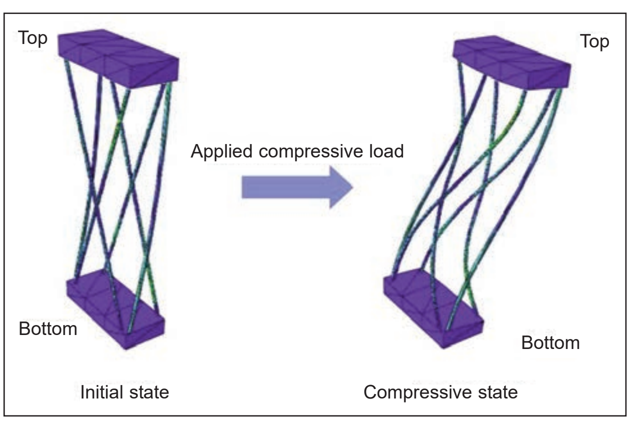

Fig. 3. The schematic of compression deformation of WSF

$$\lambda = l / L \quad (1)$$

The deformation of spacer yarns can be described by equation 2

$$\underline{x} = \underline{x}(\underline{X}) \quad (2)$$

and it follows equation 3:

$$a_i \cdot l = \frac{\delta xi}{\delta XR} \cdot a_R^{(0)} \cdot L \quad (3)$$

Thus:

$$\lambda a = F \cdot a_0 \quad (4)$$

where $a_0 = (\cos\alpha, 0, \sin\alpha)$, α is the angle between spacer yarns and the bottom horizontal plane of the matrix material. It can be calculated based on geometric parameters of spacer yarns that $\sin\alpha$ is equal to 0.882, $\cos\alpha$ is equal to 0.116. F can be expressed by:

$$F = \begin{bmatrix} \delta x1/\delta X1 & \delta x1/\delta X2 & \delta x1/\delta X3 \\ \delta x2/\delta X1 & \delta x2/\delta X2 & \delta x2/\delta X3 \\ \delta x3/\delta X1 & \delta x3/\delta X2 & \delta x3/\delta X3 \end{bmatrix} \quad (5)$$

The deformation of spacer yarns consisted of rotation and compression of spacer yarns. Exactly, the local rotation and completed compression of spacer yarns are absorbed by deformation gradient F. It supposes that the compression was caused first, then the compressed body rotated. The resolution expression of F can be calculated, as shown in equation 6:

$$F = R \cdot U \quad (6)$$

where U is Right extension tensor, R – rotation matrix. However, in the actual deformation, the computing difficulty of the rotation matrix of deformation was tremendous. In this study, supposing the composite was deformed in a material coordinate system to reduce the cost of calculation and ensure the accuracy of the calculation. The rotation matrix can be eliminated by equation 7.

$$F^T \cdot F = (R \cdot U)^T \cdot R \cdot U = U^T \cdot R^T \cdot R \cdot U = \\ = U^T \cdot U = U^2 = C \quad (7)$$

where C is Right Cauchy-Green deformation tensor. The eigenvalues of U are λ_i $(i = 1, 2, 3)$, which represent the stretch ratio for X, Y, and Z axis direction respectively. Finally, C can be expressed as:

$$C = \begin{bmatrix} \lambda_1^2 & 0 & 0 \\ 0 & \lambda_2^2 & 0 \\ 0 & 0 & \lambda_3^2 \end{bmatrix} \quad (8)$$

The deformation of spacer yarns in the compression processing can be described by equation 9:

$$\lambda^2 = a_0 \cdot F \cdot F^T \cdot a_0^T = a_0 \cdot C a_0^T \quad (9)$$

From equation 9, the deformation of spacer yarns can be determined by the initial direction of spacer yarns a_0 and the Right Cauchy-Green deformation tensor C.

As a result of the previous analysis, the silicone-rubber-matrix composite reinforced by WSF can be used as one family fibre reinforced composite. Based on the Spence Invariant Theory [17], the invariants I_i ($i = 1, 2, 3, 4, 5$) were utilized in this study to build up the model of the composite under external compressive load, where:

$$I_1 = trC = \lambda_1^2 + \lambda_2^2 + \lambda_3^2 \quad (10)$$

$$I_2 = \frac{1}{2}\left[(trC)^2 - trC^2\right] = \lambda_1^2\lambda_2^2 + \lambda_2^2\lambda_3^2 + \lambda_1^2\lambda_3^2 \quad (11)$$

$$I_3 = det\,C = \lambda_1^2\lambda_2^2\lambda_3^2 \quad (12)$$

$$I_4 = a_0 \cdot C \cdot a_0^T \quad (13)$$

$$I_5 = a_0 \cdot C^2 \cdot a_0^T \quad (14)$$

In conclusion, the total strain-energy of the composite can be expressed as $W = W_s + W_f = W(I_1, I_2, I_3, I_4, I_5)$. The strain-energy of isotropy-matrix material absorbed under outward load was represented by $W_s = W(C) = W(I_1, I_2, I_3)$. When the material is an incompressible element, the value of I_3 is equal to 1. Silicone rubber is an isotropic incompressible material, thus the $W_{(C)}$ can be described from Equation (15), which is named the Mooney-Rivlin model:

$$W_{(C)} = C_{10}(I_1 - 3) + C_{01}(I_2 - 3) \quad (15)$$

Assuming that the function $W_{(C)}$ is continuously differentiable with tensor C, and it followed that:

$$\frac{\partial W(C)}{\partial C} = \sum_{i=1}^{2} \frac{\partial W(C)}{\partial I_i} \cdot \frac{\partial I_i}{\partial C} = \frac{\partial W(C)}{\partial I_1} \cdot \frac{\partial I_1}{\partial C} + \frac{\partial W(C)}{\partial I_2} \cdot \frac{\partial I_2}{\partial C} \quad (16)$$

Among equation 16:

$$\frac{\partial I_1}{\partial C} = \frac{\partial trC}{\partial C} = \boldsymbol{I} \quad (17)$$

$$\frac{\partial I_2}{\partial C} = \frac{1}{2}\left(2trC\boldsymbol{I} - \frac{\partial tr(C^2)}{\partial C}\right) = I_1\boldsymbol{I} - C \quad (18)$$

where $\boldsymbol{I}$ is unit tensor. Second Piola-Kirchhoff stress T can be described by:

$$T = 2\frac{\partial W(C)}{\partial C} \quad (19)$$

The relationship between Second Piola-Kirchhoff stress T and Cauchy stress σ, is shown in equation 20:

$$\sigma = J^{-1} \cdot F \cdot T \cdot F^T \quad (20)$$

Substituting equation 19 into equation 21, it can obtain:

$$\sigma = \frac{1}{J}\left[W_1 \cdot B + W_2 \cdot (I_1 \cdot B - B^2)\right] \quad (21)$$

where B is the Left Cauchy-Green deformation tensor, and the structure of the eigenvalues matrix of B is equal to C. W_i is a partial derivative for the invariant ($I = 1, 2$). J is the rate of volume change. Due to the material being incompressible, the value of J is equal to 1. Supposing the compression direction was the 3 direction, during the compression processing. As a result, $\lambda_3 = \lambda$, $\lambda_1 = \lambda_2 = \lambda^{-1/2}$, $\sigma_3 = \sigma$, $\sigma_1 = \sigma_2 = 0$. The relationship between stress and strain for the matrix can be described by equation 22:

$$\sigma_s = 2\left[C_{10}(\lambda^2 - \lambda^{-1}) + C_{01}(\lambda - \lambda^{-2})\right] \quad (22)$$

The strain-energy absorbed by the reinforced structure from the external pressure was represented by $W_f = W(C, a_0 \otimes a_0^T) = W(I_4, I_5)$. The W_f was connected with the degree of deformation of spacer yarns, thus the polynomial about $(I_4 - 1)$ and $(I_5 - 1)$ was utilized to construct the strain-energy function, which was absorbed by reinforced structure, as shown following:

$$W_f = A_1(I_4 - 1) + A_2(I_4 - 1)^2 + A_3(I_5 - 1) + A_4(I_5 - 1)^2 + A_5(I_4 - 1)^3 \quad (23)$$

In equation 23:

$$\frac{\partial W(C, a_0 \otimes a_0)}{\partial C} = \sum_{i=4}^{5} \frac{\partial W(C)}{\partial I_1} \cdot \frac{\partial I_1}{\partial C} = \frac{\partial W(C)}{\partial I_4} \cdot \frac{\partial I_4}{\partial C} + \frac{\partial W(C)}{\partial I_5} \cdot \frac{\partial I_5}{\partial C} \quad (24)$$

$$\frac{\partial I_4}{\partial C} = a_0 \otimes a_0^T \quad (25)$$

$$\frac{\partial I_5}{\partial C} = 2a_0 \cdot C \cdot a_0^T \quad (26)$$

The relationship between stress and strain for reinforcement can be expressed as follow:

$$\begin{aligned}\sigma_f = {} & 2A_1(\lambda^2 - \lambda^{-1}) + \\ & + 2A_2\left[0.78(\lambda - \lambda^{-2}) + 0.01(\lambda^4 - \lambda) + (\lambda^{-1} - \lambda^2)\right] + \\ & + 2A_3\left[0.78(\lambda - \lambda^{-2}) + 0.01(\lambda^4 - \lambda)\right] + \\ & + 4A_4\left[0.61(\lambda^{-1} - \lambda^{-4}) + 0.01(\lambda^2 - \lambda^{-1}) + 0.02(\lambda^3 - 1)\right] + \\ & + 3.54A_5 + 6A_5(0.02\lambda^3 - 0.61\lambda^{-3}) + 6A_5(\lambda^2 - \lambda^{-1}) + \\ & + 12A_5(-0.78\lambda + 0.78\lambda^{-2}) + 12A_5(-0.01\lambda^4 + \lambda)\end{aligned}$$

The parameters C_{10} and C_{01} can be calculated from the nonlinear function fitting instruction by MATLAB software, based on the data of mechanical experiment for silicone rubber. The parameters A_i ($i = 1, 2, 3, 4, 5$) can be obtained based on the result of the compression experiment of WSF.

RESULTS AND DISCUSSION

The value of parameters from equation 21 and equation 26 was computed from the WSF compression experiment and the Silicone rubber mechanical experiment, as shown in table 5.

The Polynomial curve was fitted by MATLAB, based on the compression experiment data to conduct a more comprehensive analysis of the compressive behaviour of the composite. The strain value from the compression experiment of the composite was brought into the compression meso-mechanics

Table 5

THE PARAMETERS OF THE THEORETICAL MODEL							
Parameters	C_{10}	C_{01}	A_1	A_2	A_3	A_4	A_5
Value	0.0161	0.037	–5.9835	–4.5746	6.7614	–0.3910	0.000146

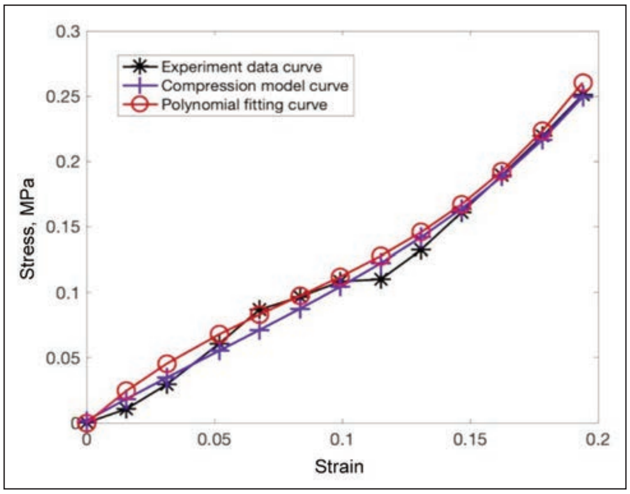

a

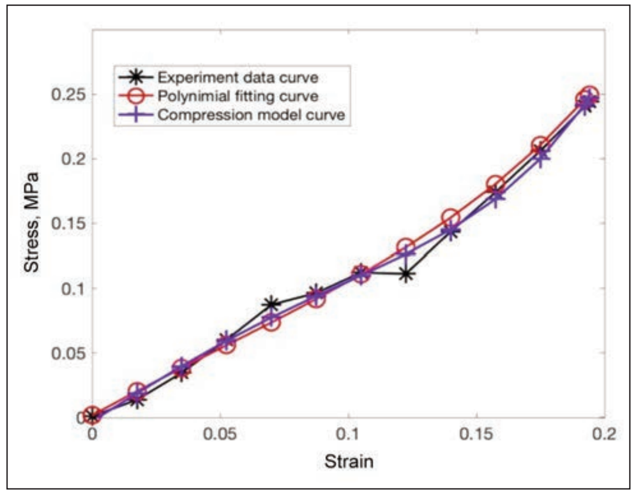

b

Fig. 3. The comparison of compression model, compression experiment and Polynomial fitting curves: *a* – Sample 1; *b* – Sample 2

theoretical model, and then the curve of stress-strain for the theoretical model was established. The curves of the compression model, compression experiment and Polynomial fitting were compared, as shown in figure 4.

It is obvious from figure 4, that the Polynomial fitting curve was mainly above the experiment data curve with a little intertwining. However, uniform contact was shown between the curve of the theoretical model and the curve of experimental results. In figure 4, *a*, the average value of the relative error between the experiment and the polynomial is 5.7453%, and the average value of the relative error between the experiment and the theoretical model is 4.9542%. In figure 4, *b*, the average value of the relative error between the experiment and the polynomial is 5.7201%, and the average value of the relative error between the experiment and the theoretical model is 4.9434%. The theoretical model had a high agreement with the experimental results, as compared with the Polynomial fitting curve. Moreover, the slope of the polynomial fitting curve has a better agreement with the experiment curve under the 12% deformation. While the slope of the theoretical curve shows a better agreement with the experimental curve between the deformation of 12% and 20%. On the other side, the deformation abilities of sample 1 and sample 2 exist difference, due to the difference within the mesh structure of the surface layer between sample 1 and sample 2. Therefore, the invariants I_i (i = 1, 2, 3, 4, 5) of sample 1 and sample 2 are different. The compression evolution of composite can be effectively simulated by the compression meso-mechanics theoretical model. However, some deviations were shown between those curves. It is supposed that in the evolution of compression, there was no shearing force existed between the reinforcement and matrix material. During the compression processing, the composite only supported compressive load and there was no friction between the spacer yarns and silicone rubber. On the other hand, the measurement error occurred, when the structure parameters were measured. Moreover, the spacer yarns are regarded as a straight bar to calculate the angle, but the spacer yarns are not completely straight, of which angle is changed. Based on the above mention, the deviation between the theoretical model and experiment results is observed during the actual compression process.

CONCLUSION

The compressive evolution of silicone-rubber-matrix composite reinforced by warp-knitted spacer fabric within 20% deformation can be efficiently simulated from the compression meso-mechanics theoretical model, which was established based on the Euler-Bernoulli beam theory and Spence Invariant constitutive theory. At the same time, the compression theoretical model shows great potential for further compressive evolution. Additionally, the elastic modulus of the composite at each stage can be approximately consulted by the slope of the theoretical model, leading to the result that the slope of the theoretical model can serve as a reference for actual production designing. It can also be a reference for the further investigation of the compression property of SRWSF, and hopefully be expanded to predict the compression feature for the variety of SRWSF.

REFERENCES

[1] Sun, Z., Jiang, X., Zhao, K., et al., *A comparative analysis of bending-torsion coupling characteristics of three-dimension angle interlocking woven and biaxial warp knitted composite blade*, In: Journal of Inner Mongolia University of Technology, 2022

[2] Si, C., Hairu, L., *Mechanical properties of 3D-structure composites based on warp-knitted spacer fabrics*, In: Autex Research Journal, 2015, 15, 2, 127–137

[3] Chao, Z., Hairu, L., *Flexural Properties of Syntactic foam Reinforced by Warp Knitted Spacer Fabric*, In: Autex Research Journal, 2016, 16, 2, 57–66

[4] Wanli, X., Pibo, M., Liwei, W., et al., *Low-velocity impact properties of composite reinforced by auxetic warp-knitted spacer fabric*, In: Journal of Sandwich Structures & Materials, 2020, 23, 6, 1972–1986

[5] Velosa, S., Rana, J.C., Fangueiro, R., et al., *Mechanical behavior of novel sandwich composite panels based on 3D-knitted spacer fabrics*, In: Journal of Reinforced Plastics and Composites, 2012, 31, 2, 95–105

[6] Wanli, X., Yaxin, S., Haitao, L., et al., *Preparation of soft composite reinforced with auxetic warp-knitted spacer fabric for stab resistance*, In: Textile Research Journal, 2020, 90, 3–4, 323–332

[7] Datta, M.K., Behera, B.K., Goyal, A., *Prediction and analysis of compression behaviour of warp-knitted spacer fabric with cylindrical surface*, In: Journal of Industrial Textiles, 2019, 48, 9, 1489–1504

[8] Zhenqian, L., Liwei, W., Bohong, G., et al., *Numerical simulation of the impact behaviors of shear thickening fluid impregnated warp-knitted spacer fabric*, In: Composites Part B: Engineering, 2015, 69, 191–200

[9] Si, C., *The Compression Meso-Mechanics Theoretical Model and Experimental Verification of Polyurethane-Based Warp-Knit Spacer Fabric Composites*, In: AATCC Journal of Research, 2021, 8, 5, 30–38

[10] Si, C., Hairu, L., *Investigation on compression properties of polyurethane-based warp-knitted spacer fabric composites for cushioning applications Part II: theoretical model and experimental verification*, In: Industria Textila, 2014, 65, 6, 340–344

[11] Chao, Z., Mingjuan, D., Zhaoling, S., et al., *Warp-Knitted Spacer Fabric Reinforced Syntactic Foam: A Compression Modulus Meso-Mechanics Theoretical Model and Experimental Verification*, In: Polymers, 2020, 12, 2, 286

[12] Yousefpour, M., Payvandy, P., Salehahmadi, M., *Investigation of physical models accuracy optimized by PSO for determining low-velocity impact behavior of warp-knitted spacer fabrics*, In: Journal of The Textile Institute, 2018, 109, 3, 312–321

[13] Zhenqian, L., Xiaoying, J., *Impact property of silicone rubber filled warp knitted spacer fabrics*, In: Textile Research Journal, 2014, 35, 9, 298–313

[14] Xiaohui, Z., Pibo, M., Huilin, X., *Compression fatigue-resistance behaviors of silicone rubber filled warp-knitted spacer fabrics*, In: Fibers and Polymers, 2017, 18, 5, 1011–1016

[15] Wang, C.M., Reddy, J.N., Lee, K.H., *Shear Deformable Beams And Plates Relationships With Classical Solutions*, Elsevier, Amsterdam-Lausanne-New York-Oxford-Shannon-Singapore-Tokyo, 2000, 14

[16] Zixiang, Z., Si, C., *Finite Element Analysis of Compression Behaviors of Silicone Rubber Composites Reinforced by Warp-Knitted Spacer Fabrics*, In: AATCC Journal of Research, 2022, 9, 5, 240–247

[17] Spencer, A.J.M., *Continuum theory of the mechanics of fiber-reinforced composites*, Springer-Verlag, Wien-New York, 1984, 16–18

Authors:

ZHOU ZI-XIANG, CHEN SI

College of Light Industry and Textile, Inner Mongolia University of Technology, Hohhot, China

Corresponding author:

CHEN SI
e-mail: ansn9119@126.com

Research into the effects of pigment printing parameters on sensorial comfort to guide garment designers in the apparel industry

DOI: 10.35530/IT.074.03.2022131

ARZU KILIÇ

ABSTRACT – REZUMAT

Research into the effects of pigment printing parameters on sensorial comfort to guide garment designers in the apparel industry

The printing process, which is an aesthetically significant process subprocess in garment design, has the potential to affect the physical properties and sensory comfort of the fabric. Due to its low cost and very fast process period and the fact that it is environmentally conscious, pigment printing is widely used in the textile industry. This study it's aimed to guide the designers in the selection of printing type for piece printing according to the fabric type by considering the print area and print pattern in the apparel industry. For this purpose, the effects of commonly used pigment printing pastes on the physical properties and sensorial comfort in knit fabrics of different constructions were studied. To that end, two different patterns were applied to three knit fabrics with different constructions by using three different pigment printing methods to assess several features of the fabrics, namely, print quality, air permeability, roughness, compressibility and bending. As a result of this study, it was observed that the printing application method and print pattern design have a significant impact on the handle properties of the fabric. Consequently, it was revealed that it is necessary to take into account the printing application method and print pattern design in the process of printed clothing design. Among the print types evaluated in this study, the best print type was determined in terms of sensorial comfort and physical properties. In addition, suggestions were made on the issues to be considered during the print design of print types with worse comfort and physical properties.

Keywords: *sensorial comfort, printing, air permeability, roughness, compressibility, bending, print design*

Cercetări privind influența parametrilor de imprimare cu pigmenţi asupra confortului senzorial pentru a ghida designerii de articole de îmbrăcăminte din industria de îmbrăcăminte

Procesul de imprimare, care reprezintă un subproces semnificativ din punct de vedere estetic în proiectarea articolelor de îmbrăcăminte, are potențialul de a afecta proprietățile fizice și confortul senzorial ale materialului textil. Datorită costului scăzut, a timpului de proces foarte scurt și a faptului că are o responsabilitate ecologică, imprimarea cu pigment este utilizată pe scară largă în industria textilă. Acest studiu îşi propune să ghideze designerii pentru selectarea tipului de imprimare pentru imprimarea piesei în funcție de tipul de material textil, luând în considerare zona de imprimare și modelul de imprimare în industria de îmbrăcăminte. În acest scop, au fost studiate influența pastelor de imprimare și pigmentare utilizate în mod obișnuit asupra proprietăților fizice și confortului senzorial ale tricoturilor cu diferite structuri. În acest scop, două modele diferite au fost aplicate la trei tricoturi cu structuri diferite, folosind trei metode diferite de imprimare cu pigment pentru a evalua mai multe caracteristici ale materialelor textile, și anume, calitatea imprimării, permeabilitatea la aer, rugozitatea, compresibilitatea și îndoirea. Ca rezultat al acestui studiu, s-a observat că metoda de aplicare a imprimării și designul modelului de imprimare au un impact semnificativ asupra proprietăților de tuşeu ale materialului textil. În consecință, s-a evidenţiat că este necesar să se țină cont de metoda de aplicare a imprimării și de designul modelului de imprimare în procesul de proiectare a îmbrăcămintei imprimate. Dintre tipurile de imprimare evaluate în acest studiu, cel mai corespunzător tip de imprimare a fost determinat din punct de vedere al confortului senzorial și al proprietăților fizice. În plus, au fost enunțate sugestii cu privire la aspectele care trebuie luate în considerare la proiectarea tipurilor de imprimare cu proprietăți fizice şi de confort mai slabe.

Cuvinte-cheie*: confort senzorial, imprimare, permeabilitate la aer, rugozitate, compresibilitate, îndoire, design de imprimare*

INTRODUCTION

In recent years, the consumer's decision to buy a product is determined not only by the clothing's aesthetic and design features but also by the element of comfort. In their daily lives, a consumer expects a high level of comfort from their preferred clothing and requires the clothing to feel comfortable.

Clothing comfort is defined as the state where the physiological, psychological, and physical harmony between the human body and its environment is gratifying. Clothing comfort is studied as two basic components which are psychological comfort and physiological comfort. Physiological comfort includes the subcomponents of thermal physiological comfort, sensorial comfort and body movement comfort [1].

The sensorial comfort of the skin characterizes the sensory input that is caused by attack styles' direct mechanical contact with the skin [2]. Sensorial comfort expresses the manner of sensory perception (sight, hearing, etc.) the surface of a certain textile evokes on the wearer and the level of gratification [3, 4], sensorial comfort is usually defined by the watch the consumer feels when the fabric contacts the skin, such as prickly, itchy, rough or smooth [5]. Sensorial comfort is a clothing field that is related to touch, humidity, pressure and thermal sensations [6]. To ensure a high level of sensorial comfort, the material that contacts the skin needs to have a structure and flexibility that would cause a pleasing sense of touch (softness, slickness), not stick to the skin, and not cause itchiness or allergic reactions. Sensorial clothing comfort is identified through several features such as feel, wettability, skin adhesion strength, surface friction factor and fabric stiffness [7].

Sensorial comfort is a multidimensional concept and impossible to define through a single physical property. Sensorial comfort is related to several fabric features such as roughness, density, flexibility, elasticity, compressibility, surface friction and thermal feature [8]. These fabric properties have been contrasted in several studies resulting in evaluations of the sensorial comfort of the clothing.

Fibre type, yarn structure, fabric structure and finishing processes, the fabric goes through are the parameters that affect sensorial comfort [5, 8–11]. Several studies have been conducted on these parameters and the state of impact of these parameters on sensorial comfort has been studied. Certain parameters focused on these studies are the impact of various fibres, mixture ratios, cross sectional fibres on sensorial comfort [5, 9, 12–15], the effect of fabric structures on sensorial comfort [2, 10, 11, 13–15] and the effect of finishing processes on sensorial comfort [15–19]. Salman et al (2021), observed that the washing process has a positive impact on the softness and resilience score while drapability, wrinkle recovery, and smoothness decrease after washing the fabric [15]. In the study conducted by Özgüney et al (2009), it was indicated that all finishing processes affect the feel of the fabric in terms of increasing roughness, but that pigment printing was the most effective bare finish process. In addition, it was also exhibited that even though the mercerization process performed before dyeing and printing result in improvements and fabric properties, impacts fabric softness negatively [17]. This study was focused on pigment printing due to the use of pigments as the major colouration method, with approximately 50% of the world textile printing market in conventional textile screen-printing [20].

In the apparel industry, where fast fashion dominates the market, piece printing becomes a frequently preferred method. Although it is a fact that the printing method and printing pattern design should be taken into account in the garment design process, the number of publications on this subject is quite limited. In today's fashion understanding, where the importance of wearing comfort takes precedence over aesthetic concerns, it is clear that the effect of the printing process on comfort is as important as the printing pattern design in customer preferences.

The objective of the study is to evaluate pigment printing in terms of physical properties and sensorial comfort properties to guide garment designers in the apparel industry. In mass production, a designed garment is produced in several colour variations and the printing pattern's dimensions vary regarding the printing area. Therefore, instead of printing on light coloured fabrics, a dark blue dyed fabric was chosen as a substrate. In total, three different water-based pigment printing pastes commonly preferred by the apparel manufacturers were prepared in different colours, and the commonly used knit fabric constructions, single jersey, rib and pique were evaluated in this study. Moreover, it is a fact that pigment printing reduces elasticity and therefore results in lower compressibility values due to the formation of a sticky film on the fabric surface [17]. Therefore, to determine the effect of these printing parameters on sensorial comfort properties, the printed knit fabrics' dimensional properties such as mass per unit area, thickness and compressibility; air permeability, handle properties including surface kinetic friction coefficient, bending properties and the print quality were tested and analyzed by using statistical evaluation.

MATERIAL AND METHOD

Material

It is aimed to guide the designers in the selection of printing paste according to the fabric type by considering the print area and print pattern in piece printing. In this context, three different commonly used water-based pigment printing pastes in piece printing were procured (Anadolu Kimya, Turkiye). As the substrates, generally preferred knit fabric constructions, single jersey, rib and pique were purchased (Ekoten Fabrics, Turkiye), which were dyed to dark blue colour with dye stuff. As the aim of the study, the commercial products were procured and the focus was on determining the effect of these commercial products on the physical properties and sensorial comfort properties, therefore the contents of the printing pastes were not researched.

In table 1, the raw materials, the yarn numbers and the knitting structures were presented. As stated in the literature, the base colour of the fabric is influential in the printing process in terms of printing quality. When a darker colour is printed on a lighter base, the visual of the print is not affected and the colour is distinctly visible. However, when a lighter colour is printed on a darker base, the colour of the print becomes obscured and clear printing is not possible [22]. For this reason, especially when printing a lighter coloured pattern on a darker coloured base, the printing is performed two or more times to get the pattern clearer. Besides, to make the colours of dark-coloured patterns printed on dark-coloured bases more clearly visible, a printing paste is used. In addition to these challenges, in the apparel industry, the designers give priority to the garment design over the clothing comfort as well as the producibility of the garment. Therefore, as in the objective of the study, the dark blue base fabric was determined for the results obtained to guide the designers as well as the manufacturers.

Table 1

THE PHYSICAL PROPERTIES OF FABRICS			
Sample number	**Raw materials**	**Yarn number (Ne)**	**Knitting structure**
Fabric 1	50% Co – 50% PES	30/1	Single Jersey
Fabric 2	50% Co – 50% PES	30/1	1x1 Rib
Fabric 3	50% Co – 50% PES	30/1	Pique

Pigment printing, which dominates the piece printing market in the apparel industry, is the printing type with the lowest cost and is highly preferred in the textile industry because the processing time is quite fast and does not harm the environment [21]. Moreover, it was indicated that all finishing processes affect the feel of the fabric in terms of increasing roughness, but that pigment printing what's the most effective and the most widely used bare finish process [17].
However, a review of the literature revealed that they were not a sufficient number of studies conducted on the effect of pigment printing on fabric handle properties including surface kinetic friction coefficient and bending properties. Therefore, taking into account various fabric structures, printing patterns and various pigment printing types, the effects of the pigment printing process extensively used in the industry on the physical properties and sensorial comfort properties of the fabric were investigated in this study.
In light of this information, the print parameters are displayed in table 2. As mentioned before, since it is difficult to print a lighter colour on a darker base, two layers of white printing paste (PT3) and one layer of black printing paste (PT2) were used. In addition, in emboss printing, it was stated by the manufacturers that the most preferred colour is white, therefore the print colour was chosen as white (PT1).
In the apparel industry, printing patterns are infinite and thousands of new patterns are designed every day. Moreover, the printing patterns' dimensions vary regarding the printing area as well as the body size. Therefore, investigating the effect of print patterns on clothing comfort is of challenge, as almost impossible to simulate all printing patterns. Thus, to achieve an evaluation of the effect of printing on sensorial comfort, two different patterns were determined (figure 1); a striped pattern of 1 cm print + 1 cm space (PP1) and a solid square pattern (PP2). The print area dimension was set at 20*20 cm to simulate larger print patterns and also to capture the measuring areas of the testing instruments. Table 3 presents all acquired samples; two different patterns printed on three knit fabrics of different constructions using three different printing pastes, including the control groups. Sample fabrics were prepared as 30*30 cm dimensions.

Print pattern code PP1   Print pattern code PP2

Fig. 1. Samples for PP1 and PP2

Table 2

PRINT PARAMETERS			
Print type code	**Printing recipe**	**Printing process**	**Printing machine**
PT 1	• 50 g/kg White Waterbased Pigment Print (Sp 240 by Antex / Anadolu Kimya) • 50 g/kg Emboss Waterbased Pigment Print (Sp 280 by Antex / Anadolu Kimya)	Printing + Fixing (160°C 2–2.5 minutes)	ROQ Oval Evolution P40 XL-18 Head
PT 2	• 48 g/kg Waterbased Pigment Print Base (XP 10 by Antex / Anadolu Kimya) • 48 g/kg Transparent Waterbased Pigment Print (Sp 220 by Antex / Anadolu Kimya) • 4 g/kg Black Waterbased Pigment Print (Fa 3010 by Antex / Anadolu Kimya)	Printing + Fixing (160°C 2–2.5 minutes)	
PT 3	• 90 g/kg White Waterbased Pigment Print (Sp 240 by Antex / Anadolu Kimya) • 10 g/kg Transparent Waterbased Pigment Print (Sp 220 by Antex / Anadolu Kimya)	First layer Printing + Drying (70–80°C/7–8 seconds) + Second layer Printing + Fixing (160°C 2–2.5 minutes)	

Table 3

EXPERIMENTAL GROUPS			
Sample number	**Knitting structure**	**Print type code**	**Print pattern code**
1	Single Jersey	without print	without print
2		PT 1	PP1
3			PP2
4		PT 2	PP1
5			PP2
6		PT 3	PP1
7			PP2
8	1*1 Rib	without print	without print
9		PT 1	PP1
10			PP2
11		PT 2	PP1
12			PP2
13		PT 3	PP1
14			PP2
15	Pique	without print	without print
16		PT 1	PP1
17			PP2
18		PT 2	PP1
19			PP2
20		PT 3	PP1
21			PP2

Method

Before performing the tests, all samples were conditioned for at least 24 hours in standard atmosphere conditions (constant ambient temperature of 20±2 ºC, relative humidity of 65±2%) (TS EN ISO 139).

Mass per unit area and thickness

The mass per unit area weight of the samples they're measured in five repetitions according to TS EN 12127 standards. The thickness test for the samples was performed in accordance with TS 7128 EN ISO 5084 standards.

Paste add-on

Paste add-on values are one of the important factors that determine the quality of the print. Paste add-on values were calculated using equation 1 [23]:

$$Paste\ add\text{-}on = \frac{E_2 - E_1}{A} \quad (1)$$

Where E_2 is the after-printing weight of the fabric samples, E_1 – the before-printing weight of the fabric samples, and A – the area of samples.

Colour measurement values

The L^*, a^*, b^* values of printed fabrics were measured using a HunterLab UltraScan PRO spectrophotometer. The colour difference values (ΔE) of the samples were calculated by reference to the back side of the unprinted sample and using equation 2 [23, 24].

$$\Delta E = \sqrt{(\Delta L^*)^2 + (\Delta a^*)^2 + (\Delta b^*)^2} \quad (2)$$

where ΔE is the colour difference value, L^* – the brightness value, a^* – red/green colour value, b^* – yellow/blue colour value.

Air permeability

Air permeability is an important property, which determines the ability of air to flow through the fabric. Ten repetitions were conducted for each fabric using the Textest FX 3300 air permeability instrument (Textest Instruments AG, Switzerland) at a pressure of 100 Pa in a 5 cm^2 measurement area according to TS 391 EN ISO 9237 standards.

Compressibility

The response of fabric thickness to the forces applied perpendicular to its surface is known as the fabric compressibility behaviour. The fabric compatibility tests the performed via digital thickness gauge in 5 repetitions for each experimental group. To determine the thickness loss that occurred in the samples, compression values were measured during the dynamic loading/charging process. The compression values of weights were coded from A to G in a way to indicate the total compression value. The pressure values applied by the presser foot without extra weight were as follows; 2 kPa, A: 5 kPa, B: 10 kPa, C: 20 kPa, D: 50 kPa, E: 100 kPa, F: 150 kPa, G: 200 kPa. During the measurement of compressibility, the measurement was started as the presser foot was logged word onto the sample, the weights were carefully added one by one, and the thickness for each weight was recorded.

Kinetic friction coefficient

The kinetic friction coefficient is one of the significant indicators in determining fabric handle [25, 26]. For the measurement of the fabric kinetic friction coefficient, the Frictorq (Fabric friction tester) device was used. The Frictorq device uses rotation momentum to determine the kinetic friction coefficient of the fabric [27]. Measurement of five repetitions was performed for each fabric in accordance with ISO 21182 standards. Following the measurement, the kinetic friction coefficient value (μkin) was calculated using rotation power values varying throughout the movement of the device lasting for 20 seconds.

Circular bending rigidity

The circular bending rigidity tests for the fabrics were performed according to ASTM D 4032. According to this method, the force resulting from the act of the simple fabric being pushed through a circle with the help of a piston is measured as an indicator of the bending feature of the fabric [17]. In this process, the maximum force required to push the fabric through the hole is an indicator of Fort fabric rigidity (resistance to bending) [28].

Statical analyses

SPSS software was used for the statistical analysis of the data acquired in the study. One Way Anova and univariate tests were performed to investigate the individual effects of each parameter and interaction on thickness, kinetic friction coefficient, circular bending rigidity and air permeability. Post hoc analyses were made using the Duncan test to determine which mean values of the groups were significant. All test results were considered at a 0.05 significance level.

RESULTS AND DISCUSSION

The mean values of the test results for the group used in the experiment conducted to investigate the effect of printing on sensorial comfort are presented in table 4.

Mass per unit area

The mean mass per unit area data for the samples is included in table 4. When the data is considered, the highest values for mass per unit area were observed as expected in samples that were printed by PT3 resulting from the two-layered printing structure. The PT3 printing type is followed by PT1 and PT2 printing types. The statistical analysis of the data indicates that the difference between samples without printing and those with printing in terms of weight is statistically significant (p = 0,000); however, the difference between PT1 and PT2 (p = 0.963), the difference between PT1 and PT3 (p = 0,999) and the difference between PT2 and PT3 (p = 1.000) are not statistically significant.

Thickness

There is a significant relationship between fabric thickness and compressibility behaviour and feel, fluidity, comfort and thermal insulation [29, 30]. It was observed that the mean thickness values for fabric samples ranged between 0.429 mm and 1.141 mm (table 4). According to the Oneway Anova test, the effect of the fabrics' knit structure (p = 0.001), printing type (p = 0.000) and printing pattern (p = 0.000) on fabric thickness is statistically significant. For all three knit structures, it was observed that the PT1 printing type had the highest values in terms of thickness and this is considered to stem from the fact that the PT1 printing type is embossed printing. The samples printed according to PT3 and PT2 printing types were also observed to follow these samples. Considering thickness in the statistical analysis conducted, the difference between printing types is statically significant; the difference between PT1 and PT2 at (p = 0.000), the difference between PT1 and PT3 at (p = 0.000) and the difference between PT2 and PT3 at (p = 0.006). On the other hand, there was no significant difference between PP1 and PP2 patterns.

Paste add-on

The paste add-on values of samples are given in table 5. When the data were analyzed, the highest values for the paste add-on were seen in the samples printed with PT3, as expected. It is thought that this situation is caused by the double-layer printing in the

Table 4

MEAN VALUES OF THE TEST RESULTS

Sample number	Knit structure	Print type	Print pattern	Mass per unit-area (g/m^2)	Thickness (mm)	Relative compress-ibility (%)	Friction coefficient (μkin)	Circular bending rigidity (N)	Air permeability (l/m^2/s)
1	Single Jersey	without print	without print	151	0.429	0.388	0.344	3.08	659.1
2		PT1	PP1	198.9	0.770	0.321	0.383	13.65	292.1
3			PP2	230.4	0.570	0.319	0.302	35.45	0
4		PT2	PP1	175.3	0.501	0.354	0.254	3.87	309.0
5			PP2	199.6	0.499	0.339	0.227	7.87	171.2
6		PT3	PP1	249.5	0.529	0.297	0.343	6.30	305.4
7			PP2	314	0.504	0.256	0.395	29.00	0
8	1*1 Rib	without print	without print	188.4	0.656	0.447	0.379	4.12	963.0
9		PT1	PP1	262.5	0.964	0.329	0.530	25.02	381.4
10			PP2	289.8	0.807	0.286	0.184	58.80	0
11		PT2	PP1	223.7	0.743	0.406	0.207	7.44	513.7
12			PP2	243	0.731	0.336	0.144	12.10	409.5
13		PT3	PP1	324.2	0.797	0.345	0.281	11.65	448.3
14			PP2	399.6	0.744	0.300	0.335	43.66	0
15	Pique	without print	without print	210	0.736	0.438	0.354	4.88	696.1
16		PT1	PP1	269.5	1.141	0.346	0.498	34.44	314.2
17			PP2	298.8	0.844	0.299	0.444	66.24	0
18		PT2	PP1	236	0.772	0.434	0.294	8.43	445.4
19			PP2	256.2	0.763	0.359	0.257	13.66	394.9
20		PT3	PP1	333.8	0.825	0.343	0.384	34.23	325.2
21			PP2	406.9	0.778	0.331	0.271	48.69	0

PT3. This printing type is followed by PT1 and PT2 printing types, respectively. It is also seen that PP1 has lower values than PP2 due to its grid structure. When Paste add-on values are examined in terms of knitting structure, it is seen that the highest values are obtained in 1*1 Rib knitting structure in all three printing types, followed by Pique and single jersey fabrics, respectively.

Table 5

THE PASTE ADD-ON VALUES OF SAMPLES			
Knit structure	**Print type**	**Paste add-on values**	
		PP1	**PP2**
Single Jersey	PT1	47.9	79.4
	PT2	24.3	48.6
	PT3	98.5	163
1*1 Rib	PT1	74.1	101.4
	PT2	35.3	54.6
	PT3	135.8	211.2
Pique	PT1	59.5	88.8
	PT2	26	46.2
	PT3	123.8	196.9

Colour measurement values

The colour measurement and DE values of the back sides of fabrics are given in table 6. When the literature is examined, it is seen that if the ΔE value is less than "1", it is assumed that there is no colour difference between the samples [23].

When the data were examined, it was observed that the lowest ΔE values were obtained in the 1*1 Rib knit structure. In the rib knit structure, ΔE values were found to be lower than "1" in PT2 (0.83) and PT3 (0.96) print types, and it can be said that there is no colour difference between the back surface of the fabric and the unprinted fabric in these two print types. It was seen that ΔE values were close to "1" in PT2 (1,12) and PT3 (1.16) print types in the pique knit structure. For single jersey knit structure, the ΔE values obtained in PT1 (3.84) and PT3 (2.89) print types were greater than "1", which indicates that there is a colour difference between the back surface of the fabric and the unprinted fabric in these two print types. In the single jersey knit structure, the ΔE value is close to "1" in the samples obtained with the PT2 (1.05) print type, unlike the other two print types. This shows that there is no colour difference between the back surface of the fabric and the unprinted fabric in the PT2 print type in a single jersey knit structure. As a result, in all three knitting structures, the lowest ΔE values were reached with the PT2 printing type, and the highest ΔE values were reached with the PT3 printing type (table 6). When are all the samples are considered for three types of a knit structures, the lowest penetration of printing paste into the fabric was found to be in 1*1 Rib fabrics.

Table 6

COLOUR MEASUREMENT VALUES OF PRINTED FABRICS (BACK SIDE)					
Knit structure	**Print type**	**Colour values (back side)**			
		L*	**a***	**b***	**DE**
Single Jersey	WP	32.71	3.25	–34.39	-
	PT1	36.51	3.02	–34.83	3.84
	PT2	32.11	2.79	–33.66	1.05
	PT3	35.35	3.33	–35.8	2.99
1*1 Rib	WP	33.57	1.6	–33.19	-
	PT1	36.29	1.52	–33.97	2.83
	PT2	32.76	1.42	–33.32	0.83
	PT3	33.52	1.98	–34.06	0.96
Pique	WP	32.88	2.96	–34.6	-
	PT1	33.2	3.14	–36.14	1,58
	PT2	31.87	2.93	–35.07	1.12
	PT3	32.69	3.32	–35.69	1.16

Air permeability

The mean values of air permeability for the samples are displayed in table 4 and the graph created by taking the mean values into account is shown in figure 2.

The properties that displayed a statistically significant impact on the air permeability of the fabrics within the experimental group were observed as knit structure (p = 0.006), printing type (p = 0.000) and printing pattern (p = 0.000).

Univariate tests were conducted to determine the effect of print type and print pattern on air permeability

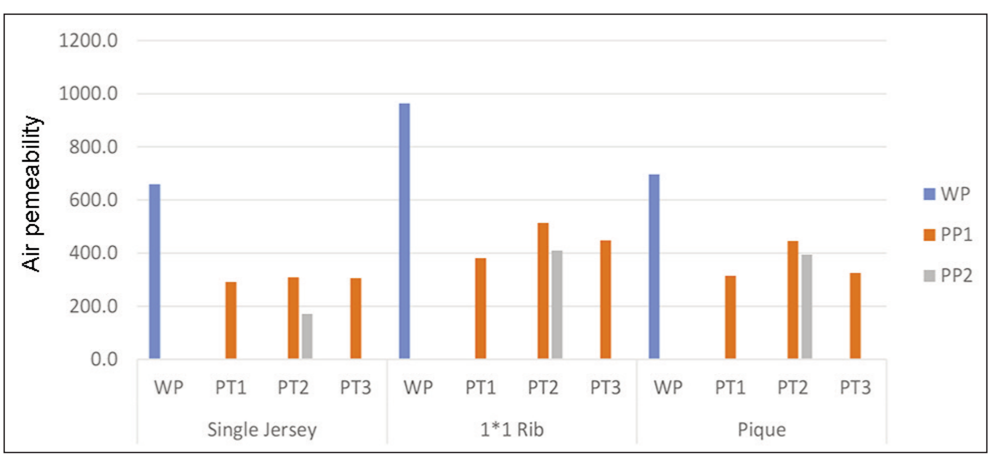

Fig. 2. Air permeability values of samples

according to the types of fabric. The results achieved revealed that the effect of print type (p = 0.000) and knit structure (p = 0.000) on air permeability values were significant (table 7). Moreover, the effect of print type and knit structure interaction on air permeability is statistically significant (p = 0.000). It is believed that, since both print material (observed power: 1.000) and knit structure (observed power: 1.000) have very powerful effects, the interaction between these two variables also becomes significant. When air permeability values are analyzed by taking into account the knit structure, it is seen that the air permeability of the rib knit structure this higher than the other knit structures, similar to what Selli and Turhan [31] found in their study (figure 2).

Air permeability is a test result that is related to the porousness of the fabric [32]. The reason why the highest values are found in rib knit fabrics is thought to be because this type of fabrics has higher porousness because of their different thickness and volume properties.

The interaction between print pattern and knit structure was statistically significant, similar to the interaction of print type and knit structure, due to the dominant effect of the parameters (table 7).

Table 7

THE UNIVARIATE ANALYSIS RESULTS: AIR PERMEABILITY

Source	Air permeability		
	F	Sig.	Observed power
Print type	150.696	0.000	1.000
Knit structure	21.254	0.000	1.000
Print type * Knit structure	4.202	0.001	0.977
Print pattern	33.071	0.000	1.000
Knit structure	393.520	0.000	1.000
Print pattern * Knit structure	5.737	0.000	0.980

According to the univariate test results where print pattern and knit structure were taken as parameters and their effect on air permeability was investigated, it is observed that the impact of print pattern and knit structure on air permeability is statistically significant. Analysis of air permeability values supports that the air permeability without printed fabrics is much higher than printed fabrics and that the printing process significantly decreases air permeability. It is considered that this results from the fact that the print material covers the pores of the fabric in a way to prevent air permeability. PT1 and PT3 samples printed with PP2 patterns were observed to permeate no air in all three knit structures. On the other hand, samples printed with the PP1 pattern were considered to have air permeability through the pattern's spaced parts, but not through the printed parts. Regarding the PT2 print type, air permeability values were able to be measured for both patterns and this was the print type with the highest level of air permeability among all three print types.

According to the Duncan test done to compare air permeability with regard to print types, three different subsets were formed. According to the achieved results, the samples printed with the PT1 print type had the lowest air permeability values for all three knit structures, but the PT1 and PT3 print types displayed no statistically meaningful difference (p = 0.934) and were placed in the same subset (table 8). When the results are analyzed, it can be observed that the air permeability value presents a steep decline in all three print types compared to nonprint fabrics, and the difference between nonprinted and printed fabrics is significant (p = 0.000).

Table 8

MULTIPLE COMPARISONS OF AIR PERMEABILITY VALUES

Print type	N	Air permeability		
		Subset		
		1	2	3
PT1	60	164.62		
PT3	60	179.82		
PT2	60		373.95	
without print	30			772.73
Sig.		0.597	1.000	1.000

Kinetic friction coefficient

The mean values of the kinetic friction coefficient for the samples are displayed in table 4 and the graph created by taking the mean values into account is shown in figure 3.

The analysis of the data belonging to the sample's kinetic friction coefficient reveals that the PT2 print type has the lowest values (0.144–0.294) for all three knit structures (table 4). The lower the kinetic friction coefficient is, the smoother the product is [33]. Therefore, it is deduced that smoother products were

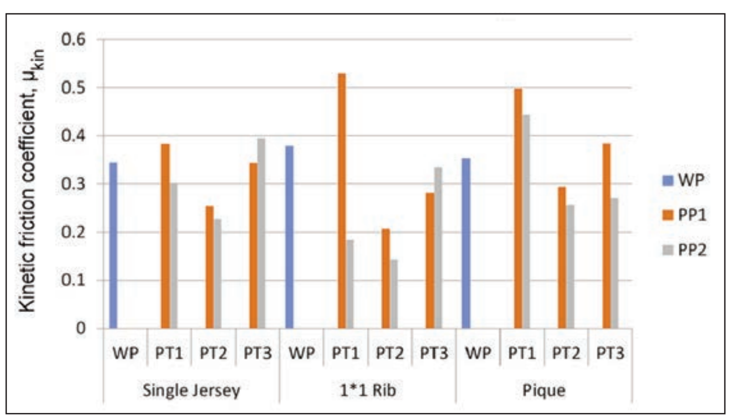

Fig. 3. Kinetic friction coefficient values of samples

Table 9

THE UNIVARIATE ANALYSIS RESULTS: KINETIC FRICTION COEFFICIENT			
Source	Kinetic friction coefficient		
	F	Sig.	Observed power
Print type	21.188	0.000	1.000
Knit structure	3.412	0.037	0.629
Print type * Knit structure	2.628	0.021	0.836
Print pattern	6.475	0.002	0.897
Knit structure	1.381	0.256	0.291
Print pattern * Knit structure	1.561	0.191	0.466

achieved through the PT2 print type compared to the other printing types involved in the study. The statistical analysis of print types shows that in terms of kinetic friction coefficient, the difference between PT1 and PT2 ($p = 0.000$), the difference between PT1 and PT3 ($p = 0.047$) and the difference between PT2 and PT3 ($p = 0.000$) were statistically significant.

The analysis of print patterns reveal starts the difference between the print patterns used in the study is statistically significant ($p = 0.004$). It was observed that due to its striped structure, PP1 caused the roughness value to increase and that, especially the embossed print structure off the PT1 print type enhanced this increase (figure 3). Moreover, it is believed that the lower value of PP2 led to the perception that the roughness of the solid pattern was lower.

According to the results of the Oneway Anova test conducted, it was observed that the effects of the knit structure ($p = 0.045$), the print type ($p = 0.003$) and the print pattern ($p = 0.045$) on the kinetic friction coefficient are statistically significant.

The statistical data regarding the effect of print type and print pattern on kinetic friction coefficient according to types of fabric are presented in table 9.

Upon analysis of the print type and knit structure on kinetic friction coefficient values, it was detected that the difference between print types ($p = 0.000$) and knit structure ($p = 0.037$), and as a result, the difference between their interactions ($p = 0.021$) were statistically significant (table 9). According to the results of the univariate test conducted to determine the parameters of print pattern and knit structure on kinetic friction coefficient values, it was observed that while the effect of print pattern on kinetic friction coefficient values is statistically significant, the difference between knit structure and therefore, the interaction between the two variables ($p = 0.191$) was not statistically significant (table 9).

Relative compressibility

As the starting thickness values of the samples are different from each other, to compare their compressibility accurately, their relative compressibility values were taken into account and calculated according to the following formula [34, 35]:

$$\text{Relative compressibility (\%)} = (h_2 - h_1) / h_2 * 100 \quad (3)$$

Where h_2 is the thickness of fabric under low weight (A: 5 kPa) and h_1 – the thickness of fabric under higher weight (G: 200 kPa).

The relative compressibility values calculated according to the gathered data are shown in table 4 and graph in figure 4. Upon analysis of the relative compressibility values of the samples, WP was observed to be higher, and thus, it was concluded that the printing process has an effect that decreases the relative compressibility of the material.

The values belonging to printed samples have revealed that the values for the samples prepared with the PT2 print type were higher than the other two print types. In addition, the analysis done in terms of print patterns has indicated higher values for the PP1 print pattern. According to these results, it is possible to conclude that in terms of the ability to absorb more energy during the compression process, the PT2 print type is more efficient than the other print types that add a PP1 print pattern than PP2.

Circular bending rigidity

The mean values of circular bending rigidity for the samples are displayed in table 4 and the graph created by taking the mean values into account is shown in figure 5.

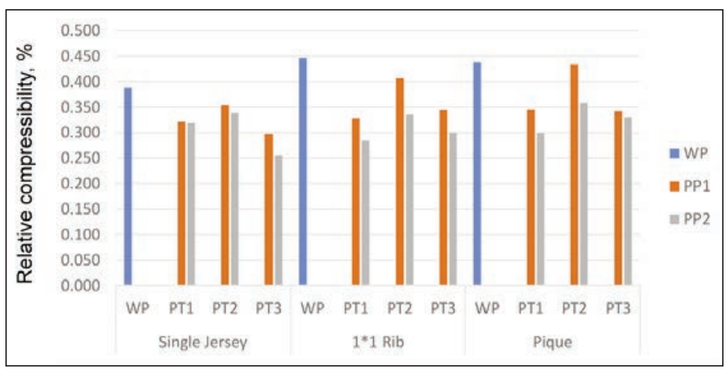

Fig. 4. Relative Compressibility values of samples

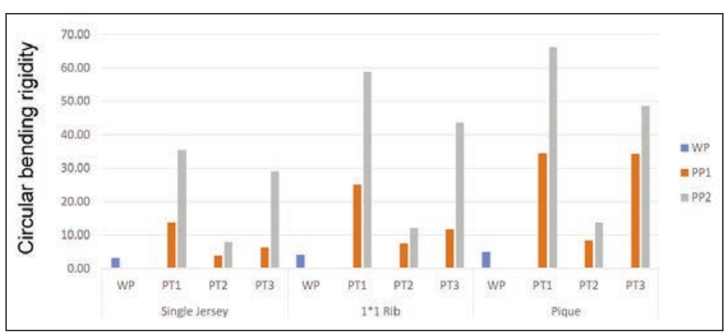

Fig. 5. Circular bending rigidity values of samples

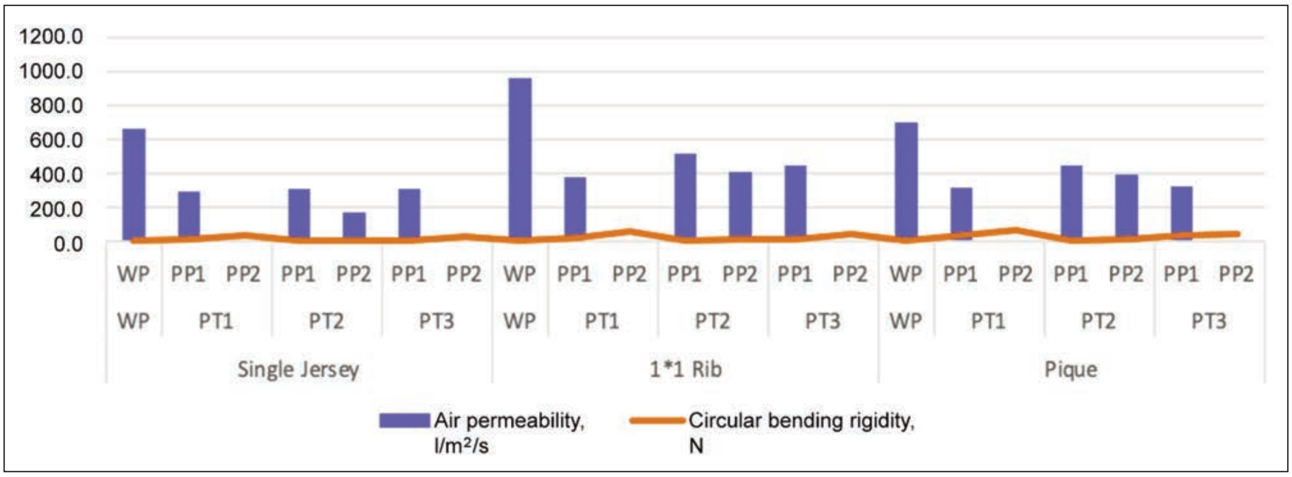

Fig. 6. Air permeability versus circular bending rigidity

The bending behaviour of fabric it's highly significant for fabric producers, garment designers and in apparel production [28]. The analysis of test results shows that the highest values were observed for PT1 print type for all three knit structures and the lowest values were found for PT2. As the bending rigidity of a fabric increases, so does the stiffness of the material [34]. When the fabric is stiffer, the handle of the fabric worsens [36]. Therefore, it can be observed that the materials printed which PT2 were softer than the others. It is believed that the embossed print structure causes the material to become stiffer. In terms of a knit structure, the lowest values were presented for single jersey fabrics and therefore, the stiffness of these materials was lower than the other knit structures, and the highest values were observed in pique fabrics. Consequently, it can be stated that the samples printed on pique fabrics are stiffer than the other samples. Statistical consideration of the gathered data, and regarding Oneway Anova test results, revealed that the effect of a knit structure, print type ($p = 0.000$) and print pattern ($p = 0.000$) on circular bending rigidity were statistically significant.

It is observed that the difference between without printed samples and PT2 print type is statistically insignificant ($p = 0.511$). When the difference between print types is investigated, it is observed that the difference between PT1 and PT2 ($p = 0.000$), the difference between PT1 and PT3 ($p = 0.004$) and the difference between PT2 and PT3 ($p = 0.000$) were statically significant.

Moreover, the difference between print patterns is statistically significant ($p = 0.000$). For each print type, the PP1 print pattern presented lower values than PP2. It is believed that the fact that the PP2 print pattern is applied to the whole surface increases circular bending rigidity and therefore, causes the material to become stiff.

To determine the effects of print type and print pattern on circular bending rigidity according to knit structure, univariate tests were conducted (table 10).

Analysis of print type and knit structure on circular bending rigidity shows that the difference between

Table 10

THE UNIVARIATE ANALYSIS RESULTS: CIRCULAR BENDING RIGIDITY

Source	Circular bending rigidity		
	F	Sig.	Observed power
Print type	13.054	0.000	0.997
Knit structure	54.061	0.000	1.000
Print type * Knit structure	2.720	0.018	0.850
Print pattern	5.709	0.005	0.855
Knit structure	36.174	0.000	1.000
Print pattern * Knit structure	1.056	0.382	0.322

print types ($p = 0.000$) and the difference between knit structures ($p = 0.000$) are statistically significant, and it is believed that the effects of the print material (observed power: 0.997) and the knit structure (observed power: 1.000) are very strong, resulting in the fact that the interaction of these two variables also become significant ($p = 0.018$) (table 10).

According to the univariate test results where the effects of the parameters of print pattern and knit structure on circular bending rigidity were investigated, it was observed that while the effects of the print pattern ($p = 0.005$) and knit structure ($p = 0.000$) on circular bending rigidity were statistically significant, the interaction between the two variables ($p = 0.382$) was not (table 10).

As filaments in fabrics with more fluidity will move more freely, air permeability is more easily allowed [37]. In support of the literature, samples with low circular bending rigidity values, and thus, higher fluidity, displayed higher air permeability values (figure 6).

CONCLUSION

In recent years, customer demands in the fashion and apparel sectors have increased, just as in all other sectors, and the comfort of the produced garment is present as a significant factor in the purchasing decision. It is important to avoid subprocesses like printing, which is one of the aesthetic and design properties of a garment and does not impose a negative effect on the physical and comfort properties of the garment. Printing is an especially important subprocess in the adornment of knit garments. This study focused on pigment printing, which is highly preferred in the textile industry since it is the lowest cost print type, the processing time is quite fast and it is environmentally friendly [21].

Based on this research the following conclusions can be drawn out:

- Regarding the test results of PT1, which was applied as a single layer, it had the highest thickness in all three knitting structures and the air permeability values were lower than the PT2 and PT3. Therefore, it is recommended not to be used in patterns that cover a large surface, particularly in the chest and back areas of the garment where sweating is intense, especially in summer clothes. In addition, it is recommended not to use this printing type, especially in 1*1 rib fabric structure, since the surface friction coefficients of the samples prepared with PT1 were higher than other printing types, thus a rougher surface was obtained. Moreover, it was observed that the bending rigidity of the samples prepared using PT1 printing paste was higher than the others. This reveals that the samples obtained with this printing paste are stiffer than the others. Consequently, it is recommended that this printing paste, which is used to achieve special effects, should be used in small-sized patterns.
- The analyses made regarding the conducted tests revealed that the print type coded as PT2 presented the best results in terms of kinetic friction coefficient, compressibility and circular bending rigidity, which impact the physical properties, air permeability and sensorial comfort of the fabric. In addition, especially in 1*1 rib and pique fabrics, this type of printing causes the lowest penetration to the back side of the fabric.
- For PT3, concerning results obtained, it was observed that the highest values for the mass per unit showed by these samples due to the double-layer printing structure, as expected. It was understood that the air permeability values of the samples obtained with this printing type were similar to those obtained with PT1 and that airflow did not occur, especially in large-area patterns. It has been observed that this printing type had higher values compared to the unprinted samples in terms of handle properties such as smoothness and stiffness. For this reason, it is recommended to choose small-sized print patterns for garments in which this print type will be used and to choose a light colour base in the designs that are desired to be smooth and soft, since they are applied in double layers to cover the dark coloured bases.
- Likewise, it was observed that the PP1 print pattern, which did not cover the whole surface due to its striped structure, displayed better values in terms of air permeability, compressibility and circular bending rigidity.

Considering the results, it is recommended that the print type and print pattern to be used in the clothing design step should be chosen to not cause problems in terms of sensorial comfort. PT2 print type could be prioritized for areas that may face a higher level of compression due to its space of use such as the back piece of the garment and when PT1 and PT3 print types are to be used, the print area should not be too large and not to cover the surface completely with printing paste in the patterns created, and to design patterns so that the ground fabric can be seen. It is believed that the conducted study wheel assists fashion designers and apparel producers in terms of print design.

REFERENCES

[1] Öner, E, Okur, A., *Materyal, Üretim Teknolojisi ve Kumaş Yapısının Termal Konfora Etkileri*, In: Textile and Engineer, 2010, 17, 80

[2] Nawaz, N., Troynikov, O., Watson, C., *Evaluation of surface characteristics of fabrics suitable for skin layer of firefighters' protective clothing,* In: Physics Procedia, 2011, 22, 478–486

[3] Çivitci, Ş., Dengin, S., *Koşu Giysileri Konforunun Kullanıcılar Tarafından Değerlendirilmesi Üzerine Bir Araştırma,* In: International Journal of Sport Culture and Science, 2016, 2 (Special Issue 1), 553–569

[4] Bilgi, M., Kalaoğlu, F., *Özel Apre Tekniklerinin Askeri Kumaşların Performans ve Konforu Üzerindeki Etkileri*, In: Textile and Apparel, 2010, 20, 4

[5] Atalie, D., Rotich, G.K., *Impact of cotton parameters on sensorial comfort of woven fabrics*, In: Research Journal of Textile and Apparel, 2020, 24, 3, 281–302

[6] Tadesse, M.G., Loghin, C., Dulgheriu, I., Loghin, E., *Comfort Evaluation of Wearable Functional Textiles,* In: Materials, 2021, 14, 6466

[7] Marmaralı, A., Oğlakçıoğlu, N., *Giysilerde Isıl Konfor*, In: 11. Ulusal Tesisat Muhendisliği Kongresi, , İzmir, Turkey, 2013, 1957–1963

[8] Bartkowiak, G., Frydrych, I., Komisarczyk, A., Greszta, A., *Fabric Selection for the Reference Clothing Destined for Ergonomics Test of Protective Clothing – Sensorial Comfort Point of View,* In: Autex Research Journal, 2017, 17, 4, 303–312

[9] Kayseri, G.Ö., Özdil, N., Menguç, G.S., *Sensorial comfort of textile materials Woven fabrics,* In: InTech, 2012, 235–266

[10] Nayak, R., Kanesalingam, S., Houshyar, S., Wang, L., Padhye, R., Vijayan, A., *Evaluation of thermal, moisture management and sensorial comfort properties of superabsorbent polyacrylate fabrics for the next-to-skin layer in firefighters' protective clothing*, In: Textile Research Journal, 2018, 88, 9, 1077–1088

[11] Atalie, D., Ferede, A., Rotich, G.K., *Effect of weft yarn twist level on mechanical and sensorial comfort of 100% woven cotton fabrics,* In: Fash. Text., 2019, 6, 3
[12] Behera, B.K., Mishra, R., *Comfort properties of non-conventional light weight worsted suiting fabrics*, In: Indian Journal of Fibre and Textile Research, 2007, 32
[13] Kaplan, S., Okur, A., *The meaning and importance of clothing comfort: A case study for Turkey,* In: Journal of Sensory Studies, 2008, 23, 5, 688–706
[14] Süpüren, G., Ozdil, N., Leskovsek, M., Demsar, A., *Surface properties of wool and various luxury fibres*, In: Fibre Society Spring Conference, Bursa, Turkey, 2010, 12–14
[15] Salman, M., Iftikhar, F., Khan, M.O., Tanveer, H., Naseer, A., Fazal, M.Z., Javed, Z., Naeem, M.S., *Development and Characterization of Knitted Fabrics for Better Sensorial Comfort Properties in Sportswear by Using Grey Rational Analysis*, In: Journal of Natural Fibres, 2021, 1–15
[16] Ajayi, J.O., *Fabric Smoothness, Friction, and Handle,* In: Textile Research Journal, 1992, 62, 52–59
[17] Özgüney, A.T., Taşkın, C., Özçelik, G., Gürkan Ünal, P., Özerdem, A., *Handle Properties of the Woven Fabrics Made of Compact Yarns*, In: Textile and Apparel, 2009, 19, 2, 108–113
[18] Robinson, K.J., Chambers, I.V.E., Gatewood, B.M., *Influence of pattern design and fabric type on the hand characteristics of pigment prints*, In: Textile Research Journal, 1997, 67, 11, 837–845
[19] Jeguirim, S.E.G., Dhouib, A.B., Sahnoun, M., Cheikhrouhou, M., Njeugna, N., Schacher, L., Adolphe, D., *The tactile sensory evaluation of knitted fabrics: effect of some finishing treatments*, In: Journal of Sensory Studies, 2010, 25, 2, 201–215
[20] Hees, U., Freche, M., Kluge, M., Provost, J., Weiser, J., *Developments in textile ink jet printing with pigment inks*, In: In NIP & Digital Fabrication Conference, Society for Imaging Science and Technology, 2002, 1, 242–245
[21] Jiang, J., Shen, Y., Yu, D., Wu, M., Yang, L., Li, S., *Sustainable washing□free printing of disperse dyes on polyester fabrics enabled by crosslinked fluorosilicone modified polyacrylate binders*, In: Polymers for Advanced Technologies, 2021, 32, 2, 641–650
[22] Yüksel, D., *Farklı Özelliklerdeki Tekstil Desenlerinin Günümüzdeki Baskı Stilleri ile Basılması*, Doctoral dissertation, Marmara University Turkey, 2010, 261478
[23] Çatal, D.O., Özgüney, A.T., Kumbasar, E.P.A., *The influence of rheological properties of the pretreatment thickeners on ink-jet printing quality,* In: Textile and Apparel, 2012, 22, 4, 309–316
[24] Özomay, M., Özomay, Z., *The effect of temperature and time variables on printing quality in sublimation transfer printing on nylon and polyester fabric*, In: Avrupa Bilim ve Teknoloji Dergisi, 2021, 23, 882–891
[25] Lima, M., Hes, L., Vasconcelos, R., Martins, J., *Frictorq, a novel fabric surface tester: A progress report*, In: Journal of Textile Engineering, 2005, 51, 3+4, 40–46
[26] Lima, M., Vasconcelos, R., Abreu, M.J.A.M., Silva, M.E., *Comparative study of friction coefficient in nonwovens usin frictorq, fabric friction tester*, In: Proceedings of the 6th AUTEX 2006 Conference, 2006
[27] Süpüren Mengüç, G., Özçelik Kayseri, G., Özdil, N., *Yün içeren çeşitli kumaşlarin pürüzlülük özelliğinin incelenmesi*, In: Textile and Engineer, 2019, 26, 116, 360–364
[28] Eryürük, S.H., Kalaoğlu, F., Bahadır, S.K., Sarıçam, C., Jevsnık, S., *The evaluation of stiffness and drape behaviour of wool fabrics,* In: Textile and Engineer, 2015, 22, 98
[29] Majumdar, A., Saha, S.S., *A novel fabric thickness and compression tester using magnetic inductance principle,* In: Journal of the Textile Institute, 2008, 99, 4, 359–362
[30] Yıldız, E.Z., Özdil, N., *Subjective and objective evaluation of the handle properties of shirt fabric fused with different woven interlinings*, In: Textile and Apparel, 2014, 24, 1, 47–55
[31] Selli, F., Turhan, Y., *Investigation of air permeability and moisture management properties of the commercial single jersey and rib knitted fabrics*, In: Textile and Apparel, 2017, 27, 1, 27–31
[32] Sitotaw, D.B., *Effect of Twist Multipliers on Air Permeability Property of Single Jersey and Rib 1x1 Knitted fabrics*, In: Journal of Textile and Apparel Technology and Management, 2016, 10, 1
[33] Özgen, B., Altaş, S., *The investigation of thermal comfort, moisture management and handle properties of knitted fabrics made of various fibres*, In: Textile and Apparel, 2014, 24, 3, 272–278
[34] Mengüç, G.S., Özgüney, A.T., Dalbaşi, E.S., Özdil, N., *A comparative study on handle properties of bamboo and cotton fabrics*, In: Industria Textila, 2019, 70, 3, 278–284, http://doi.org/10.35530/IT.070.03.1538
[35] Özdil, N., Bozdoğan, F., Özçelik Kayseri, G., Süpüren Mengüç, G., *Compressibility and Thickness Recovery Characteristichs of Carpets*, In: Journal of Textile and Apparel, 2012, 22, 3
[36] Özçelik, G., Süpüren, G., Gülümser, T., Tarakçıoğlu, I., *A Study on Subjective and Objective Evaluation of the Handle Properties of Shirt Fabrics,* In: Fibres and Textiles in Eastern Europe, 2008, 16, 3, 56–62
[37] Kaynak, H.K., Babaarslan, O., *Investigation of the effects of filament fineness on the performance properties of microfibre knitted sportswear fabrics,* In: Textile and Engineer, 2010, 17, 78, 20–24

Author:

ARZU KILIÇ

Ege University, Fashion and Design Faculty, Department of Fashion Design, Bornova, İzmir, Türkiye

Corresponding author:

ARZU KILIÇ
e-mail: arzu.senkilic@ege.edu.tr

Non-invasive analytical methods applied in the study of cultural heritage artefacts

DOI: 10.35530/IT.074.03.202220

BAHODIR SAFAROV
LILIANA INDRIE
MONICA COSTEA
ALEXANDRU TURZA
KOMIL AVAZOV
STEFAN BAIAS
DORINA CAMELIA ILIEȘ
MIHAELA ZDRINCA
EMILIA PANTEA
GABRIELA ILIEȘ
NICOLAIE HODOR
ANA CORNELIA PERES

ABSTRACT – REZUMAT

Non-invasive analytical methods applied in the study of cultural heritage artefacts

Ethnographic heritage textiles may be subject to risks generated in particular by various factors in close connection with the microclimate of the storage and exposure areas. In accordance with the current European trends of pest prevention and reduction and response to the infestation/contamination of the cultural heritage, the research direction of this study aimed at investigating the degradation of some women's clothing items, around 80–100 year-old, made of natural fibres, namely cotton. Throughout this paper, an essential aspect was taken into account for establishing a preventive or curative conservation strategy, namely the characterization of the fabric from which the three shirts are made. Thus, some physical and structural characteristics were determined by making use of different types of analyses: FTIR spectroscopy, the spectra specific for cotton; the microbiological analyses showed the presence of Bacillus subtilis and Rhizobium radiobacter, Staphylococcus aureus and Streptococcus pyogenes, which are not considered pathogenic or toxigenic to humans with the normal function of the immune system.

Keywords: *textiles, cultural heritage, non-invasive, conservation, fungi, FTIR*

Metode analitice non-invazive aplicate în studiul artefactelor din patrimoniul cultural

Textilele de patrimoniu etnografic pot fi supuse unor riscuri generate de diverși factori, care sunt în strânsă legătură cu microclimatul spaţiilor de depozitare și expunere. În conformitate cu tendințele europene actuale de prevenire și reducere a dăunătorilor și ca răspuns la contaminarea patrimoniului cultural, acest studiu vizează investigarea degradării unor articole de îmbrăcăminte cu o vechime de aproximativ 80-100 de ani, din fibre naturale de bumbac. În lucrare s-a ținut cont de un aspect esențial pentru stabilirea unei strategii de conservare preventivă sau curativă, și anume caracterizarea țesăturilor din care sunt confecționate cele trei cămăși. Astfel, au fost determinate unele caracteristici fizice și structurale, folosind diferite tipuri de analize: spectroscopie FTIR, spectre specifice fibrelor celulozice, tipice bumbacului; analizele microbiologice au evidențiat prezența Bacillus subtilis și Rhizobium radiobacter, Staphylococcus aureus și Streptococcus pyogenes, care nu sunt considerate patogeni sau toxigeni pentru persoanele cu sistem imunitar normal.

Cuvinte-cheie: *textile, patrimoniu cultural, non-invaziv, conservare, fungi, FTIR*

INTRODUCTION

Subject to the effects of globalization, some heritage items are stored or exhibited in museums, archives, libraries, archaeological sites, etc., and others have even disappeared or are at high risk in this regard. The conservation of cultural heritage, and the development of sustainable and innovative conservation techniques that do not affect the integrity of the item, all these are considered challenges to which interdisciplinary teams of specialists are subjected: preservationists, restorers, custodians, historians, archivists, biologists, chemists, physicists, geographers, ethnologists, bioinformaticians etc. [1, 2]. Textile heritage is the cultural expression of a nation through the social status of the holder as well as the regional and local characteristics transposed into the symbolism represented [3]. Heritage textile items, fabrics, yarn arrangement, and embroidery used in fabric making are tools for knowing the details of daily life in general, customs, values and behaviour of our ancestors. The restoration/ conservation actions and the strategies established to this end are based on studies and thorough analyses that provide information related to the characterization of textile materials [4]. Biological, physical and chemical factors, under the influence of anthropogenic activity and environmental factors, act in time, slowly or brutally, leading to the deterioration/biodeterioration of valuable items of the cultural heritage. The operation of this mechanism takes place within an open and dynamic system: human/artefact/environment. Microorganisms can contribute to the deterioration/biodeterioration of artefacts, especially those made of natural threads (e.g., cotton), fibres with cellulose predominantly in their composition (about 94%), proteins 1.3% [5–6], being wrapped by a protective waxy cuticle. Also, the biological particles in aerosols (e.g., spores, toxins, allergens, etc.) present a potential risk not only to the heritage item but also to human health (visitors, users, curators, etc.). Identifying the type of fibres from which a heritage item is made sometimes allows for approximating the age of an artefact, the type of climate or trade routes and the manufacturing process used [7].

Literature review

Kavkler et al. [8] use the applications of Fourier-transform infrared spectroscopy (FTIR) to determine the degree of biodegradation of historical textiles stored in museums in Slovenia, especially those based on protein components compared to cellulosic ones. Thus, more intense biodegradation processes were underlined in the internal part of the fibres compared to their superficial part, these being caused both by microorganisms and other deterioration agents. Margariti et al. [9] support the use of FTIR microspectroscopy as a non-invasive and non-destructive technique in the study to preserve archaeological textiles. Peets et al. [10] prove that FTIR is a useful, non-invasive technique to identify textile fibres, discussing the advantages, but also some disadvantages. A range of spectra specific to different ranges of fibres is made available by the authors to those interested, in support in identifying the types of fibres.

Studies regarding the biodegradation of cultural heritage have been conducted by researchers such as Montegut et al. [11], Szostak-Kotowa [12], Abdel-Kareem [13], Arshad and Mujahid [14], Gutarowska et al. [15], Brzozowska et al. [16], Kumar and Shah [17], Sanders et al. [18], Trovão and Portugal [19], Unković et al. [20], Romero et al. [21] etc. In Romania, we mention the most recent research studies of different work groups, such as Radulescu et al. [22], Ilieș et al. [23–26], Marcu et al. [27], Bou-Belda et al. [28], Indrie et al. [29], Albu et al. [30], Wendt et al. [31], Gaceu et al. [32] etc.

MATERIALS AND METHODS

The study considered the analysis of two women's clothing items from Maramures County, Romania and a men's traditional cloth from Beius region, Romania, around 80–100 years old, made of cotton, belonging to private collections (figures 1, 2 and 3).

Both shirts originating from the Maramureș region are made of cotton cloth. They are large, both on the body and arms, which gives them a sense of greatness. They have long sleeves, up to the wrist.

Textile object no. 1 (figure 1, *a* and *b*) – Female shirt from Maramureș region. It has the size of the chest. When the shirt is dressed, a simple lower part named "stan" (figure 2, *a*) is added, or on special occasions, it has a richly decorated lower part (figure 2, *b*). Around the neck, it has a very wide lace with patterns of twigs, leaves and rose flowers, made of holes sewn on the edges called "fereşti". They have an angular appearance, resulting from broken lines and chained squares. Holes are achieved by cutting and hemming with the needle, by seaming on the threads. At the cuff, the sleeve is tightened through folds, but it widens towards the large-sized embroidery with floral patterns. The embroidery at the base of the neck (covering the cloth on the chest), from the shoulders and from the cuff is called "bezeri". Being stitched only at the top, they move in the wind and while walking. They are provided with two or three rows of holes, "fereşti". Folds are also present at the shoulders and chest area. All models have the colour of the canvas (white). The embroidery surrounds the neck, forming a zigzag called "șânguială". The cuffs have eight folds, four "scărițe" and two "suveici". The edges are provided with "boți" (thread nodes).

a *b*

Fig. 1. Object 1. Short traditional cloth, Romania: *a* – entire product; *b* – sample

a *b*

Fig. 2. Object 2. Long traditional cloth, Romania: *a* – entire product; *b* – sample

a *b*

Fig. 3. Object 3. Romanian traditional cloth, Beius area, Romania: *a* – entire product; *b* – sample

Buttons and loops present on the new shirt have been lost over time. Their traces are visible in the neck area.

Textile object no. 2 (figure 2, *a* and *b*) – Female shirt from Maramureș region. This shirt is complete, including the simple lower part named "stan". Around the neck, it is provided with very wide lacework, with no "bezeri" in the chest area. It has a closure system made of "guriță" and "chetori" (loops). The loops are provided with "ciucalăi" (also known as "ciucuri" (tassels) in certain ethnographic areas). They have two colours: white and the colour of the pumpkin flower. The pattern in the neck area is complex. We describe it from the bottom up: folds alternating with embroidery made of holes. Followed by "scărița mășcată" (big). Next, the layer of "suveicuțe", followed by "scărițe". Again, a layer of "suveicuțe", a layer of "scărițe", followed by another layer of "suveicuțe". Thus, there are three layers of "suveicuțe" separated by two layers of "scărițe". In the upper area, tusk-shaped pieces of cloth are sewn with a needle. Above we can see a layer of "pupi" (round ornaments) of different colours (white and the colour of the pumpkin flower). The pattern of the neck embroidery is called "formă într-un vârf și gaură" (shape in a tip and hole). The shoulder area presents small "bezeri" on a small pattern also in "formă într-un vârf și gaură". The pattern on the shoulders has a row of 'S' in a horizontal position, just like the interrupted and stylised "water stream" from the Dacian ceramics. At the cuff, the sleeve is tightened through folds, but it widens towards the small-sized embroidery with clover leaf patterns, and holes made with the tip of the spindle and sewn along the entire length of the circle. The narrowest part of the sleeve, at the cuff, is adorned with a chain of rhombuses. This type of rhombus is often found in Romanian folk art in and around the Carpathians, both in fabrics as well in wood hand-chiselling and carving. The rhombuses found on the cuffs are adorned with flowers made of double „greblușe" (rakes), of different colours, framed by four folds, two layers of "scărițe" and "boți". The pattern in the neck area is highly adorned (folds, tusk-shaped items, "scărițe", "suveicuțe" etc.). The most complex patterns are present at the neck, shoulders and cuffs.

The object of the investigated patrimony (figure 3, *a*) is stored in an ethnographic museum in Romania. It is a men's shirt, dating about 80–100 years, from the area of Beius region, Romania. The men's shirt is an important piece of Romanian folk costume. It is a homemade cotton cloth and hand-woven. The shirt is cut much wider than the body and has a light puffy look. At the same time, the sleeves are wide. It has great robustness and vigour and does not bend easily on the body, it does not mould to it. The grandeur, sobriety, prestige and elegance are considerable advantages. In summer, it offers a cool atmosphere and in winter, the shirt is worn under other clothes, keeping a lot of warmth, because between its folds it retains real air cushions that have a thermal insulation effect. All the ornamentation of the garment is done by hand, sewn with a needle. The body of the shirt is crimped at the base of the neck. Above the wrinkle, a beautiful ornate collar is sewn. Its pattern, coloured in dark brown, is strongly geometrized by a series of squares (sometimes rhombuses) tied/coupled in the corners. At the bottom of the shirt, there is a simple hem. The wide sleeves are tightened at the wrist by a wrinkled cuff (sleeve, collar). The crease is similar to the shoulder, where the sleeve is attached to the body of the shirt. The simplicity of the shirt, especially specific to men's garments, with patterns of the same colour as the bottom (white) applied by sewing on the fabric and the additional presence of a single colour (dark brown), gives the shirt a special sobriety and beauty [49].

The study on how environmental conditions have left their mark on the type and characteristics of the textile material from which the two shirts has targeted two lines of research:

i) to determine the microbiological aspects associated with the clothing items analysed in the framework of the study it was aimed to determine the total number of bacteria, respectively the total number of fungi in the fabric. The microbiological tests were performed in the speciality laboratories at the Institute of Microbiology of the Republic of Uzbekistan. The working procedure was aimed at maintaining aseptic conditions and the following working methodology was used: the tests were carried out on the three samples specific to the two shirts originating from Maramureş and Beiuș regions (figure 1, *b*; figure 2, *b*; figure 3, *b*) made of cotton fabric. Samples from the textile samples surface (six) were collected using sterile cotton swabs [33, 34], on a surface of approximately 1 cm^2/each sample. Cotton swabs were treated by immersion in one millilitre of sterile water. Three Petri plates measuring 90–100 mm in diameter were used for each sample. To determine the microbiological load, three culture media were used: Saline solution; Nutrient Agar (Himedia); Nutrient Sabureau medium (Himedia). If the colony growth was not noticed at a 1:10 dilution of the samples, the results should be considered as follows: 1 ml of the sample contains less than 10 bacteria.

ii) Fabrics are characterized by both their basic properties (flexibility, durability, etc.) and other characteristics that leave their mark on their appearance and behaviour under different conditions of use. The behaviour of the material under different environmental conditions is determined by the functional combination of the properties of the fabric and the characteristics and structure of the raw material. To highlight this fusion structure – type of material – behaviour, under different environmental conditions, we analysed some of the main general properties of the fabrics: structural properties and physical properties. The textile material from which the two shirts are made was subjected to several physical and structural tests, as follows:

1. Mesh density test was performed according to the European standard (EN ISO) 7211/2.

2. The thickness of the layer is a factor that affects the durability, permeability, fluidity and similar properties of the fabric being directly influenced by the diameter and number of threads in the textile material. The specific test for determining the thickness was carried out according to ASTM D1777.
3. Air permeability is a measure of the amount of airflow passing through a certain area of fabric at a certain time. The air permeability test was carried out according to ASTM D737-04 (2012).
4. Abrasion is the physical destruction of yarns, fibres and fabrics as a result of rubbing a textile surface against another surface. There is a close connection between abrasion and durability. Abrasion tests can contribute to the overall durability assessment.
5. Hygroscopicity is the property of fibres to accumulate and release water vapours in the atmosphere. Fibres retain a quantity of water that is influenced by their chemical composition and structure and the parameters of the microclimate to where they are stored or exposed. The hygroscopicity of the types of fibres influences the hygienic and comfort qualities of the textile garments and it is important to know the value to adjust to the technological processes and areas of use [35].

The samples were inserted in separate weighing vials, and placed openly in a water desiccator, where the relative humidity is predetermined at (98±1)%, and the time frame is 4h. After this time frame, they are closed and removed from the desiccator, and their weighing and drying are performed at a temperature of (107±2)°C (the drying temperature is (68±2)°C). After drying and cooling in a desiccator filled with dehydrated calcium chloride, the sample vials are weighed to constant mass using the analytical balance. The calculation formula used is:

$$H = (mB - mC) / mC \times 100 \ (\%) \tag{1}$$

where *mB* is the mass of the moistened elementary sample, in grams (g), and *mC* – mass of an elementary sample, after drying to constant mass, in grams (g).

Another indicator which characterises the mass of a unit area is the *areal density of fabric* (g/m^2). The recorded values of this indicator characterize the thickness of the warp and weft threads and the density of the fabric. Variations of this indicator can range on a fairly large scale of values, depending on the type of material, namely fluctuations which tend to increase the values of this indicator can be followed: after dressing up, printing, cutting, etc., as well as fluctuations which tend to decrease the values are recorded in cases of washing, bleaching, boiling, etc. of the fabric.

The determination of the fabric areal density: elementary samples are preliminarily conditioned to equilibrium humidity by keeping them under standard climatic conditions in an unstressed state, for at least 24 hours. In turn, each elementary sample is placed on a surface suitable for cutting, a metal template (cutter) is placed in the center, along which a square sample of 10 × 10 cm (or a round one with an area of 100 cm^2) is cut out. The elementary sample is weighed with an accuracy of ± 0.001 g while ensuring the safety of the threads. From the mass of the elementary sample, calculate the mass per unit area of tissue using the formula:

$$m_{oa} = m \times 100 \tag{2}$$

where m_{oa} is the mass per unit area of fabric (per square meter) after conditioning under standard test climate conditions in g and *m* – the mass of the elementary sample in g.

In dry friction – initially, the dry sample is placed and set inside the tester. The second stage provides for the application of a strip of cotton material (about 50×50 mm) on the friction rod of the device, aiming for the friction surface to be smooth. The test must start on an elementary sample in one of the extreme positions of the rod, the device acting for 10 round trips, length of 100 mm, timing 10 s, and a load of 9 N. The tests are performed for the cotton cloth in wet and dry conditions. Thus, the material sample is immersed in distilled water (for 5 minutes); subsequently, squeezing is performed (the liquid content remaining in the cotton fabric is approximately equal to the weight of the adjacent cloth). The last stage of the test sets out to test the dry sample (GOST 9733.0-83 (Section 4)).

To identify the influence of the microclimate on the chemical properties of the textile material from which the three shirts originating from the Maramureş and Beiuș regions are made, we have collected samples taken from the three textile materials and analysed them, making use of the IR spectroscopy technique (FTIR). This technique is characterised by sensitivity, specificity and non-destructive nature, being minimally invasive. The application of FTIR for the analysis can be achieved for a fairly wide range of types of materials: e.g., historical fibres, paper, ceramic, etc. [36, 37]. FTIR test was done on the main components: the support textile fibre, very common when making old-time clothing items. Chemical changes can also be noted and even quantified, due to the ageing process of materials, especially those made of natural fibres, which is particularly important for the processes of conservation and restoration [38].

To analyse the type of fibre the chemical analysis of the efflorescence present on the sample was performed by infrared spectroscopy with a Miracle Accessory ZnSe S2PE infrared spectrometer (This ATR MIRacle Single Reflection Accessory includes the MIRacle base optics, a zinc selenide (ZnSe) crystal plate, a high-pressure clamp with three interchangeable tips, purge tubes, and a mount for the Spectrum Two spectrometer.

As for the *microbiological tests*, each fabric sample was processed as follows: for a weight of 0.7 g, 5 ml of saline was added. Next, they were placed under a magnetic stirrer for 30 minutes, leaving them for 3–4 hours at room temperature. 100 ml from each sample was added to the Petri plates with the nutrient

Agar. This was done evenly on the surface, using a spatula. Subsequently, the plates were incubated for 5 days at 37°C. Counting the bacterial colonies, grown on three plates, was achieved after an interval of 48 hours and 5 days, respectively. The mean value was identified as having multiplied by the dilution index and thus it was calculated the number of bacteria in 1 g of sample. The test was performed also using Petri plates with Sabouraud medium. The incubation of cultures was carried out at 20°C for 5 days. Counting the colonies of fungi and mould on three plates was carried out at the first stage of these types of tests with another culture medium; next, the number of fungi within 1 g of the sample was calculated by multiplying the mean value of the number of colonies by the dilution index.

RESULTS AND DISCUSSION

As for sample, object no 1 (MPA medium) – determination of the total number of germs revealed – 45 bacteria in 1 g of tissue; in the Sabouraud medium determination showed – 23 fungi in 1 g of tissue (GF XX1: 197).

When identifying samples of isolated cultures by MACLI-TOF mass spectrometry, using VITEK MS biometric analyzer, the following types of microorganisms were found: sample 1 (MPA) – bacterium *Bacillus subtilis*.

Object no. 2 sample: determination of the total number of germs showed 21 bacteria in 1 g of tissue, while in Sabouraud medium 23 fungi were determined in 1 g of tissue (GF XX1, part one page 197). When identifying culture samples isolated by MACLI-TOF mass spectrometry, using VITEK MS biometric analyzer, the bacterium – *Rhizobium radiobacter* was identified on the Sample, object 2 (MPA)

As for pathogenicity, the microbiological tests indicate the presence of *Bacillus subtilis* on sample object 1. This is a conditional pathogen, which can be often found in the dust; mainly it can be part of the normal microbiota of the human skin surface, and it is also found in the environment: in soil, dust, water and air. *Bacillus subtilis* is not considered pathogenic or toxigenic to humans with the normal function of the immune system, animals or plants [39]. On the sample object no. 2 – *Rhizobium radiobacter* was identified. A phytopathogen is known, and it represents conditional pathogenicity in people with intravascular devices suffering from immunodeficiency diseases [40, 41].

For the third object sample, Petri dishes with Sabouraud medium were used. The cultures were incubated for 5 days at a temperature of 20°C. After 5 days, the total number of fungi and mould colonies was counted on three plates, the mean value was found and multiplied by the dilution index and the number of fungi in 1 g of sample was calculated [50–52]. For the sample from (Sabouraud's medium) – 1,855 fungi in 1 g of tissue were calculated. For bacterial identification from cultures, we worked on VITEK® MS, an automated mass spectrometry microbial identification system that uses Matrix Assisted Laser Desorption Ionization Time-of-Flight (MALDI-TOF) technology. *Streptococcus pyogenes* has been identified but this species is not found in the list of microorganisms associated with the biodegradation of textiles mentioned by Pyzik [53]. If the clothing is worn, it should be borne in mind that the pH of the skin may change, which could lead to the exacerbation of pathogenic bacteria. *Staphylococcus aureus* and *Streptococcus pyogenes* [18].

Streptococci are gram-positive cocci hosted by humans and various animals. Streptococci are also present in the environment in dust, soil, air, and water. Most species are present in the normal flora in the respiratory tract, gastrointestinal tract, genitals and skin. Some species are pathogenic and can cause infectious diseases: erysipelas, impetigo, scarlet fever, rheumatism, cellulite, etc. Some studies show the possibility of transmitting bacteria such as

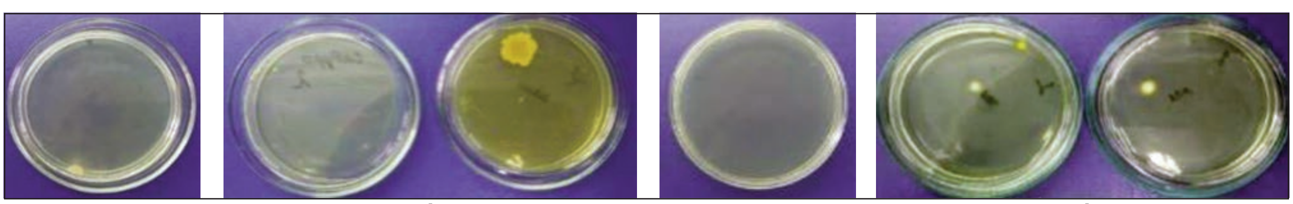

a ***b*** ***c*** ***d***

Fig. 4. The Petri plates different medium, a sample of textile object 1: *a* – Sample object 1 (MPA); *b* – Sample object 1 (Sabouraud); *c* – Sample object 1 (Sabouraud); *d* – Sample object 1 (MPA)

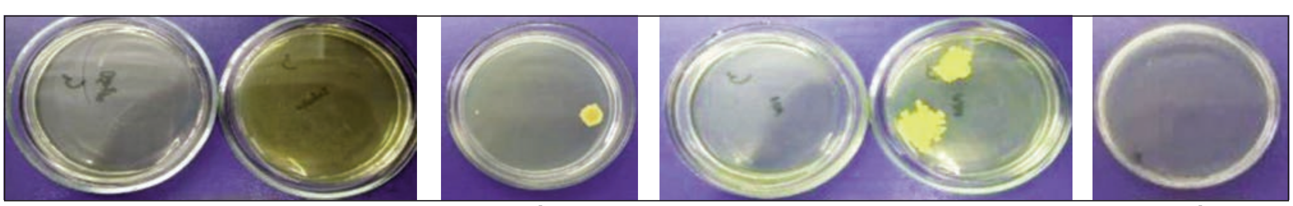

a ***b*** ***c*** ***d***

Fig. 5. The Petri plates, different medium, sample object no. 2: *a* – Sample object 2 (Sabouraud); *b* – Sample object 2 (Sabouraud); *c* – Sample object 2 (MPA); *d* – Sample object 2 (MPA)

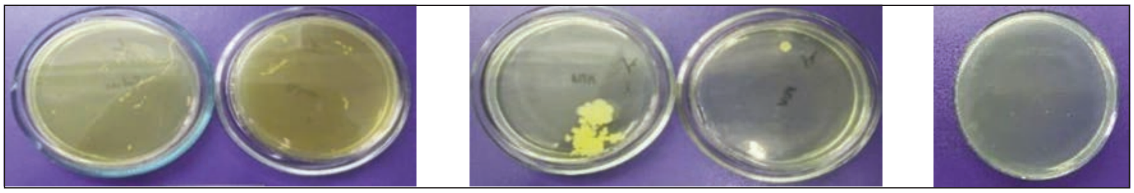

a *b* *c*

Fig. 6. The genera of fungi, *Streptococcus pyogenes*, identified on the sample, in different medium: *a* – Sabureau medium; *b* – MPA medium; *c* – Saline medium

Table 1

INDICATORS VALUES (TEST DONE AT CENTEXUZ RESEARCH CENTER, UZBEKISTAN)				
№	**Indicators**	**Sample object 1**	**Sample object 2**	**Sample object 3**
1	Surface density (g/m^2)	318.2	348.4	326.5
2	Thickness (mm)	0.6	0.7	0.56
3	Air permeability (cm^2/cm^2.sec.)	54.8	21.8	53.6
4	Abrasion cycle	18000	21000	19500
5	Hygroscopicity (%)	11.01	11.26	11.62

Table 2

INDICATORS - COMPLEX OF TESTING LABORATORIES AT JV LLC “UZBEK-TURK TEST CENTER”, UZBEKISTAN				
№	**Indicators**	**Sample object 1**	**Sample object 2**	**Sample object 3**
1	Breaking load (N)	513.8	602.4	567.9
2	Specific surface electrical resistance (Ω)	2.1 x 107	3.5 x 108	1.1 x 108
3	Colour fastness to washing (points)	-	4	-
4	Colour fastness to organic solvent (points)	-	4	-
5	Colour fastness to dry friction (points)	-	4	-

methicillin-resistant staphylococci, and gram-negative bacteria, including streptococci on clothes (white robes, uniforms-cuffs, seams on the waist, pockets) clothes that can represent a bacterial microdeposit and a channel of bacterial spread [54, 55]. For any person with natural immunity, the streptococci do not pose any danger [56, 57].

Identification of the influence that the environmental conditions have had on the structure of the textile material from which the two shirts are made, rendered by the same indicators which were evaluated at the Complex of testing laboratories at JV LLC “Uzbek-Turk Test Center”, Uzbekistan, can be viewed in table 1 and table 2.

FTIR spectrometers. Fourier-transform infrared spectroscopy (FTIR) spectroscopy technique was chosen to characterize, especially from a physical point of view, the surface of the material and to give some clues regarding the degradation of the fibres. The FTIR spectra present specific cellulosic fibre peaks, typical for cotton (figures 7 and 8).

Fourier spectroscopy. With the help of Fourier spectrometers, the entire spectrum can be recorded simultaneously. Because in the interferometer an entrance opening of a larger size is permissible than the slit of spectral instruments with a dispersing element. Non-invasive and label-free Raman spectroscopy is an ideal analytical tool for fabric analysis non requiring sample homogenization. It is possible to extract the full range of chemical information without the need for biomolecular orientation, markers, stains or dyes. Unlike many other methods of analysis, such as Western blotting, gas chromatography/mass spectrometry, and time-of-flight mass spectrometry with laser ionization and desorption from a liquid matrix (MALDI-TOF).

FTIR spectra of both samples are showing similar bands and are presented in figures 7, 8 and 9.

The intense band at 3320 cm^{-1} is specific to the hydroxyl (O-H) groups corresponding to cellulose, lignin and water [42]. The 2890 cm^{-1} peak is associated with the stretching vibration of the C-H groups present in the composition of cellulose and hemicellulose [43], while the less intense peak at 1628 cm^{-1} can be correlated with the presence of O-H bending vibration of water from fibre [44]. The fact that the peak corresponding to the water is weak can be correlated with the age of the material. The presence of the sharp peak at 1740 cm^{-1} is characteristic of the carboxyl group from hemicellulose [45].

The 1426 cm^{-1} band is associated with the symmetrical bending of CH_2 groups in cellulose. The weak absorption bands between 1360 and 1300 cm^{-1} are

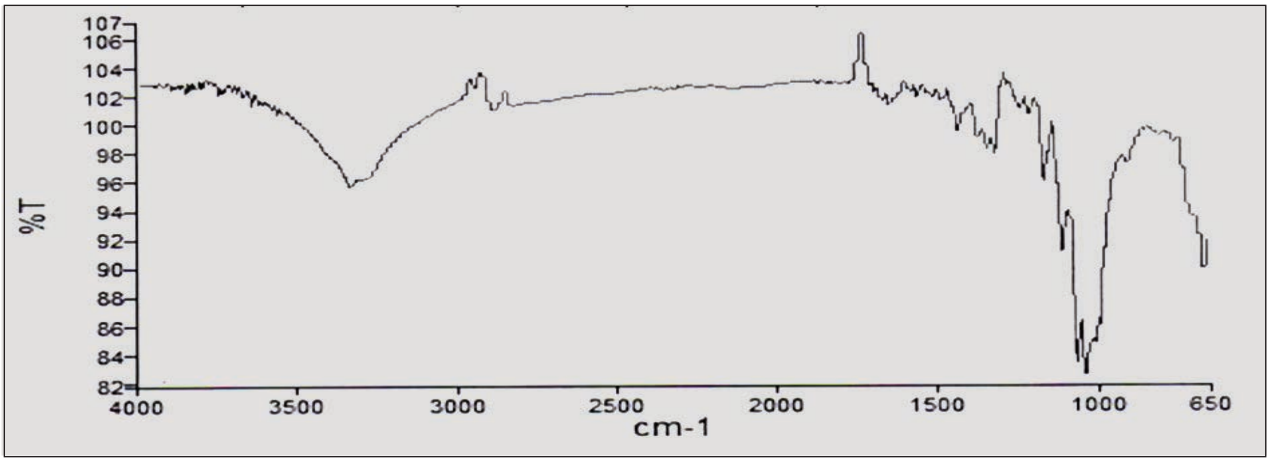

Fig. 7. FTIR-ATR spectra of cotton fibres, sample object no. 1

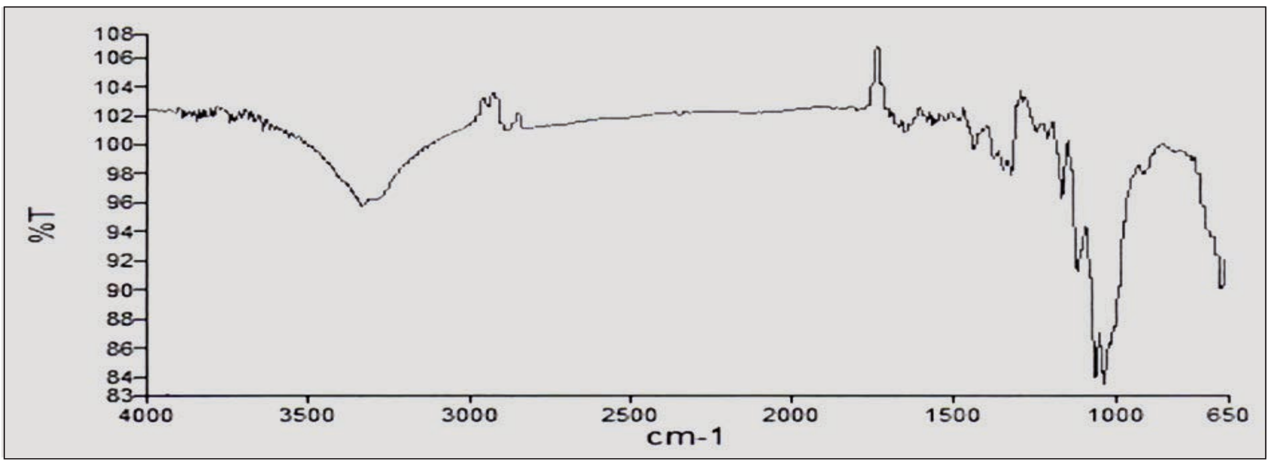

Fig. 8. FTIR-ATR spectra of cotton fibres, for sample object no. 2

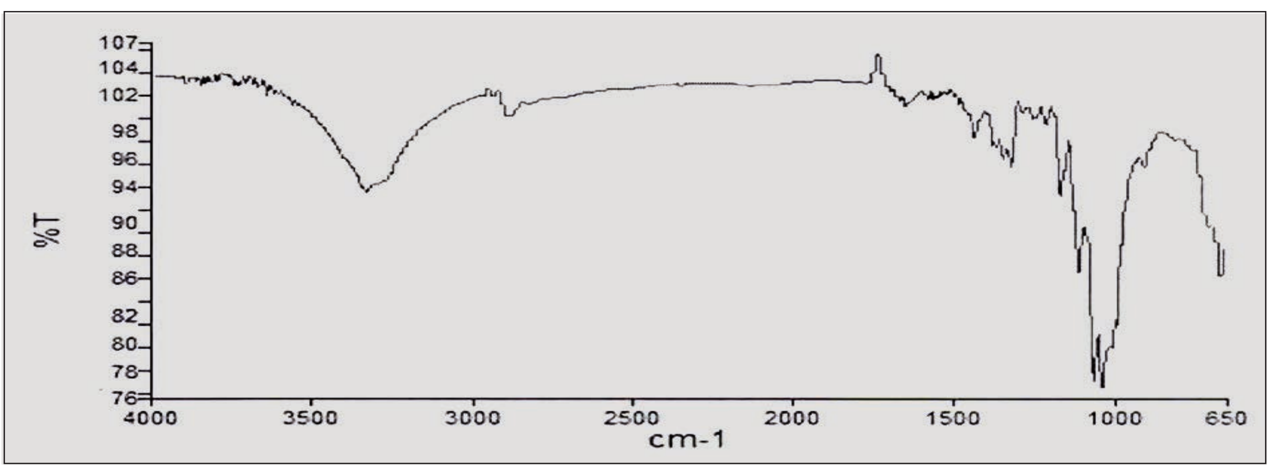

Fig. 9. FTIR-ATR spectra of cotton fibres, for sample object no. 3

due to the bending vibrations of the C-H and C-O groups in the rings of cellulose polysaccharides. The intense bands observed at 1030 cm^{-1} correspond to the stretching vibrations of (C-O) and (O-H) groups from cellulose polysaccharides. The weaker peak at 892 cm^{-1} indicates the existence of β-glycosidic bonds between monosaccharides [45].

At high wavenumbers, the broad and intense band appearing at 3325 cm^{-1} represents the hydroxyl (O-H) groups, specific to cellulose, lignin and water [42]. Further, at lower frequencies (2895 cm^{-1}) peak can be assigned with the stretching vibration of C-H groups of cellulose and hemicellulose [43].
The sharp band at 1745 cm^{-1} is assigned with the carboxyl group from hemicellulose [44]. The band at

Table 3

SPECTRAL ANALYSES ON THE INVESTIGATED SAMPLE				
Name (ID)	**Description**	**Search range**	**Libraries searched**	**Execution summary**
		Overlap	Library 1, polyatr, ATR Polymer Introductory Library, Library NDFIBS	
HitSpectrumID	**HitDescription**	**HitCorrelation**	**LibraryName**	**Library description**
F00352	FB352.SP FB352, SNOW FLAKE, COTTON, WONOCO, COPYRIGHT NICODOM 2007 IR- S	0.946613	NDFIBS	

Source: Analyses made complex of testing laboratories at JV LLC "Uzbek-Turk Test Center".

1628 cm^{-1} is assigned with the O-H bending vibration of water from fibre [45].

Considering the fingerprint region (less than 1500 cm^{-1}) the 1429 cm^{-1} peak is specific to the symmetrical bending of CH_2 groups in cellulose. Absorption bands seen in the 1365 and 1300 cm^{-1} region are characteristic of bending vibrations of the C-O and C-H groups of polysaccharides cellulose rings. Intense bands present at 1035 cm^{-1} are assigned with the (C-O) and (O-H) stretching vibrations from cellulose polysaccharides. At 890 cm^{-1}, the weaker peak shows the existence of β-glycosidic bonds between monosaccharides [44].

IR spectra recorded for reference samples (figures 7, 8 and 9) have absorption strips located in the frequency regions characteristic of cellulose [46–48]. From the analysis of the IR spectra recorded for the studied textiles, it is noted that the microclimate factors do not affect the molecular structure of the cellulosic chain, for any of the samples under analysis.

CONCLUSIONS

The different behaviour of the studied materials during the treatments can be explained by: the secondary, supramolecular and crystalline organisation of the cellulose, alternating amorphous and crystalline areas in the crystalline structure of the cellulose, the presence of microscopic and submicroscopic voids in the structure of the fibres, as well as the presence of the other main chemical components – hemicelluloses and lignin – in the structure of textile fibres. FTIR spectroscopy applications on biodegraded historical textiles is a successful non-invasive technique which can underline the fabric decay caused by microorganisms, but also by other deterioration agents. At the microbiological tests, the bacteria species *Bacillus subtilis* and *Rhizobium radiobacter* were isolated and identified, being the main part of the normal microbiota of the human skin surface, and they are not dangerous to a person with the normal function of the immune system and its presence can be also in the environment: in soil, dust, water and air. The strategies and tools used for investigations (microbiological etc.) of cultural heritage objects are not standardized, being in continuous development, each with advantages and disadvantages depending on the type and purpose of the study, but especially on the available infrastructure [2, 58–62]. If the clothing is worn, it should be borne in mind that the pH of the skin may change, which could lead to the exacerbation of pathogenic bacteria. *Staphylococcus aureus* and *Streptococcus pyogenes* [54].

Insights: New/unconventional methods of protection are necessary to be identified and tested against the influence of microclimate conditions in the ageing processes of cellulosic materials from ethnographic textile collections. In the context of future research, we will be taken into account the study on the effects of the main microclimate factors (temperature, humidity, lighting, etc.) on the permanence and durability characteristics of textiles made of cellulosic materials. Their action on natural pigments will also be analysed, using other investigation techniques such as High-performance liquid chromatography, SEM analysis etc.

ACKNOWLEDGEMENT

The research has been funded by the University of Oradea. The research undertaken was made possible by the equal scientific involvement of all the authors concerned.

REFERENCES

[1] Mukesh, M., Norlaila, H., Khaliq, A.A., *A study of the digitization process to preserve the culture and heritage of a civilization using natural language processing and it's impact on the social, economic and scientific aspects*, In: Journal of Theoretical and Applied Information Technology, 2018, 96, 16, 5550–5568

[2] Piñar, G.S., *Natural sciences at the service of art and cultural heritage: an interdisciplinary area in development and important challenges*, In: Microbial Biotechnology, 2021, 14 3, 806–809, https://doi.org/10.1111/1751-7915.13766

[3] Kočevar, T.N., *3D Visualisation of a Woman's Folk Costume,* In: M. Ioannides (Ed.), Marie Skłodowska-Curie Initial Training Network for Digital Cultural Heritage, Olimje: Springer, Cham, 2017, 304–323, https://doi.org/10.1007/978-3-319-75826-8

[4] Olaru, A., *Cercetări privind protecţia şi conservarea textilelor etnografice aparţinând patrimoniului cultural*, Teză de doctorat, Universitatea Tehnică „Gheorghe Asachi" din Iaşi, Facultatea de Inginerie Chimică şi Protecţia Mediului, 2014

[5] Dochia, M., Sirghie, C., Kozłowski, R.M., Roskwitalski, Z., *Cotton fibres,* In: Handbook of natural fibres, Woodhead Publishing Limited, Volume 1: Types, properties and factors affecting breeding and cultivation, Edited by Ryszard M. Kozłowski, 2012, 11–23

[6] Di Carlo, E., Chisesi, R., Barresi, G., Barbaro, S., Lombardo, G., Rotolo, V., Sebastianelli, M., Travagliato, G., Palla, F., *Fungi and Bacteria in Indoor Cultural Heritage Environments: Microbial-related Risks for Artworks and Human Health,* In: Environment and Ecology Research, 2016, 4, 5, 257–264, https://doi.org/10.13189/eer.2016.040504

[7] Raditoiu, V., Chican, I.E., Raditoiu, A., Fierascu, I., Fierascu, R.C., Fotea, P., *Application of Fourier-transform infrared spectroscopy (FTIR) for the study of cultural heritage artifacts,* In: International Conference on VR Technologies in Cultural Heritage. Springer, Cham, 2018, 3–9

[8] Kavkler, K., Gunde-Cimerman, N., Zalar, P., Demšar, A., *FTIR spectroscopy of biodegraded historical textiles,* In: Polymer degradation and stability, 2011, 96, 4, 574–580

[9] Margariti, C., *The application of FTIR microspectroscopy in a non-invasive and non-destructive way to the study and conservation of mineralised excavated textiles,* In: Heritage Science, 2019, 7, 1, 1–14

[10] Peets, P., Leito, I., Pelt, J., Vahur, S., *Identification and classification of textile fibres using ATR-FT-IR spectroscopy with chemometric methods,* In: Spectrochimica Acta Part A: Molecular and Biomolecular Spectroscopy, 2017, 173, 175–181

[11] Montegut, D., Indictor, N., Koestler, R.J., *Fungal deterioration of cellulosic textiles: a review,* In: International biodeterioration, 1991, 28,1–4, 209–226

[12] Szostak-Kotowa, J., *Biodeterioration of textiles,* In: International Biodeterioration & Biodegradation, 2004, 53, 3, 165–170

[13] Abdel-Kareem, O., *Evaluating the combined efficacy of polymers with fungicides for protection of museum textiles against fungal deterioration in Egypt,* In: Polish Journal of Microbiology, 2010, 59, 4, 271–280

[14] Arshad, K., Mujahid, M., *Biodegradation of textile materials,* University of Borås/Swedish School of Textiles, 2011

[15] Gutarowska, B., Pietrzak, K., Machnowski, W., Milczarek, J.M., *Historical textiles–a review of microbial deterioration analysis and disinfection methods,* In: Textile Research Journal, 2017, 87, 19, 2388–2406

[16] Brzozowska, I., Bogdanowicz, A., Szczęsny, P., Zielenkiewicz, U., Laudy, A., *Evaluation of bacterial diversity on historical silk velvet textiles from the Museum of King John III's Palace at Wilanów, Poland*, 2017

[17] Deepti, K., Shah, N.R., *Biodeterioration in Textiles: A Review,* In: International Journal of Interdisciplinary Research in Arts and Humanities, 2018, 3, 1, 167–175

[18] Sanders, D., Grunden, A., Dunn, R.R.*, A review of clothing microbiology: the history of clothing and the role of microbes in textiles,* In: Biology Letters, 2021, 17, 1, https://doi.org/10.1098/rsbl.2020.0700

[19] Trovão, J., Portugal, A., *Current knowledge on the fungal degradation abilities profiled through biodeteriorative plate essays,* In: Applied Sciences, 2021, 11, 9, 4196

[20] Unković, N., Dimkić, I., Stupar, M., Stanković, S., Vukojević, J., Ljaljević Grbić, M., *Biodegradative potential of fungal isolates from sacral ambient: in vitro study as risk assessment implication for the conservation of wall paintings,* In: PLoS One, 2018, 13, 1

[21] Romero, S.M., Giudicessi, S. L., Vitale, R.G., *Is the fungus Aspergillus a threat to cultural heritage?,* In: Journal of Cultural Heritage, 2021, 51, 107–124

[22] Rădulescu, H.C., Perdum, E., Mitran, C.E., Dincă, L.C., Lazăr, V., *Biodeteriogenic capacity of a microfungal species isolated from textile cultural heritage items on contemporary wool materials,* In: The Publishing House of Romanian Academy Series B, 2018, 20–167

[23] Ilieş, D.C., Herman, G.V., Caciora, T., Ilieş, A., Indrie, L., Wendt, J.A., Axinte, A., Diombera, M., Lite, C., Berdenov, Z., Albu, A., *Considerations regarding the research for the conservation of heritage textiles in Romania*. In: Waste in Textile and Leather Sectors. IntechOpen, 2020

[24] Ilieş, D.C., Indrie, L., Ilieş, A., Marcu, F., Axinte, A., Burtă, L., Herman, G.V., Atasoy, E., Baidog, A., Iovan, C., Albu, A., Costea, M., Wendt, J.A., *Investigation of old textiles using scanning electron microscopy*. In: Journal of Environmental Biology, 2020, 41, 2, 499–504

[25] Ilieș, D.C., Marcu, F., Caciora, T., Indrie, L., Ilieș, A., Albu, A., Costea, M., Burtă, L., Baias, Ș., Ilieș, M., Sandor, M., Herman, G.V., Hodor, N., Ilieș, G., Berdenov, Z., Huniadi, A., Wendt, J.A., *Investigations of museum indoor microclimate and air quality. Case study from Romania,* In: Atmosphere, 2021, 12, 2, 286

[26] Ilieș, D.C., Hodor, N., Indrie, L., Dejeu, P., Ilieș, A., Albu, A., Caciora, T., Ilieș, M., Barbu-Tudoran, L., Grama, V., *Investigations of the Surface of Heritage Objects and Green Bioremediation: Case Study of Artefacts from Maramureş, Romania,* In: Applied Sciences, 2021, 11, 14, 6643.

[27] Marcu, F., Ilieș, D.C., Wendt, J.A., Indrie, L., Ilies, A., Burta, L., Caciora, T., Herman, G.V., Todoran, A., Baias, Ș., Albu, A., Gozner, M., *Investigations regarding the biodegradation of the cultural heritage. Case study of traditional embroidered peasant shirt (Maramures, Romania),* In: Romanian Biotechnological Letters, 2020, 25.2: 1362–1368

[28] Bou-Belda, E., Indrie, L., Ilieș, D.C., Hodor, N., Berdenov, Z., Herman, G., Caciora, T., *Chitosan – a non-invasive approach for the preservation of historical textiles,* In: Industria Textila, 2020, 71, 6, 576–579, http://doi.org/10.35530/IT.071.06.1756

[29] Indrie, L., Bonet-Araci, M., Ilies, D.C., Albu, A., Ilies, G., Herman, G., Baias, Ș., Costea, M., *Heritage ethnographic objects-antimicrobial effects of chitosan treatment,* In: Industria Textila, 2021, 72, 3, 284–288, http://doi.org/10.35530/IT.072.03.1812

[30] Albu, A.V., Caciora, T., Berdenov, Z., Ilies, D.C., Sturzu, B., Sopota, D., Herman, G.V., Ilies, A., Kecse, G., Ghergheles, C.G., *Digitalization of garment in the context of circular economy,* In: Industria Textila, 2021, 72,1, 102–107, https://doi.org/ 10.35530/IT.072.01.1824

[31] Wendt, J.A., Indrie, L., Dejeu, P., Albu, A., Ilieș, D.C., Costea, M., Caciora, T., Ilieș, G., Hodor, N., Josan, I., Berdenov, Z., Grama, V., Safarov, B., *Natural sources in preventive conservation of naturally aged textiles,* In: Fibres & Textiles in Eastern Europe, 2021

[32] Gaceu, O., Ilieș, D.C., Baias, Ș., Georgiță, M., Ilieș, A., Caciora, T., Indrie, L., Albu, A., Herman, G.V., Baidog, A., Buhaș, R., Marcu, F., Șipoș, L., Hodor, N., *Microclimatic characteristics and air quality inside the National Archives of Bihor County, Romania,* In: Environmental Engineering & Management Journal (EEMJ), 2021, 20, 3

[33] Ciferri, O., *Microbial degradation of paintings,* In: Applied and Environmental Microbiology, 1999, 65, 3, 879–885

[34] Fernandes, P., *Applied microbiology and biotechnology in the conservation of stone cultural heritage materials,* In: Applied Microbiology and Biotechnology, 2006, 73, 2, 291–296

[35] Bordeianu, D., Tefnologii și utilaje în filaturi, Available at: http://www.tex.tuiasi.ro/biblioteca/carti/CURSURI/Prof.%20Dr.%20Ing.%20Demetra%20Bordeianu/FCP%20II%20PDF/cap5a.pdf [Accessed on November 2021]

[36] Akyuz, T., Akyuz, S., Balci, K., Gulec, A., *Investigations of historical textiles from the Imperial Pavilion (Hunkar Kasri) of the new mosque Eminonu-Istanbul (Turkey) by multiple analytical techniques,* In: Journal of Cultural Heritage, 2017, 25, 180–184

[37] Mai, H., Yang, Y., Jiang, H., Wang, B., Wang, C., *Investigating the materials and manufacture of Jinzi: The lining of Futou (Chinese traditional male headwear) from the Astana Cemeteries, Xinjiang, China,* In: Journal of Cultural Heritage, 2017, 27, 116–124

[38] Higgitt, C., Harris, S., Cartwright, C., Cruickshank, P.*, Assessing the potential of historic archaeological collections: a pilot study of the British Museum's Swiss lake village textiles,* In: British Museum technical research bulletin, 2011, 5, 81–94

[39] Priest, F.G., Goodfellow, M., Todd, C., *The genus Bacillus: a numerical analysis,* In: The Aerobic Endospore-forming Bacteria. Classification and Identification, 1981, 91–103

[40] Chen, C.Y., Hansen, K.S., Hansen, L.K., *Rhizobium radiobacter as an opportunistic pathogen in central venous catheter-associated bloodstream infection: case report and review,* In: Journal of Hospital Infection, 2008, 68, 3, 203–207

[41] Lai, C.C., Teng, L.J., Hsueh, P.R., Yuan, A., Tsai, K.C., Tang, J.L., Tien, H.F., *Clinical and microbiological characteristics of Rhizobium radiobacter infections,* In: Clinical Infectious Diseases, 2004, 38, 1, 149–153

[42] Tomczak, F., Satyanarayana, K.G., Sydenstricker, T.H.D., *Studies on lignocellulosic fibres of Brazil: Part III–Morphology and properties of Brazilian curauá fibres,* In: Composites Part A: Applied Science and Manufacturing, 2007, 38, 10, 2227–2236, https;//doi.org/10.1016/j.compositesa.2007.06.005

[43] Satyanarayana, K.G., Guimarães, J.L., Wypych, F., *Studies on lignocellulosic fibres of Brazil. Part I: Source, production, morphology, properties and applications,* In: Composites Part A: Applied Science and Manufacturing, 2007, 38, 7, 1694–1709, https://doi.org/10.1016/j.compositesa.2007.02.006

[44] De Rosa, I.M., Kenny, J.M., Puglia, D., Santulli, C., Sarasini, F., *Morphological, thermal and mechanical characterization of okra (Abelmoschus esculentus) fibres as potential reinforcement in polymer composites,* In: Composites Science and Technology, 2010, 70, 1, 116–122, https://doi.org/10.1016/j.compscitech.2009.09.013

[45] Romanzini, D., Ornaghi Junior, H.L., Amico, S.C., Zattera, A.J., *Preparation and characterization of ramie-glass fibre reinforced polymer matrix hybrid composites,* In: Materials Research, 2012, 15, 3, 415–420, http://dx.doi.org/10.1590/S1516-14392012005000050

[46] Garside, P., Wyeth, P., *Identification of cellulosic fibres by FTIR spectroscopy differentiation of flax and hemp by polarized ATR FTIR,* In: Studies in Conservation, 2006, 51, 3, 205–211

[47] Malutan, T., Nicu, R., Popa, V.I., *Contribution to the study of hydroxymetylation reaction of alkali lignin,* In: BioResources, 2008, 3, 1, 13–20

[48] Rozmarin, G., *Macromolecular fundamentals of wood chemistry,* In: Macromolecular Fundamentals of Wood Chemistry, 1984

[49] Ilieș, A., Hurley, P.D., Ilies, D.C., Baias, S., *Tourist animation – a chance adding value to traditional heritage: case study in the Land of Maramures (Romania)*, In: Revista de Etnografie și Folclor, 2017, New Series 1–2

[50] Cernei, E.R., Maxim, D.C., Mavru, R., Indrei, L.L., *Bacteriological analysis of air (aeromicroflora) from the level of dental offices in Iaşi County Romanian*, In: Journal of Oral Rehabilitation, 2013, 5, 4

[51] Gary, W., Procop, M.D., Elmer, W.M.S., *Koneman's Color Atlas and Textbook of Diagnostic Microbiology*, Lippincott Williams Wilkins, 7th Edition, 2016

[52] Buiuc, D., Negut, M., *Tratat de Microbiologie Clinica (Treatise on Clinical Microbiology)*, *3rd 559 ed*., Editura Medicala, 560 București, Romania, 2009

[53] Pyzik, A., Ciuchcinski, K., Dziurzynski, M., Dziewit, L., *The Bad and the Good – Microorganisms in Cultural Heritage Environments – An Update on Biodeterioration and Biotreatment Approaches,* In: Materials, 2021, 14, 177, https://doi.org/ 10.3390/ma14010177

[54] Oliveira, A.C., Medeiros, S., Marlene das, D., Garbaccio, J., *Clothing of Health Care Professional as potential reservoirs of microorganisms: an integrative review,* In: Texto &Contexto Enfermagem, 2012, 21, 3, 684–691

[55] Handorean, A., Charles, E., Robertson, J., Kirk, H., Frank, D., Hull, N., Kotter, C., Stevens, J.M., Baumgardner, D., Norman, R., Pace, R.N., Hernandez, M., *Microbial aerosol liberation from soiled textiles isolated during routine residuals handling in a modern health care setting,* In: Microbiome, 2015, 3

[56] Krzyściak, W., Pluskwa, K.K., Jurczak, A., et al., *The pathogenicity of the Streptococcus genus,* In: Eur. J. Clin. Microbiol. Infect. Dis., 2013, 32, 1361–1376. https://doi.org/10.1007/s10096-013-1914-9

[57] Katelin, L., Davis, O.G., Shyamesh, K., Edward, J.D.Jr., *Pathology Associated With Streptococcus spp. Infection*, In: Baboons (Papio spp.*),* 2020, 57, 5, PubMed, https://doi.org/10.1177/0300985820941496

[58] Herman, G.V, Caciora, T., Ilies, D.C., Ilies, A., Deac, A., Sturza, A., Sonko ,S.M., Suba, N.S., Nistor, S., *3D Modeling of the Cultural Heritage: Between Opportunity and Necessity*, In: Journal of Applied Engineering Sciences, 2020, 10, 1, 27–30, https://doi.org/10.2478/jaes-2020-0005
[59] Elnashar, E.A., Indrie, L., Ilieş, D.C., Zlatev, Z., Herman, G.V., Secan, C., Wendt, J.A., *Rare Romanian Ethnographic Textiles-Reverse Engineering of Fabrics for Fashion Trends,* In: Sustainability, 2022, 14, 6859, https://doi.org/10.3390/su14116859
[60] Indrie, L., Affandi, N.D.N., Díaz-García, P., Haji, A., Ilies, D.C., Zlatev, Z., Taghiyari, H.R., Grama, V., Farima, D., *Mechanical and Morphological Properties of Cellulosic Fabrics Treated with Microencapsulated Essential Oils,* In: Coatings, 2022, 12, 1958, https://doi.org/10.3390/coatings12121958
[61] Al Fahmawee, E.A.D., Jawabreh, O., *Sustainability of green tourism by international tourists and its impact on green environmental achievement: Petra heritage, Jordan,* In: GeoJournal of Tourism and Geosites, 2023, 46, 1, 27–36, https://doi.org/10.30892/gtg.46103-997
[62] Glevitzky, M., Aleya, L., Vica, M.L., Dumitrel, G.A., Avram, M., Tit, D.M., Popa, M., Popa, V.C., Behl, T., Bungau, S., *Assessing the microbiological contamination along with environmental factors of old books in the 1490-founded Bistrița Monastery, Romania*, In: Environ. Sci. Pollut. Res., 2021, 8743–8757, https://doi.org/10.1007/s11356-020-

Authors:

BAHODIR SAFAROV[1], LILIANA INDRIE[2], MONICA COSTEA[3], ALEXANDRU TURZA[4], KOMIL AVAZOV[5], STEFAN BAIAS[6], DORINA CAMELIA ILIEȘ[6], MIHAELA ZDRINCA[7], EMILIA PANTEA[3], GABRIELA ILIEȘ[8], NICOLAIE HODOR[9], ANA CORNELIA PERES[3]

[1]Samarkand State University, Department of Digital Economy,
Samarkand 140104, Uzbekistan
e-mail: safarovb@rambler.ru

[2]University of Oradea, Faculty of Energy Engineering and Industrial Management, Department of Textile, Leather and Industrial Management, Oradea, Romania
e-mail: lindrie@uoradea.ro

[3]University of Oradea, Faculty of Environmental Protection, Oradea, Romania
e-mail: emilia.pantea@uoradea.ro, peresana@uoradea.ro

[4]National Institute for R&D of Isotopic and Molecular Technologies, Cluj-Napoca, Romania
e-mail: turzaalex@yahoo.com

[5]Tashkent Institute of Textile and Light Industry, Head of the Department of Scientific Research, Innovation, Scientific and Pedagogical Personnel Training, Tashkent 100012, Uzbekistan
e-mail: komil.avazov@mail.ru

[6]University of Oradea, Faculty of Geography, Tourism and Sport, Oradea, Romania
e-mail: sbaias@uoradea.ro, dilies@uoradea.ro

[7]University of Oradea, Faculty of Medicine and Pharmacy, Oradea, Romania
e-mail: mzdrinca@yahoo.com

[8]Babes-Bolyai University, Faculty of Geography, Extension at Sighetu Marmatiei, Romania
e-mail: gabriela.ilies@ubbcluj.ro

[9]Babes-Bolyai University, Faculty of Geography, Cluj-Napoca, Romania
e-mail: nicolaie.hodor@ubbcluj.ro

Corresponding author:

MONICA COSTEA
mcostea@uoradea.ro

Application of grape seed coating for antibacterial cotton fabric

DOI: 10.35530/IT.074.03.202217

FEYZA AKARSLAN KODALOĞLU HILAL DEMİRALAY

ABSTRACT – REZUMAT

Application of grape seed coating for antibacterial cotton fabric

Microorganisms can reproduce rapidly on textile surfaces. It is known that textile surfaces used especially in hospitals cause the spread of infections and pose a danger. In recent years, instead of synthetic and heavy metal applications, the interest in obtaining environmentally friendly and natural plant-based antibacterial materials and textile applications has been increasing day by day. Grape skins and seeds, rich in polyphenolic compounds, are waste products from winemaking. The evaluation of such waste products is of great importance. In this study, grape seed, which is stated to have antibacterial activity in many studies, was applied to cotton textile material with the coating method and it was aimed to gain antibacterial properties to the fabric. As a result of the colour fastness tests performed according to the ISO 105-C06 standard, it was not observed that the coating process had a negative effect on the washing fastness of the fabrics. The wash fastness value of all coated fabrics is 5. As a result of the washing fastness test, it was seen that the coated fabrics were resistant to washing. As a result of the friction fastness tests performed according to the TS EN ISO 105-X12 standard, it was observed that the coated fabrics were resistant to friction. When the breaking strength and breaking elongation values of the coated fabrics were examined as a result of the strength test performed according to the TS EN ISO 13934-1 standard, it was observed that the tensile strength and elongation at break of the coated fabrics increased. Antibacterial tests against E. coli and S. aureus bacteria were performed on treated fabrics according to the AATCC 100 antibacterial test method. It is obtained as a result of the coating process for 60% coverage. As a result of the coating process, better results were obtained against E.coli bacteria. It was observed that the antibacterial properties improved as the coating rate increased. As a result of the tests, antibacterial activity was provided against both bacteria. An acceptable level of antibacterial activity was detected in the antibacterial tests of the washed fabrics.

Keywords: *grape seed, coating, cotton fabric, antibacterial activity*

Aplicarea acoperirii cu semințe de struguri pentru material textil antibacterian din bumbac

Microorganismele se pot reproduce rapid pe suprafețele textile. Se știe că suprafețele textile folosite în special în spitale provoacă răspândirea infecțiilor și reprezintă un pericol. În ultimii ani, în locul aplicațiilor din metale sintetice și grele, interesul pentru obținerea de materiale antibacteriene și aplicații textile ecologice și naturale pe bază de plante a crescut pe zi ce trece. Coji și semințele de struguri, bogate în compuși polifenolici, sunt produse reziduale din vinificație. Evaluarea unor astfel de deșeuri este de mare importanță. În acest studiu, sămânța de struguri, despre care se spune în multe studii că are activitate antibacteriană, a fost aplicată pe material textil din bumbac prin metoda de acoperire și a avut ca scop obținerea de proprietăți antibacteriene pentru suportul textil. În urma testelor de rezistență a culorii efectuate conform standardului ISO 105-C06, nu s-a observat un efect negativ al procesului de acoperire asupra rezistenţei la spălare a materialelor textile. Valoarea rezistenței la spălare a tuturor materialelor textile acoperite este 5. Ca rezultat al testului de rezistență la spălare, s-a observat că materialele textile acoperite sunt rezistente la spălare. În urma testelor de rezistență la frecare efectuate conform standardului TS EN ISO 105-X12, s-a observat că materialele textile acoperite erau rezistente la frecare. Când au fost examinate valorile rezistenței la rupere și alungirii la rupere ale materialelor textile acoperite ca urmare a testului de rezistență efectuat conform standardului TS EN ISO 13934-1, s-a observat că rezistența la rupere și alungirea la rupere au crescut. Testele antibacteriene împotriva bacteriilor E. coli și S. aureus au fost efectuate pe materialele textile tratate conform metodei de testare antibacteriană AATCC 100. Se obține ca rezultat al procesului de acoperire pentru o acoperire de 60%. Ca urmare a procesului de acoperire, s-au obținut rezultate mai bune împotriva bacteriilor E.coli. S-a observat că proprietățile antibacteriene s-au îmbunătățit odată cu creșterea ratei de acoperire. În urma testelor, a fost asigurată activitate antibacteriană împotriva ambelor bacterii. Un nivel acceptabil de activitate antibacteriană a fost detectat în testele antibacteriene ale materialelor textile spălate.

Cuvinte-cheie: *sămânță de struguri, acoperire, material textil din bumbac, activitate antibacteriană*

INTRODUCTION

Grape (Vitis vinifera L.) is known as the raw material source of fruit juice and especially wine industry, and grape pulp is known as the main waste of grape processing enterprises. Tens of tons of pulp are released after the grape, which is one of the most grown fruits in the world, is processed in each harvest period. Its rich bioactive components make grape pomace a very profitable raw material for different sectors, the importance of which is increasing day by day [1, 2]. Grape seeds, whose antioxidant, anti-inflammatory and antimicrobial properties have been reported many times in the literature [3–5] constitute 38–52% of the grape pomace on a dry weight basis [6]. For this reason, the evaluation of grape seeds and extract and recycling of waste is an economically important approach.

Microorganisms can reproduce rapidly on textile surfaces under the influence of moisture, nutrients and temperature [7–9]. Undesirable odours and stains may occur on textile surfaces with the reproduction of microorganisms. In addition, colour change and a decrease in strength can be observed on the textile surface [10]. For this reason, as a result of increasing customer demands, antibacterial products obtained by processing the textile product with substances with antibacterial properties to eliminate or minimize the effect of microorganisms that harm the product and the user have come to the fore. It is very important to provide protection against microorganisms, especially in hospitals and schools, in terms of human health [11]. It is known that many textile surfaces such as bedspreads, sheets, aprons, uniforms, towels, and curtains used in hospitals cause the spread of infections and pose a danger. In a study, it was determined that *Staphylococcus aureus* bacteria, which is the most basic resistant bacteria for nosocomial infections, is found in 65% of nurse aprons [12]. E. coli is a bacterium that is abundant in the intestines of humans and animals. Some varieties cause epidemics transmitted by food and water, causing intestinal and urinary tract infections. These bacteria are the most dangerous and resistant, and it is known that 10% of the infections they cause result in death.

The main methods applied to impart antibacterial activity to textile materials can be classified as follows [13–29]: (a) by surface application; (b) by incorporating suitable bioactive substances into polymer melts before extrusion; (c) by coating technology; (d) with natural substrates; (e) using sol-gel technology; (f) by spraying or foaming technique; (g) by chemical or physical modification of the substrate and/or the active agent; (h) with green chemistry approaches. Determination of the most appropriate physicochemical and/or chemical techniques or methods is depended on the fibre type, the fabric, the chemical structure of the active agent, the equipment, and the desired performance properties.

In recent years, instead of synthetic and heavy metal applications, the interest in obtaining environmentally friendly and natural plant-based antibacterial substances and textile applications has been increasing day by day. In this study, grape seed, which is stated to have antibacterial activity in many studies, was applied to cotton textile material with different rates of coating method and the fabric gained antibacterial properties. Antibacterial tests against E. coli and S. aureus bacteria were performed on the treated fabrics. In addition, strength tests and washing and rubbing fastness tests of the fabrics were made and evaluated.

MATERIALS AND METHODS

In this study, 100% cotton woven fabrics were used. The properties of these fabrics are shown in table 1.

Table 1

FEATURES OF COTTON FABRIC

Cotton fabric	Density (wire/cm)	Yarn number (Nm)	Fibre type	Weight (g/m²)
Weft	13	20	Cotton	230
Warp	27	34	Cotton	

In this study, Tubicoat CRO water-based coating chemical used in coating applications was used in textiles supplied by CHT Tekstil and Chemistry. Tubicoat is a white paste-like acrylic dispersion coating chemical with an anionic character pH value of 8.5–9.5. Tubicoat forms a soft, non-sticky, wash-resistant and transparent film layer. Tubicoat is applied as a top coat. Tubicoat is suitable for direct use without dilution.

By coating, the physical and characteristic properties of fabrics are improved. Some features that cannot be gained with the existing structure of the fabric are gained by coating. Squeegee coating, wire-wrapped roller coating, cylinder coating, rotary stencil coating, spray coating, extrusion coating, powder coating, calender coating, transfer coating, sol-gel coating, and plasma coating methods are used in the coating. In this study, the squeegee coating method was used. The squeegee coating method is shown in figure 1.

The coating paste was prepared by mixing grape seed and auxiliary coating chemicals prepared at a micron scale at different rates (40%, 50% and 60%). After the fabric to be coated is fixed on a flat surface, a smooth and even population of the coating paste (paste) on the fabric is ensured with the help of the template and squeegee. Then, drying at 100 °C for 12 minutes and fixation at 120 °C for 3 minutes, the application was completed.

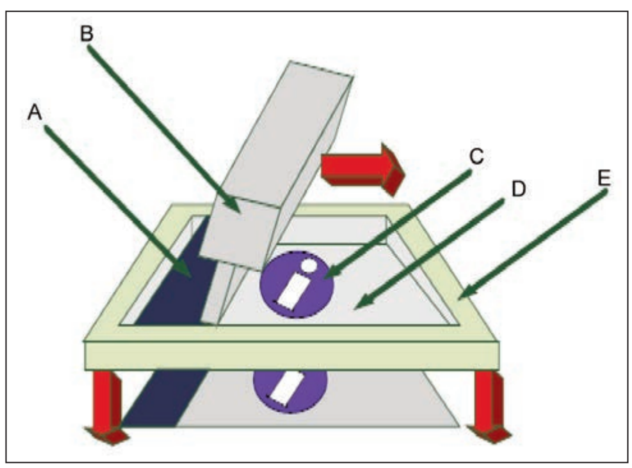

Fig. 1. Coating method: A – covering material; B – scraper (knife); C – tension cloth (gauze); D – template (frame); E – the picture that will appear if a picture is desired

In figure 1, it is shown that the grape seed is coated on the fabric using a coating chemical using a squeegee. The fabrics used in the study and the applications made are shown in table 2.

Table 2

APPLICATIONS	
Fabric	**Application**
1	Untreated fabric
2	40% Coated fabric
3	50% Coated fabric
4	60% Coated fabric

Before all tests were carried out, the fabrics were conditioned for 24 hours under laboratory conditions. To determine the washing sensitivities of the fabrics with an antibacterial finish, 1-5-10 repeated washings were carried out according to the TS EN ISO 105-C06 standard. Detergent and pure water for washing fastness test; *Staphylococcus aureus* (ATCC 6538) and *Escherichia coli* (ATCC 35218) bacteria, purified water and agar materials were used for antibacterial tests. Coated fabric images are given in figure 2.

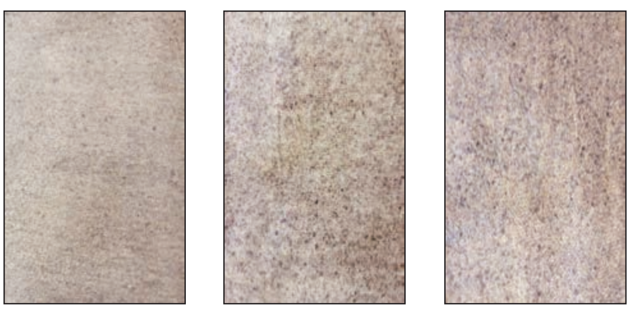

a *b* *c*

2. Fabrics coated with grape seed:
a – 40%; *b* – 50%; *c* – 60%

AATCC 100 antibacterial test method was used to quantitatively investigate the antibacterial properties of woven fabrics that were coated. To determine the effect of coating methods applied to woven fabrics on the tensile strength of fabrics, the tensile strength test of Llyod brand LR5K model strength tester according to TS EN ISO 13934-1 standard, To determine the effect of the washing process on fabrics, washing fastness test in ISO 105-C06 standard and to determine the effect of friction on fabrics, friction fastness test according to TS EN ISO 105-X12 standard was applied.

FINDINGS

Antibacterial test

In this study, AATCC 100 test method was used to determine antibacterial properties. This method is a test used to quantitatively determine the antibacterial properties of textile materials. According to this method, samples are placed in sterile containers. The number of colours that can absorb 1 ml of inoculum without leaving any liquid is determined. 1 ml of 100,000 CFU/ML inoculum is allowed to circulate throughout the heap to the samples. The inoculated inoculum is incubated for a certain contact time. At the appropriate test time, the neutralizing liquid is added to each vessel and shaken for one minute to incorporate the inoculum into the test. Serial dilutions are made and the plates are incubated. Colonies collected after incubation are counted and the percentage is calculated according to their decrease.

According to AATCC 100 antibacterial test method, fabrics' antibacterial activity values are given in table 3 against S. aureus and antibacterial activity values are given in table 4 against E. coli. In AATCC 100 Antibacterial test method, (–) values indicate a decrease in the number of bacteria, and (–) 100 indicates that all bacteria are dead. If the bacterial reductions in the media are calculated greater than 99.99%, they are considered to be "excellent", "good" if calculated between 99% and 99.99%, and "acceptable" if calculated between 0–99%.

Table 3

ANTIBACTERIAL ACTIVITY OF SAMPLES AGAINST S. AUREUS		
Fabrics	**Bacteria reduction (%)**	**Evaluation**
2	–66.67	acceptable
3	–75	acceptable
4	–89.18	acceptable

Table 4

ANTIBACTERIAL ACTIVITY OF SAMPLES AGAINST E.coli		
Samples	**Bacteria reduction (%)**	**Evaluation**
2	–89.4	acceptable
3	93.7	acceptable
4	–99.98	good

As seen in table 3 and table 4, for the 60% coated fabric, there was a reduction of 89.18% against S. aureus bacteria and a decrease of 99.98% against E. coli bacteria. The result was evaluated as 'acceptable' for S. aureus bacteria and 'good' for E. coli bacteria. For the 50% coated fabric, there was a 75% reduction against S. aureus bacteria and a 93.7% reduction against E. coli bacteria, and each person was evaluated as 'acceptable'. For the 40% coated fabric, there was a 66.67% reduction against S. aureus bacteria and an 89.4% reduction against E. coli bacteria, and it was evaluated as 'acceptable'. It was observed that as the coating rate increased, the antibacterial properties increased. As a result of the coating process, better results were obtained against E. coli bacteria.

Tensile strength

Tensile strength and elongation at break values of the samples are given in table 5.

Table 5

TENSILE STRENGTH AND ELONGATION VALUES OF SAMPLES

Fabrics	Tensile strength (N)		Elongation at break (%)	
	Warp	Weft	Warp	Weft
1	1077	285	29	75
2	1200	315	27	78
3	1226	317	30	82
4	1245	322	34	84

When the breaking strength and breaking elongation values given in table 5 are examined, it is seen that the breaking strength and breaking elongation values of the coated fabrics have increased.

Friction fastness

Friction fastness values of the samples are given in table 6.

Table 6

FRICTION FASTNESS VALUES OF SAMPLES

Fabrics	Friction fastness	
	Dry	Wet
2	5	4–5
3	5	4–5
4	5	4

When table 6 is examined, it is seen that the coating process does not affect the dry friction fastness of the fabrics, but it is effective on the wet friction fastnesses. The dry friction fastness of coated samples is 5, wet friction fastness is 4, 4–5.

Table 7

WASHING FASTNESS VALUES OF SAMPLES

Fabrics	Fading					
	Acetate	Cotton	Polyamide	Polyester	Acrylic	Wool
2	5	5	5	5	5	5

Washing fastness

The washing fastness values of the samples are given in table 7.

When table 7 is examined, no negative effect of the coating process on the washing fastness of the fabrics was observed. The washing fastness value of all coated fabrics is 5. As a result of the washing fastness test, it was seen that the coated fabrics were resistant to washing.

RESULTS AND DISCUSSION

The research of new technologies and new materials for the development of antibacterial textiles has been one of the topics of interest to researchers in recent years. Grape skins and seeds, rich in polyphenolic compounds, are waste products from winemaking. The evaluation of such waste products is of great importance. In this study, the use of grape seed in textiles has been investigated to give antibacterial activity to cotton fabrics. In this study, the coating method (squeegee coating) was used. 1-5-10 repeated washings were made to determine the washing resistance. It was not observed that the coating process had a negative effect on the washing fastness of the fabrics. The washing fastness value of all coated fabrics is 5. As a result of the washing fastness test, it was seen that the coated fabrics were resistant to washing. It has been observed that the coating process does not affect the dry rubbing fastness of the fabrics, but it is effective on the wet rubbing fastnesses. In general, it has been observed that the coated fabrics are resistant to friction. When the tensile strength and elongation at break values were examined, it was observed that the tensile strength and elongation at break of the coated fabrics increased. Antibacterial tests were carried out against E. coli and S. aureus bacteria on the treated fabricsGood antibacterial properties were obtained as a result of the coating process for 60% coating. As a result of the coating process, better results were obtained against E. coli bacteria. It was observed that the antibacterial properties improved as the coating rate increased. As a result of the tests, antibacterial activity was provided against both bacteria. In the antibacterial tests of the washed fabrics, an acceptable level of antibacterial activity was detected.

REFERENCES

[1] Barba, F.J., Zhu, Z., Koubaa, M., Sant'ana, A.S., *Green alternative methods for the extraction of antioxidant bioactive compounds from winery wastes and by-products,* In: Trends Food Sci. Tech., 2016, 49, 96–109

[2] Demirtaş, İ., Pelvan, E., Özdemir, İ.S., Alasalvar, C., Ertaş, E., *Lipid characteristics and phenolics of native grape seed oils grown in Turkey,* In: Eur. J. Lipid. Sci. Tech., 2013, 115, 641–647

[3] Oliveira, D.A., Salvador, A.A., Smânia, A., Smânia, E.F., Maraschin, M., Ferreira, S.R., *Antimicrobial activity and composition profile of grape (Vitis vinifera) pomace extracts obtained by supercritical fluids,* In: J Biotechnol., 2013, 164, 3, 423–432

[4] Sofi, F.R., Raju, C.V., Lakshmisha, I.P., Singh, R.R., *Antioxidant and antimicrobial properties of grape and papaya seed extracts and their application on the preservation of Indian mackerel (Rastrelliger kanagurta) during ice storage,* In: J. Food Sci. Technol., 2016, 53, 1, 104– 117
[5] Soto, M.L., Falqué, E., Domínguez, H., *Relevance of natural phenolics from grape and derivative products in the formulation of cosmetics,* In: Cosmetics, 2015, 2, 3, 259–276
[6] Teixeira, A., Baenas, N., Dominguez-Perles, R., Barros, A., Rosa, E., Moreno, D.A., Garcia-Viguera, C., *Natural bioactive compounds from winery byproducts as health promoters,* In: Int. J. Mol. Sci., 2014, 15, 15638–15678
[7] Cheng, W., Liu, W., Wang, Q., Wang, P., Zhou, M., Yu, Y., *Durable hydrophobic and antibacterial textile coating via PDA/AgNPs/ODA in situ assembly,* In: Cellulose, 2022, 29, 1175–1187
[8] Ye, Z., Li, S., Zhao, S., Deng, L., Zhang, J., Dong, A., *Textile coatings configured by double-nanoparticles to optimally couple superhydrophobic and antibacterial properties,* In: Chemical Engineering Journal, 2021, 420, 127680, 1–14
[9] Chen, M., et al., *Durably antibacterial cotton fabrics coated by protamine via Schiff base linkages,* In: International Journal of Biological Macromolecules, 2023, 227, 1078–1088
[10] Oğuz, N.S., *Antibacterial fabric production with radiation shielding property and investigation of its properties,* Süleyman Demirel University, Institute of Natural Sciences, PhD thesis, Isparta, 2019
[11] Devrent, N., Yılmaz, N.D., *Tekstil Endüstrisinde Kullanılan Antimikrobiyel Lifler,* In: Nonwoven Technical Textiles Technology Dergisi, 2004, 4, 48–55
[12] Boryo, D. E. A., *The effect of microbes on textile material: a review on the way-out so far,* In: The International Journal of Engineering and Science (IJES), 2013, 2, 8, 09–13
[13] Lee, H.J., Yeo, S.Y., Jeong, S.H., *Antibacterial effect of nanosized silver colloidal solution on textile fabrics,* In: Journal of Materials Science 2003, 38, 2199–2204
[14] Zhang, Z., et al., *Antibacterial properties of cotton fabrics treated with chitosan,* In: Textile Research Journal, 2003, 73, 12, 1103–1106
[15] Lim, S.H., Hudson, S.M., *Review of chitosan and its derivatives as antimicrobial agents and their uses as textile chemicals,* In: Journal of Macromolecular Science, Part C: Polymer Reviews, 2003, 43, 2, 223–269
[16] Kamel, M.Y., Hassabo, A.G., *Anti-microbial finishing for natural textile fabrics,* In: Journal of Textiles, Coloration and Polymer Science, 2021, 18, 2, 83–95
[17] Mahltig, B., Haufe, H., Böttcher, H., *Functionalisation of textiles by inorganic sol–gel coatings,* In: Journal of Materials Chemistry, 2005, 15, 41, 4385–4398
[18] Tawiah, B., Badoe, W., Fu, S., *Advances in the development of antimicrobial agents for textiles*: *The quest for natural products. Review,* In: Fibres & Textiles in Eastern Europe, 2016, 3, 117, 136–149
[19] Gao, Y., Cranston, R., *Recent advances in antimicrobial treatments of textiles,* In: Textile Research Journal, 2008, 78, 1, 60–72
[20] Dastjerdi, R., Montazer, M., *A review on the application of inorganic nano-structured materials in the modification of textiles: focus on anti-microbial properties,* In: Colloids and Surfaces B: Biointerfaces, 2010, 79, 1, 5–18
[21] Ibrahim, N.A., et al., *Innovative multi-functional treatments of ligno-cellulosic jute fabric,* In: Carbohydrate polymers, 2010, 82, 4, 1198–1204
[22] Shahid, M., Mohammad, F., *Green Chemistry Approaches to Develop Antimicrobial Textiles Based on Sustainable Biopolymers- A Review,* In: Industrial & Engineering Chemistry Research, 2013, 52, 15, 5245–5260
[23] Kasiri, M.B., Safapour, S., *Natural dyes and antimicrobials for green treatment of textiles,* In: Environmental Chemistry Letters, 2014, 12, 1, 1–13
[24] Sharkawy, A., Fernandes, I.P., Barreiro, M.F., Rodrigues, A.E., Shoeib, T., *Aroma-loaded microcapsules with antibacterial activity for eco-friendly textile application: synthesis, characterization, release, and green grafting,* In: Industrial & Engineering Chemistry Research, 2017, 56, 19, 5516–5526
[25] Fiedot-Toboła, M., Ciesielska, M., Maliszewska, I., Rac-Rumijowska, O., Suchorska-Woźniak, P., Teterycz, H., Bryjak, M., *Deposition of zinc oxide on different polymer textiles and their antibacterial properties,* In: Materials, 2018, 11, 707, 1–16
[26] Beşen, B.S., *Production of disposable antibacterial textiles via application of tea tree oil encapsulated into different wall materials,* In: Fibers and Polymers, 2019, 20, 2587–2593
[27] Das, S., Natarajan, S., *Antibacterial activity of chitosan in textiles–A review,* In: Man-Made Textiles in India, 2022, 50, 3, 96–100
[28] Lange, A., Sawosz, E., Wierzbicki, M., et al., *Nanocomposites of Graphene Oxide-Silver Nanoparticles for Enhanced Antibacterial Activity: Mechanism of Action and Medical Textiles Coating,* In: Materials, 2022, 15, 9, 3122
[29] Massella, D., Giraud, S., Guan, J., Ferri, A., Salaün, F., *Textiles for health: A review of textile fabrics treated with chitosan microcapsules*, In: Environmental Chemistry Letters, 2019, 17, 1787–1800

Authors:

FEYZA AKARSLAN KODALOĞLU[1], HILAL DEMİRALAY[2]

[1]Süleyman Demirel University, Department of Textile Engineering, 32260, Isparta, Turkey

[2]Isparta Health Directorate, No. 71 Family Health Center, 32300, Isparta, Turkey
e-mail: demiralay.hilal@gmail.com

Corresponding author:

FEYZA AKARSLAN KODALOĞLU
e-mail: feyzaakarslan@sdu.edu.tr

Research on modelling and stability of seamless dust removal system based on generalized system

DOI: 10.35530/IT.074.03.202236

HAIWEN MAO YAN HONG

ABSTRACT – REZUMAT

Research on modelling and stability of seamless dust removal system based on generalized system

The dedusting system is the parameter selection and the degree of cooperation between several dust collector components. The stability of the system plays a decisive role in the dust removal efficiency of the whole system. The existing dust removal system model is a mechanism model, and the bag size, filter bag distribution and other parameters are optimized by simulation results. It cannot provide a model reference for the use of a new filter bag. In this research, the generalized model of the dust removal system is established by MATLAB. The factors affecting the service life of filter bag and dust removal efficiency of dust removal system are analysed. A differential equation is used to describe the influence of these factors. The dynamic model of the dust removal system is established. When considering the problem of flue gas emission, the algebraic equation with dust is constructed. The model of the bag-type dust removal system is described by a generalized system. Finally, the model's stability is analysed using the method of generalized system analysis, and the necessary and sufficient conditions for the stability of the model are obtained. Given the advantages of a seamless filter bag in filtration efficiency and mechanical properties, the stability of the system is studied. The results show that the system stability increases by 55.4% and 41.9% respectively. The performance of the filter bag is introduced into the modelling of the dust removal system, which plays a key role in the overall evaluation of the filter bag.

Keywords: *seamless filter bag, generalized system, dust removal system, system stability*

Cercetări privind modelarea și stabilitatea sistemului de îndepărtare a prafului pentru sacul filtrant fără cusătură pe baza unui sistem generalizat

Sistemul de desprăfuire reprezintă selecția parametrilor și gradul de conlucrare dintre mai multe componente ale colectorului de praf. Stabilitatea sistemului joacă un rol decisiv în eficiența de îndepărtare a prafului întregului sistem. Modelul existent de sistem de îndepărtare a prafului este un model de mecanism, iar dimensiunea sacului, distribuția sacului filtrant și alți parametri sunt optimizați prin rezultatele simulării. Nu se poate furniza model de referință pentru utilizarea noului sac filtrant. În această cercetare, modelul generalizat al sistemului de îndepărtare a prafului este stabilit utilizând MATLAB. Sunt analizați factorii care afectează durata de viață a sacului filtrant și eficiența de reținere a prafului de către sistemul de îndepărtare a prafului. Ecuația diferențială este utilizată pentru a descrie influența acestor factori. Se stabilește modelul dinamic al sistemului de îndepărtare a prafului. Apoi, luând în considerare problema emisiei de gaze arse, se construiește ecuația algebrică pentru praf. Modelul de sistem de îndepărtare a prafului tip sac este descris de sistemul generalizat. În sfârșit, se analizează stabilitatea modelului prin utilizarea metodei analizei generalizate a sistemului și se obțin condițiile necesare şi suficiente pentru stabilitatea modelului. Având în vedere avantajele sacului filtrant fără cusătură în ceea ce privește eficiența filtrării și proprietățile mecanice, se studiază stabilitatea sistemului. Rezultatele arată că stabilitatea sistemului crește cu 55,4% și, respectiv, 41,9%. Performanța sacului filtrant este introdusă în modelarea sistemului de îndepărtare a prafului, care joacă un rol cheie în evaluarea generală a sacului filtrant.

Cuvinte-cheie: *sac filtrant fără cusătură, sistem generalizat, sistem de îndepărtare a prafului, stabilitatea sistemului*

INTRODUCTION

The dedusting system was the parameter selection and the degree of cooperation between several components of the dust collector, which included several parts, a filter bag, bag type, ash hopper, air inlet and outlet, etc. [1–3]. Dust removal stability determined the stability of each component during operation. It played a decisive role in the dust removal efficiency of the whole system [4–7]. The performance of the filter bag was the key factor affecting the efficiency and stability of the dust removal system. Therefore, the performance of the filter bag was introduced into the modelling of the dust removal system, which played a key role in the overall evaluation of the filter bag [8–10].

Many factors need to be considered to model the entire dust removal system. The uncertainty of these factors was greater. Therefore, there were few researched on it. Chang analysed the operation stability of the bag-type dust removal system in a garbage incineration plant and established the qualitative relationship between the factors affecting the operation stability of the dust removal system. Then through the quantitative treatment of each influence factor, using the primary and secondary factor analysis method and fuzzy mathematical evaluation matrix mathematical modelling, the study of the smooth operation of the dust removal system seamless dust removal system research qualitative generalized system and the quantitative relationship between the influence factors was obtained. The model was optimized to improve the stability of the new dedusting process [11]. Liu quantified the factors that may affect the dust removal efficiency of bag-type dust removal system by establishing a mechanism model. Its influence on dust removal efficiency with time was analysed. The stability of the bag-type dust removal system was studied and evaluated by the coefficient of variation of dust removal efficiency under normal working conditions in the same year. Finally, the influence of the new process on the stability of the dust removal system was studied in the waste incineration plant. The model was employed to predict the maximum expansion scale of the enterprise and provide relevant suggestions for the detection of environmental protection departments [12]. Combined with the calculation model of the dust removal system, the further development of the simulation model of the EAF comprehensive process was proposed by Merier [13]. Further chemical composition and gas radiation were added to improve gas phase calculations. The results obtained from the EAF process model were used for subsequent calculations of the dust removal system model, such as predicting waste heat recovery potential, cooling system load, or analysing the post-combustion process. The deterministic implementation of these two models allowed for quick and easy adaptation of various EAF and detailed study of energy distribution and mass transfer within EAF. The model could be used in the design and control strategy of electric furnace. The existing dust removal system model was a mechanism model, and the bag size, filter bag distribution, ash bucket size, inlet and outlet location and other parameters were optimized through the simulation results, and the change of process parameters did not include the filter bag property. It had no reference value for the use of a filter bag and could not provide a model reference for the use of a new filter bag.

The establishment of the dust removal system model was to further explain the advantages of weft-knitted biaxial seamless air filter material in the improvement of mechanical properties and filtration efficiency in practical application. A generalized system was employed to model the dust removal system. Matlab was employed to simulate the stability of the dust removal system, which could better analyse the stability of the dust removal system. The dedusting efficiency and stability of the system were studied by changing the life of the filter bag and the initial dedusting efficiency. It was proved that the use of a seamless filter bag played a positive role in improving the efficiency and stability of the whole dust removal system. It provided a theoretical reference for the application of a seamless filter bag.

MODELLING ASSUMPTION

Aiming at the stability of the dust removal system, the stability of the dust removal system studied in this research was comprehensively measured by the service life of the filter bag, the dust removal efficiency and the total amount of flue gas emissions. In the process of dust removal, all factors were changing. To facilitate this research, the system stability was defined when the above three factors kept a certain value unchanged during the system operation. The shorter the time for the system to reach stability, the higher the corresponding system stability was.

Firstly, the factors affecting the service life of the filter bag and the dust removal efficiency of the dust removal system were analysed. The differential equation was applied to describe the influence of these factors on the service life of the filter bag and the dust removal efficiency of the dust removal system. The dynamic model of the dust removal system was established. Secondly, considering the problem of flue gas emission, the algebraic equation with dust was constructed. The model of the bag-type dust removal system is described by a generalized system. Finally, the stability of the model was analysed by using the method of generalized system analysis. The necessary and sufficient conditions for the stability of the model were obtained. The following assumptions were made for the successful establishment of the model and the smooth operation.

Assumption 1: The failure of the ash transport system during the operation of the dust removal system was not considered.

Assumption 2: The influence of the control system on the dust collector was not considered.

Assumption 3: The proportion of waste incineration to flue gas remained unchanged.

Assumption 4: The pressure difference in the furnace did not change during the operation of the system.

Assumption 5: The scale of an incinerator was multiplied by the efficiency of dust removal.

INFLUENCING FACTORS OF MODEL

To make a better explanation of the solution of the equation, the Hurwitz theorem was introduced here. Its content was below. The necessary and sufficient condition for the stability of the system was that all eigenvalues of the coefficient matrix *A* of the system had non-positive real parts. In addition, its eigenvalues with zero real part were simple roots of its minimal polynomial. The asymptotic stability of the system was required if all eigenvalues of the system coefficient matrix *A* had negative real parts.

The influence factors of the dust removal system were mainly divided into two parts. The first part was the factors affecting the service life of filter bag. The second part was the factors affecting the dust removal efficiency of the system.

The factors affecting the service life of the filter bag

Uneven distribution of flue gas

The local filter wind speed in the air chamber was too high. This caused the dust to increase the impact and wear of the filter bag. The degree of uneven distribution of flue gas is expressed by $d_1, d_1 \in [0,1]$. When the value was 1, it indicated that the flue gas was not evenly distributed. However, when the value was 0, it indicated that the flue gas was evenly distributed and hardly wear the filter bag.

Pressure difference in the furnace

A larger differential pressure means that the filter bag was subjected to greater resistance during operation. This was one of the reasons why the damage of the filter bag is aggravated. The pressure difference in the furnace was set as p_1. The larger its value was, the more the service life of the filter bag was reduced.

Distance between filter bags

The distance between the filter bags was too small. This could cause wear and tear between filter bags or flexion of cage bones. The gap between the cage bone and the bottom of the filter bag was too small. This could cause impact wear between the filter bag and the cage bone. Therefore, the influence of the direct distance of the filter bag on the service life of the filter bag was considered. In addition, the distance between the filter bags was set as d_2.

Cleaning times of the filter bag

Cleaning the filter bag too often would accelerate the wear of the filter bag. It would also affect the service life of the filter bag. The filter bag cleaning times were set as n.

Temperature of the flue gas

It was easy to damage the filter bag when the flue gas temperature exceeded 220 °C. This could greatly reduce the life of the filter bag. Therefore, the influence of flue gas temperature on the service life of the filter bag was also considered. It was set as γ_3 and meets the following conditions.

$$\text{if } T_2 \leq 220, \text{ then } \gamma_3 = 0$$

The factors affecting system dust removal efficiency

Temperature of the flue gas

The temperature of incoming flue gas was strictly controlled between 130 °C and 220 °C. Flue gas condensation was easy to occur when the temperature was lower than 130 °C. Dust adsorption on the filter bag was not easy to fall off. e of the flue gas was set as γ_3 and meets the following conditions.

$$\text{if } T_2 \geq 130, \text{ then } \gamma_3 = 0$$

Air leakage

Air leakage leads to fly ash plate and agglomerate, blocking the filter bag and affecting the filtering effect. Caking in the chamber and tube wall affected the conveying effect of fly ash. The influence factor is set as a_1, $a_1 \in [0,1]$. If the value was set to 1, the filtering effect was greatly affected. If the value was set to 0, the filtering effect was almost unaffected.

Leakage in flue and body

Leakage of the flue and body leads to condensation of flue gas. The condensation precipitated acidic liquid, leading to serious corrosion of the dust collector structure. Inhaling rainwater on rainy days further aggravated the damaging effects of caking, acid, etc. This impact factor was as a_2, $a_2 \in [0,1]$. When the value was 1, it had a great influence on the life of the filter bag. When the value was 0, it basically had no influence.

MODEL ESTABLISHMENT OF DUST REMOVAL SYSTEM

According to the analysis of the influencing factors of the system in the preparation part of the above model, the differential equation of the service life of the filter bag can be obtained as shown in equation 1. In the equation, α_1 is the influence factors of mechanical properties of filter bags on service life, d_1 – the degree of irregularity in the distribution of flue gas, d_2 – the interaction factor between two filter bags, n – the influence of filter bag cleaning times on filter bag life.

$$T'(t) = \alpha_1\rho(t)T(t) - (1 - d_1)T(t) - d_2T^2(t) - nT(t) \quad (1)$$

Based on the above analysis of the influencing factors of the system dust removal efficiency, the differential equation of the system dust removal efficiency can be obtained as shown in equation 2. In this formula, n is the influence of cleaning times on dust removal efficiency, a_1 and a_2 – the influence factors of air leakage and water leakage on dust removal efficiency respectively, α_2 – the influence of the service life of filter bag on dust removal efficiency.

$$\rho'(t) = n\rho(t) - a_1\rho(t) - a_2\rho(t) - \alpha_2\rho(t)T(t) \quad (2)$$

The ceiling of total emissions per unit area around incineration plants shall be set. The total amount of flue gas discharged was equal to the flue gas produced by garbage incineration minus the flue gas discharged by the dust removal system. The algebraic equation about the total amount of flue gas discharged was given below, as shown in equation 3. In this formula, β is the conversion rate of garbage to flue gas, S – the conversion rate of garbage to flue gas, M – the amount of garbage treated per unit area of the standard incinerator, m – the amount of filter bags, $\rho(t)$ – the filtration efficiency.

$$N(t) = (\beta - m\rho(t))SM \quad (3)$$

According to equations 1, 2 and 3, the model of the dust removal system was shown in equation 4.

$$\begin{cases} T'(t) = \alpha_1\rho(t)T(t) - (1 - d_1)T(t) - d_2T^2(t) - nT(t) \\ \rho'(t) = n\rho(t) - a_1\rho(t) - a_2\rho(t) - \alpha_2\rho(t)T(t) \\ 0 = (\beta - m\rho(t))SM - N(t) \end{cases} \quad (4)$$

STABILITY ANALYSIS OF DUST REMOVAL SYSTEM

Equation 4 could be expressed as follows:

$$A(t)X'(t) = (T(t), \rho(t), N(t))$$

In this formula,

$$X(t) = G(T(t), \rho(t), N(t))$$

$$A(t)=\begin{bmatrix}1 & 0 & 0\\ 0 & 1 & 0\\ 0 & 0 & 0\end{bmatrix}$$

$$G\big(T(t),\rho(t),N(t)\big)=$$

$$=\begin{bmatrix}\alpha_1\rho(t)T(t)-(1-d_1)T(t)-d_2T^2(t)-nT(t)\\ n\rho(t)-a_1\rho(t)-a_2\rho(t)-\alpha_2\rho(t)T(t)\\ (\beta-m\rho(t))SM-N(t)\end{bmatrix}$$

$$\begin{cases}\alpha_1\rho(t)T(t)-(1-d_1)T(t)-d_2T^2(t)-nT(t)=0\\ n\rho(t)-a_1\rho(t)-a_2\rho(t)-\alpha_2\rho(t)T(t)=0\\ (\beta-m\rho(t))SM-N(t)=0\end{cases}$$

Three equilibrium points are solved according to the system formula.

$$P_1=(0,0,MS),\ \ P_2=\Big(\frac{d_1-n-1}{d_2},0,\beta MS\Big)$$

$$P_3=\left(\frac{n-a_1-a_2}{\alpha_2},\ \frac{\alpha_2-a_1d_2-a_2d_2-\alpha_2d_1+\alpha_2n+nd_2}{\alpha_1+\alpha_2},\ \frac{MS(a_1d_2m-\alpha_2m+a_2d_2m+\alpha_2d_1m-\alpha_2nm-d_2nm+\beta\alpha_1\alpha_2)}{\alpha_1+\alpha_2}\right) \quad (5)$$

Subsequently, the stability of model 4 at the above three equilibrium points was researched. The Jacobian determinant of the system was shown in formula 6.

$$J_p=\begin{vmatrix}\alpha_1\tilde{\rho}-(1-d_1)-2d_2\tilde{T}-n & \alpha_1\tilde{T} & 0\\ -\alpha_2\tilde{\rho} & n-a_1-a_2-\alpha_2\tilde{T} & 0\\ 0 & -mSM & -1\end{vmatrix} \quad (6)$$

Firstly, the stability at the point P_1 was considered. The Jacobian determinant of the characteristic equation of the dust removal system 5-4 at the point P_1 was as follows.

$$\det\left|\lambda-J_p\right|_{p_1}=$$

$$=\begin{vmatrix}\lambda-[\alpha_1\tilde{\rho}-(1-d_1)-2d_2\tilde{T}-n] & -\alpha_1\tilde{T} & 0\\ \alpha_2\tilde{\rho} & \lambda-(n-a_1-a_2-\alpha_2\tilde{T}) & 0\\ 0 & SM & \lambda+1\end{vmatrix}_{p_1}$$

$$=(\lambda+1-d_1+n)(\lambda-n+a_1+a_2)(\lambda+1)$$

The above system has three characteristic roots as follows.

$$\lambda_1=d_1-1-n$$
$$\lambda_2=n-a_1-a_2$$
$$\lambda_3=-1$$

According to the Hurwitz theorem, when the dust removal system meets $\lambda_1<0$, $\lambda_2<0$, $\lambda_3<0$, the dust removal system is asymptotically stable at the point P_1 as shown in equation 7. It could be concluded that when the coefficient of the dust removal system meet condition 7, the dust removal system 4 was asymptotically stable at the point P_1.

$$\begin{cases}d_1-1-n<0\\ n-a_1-a_2<0\end{cases} \quad (7)$$

Secondly, the stability at the point P_2 was considered. The Jacobian determinant of the characteristic equation of the dust removal system 4 at a point P_2 was as follows.

$$\det\left|\lambda-J_p\right|_{p_2}=$$

$$=\begin{vmatrix}\lambda-[\alpha_1\tilde{\rho}-(1-d_1)-2d_2\tilde{T}-n] & -\alpha_1\tilde{T} & 0\\ \alpha_2\tilde{\rho} & \lambda-(n-a_1-a_2-\alpha_2\tilde{T}) & 0\\ 0 & SM & \lambda+1\end{vmatrix}_{p_2}$$

$$=(\lambda+d_1-n-1)\left(\lambda-n+a_1+a_2+\alpha_2\frac{d_1-n-1}{d_2}\right)(\lambda+1)$$

The above system has three characteristic roots as follows.

$$\lambda_1=-d_1+1+n$$
$$\lambda_2=n-a_1-a_2-\alpha_2\frac{d_1-n-1}{d_2}$$
$$\lambda_3=-1$$

According to the Hurwitz theorem, when the dust removal system meets $\lambda_1<0$, $\lambda_2<0$, $\lambda_3<0$, the dust removal system is asymptotically stable at the point P_2 as shown in equation 8. It could be concluded that when the coefficient of the dust removal system meet condition 8, the dust removal system 4 was asymptotically stable at the point P_2.

$$\begin{cases}-d_1+1+n<0\\ n-a_1-a_2-\alpha_2\dfrac{d_1-n-1}{d_2}<0\end{cases} \quad (8)$$

Secondly, the stability at the point P_3 was considered. The Jacobian determinant of the characteristic equation of the dust removal system 4 at the point P_3 was as follows.

$$\det\left|\lambda-J_p\right|_{p_3}=$$

$$=\begin{vmatrix}\lambda-[\alpha_1\tilde{\rho}-(1-d_1)-2d_2\tilde{T}-n] & -\alpha_1\tilde{T} & 0\\ \alpha_2\tilde{\rho} & \lambda-(n-a_1-a_2-\alpha_2\tilde{T}) & 0\\ 0 & mSM & \lambda+1\end{vmatrix}_{p_3}$$

$$=\{[\lambda-(\alpha_1\rho-(1-d_1)-2d_2T-n)]\cdot$$

$$\cdot[\lambda-(n-a_1-a_2-\alpha_2T)]+\alpha_1\alpha_2T\rho\}(\lambda+1)=$$

$$=\left(\begin{matrix}\lambda^2+(a_1+a_2-d_1+A_1+A_2+A_3+1)\lambda+\\ (a_1+a_2-n+A_3)(n-d_1+A_1+A_2+1)-\dfrac{\alpha_1(a_1+a_2-n)A_4}{\alpha_1+\alpha_2}\end{matrix}\right)(\lambda+1)$$

$$A_1=\frac{\alpha_1(a_1+a_2-n)}{\alpha_2},\ \ A_2=\frac{2d_2A_4}{\alpha_1+\alpha_2},\ \ A_3=\frac{\alpha_2A_4}{\alpha_1+\alpha_2}$$

$$A_4=\alpha_2-a_1d_2-a_2d_2-\alpha_2d_1-\alpha_2n-d_2n$$

The system had three characteristic roots, among which $\lambda_1=-1<0$. The other two roots were determined by equation 9.

$$\left(\begin{array}{l}\lambda^2 + (a_1 + a_2 - d_1 + A_1 + A_2 + A_3 + 1)\lambda + \\ (a_1 + a_2 - n + A_3)(n - d_1 + A_1 + A_2 + 1) - \dfrac{\alpha_1(a_1 + a_2 - n)A_4}{\alpha_1 + \alpha_2}\end{array}\right) = 0 \quad (9)$$

It was known that both roots of the equation had negative real parts when the coefficients satisfied the following conditions through Weida's theorem.

$$\begin{cases} a_1 + a_2 - d_1 + A_1 + A_2 + A_3 + 1 > 0 \\ (a_1 + a_2 - n + A_3)(n - d_1 + A_1 + A_2 + 1) - \dfrac{\alpha_1(a_1 + a_2 - n)A_4}{\alpha_1 + \alpha_2} > 0 \end{cases}$$

According to the Hurwitz theorem, when the dust removal system meets $\lambda_1 < 0$, $\lambda_2 < 0$, $\lambda_3 < 0$, the dust removal system is asymptotically stable at the point P_3 as shown in equation 10. It could be concluded that when the coefficient of the dust removal system meet condition 10, the dust removal system 4 was asymptotically stable at the point P_3.

$$\begin{cases} a_1 + a_2 - d_1 + A_1 + A_2 + A_3 + 1 > 0 \\ (a_1 + a_2 - n + A_3)(n - d_1 + A_1 + A_2 + 1) - \dfrac{\alpha_1(a_1 + a_2 - n)A_4}{\alpha_1 + \alpha_2} > 0 \end{cases} \quad (10)$$

Since the service life of the filter bag and the dust removal efficiency of the system were both positive numbers, the stability of the system only considered the stability of the system at the positive equilibrium point. That was, the following stability premise was the stability at the positive equilibrium point. Therefore, the premise of stability was to meet the conditions of the point P_3.

To verify that the theorem conditions could ensure the stability of the dust removal system, the relevant parameters set was shown in table 1. The number of filter bags represented the relative number (unit: 10,000).

The system status response was shown in the following two figures. Figure 1 shows the service life diagram of the filter bag. Figure 2 shows the smoke emission chart. The values in the figure represent relative sizes, not specific values. It could be seen from the figures that the system could finally reach a stable state within a certain period. Therefore, the solution of the equilibrium point P_3 was reasonable and reliable.

RESULTS AND DISCUSSION

Influence of mechanical properties on filter bag life

In this model, α_1 was not the specific mechanical property value, which represented the influence factors of mechanical properties of filter bag on service life. The parameter was set to four different values, 1, 2, 3, and 4. The increase in this value represented the improvement of the mechanical properties of the filter bag itself. The influence of the parameter α_1 on the life of the filter bag was shown in figure 3. It was obvious in this figure that the overall performance of the system would eventually be stable when the system changes the influence factor of the mechanical properties of the filter bag on the service life. The greater the influence factor of the mechanical properties of the filter bag on the service life, the longer the service life of the filter bag system was. The life of the filter bag at different values was shown in table 2.

Table 1

PARAMETER SETTINGS								
Parameter	α_1	α_2	a_1	a_2	β	m	S	M
Number	1	0.5	0.5	0.5	0.8	0.01056	10	1

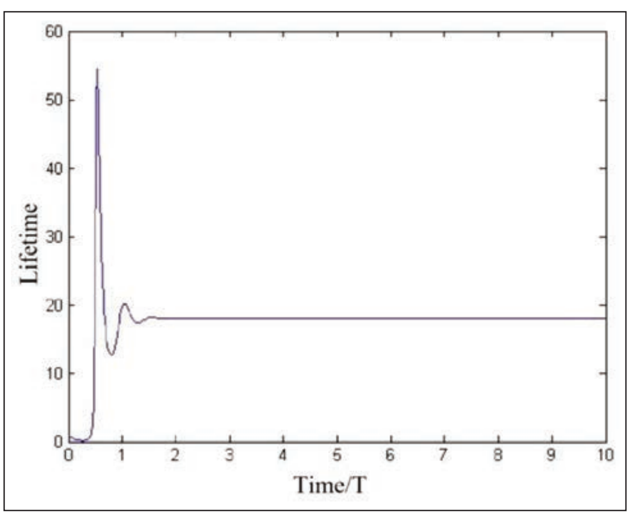

Fig. 1. The service life diagram of the filter bag

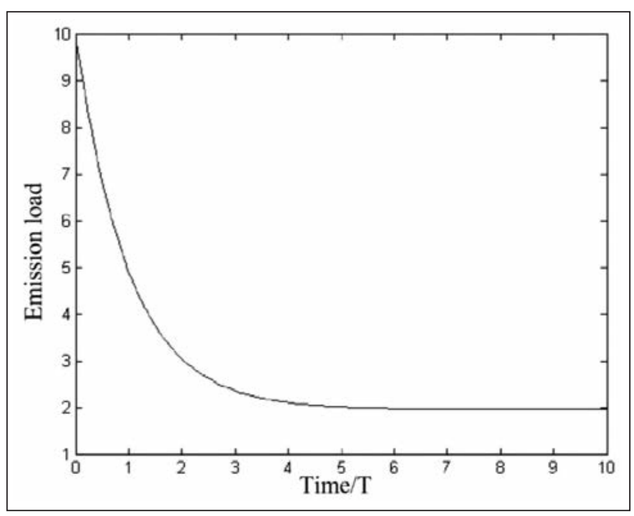

Fig. 2. The smoke emission chart

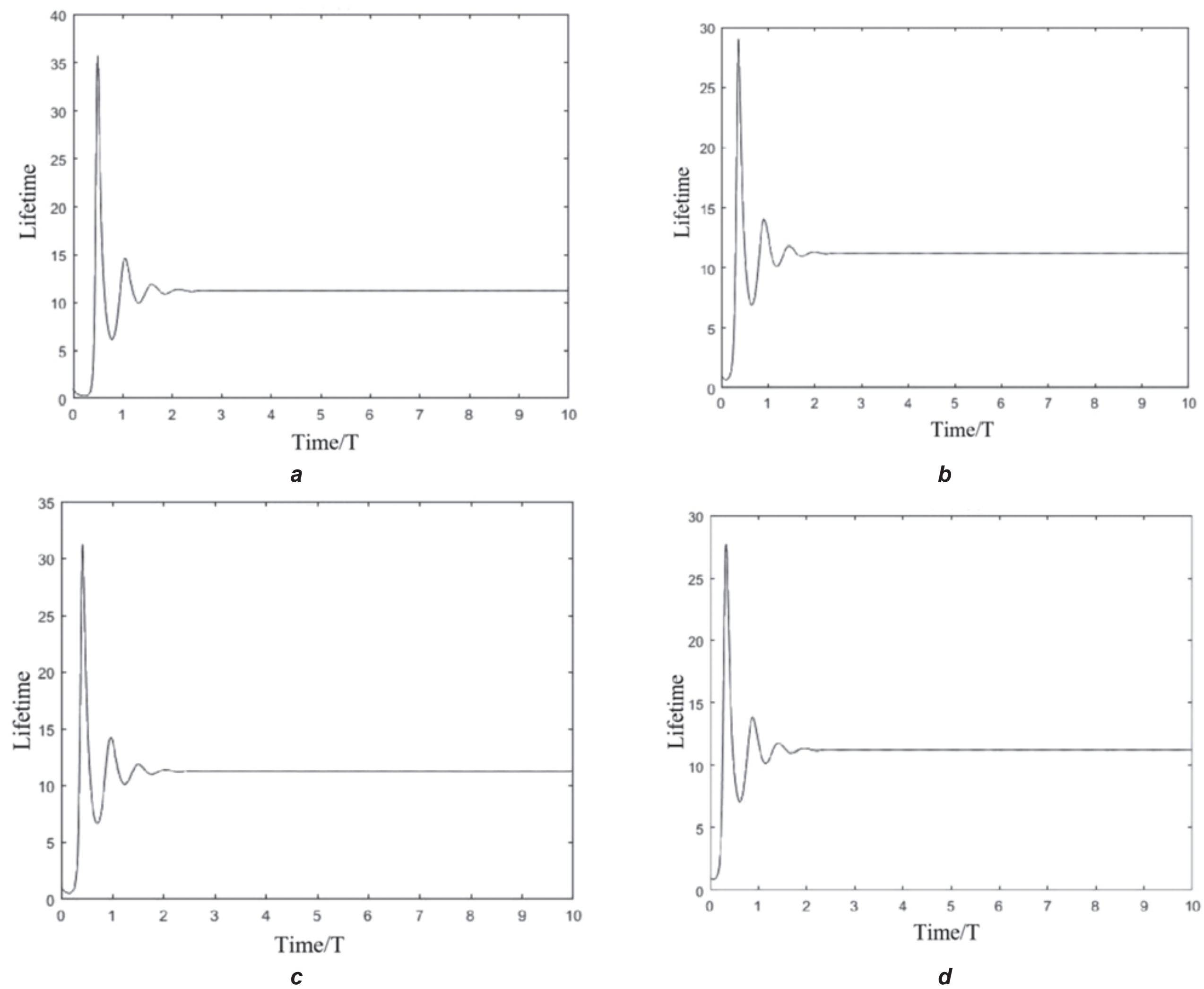

Fig. 3. Influence of different mechanical properties on filter bag life and system stability:
a – $\alpha_1 = 1$; *b* – $\alpha_1 = 2$; *c* – $\alpha_1 = 3$; *d* – $\alpha_1 = 4$

Table 2

THE LIFE OF THE FILTER BAG AT DIFFERENT VALUES

α_1	The life of the filter bag
1	11.2
2	12.8
3	15.0
4	17.9

Table 3

THE INFLUENCE OF THE PARAMETER α_2 ON THE DEDUSTING EFFICIENCY OF THE SYSTEM AND THE STABILIZATION TIME OF THE SYSTEM

α_2	The stabilization time	The dedusting efficiency
0.5	2.35	16.15
1	2.72	14.99
1.5	4.01	13.51
2	5.28	12.75

Influence of service life on dust removal efficiency of filter bag

In this model, α_2 represented the influence factor of the service life of filter bag on dust removal efficiency. The parameter was set to four different values, 0.8, 1, 1.5 and 2. The increase of this value represented the greater impact of the service life of the filter bag on dust removal efficiency. Therefore, the service life of the filter bag was lower. The influence of the parameter α_2 on dust removal efficiency was shown in figure 4. It was obvious in this figure that the overall performance of the system tend to be stable when the system changed the influence factor of the service life of the filter bag on the dust removal efficiency. However, when the parameter α_2 was set to different values, the dust removal efficiency of filter bags was different. Table 3 shows the impact of the parameter on the dust removal efficiency and system stabilization time. As the parameter α_2 increased, so did the time to system stability. The efficiency of dusting declined, which indicated the reduction of the service life of the filter bag. The dust removal efficiency

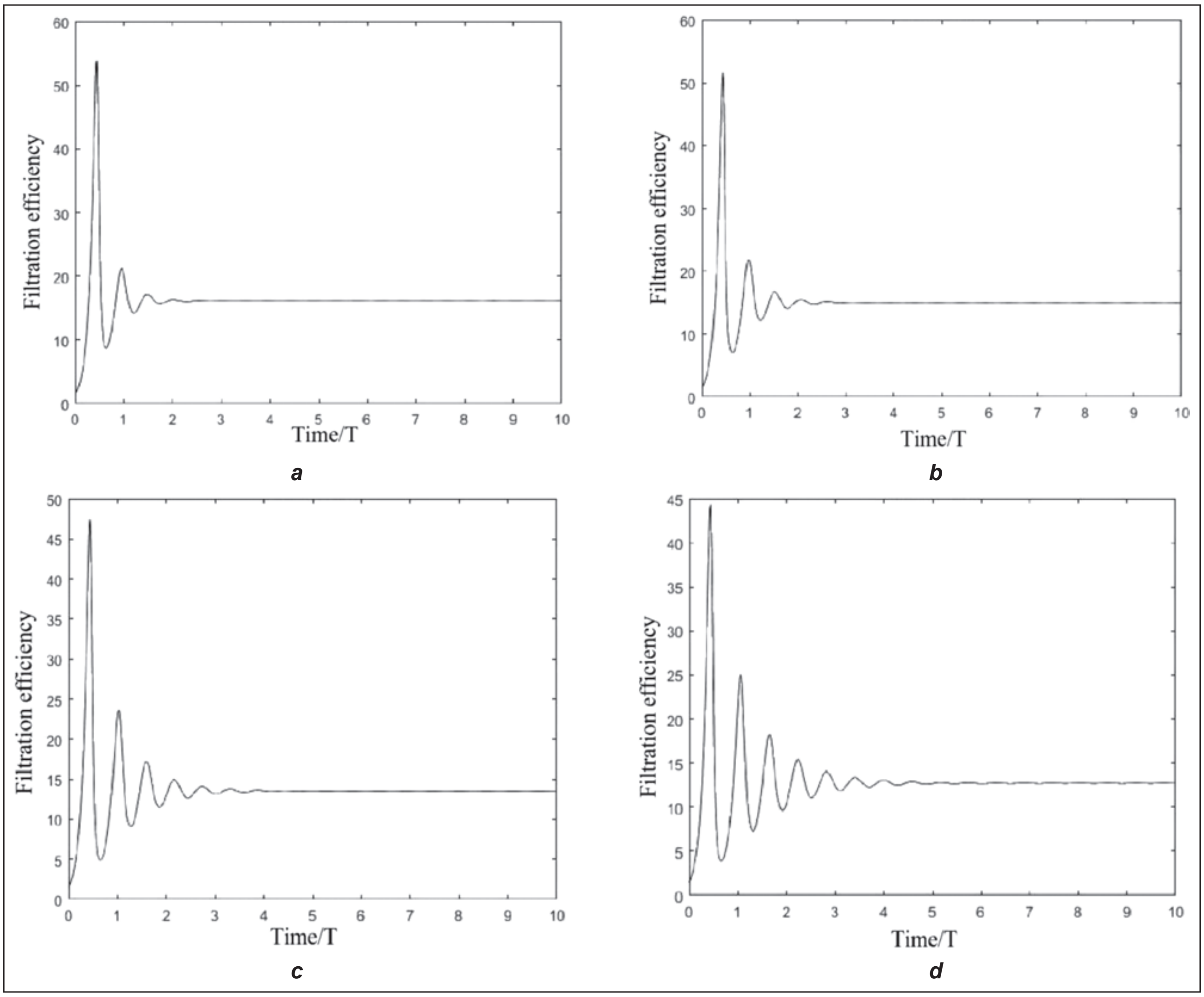

Fig. 4. Influence of different filter bag life on dedusting efficiency and system stability:
a – $\alpha_2 = 0.5$; *b* – $\alpha_2 = 1$; *c* – $\alpha_2 = 1.5$; *d* – $\alpha_2 = 2$

of the system decreased. The time to reach stability increased, which was not conducive to the continuous operation of the whole dust removal system.

Influence of initial filtration efficiency on dust removal efficiency

Compared with the traditional filter bag, the seamless filter bag not only improved in mechanical properties but also improved filtration performance to a certain extent. In the model, the employment of a seamless filter bag was shown the improvement of dust removal efficiency ρ_0 in the initial state. Four different initial dust removal efficiency values were adopted in this experiment, which were 0.1, 0.5, 1 and 1.5 respectively. The larger the value was, the greater the initial dust removal efficiency of the filter bag was. The impact of this value on dust removal efficiency and system stability was shown in figure 5.

It was obvious in this figure that the system's overall performance tends to be stable when the system changes the initial value of dust removal efficiency. However, the time reached stability was different. The time when the system reaches stability with different initial dust removal efficiencies was listed in table 4. It was obvious from the table, when the initial value was larger, the time for the system to reach stability was shorter, and the overall operation effect of the system was better.

Table 4

THE TIME FOR DUST REMOVAL EFFICIENCY TO REACH STABILITY AT DIFFERENT INITIAL VALUES

Initial value of dust removal efficiency	The time the system reaches stability
0.1	2.0370
0.5	1.4826
1.0	1.3279
1.5	1.1872

The seamless filter bag researched in this paper could improve the initial value of dust removal. Seamless filter bag played a positive role in improving the stability of the whole filtration system. Therefore, for the model of the air filter bag, the time spent to stabilize the dust removal system was taken as the standard of system stability performance. The calculation formula for system stability was shown in equation 11. The function of the dust removal system

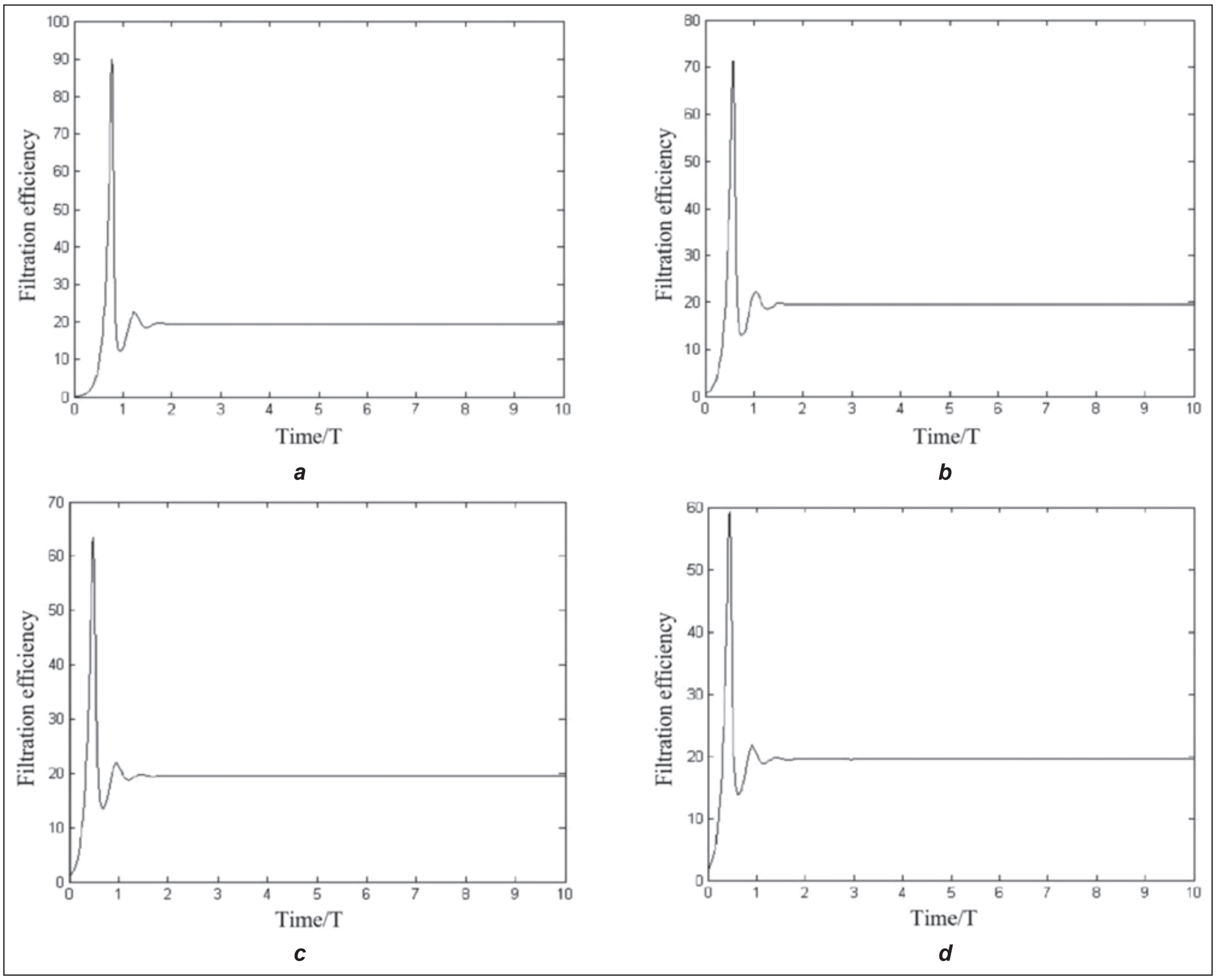

Fig. 5. Influence of different initial filtration efficiency on dust removal efficiency and system stability:
a – $\rho_0 = 0.1$; *b* – $\rho_0 = 0.5$; *c* – $\rho_0 = 1$; *d* – $\rho_0 = 1.5$

was shown in equation 12. The system stability time was the time that the dust removal system passes when the derivative of the dust removal efficiency function was equal to 0. Equation 13 was obtained after taking the derivative. The time for the system to reach stability was shown in equation 14.

$$\begin{cases} T'(t) = \alpha_1\rho(t)T(t) - (1 - d_1)T(t) - d_2T^2(t) - nT(t) \\ \rho'(t) = n\rho(t) - a_1\rho(t) - a_2\rho(t) - \alpha_2\rho(t)T(t) \end{cases} \quad (11)$$

$$\rho(t) = \rho_0 e^{(a_1 + a_2 + \alpha_2 T - n)t} \quad (12)$$

$$\rho'(t) = (a_1 + a_2 + \alpha_2 T - n)\rho_0 e^{(a_1 + a_2 + \alpha_2 T - n)t} \quad (13)$$

$$T = \frac{n - a_1 - a_2}{\alpha_2 \rho_0} \quad (14)$$

Therefore, the reduction of time for the system to reach stability was regarded as the standard for improving the stability of the dust removal model. When the initial value was raised, it was calculated according to equation 15. When the seamless filter bag was employed, the stability of the dust removal system model was improved by 20%.

$$\frac{1.4826 - 1.1872}{1.4826} = 20\% \quad (15)$$

CONCLUSIONS

- In this research, a bag dust removal system model based on a generalized system was obtained by analysing various influencing factors of the bag dust removal system, which was composed of three differential equations, the service life of the filter bag, system dust removal efficiency and total amount of flue gas emission.
- The stability of the dust removal model was analysed by means of the stability analysis of the generalized system. The dedusting model could reach a stable equilibrium point under certain conditions. Finally, the time when the dust removal model reaches stability was employed as the standard to measure the stability performance of the system.
- By increasing the influence factor of the mechanical properties of the filter bag on the service life, the system would be stable. However, with the increase in the service life of the filter bag, the higher the dust removal efficiency of the system was, the shorter the time for the system to reach stability was, and the stability of the system improved by 55.4%. By increasing the initial value of dust removal efficiency, the system's overall performance tends to be stable. But the time to stability was

different. The larger the initial value of dust removal efficiency was, the shorter the time for the system to reach stability was. System stability was improved by 41.9 %. The research showed that the employment of seamless filter bag with high mechanical properties and filtration performance had significantly improved the stability of the dust removal system. It provided a theoretical reference for the application of seamless filtration materials.

ACKNOWLEDGEMENTS

This work was supported by the National Natural Science Foundation of China, China Association for Science and Technology Youth Support Talent Project, Hong Kong Polytechnic University GBA Startup Postdoc Programme 2022, and Jiangsu Province Engineering Research Center of Special Functional Textile Materials.

REFERENCES

[1] Hong, S.G., Jung, Y.J., et al., *A study on the optimization design of pulse air jet system to improve bag-filter performance,* In: Journal of the Korea Academia-Industrial cooperation Society, 2012, 13, 8, 3792–3799

[2] Ilić, M., Milutinović, S., et al., *Selection of a dedusting system for the lime stone preparation plant in the deposit "Zagradje-5"*, In: Mining and Metallurgy Engineering Bor, 2020, 3–4, 57–66

[3] Matelli, J.A., *Heat recovery of dedusting systems in electric arc furnaces: concept of a bottoming cogeneration plant and techno-economic analysis*, In: Journal of the Brazilian Society of Mechanical Sciences and Engineering, 2018, 40, 1, 1–14

[4] Omelchenko, E., Trushkova, E., et al., *Study of the Effectiveness of Innovative Air Purification Systems Used in the Design of Road Construction Enterprises*, In: Transportation Research Procedia, 2022, 61, 594–599

[5] Dock, J., Janz, D., et al., *Time-and component-resolved energy system model of an electric steel mill*, In: Cleaner Engineering and Technology, 2021, 4, 100223

[6] Dong, J., Tang, Y., et al., *Environmental consequences of an ultra-low emission retrofit in coal-fired power plants from a life cycle perspective,* In: Waste Disposal & Sustainable Energy, 2021, 3, 4, 309–323

[7] Wu, Q., Gu, M., et al., *Synergistic removal of dust using the wet flue gas desulfurization systems*, In: Royal Society Open Science, 2019, 6, 7, 181696

[8] Guo, L., Nie, W., et al., *The dust diffusion modeling and determination of optimal airflow rate for removing the dust generated during mine tunnelling,* In: Building and Environment, 2020, 178, 106846

[9] Li, Y., Cao, L., et al., *Semi-Interpenetrating Polymer Network Biomimetic Structure Enables Superelastic and Thermostable Nanofibrous Aerogels for Cascade Filtration of PM2.5,* In: Advanced Functional Materials, 2020, 30, 14, 1910426

[10] Liu, Q., Nie, W., et al., *A study on the dust control effect of the dust extraction system in TBM construction tunnels based on CFD computer simulation technology*, In: Advanced Powder Technology, 2019, 30, 10, 2059–2075

[11] Chang, P., Chen, L., et al., *Modeling and optimization of operation stability of bag-type dust removal system*, In: Construction Machinery Technology and Management, 2017, 30, 6, 66–71

[12] Liu, B.D., Jia, P.Y., et al., *Stability model and simulation of bag dust removal system*, In: Mathematical Modeling and its Applications, 2017, 6, 1, 39–52

[13] Meier, T., Kolagar, A.H., et al., *Process modelling and simulation of an EAF and its dedusting system*, In: Chernye Metally, 2018, 2, 18–24

Authors:

HAIWEN MAO[1,2], YAN HONG[3]

[1]Changzhou Vocational Institute of Textile and Garment, College of Textile,
No. 53 Gehu Road Changzhou, 213164, Changzhou, China,

[2]Jiangsu Province Engineering Research Center of Special Functional Textile Materials,
No. 53 Gehu Road Changzhou, 213164, Changzhou, China,

[3]Soochow University, College of Textile and Clothing Engineering, No.1 Shizi Street Suzhou, 215026, Suzhou, China,

Corresponding author:

HAIWEN MAO
e-mail: maohw91@163.com
YAN HONG
e-mail: hongyan@suda.edu.cn

Emotions and fashion: how garments induce feelings to the sensory system

DOI: 10.35530/IT.074.03.202253

DUJE KODŽOMAN
ALENKA PAVKO ČUDEN
VANJA ČOK

ABSTRACT – REZUMAT

Emotions and fashion: how garments induce feelings to the sensory system

Emotional design is the concept of creating a design that evokes emotions, which results in pleasant user experiences. It is important because emotions influence decision-making and affect both our attention and memory. Although clothing has a direct impact on our mood and attitude, fashion is rarely given attention as an area where emotions play an important role in the design process. We have summarized the existing data on this topic using a secondary research method. This review aims to explore whether garments induce senses and sensory experiences, what is the importance of emotional branding and brand experience, and how fashion brands employ sense marketing. After a theoretical review of the literature, in the results section, we present a brief overview of evoking the senses with specific examples from the fashion industry. The findings of the review indicate that the relationship between emotions, senses and fashion can be seen through: the colour of the fabric (sense of sight), the store interior (sense of sight and touch), the scents in the store (sense of smell), the interaction between skin and fabric or touching the textiles (sense of touch), and finally the music in the store (sense of hearing).

Keywords: *fashion, emotion, senses, sensory evaluation, sensory system*

Emoțiile și moda: cum induce îmbrăcămintea sentimente în sistemul senzorial

Designul emoțional este conceptul de a crea un design care evocă emoții, care au ca rezultat experiențe plăcute pentru utilizator. Este important pentru că emoțiile influențează luarea deciziilor și ne afectează atât atenția, cât și memoria. Deși îmbrăcămintea are un impact direct asupra stării de spirit și a atitudinii noastre, modei i se acordă rar atenție ca zonă în care emoțiile joacă un rol important în procesul de design. Am rezumat datele existente pe această temă folosind metoda de cercetare secundară. Scopul acestui studiu este de a explora dacă articolele de îmbrăcăminte induc simțuri și experiențe senzoriale, care este importanța brandingului emoțional și a experienței de brand și cum folosesc brandurile de modă marketingul senzorial. După analiza teoretică a literaturii de specialitate, în secțiunea de rezultate prezentăm un rezumat al evocării simțurilor cu exemple specifice din industria modei. Rezultatele studiului indică faptul că relația dintre emoții, simțuri și modă poate fi văzută prin: culoarea materialului textil (simțul văzului), interiorul magazinului (simțul văzului și simţul tactil), mirosurile din magazin (simțul olfactiv), interacțiunea dintre piele și materialul textil sau atingerea textilelor (simțul tactil), și în final muzica din magazin (simțul auzului).

Cuvinte-cheie*: modă, emoţie, simțuri, evaluare senzorială, sistem senzorial*

INTRODUCTION

We live in a society with a growing interest in unique and personalized products, seeking authentic experiences. Scientists who studied design twenty years ago began to discuss several relevant affective phenomena in design, such as pleasure, mood, and emotion. This research resulted in the creation of a relatively new concept – emotional design [1]. It is a concept that refers to a type of design that strives to create products that induce and cause the appropriate emotions [2]. While most authors agree that useful design should include personality and emotions [1, 2], in discussions on design methodology, fashion is rarely given attention as a field in which emotion plays a significant role in the design process [3]. Emotional design is thoroughly elaborated within architectural design, web design, and product design; but there is a noticeable literature deficit regarding emotional design in the field of textile and fashion. Also, despite the recognition of consumer emotions in design practice today, a literature review of design research in the field of fashion has revealed a lack of conceptualization of consumers' emotional needs in fashion [4]. The human sensory system, such as sight, smell, touch, taste, and hearing, receives a great deal of information every day based on the feedback mechanism of cranial nerves [5, 6].

In today's commercial activities, consumers are seeking rewarding, memorable, and pleasurable consumption experiences. Thereby it is important to explore the relationship between emotions and the senses in the field of fashion design. The secondary research (desk research) method was used for data processing in this study on emotions, emotional experiences, moods, emotional branding, and sensory marketing.

GENERAL INFORMATION

The databases presented in the review were compiled and sourced from a variety of channels such as journals and magazines (61), books (17) and conference papers (4). The examined sources were the Web of Science and COBISS (Slovenian library information system), but also documents available by websites. The period included in the analysis is the period from the 1970s to recent works from 2021.

Emotions and mood

It is a universal phenomenon that mood and emotion influence the way consumers purchase clothing. One's attire or dressing style is said to be an important part of the personality representation as it gives the first impression on others, though emotion and mood are two factors of a person's personality which clothing can have an impact on [3, 7, 8].

Commonly emotions are considered within two main schools of thought [8]. Firstly, emotions are viewed as biologically given or "inherent" [9]. Secondly, emotions are viewed as "intersubjective" [10], involving active perception, identification, and management on the part of individuals [11]. Emotions can be understood as central to human behaviour because they condition our experiences (by limiting, modifying or enhancing them), substantiate the belief systems we uphold, and are an inherent aspect of all human action [8]. Illouz [12] contends that the concept of emotion usefully explains how consumption is anchored in cognition and culture (beliefs and evaluations) on the one hand, and in the motivational structure of drives within the body (affect) on the other.

According to Mehrabian and Russell [13], individuals engage or approach environmental stimuli that create pleasurable affective responses and avoid stimuli that create unpleasant affective responses. Approach responses include willingness to purchase a product and return to the site or store. Laros & Steenkamp [14] found that we choose clothing daily to cope with social circumstances and one's feelings and indicated that favourite clothes are important for controlling one's emotions and mood.

The means by which connections between emotions and clothing have been made can again be divided into two main approaches [8]. Firstly, there are those accounts which focus on women's emotional attachments to clothes, for example, wedding dresses [15], whereby clothing provides symbolic access to women's emotional pasts. The second body of work focuses more explicitly on women's relationships with clothing, beyond considering clothing to be an emotional trigger, instead documenting more deeply the relationship between clothing and female identity through wearing, selecting, and keeping clothing [16]. Recent work on emotions suggests that we consider emotion not as biologically inherent in its form and production, but instead look at the intersubjective nature of emotions [8].

Work which has considered women's relationships with clothing and fashion more generally has tended to dichotomize women's emotional connections with clothing as "positive" (playful, performative, and celebratory) or "negative" (enslaving, patriarchal or indulgent) [17]. These accounts tend to emphasize the product of emotional sensation, i.e., positive and negative emotions, rather than how emotions are produced and experienced. However, Negrin [17] does not mention men's relationship with clothing and fashion in her article.

The work of Sayer [18] illustrates those sentiments such as pride, shame, envy, resentment, compassion, and contempt are not merely abstract and temporal emotions. He asserts that sentiments are borne out of evaluative judgements that people make about how well they, or others, are being treated, and whether they have access to the things they consider affect their well-being and happiness. The way a person chooses to dress can affect their everyday life in numerous ways. The circle of friends and associates, job interview performance or how a person feels can all be affected by what the person decides to wear on daily bases [6, 7].

The affective component covers the motions and the positive and negative responses of mood [16] and is considered to be one factor of preference. Moody, Kinderman and Sinha [19] found out that both mood and personality played a role in the person's choice of clothing style but the mood had a more significant effect. Kwon [20, 21] found that clothing items with higher clothing functions had a strong positive relation with a person's mood, in the sense that, if clothing item were highly fashionable and highly individuality, it would boost the person's mood higher than a clothing item that had only one clothing function. Asare, Ibrahim and Kwesi [22] researched social and psychological factors that influenced female students' choice of clothing, they found that body image played a significant role in the selection of clothing. More specifically, the female students preferred clothing that emphasized the body parts that they were satisfied with.

When shopping for clothes women may experience uncomfortable feelings and emotions about their bodies in clothing, but in turn, engage in practices of consumption that enable the moment(s) to be experienced differently [8]. Emotion and mood were shown to be managed and reflected through clothing with implications for assistance in consumer clothing decisions. The result from Samadi [6] indicated a strong relationship between mood and emotion. There are many other factors about dressing like the colour of the dress, print, quality of fabric and design of dress are important for the person, and people do consider these factors.

Importance of emotional branding and brand experience

Emotional branding is a brand's strategy that stimulates consumers' affective state, appealing to their feelings to increase consumer loyalty toward the

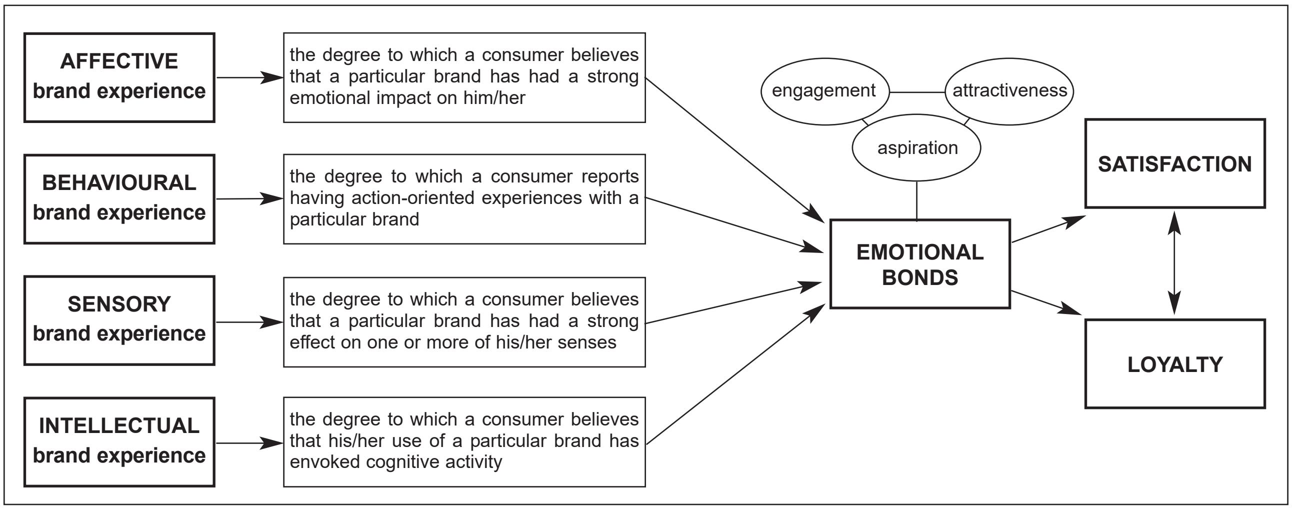

Fig. 1. Brand experiences scheme according to Brakus [27]

brand [23], and it is an extremely important strategic practice for fashion brands because it can create strong attachments between consumers and brands [24]. Emotional branding establishes itself as a critical factor in developing brand loyalty, which has been conceptualized as a long-term partnership devised to characterize consumer-brand bonds [25].

Fashion brands today must develop new strategies to capture consumer attention. Emotional branding and brand experiences can help them become more competitive and delight their customers [23]. This is particularly important because research shows that emotionally connected consumers are 52% more valuable to a brand than those who are just satisfied [23, 26].

A brand experience includes subjective sensations, feelings, and evaluations, which are internally processed responses to brand-related stimuli like brand design, visual identity, packaging, communications, and other environmental cues [27]. Therefore, a brand experience can occur at the level of a product, service, store, or marketing campaign. Based on Schmitt's [28] identification of five sensory experiences (i.e., think, feel, sense, relate, and act), Brakus et al. [27] proposed four dimensions of brand experiences: affective, behavioural, sensory, and intellectual experiences (figure 1). These experiences inspire emotional bonds and lasting impressions in consumers, leading to the success of branding efforts. Nowadays, retailers employ emotional branding to engage their customers – appealing to their needs, aspirations, dreams, and ego [29].

As marketing emphasis has shifted from the product to the creation of consumers' experiences, sensory marketing seems to be integral to stimulating excitement and pleasure [30]. As Lindstrom [31] stated, a brand's appeal to consumers' senses allows them to experience the brand more profoundly and have an emotional connection with it at a deeper level. Sensory marketing engages and triggers consumers' senses (i.e., sight, sound, feel, taste, and smell) [32]. All five senses elicit emotional responses to goods, services, and the environment [23]. In terms of ranking the senses, previous research has pointed sense of sight as being the most powerful in detecting changes and differences in the environment [33] and the sense of smell as the one triggering the most vivid memories (figure 2) [34].

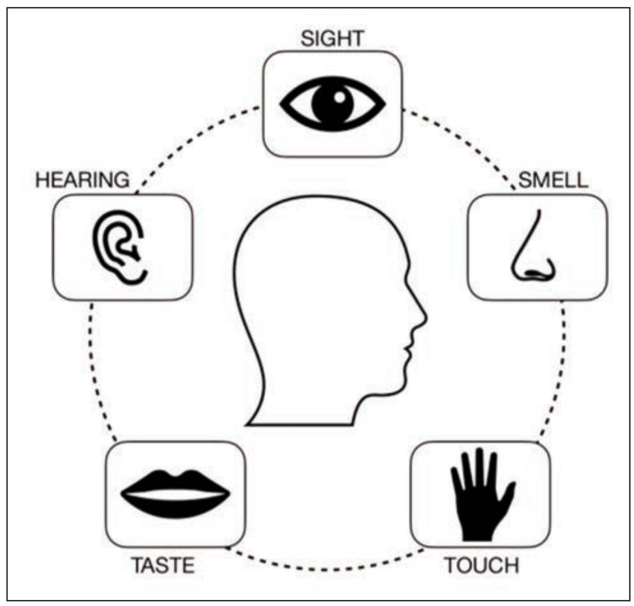

Fig. 2. The five traditionally recognized senses

Holbrook and Hirschman [35] outlined that the consumption experience can be intrinsically satisfying when the experience pleasures the senses and feelings. A lot of research support Holbrook's proposition that emotion is a key link in the consumption experience [36–38]. Mattila & Wirtz [39] showed that pleasurable stimulation from store atmospherics increased impulse buying behaviour, and the stimulating experience will enhance willingness to purchase from the online store. The stimulating (emotional) experience involved in the consumption process can be effectively represented by two dimensions, emotional arousal and emotional pleasure [40, 41]. Emotional arousal refers to the degree to which one feels stimulated, excited, or alert in the situation, whereas emotional pleasure is the evaluation dimension of affect referring to the degree to which one feels good, happy, or satisfied [42]. According to Delong and Larntz [43] preferences are composed of two components: cognitive and affective. The affective component is the emotional and overall positive and negative mood response to the object, which due to the very nature of clothing, is a very intimate experience. The cognitive component or schema, are product, aesthetic and social attributes inherent in the object which are evaluated through previous experiences, concepts, and situations of use [38].

For example, Lush, a handmade cosmetics brand, has been successful in employing sensory marketing: sight from round shapes of visually attractive products and live plants to illustrate the actual ingredients of their products; smell from the intoxicating and sweet scents; sound from knowledgeable salespeople talking actively behind a large bubbling hand bath; feel from unusual textures of the products and smooth and natural packaging; and imaginary taste from products with delicious food colours [44].

An example from the fashion industry is Chanel which has LED signage that visually promotes its signature tweed [23]. Chanel boutiques have a sitting area that features tweed chairs, plush carpet, fireplaces, and coffee tables stacked with Chanel books on each floor for visual consistency [45]. In addition, the store sprays classic Chanel No. 5 perfume to enhance the customer's olfactory sensory experience [46]. Furthermore, since touch increases the probability of purchase, it places accessories where customers can feel the products. Chanel is one of the successful brands that have utilized multi-sensory stimuli to intensify their customers' experiences.

Another fashion example was set in 2014 in Shanghai, China by the Under Armour brand. They combined striking architecture and visual effects – a panoramic film featuring Michael Phelps. After watching a 6-minute film of intensive sports training on a 270-degree panoramic screen, customers emerge in a custom-designed retail space in which several Under Armour products were exhibited.

The store itself also has an important role. More than before, fashion stores are the reference "touch-point" of the brand. They keep evolving and adapting to customers' needs. Some of them have set up a ramp for skateboarding (DC store in Bali, Indonesia), others provide a selection of books and magazines (Mulberry's first flagship in New York, USA, and many more), many have expanded into the pedestrian area with tables and beautiful flowers etc. Some of the best design achievements when it comes to fashion store interiors involve the use of unusual materials and colour combinations. Ssense's store in Montreal, Canada features a metallic interior designed by British architect David Chipperfield. The same architect designed the 1,850-metre-square store for Valentino in New York, USA. Light blue Pinta Verde marble appears throughout Celine's flagship store in Miami, which has been designed by Swiss practice Valerio Olgiati. Eduard Eremchuk on the other hand has designed pink furry changing rooms for a concept shop in Rostov-on-Don, Russia. All these examples show us an immediate way in which the fashion industry manages to stimulate the senses of sight and touch (figure 3). However, it should be emphasized that in addition to the interior, stimulation of the mentioned senses is successfully achieved also by garments with their colour and texture.

Sense marketing

Characteristics of a store's environment can have a substantial impact on consumers' shopping behaviour [47]. Previous research has shown that music [48], colour [49], lighting [50], crowding [51], and ambient scents [52] are a few atmospheric cues that affect consumers. Experiential marketers view consumers as rational yet emotional creatures that like to encounter pleasant experiences [53]. According to retailers, appealing to the senses is an important factor in these shopping experiences [53, 54]. Schmitt [53] defined sensory marketing as follows:

Sense marketing appeals to the senses with the objective of creating sensory experiences through sight, sound, touch, taste, and smell. Sense marketing may be used to differentiate companies and products, motivate customers and add value to products (e.g., through aesthetics or excitement).

The most common theoretical basis for studying the effects of atmospheric cues on shopping behaviour is

a *b* *c*

Fig. 3. Photos of: *a* – Ssense store in Montreal; *b* – concept shop in Rostov-on-Don; *c* – Celine store in Miami

based on environmental psychology [47]. One of its basic paradigms is the stimulus–organism–response (S–O–R) paradigm [13, 55, 56]. In the retail context, a store's atmosphere (S) is the stimulus that affects consumers' internal evaluations (O). These evaluations then lead to behavioural responses, that is, approach or avoidance responses (R).

Department stores such as Harrods in London, and Bloomingdale's Inc. in New York City, have experimented with olfactory marketing, diffusing different odours into their departments [47]. Individuals who enjoy the shopping experience will be more positively affected by the presence of a pleasant ambient scent in the store than people who shop for utilitarian reasons. Orth and Bourrain [57] found that the presence of an ambient scent evokes nostalgic memories. Bruner [58] stated that music has the greatest effect on consumer behaviour when consumers are either highly affective involved or low cognitively involved with the product. Because ambient scent is also an atmospheric element, it is most likely that scent influences consumers when they buy products based on emotional motives (e.g., prestigious clothing) or when they are low involved with the purchase decision.

Colour is an important factor in the visual appearance of products as well as brand recognition, and it is critical for designers to understand consumer colour preferences as part of an effective design plan [59], such as evoking emotions. Kodžoman et al. [59] examined colour preferences about attractiveness across all decades of the 20th century and found that the most unattractive colours were: Caramel Cafe (brown), Desert Sage (grey), and Sulfur Spring (green-yellow) showing that we are repelled by colours associated with negative connotations because of experiences we have had with them, while most attractive colours in their study were: Black, Pink Yarrow, and Blazing Yellow. As they stated the stability of preferences depends on the period and era we live in, all influenced by age, gender, and education.

Young-adult female consumers continue to be the most attractive targets for the fashion industry [60, 61]. And many women report that fashion plays a significant role in their lives and affects their sense of emotional well-being [62–64].

A large body of research has studied how a combined measure of positive employee-displayed actions, which has sometimes included the presence, visibility, or availability of store employees, can impact customers' attitudes, affective states, and purchase behaviour [65–68].

Söderlund [69] has explicitly examined the isolated effect of employee mere presence on key customer outcomes and found that customers entering a store with an employee present reported significantly higher levels of customer satisfaction, with their increased levels of pleasurable feelings mediating this effect [70]. Otterbring and Lu [70] replicated the main findings from Söderlund in a large Chinese sample, indicating that prior theorizing pertaining to this topic applies not only to data collected on customers in Western and individualistic societies but also to customers from Eastern and collectivist societies.

Within the economy, retail continues to grow and is now the largest and one of the most influential sectors [71]. Clothing and accessory stores are among the largest retail employers [72]. Nearly 1 million U.S. workers – almost 1% of all workers – were employed in clothing retail in 2014, which pays less than most other retail positions [73]. This industry disproportionately employs young people, not unionized, women, and racial and ethnic minorities, making it a key area to study to examine vulnerable workers [74, 75]. Research suggests that employers seek out workers who identify with the store brand [76, 77].

Selecting the clothes we wear

It is widely accepted that clothing has the potential (and is commonly used) to reflect and convey the inner self [19], e.g., self-image, mood, political affiliations, and social aspirations [78–80], but also that consumers prefer products that are consistent with their identity [81]. Raunio [82] identified three factors in the preference of clothing: physical features of clothes including skin response, size and shape of the clothes, thermal comfort, and fit (looseness and over-sized), revealing levels and visual features; the wearers' self-appearance; and associative reasons and memories. All of these factors would generate an emotional response. Raunio [82] also found that we choose clothing daily to cope with social circumstances and one's feelings. She indicated that favourite clothes are important for controlling one's emotions and therefore have regulative purposes (figure 4).

Furthermore, Kwon [20] researched the relationships between the perception of mood, self-consciousness, and the selection of clothing, and concluded that

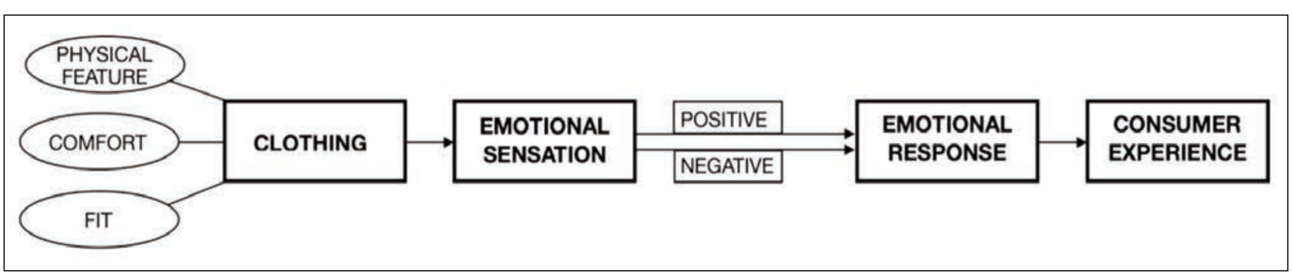

Fig. 4. Factors in the preference of clothing according to Raunio [82]

females were more sensitive to mood than men, which affected their clothing choices; and negative moods affected their choices more than positive moods. Kwon [20, 21] also showed how much one feels and their emotional baseline about themselves, can affect their choices and behaviour. These findings indicate the emotional management functions of clothing.

Tombs [83] found that outfit choices are made to match the mood and that they are a form of self-expression, but clothing can also be used to control emotions since memories attached to our clothes can evoke good or bad feelings when we wear them.

Woodward [84] conducted a study by interviewing women in their homes while they were choosing an outfit from their wardrobe (figure 5). She found that women order and re-order a personal narrative and while choosing an outfit ask them-self the question “who am I?” In several studies [8, 84, 85] women’s choices of clothing emerge as a mainly intellectual exploration of their own identity and a conscious decision about which aspects of this identity to show and underline, given the social circumstances under which the choice is made and the characteristics of the situations in which the clothes have to be worn. Studies have also shown that closer interest in clothing can correlate with increased depression, but also that over short periods after dressing, clothes can lift or change a low mood [86].

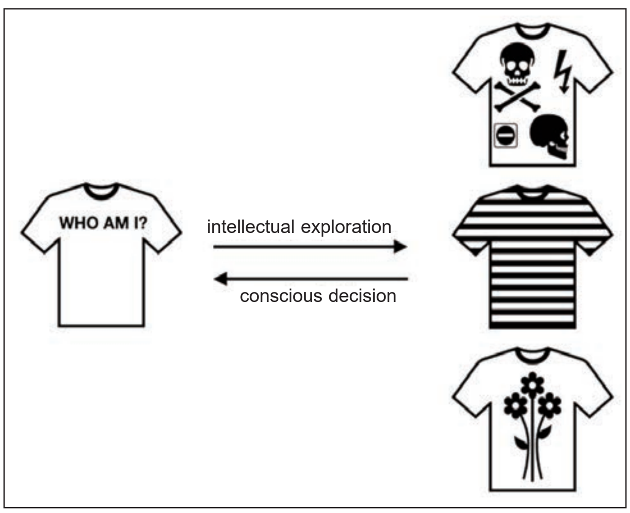

Fig. 5. Choices of clothing emerge as an intellectual exploration of identity according to Woodward [84]

Even when we are struck by the beauty of a dress, it may happen that when we put it on, we stop liking it. The power of clothing to transform the wearers is pushed to the fore and the event of selecting and wearing clothes can thus be interpreted as an encounter between a human body and objects that initiates a process of mutual becoming with either a positive or a negative outcome [87]. One’s wardrobe is known to be an extension of the diverse aspects of one’s beliefs, and the clothes we wear send powerful signals to our peers and strangers, projecting the self-image of us that we want to display.

RESULTS

Stimulus to the sense of sight can be evoked by colour fabric. By default, every garment evokes a sense of sight but it depends on colour trend. Stimulating the senses of sight depends on fashion trends that are subject to constant change. Colour trends change (or repeat) from season to season, and are set by trend scouts and trend researchers. Figure 6 shows examples of key colours in the last 3 seasons at the time of writing this review (S/S 2022, S/S 2021 I A/W 2021) as predicted by WGSN [88], as well as a brief overview of brands that have implemented these colours in their collections. However, it is not uncommon for brands to evoke a sense of sight with the store interior.

Stimulus to the sense of smell can be evoked by using fragrances (olfactometry method) in stores. Scents can generate memory-related affective reactions as they are directly processed in the brain's limbic system, which is the centre of emotions and memory. Many consumers associate the scent of citrus (the lemon-tangerine scent) with neatness and cleaning, and that is the reason we can often smell citrus in different shops, not necessarily in fashion stores. Of course, we must be aware of the fact that textiles are the holders and diffusers of the perfumes or colognes we apply on our bodies, and scented textiles can affect our mood and emotions even better than store interior scents.

Stimulus to the sense of touch can be evoked through the skin–fabric interaction, or simply by touching textiles. By default, every garment evokes a sense of touch but it depends on textiles forecast. Figure 6 shows examples of textiles forecast predicted by WGSN. The texture of the material is first determined by the way in which the material has been handcrafted or industrially processed. Skin-fabric interactions generally can be divided into active touch, i.e., the hand value of a fabric, as well as the fabric feel, when a fabric is stroked across a person’s skin. Both interactions lead to touch, which evokes sensations concerning both sensory (e.g., tactile sensitivity and discrimination) and emotional (e.g., pleasant, painful) aspects.

Stimulus to the sense of taste can be evoked so that the threads of textile fibres stimulate the taste buds. This implies the production of edible garments. There are a few examples of artistic reinterpretation of edible garments mentioned in figure 6, but this problem has not been accessed on the scientific level.

Stimulus to the sense of hearing is mostly presented in this review as an outcome of sounds played in stores since music has a profound effect on consumer behaviour. However, these stimuli can be generated as the fabrics are rubbed against one another during the movement (walking, jogging, and running).

CONCLUSION

As one of the most intimate contact items with the human body, garments can induce different feelings

SIGHT	SMELL	TOUCH	TASTE	HEARING
S/S 2022 key colours - pastels, greens • Brands which showcased these colours were: Sunnei, Nina Ricci, Roksanda, MSGM, etc. S/S 2021 key colors - A.I. Aqua, Quiet Wave and Lemon Sherbet • Brands which showcased these colours were: Alberta Ferretti, Rotate Birger Christensen, Miu Miu, Maisie Williams, etc. A/W 2021 key colours - Neo Mint, Redwood and Digital Teal • Brands which showcased these colours were: Christian Wijnants, By Far, A.W.A.K.E. mode, ALC ltd, etc.	Brands which use scent marketing are: • Chanel - Chanel no5, • Benetton - fragrance modeled after Verde cologne, • Abercrombie & Fitch - using nebulisers, etc. Department stores such as: Harrods, London and Bloomingdale's Inc., New York are using coconut blankets for the swimwear section, baby powder for the infant area and lilac for the lingerie department.	S/S 2022 textiles forecast - GOTS and BCI cottons, cupro, modal, lurex, econyl, cotton chiffon, recycled nylon. • Brands which showcased these textiles were: Marni, Missoni, Pangaia, Henrik Vibskov, Napapijri, etc. S/S 2021 textiles forecast - pure linen, hemp, jute, raw silk. • Brands which showcased these textiles were: Jil Sander, Lemaire, Hannah Culshaw, etc. A/W 2021 textiles forecast - RWS wools, GOTS cottons, linens, ramie, bamboo, nylons etc. • Brands which showcased these textiles were: Filippa K, Loewe, Sacai, Cecily Ophelia, etc.	Examples: • underwear by David Sanderson and Lee Brady, called "Candypants" • photo series "Hunger Pains" by Ted Sabarese featuring clothing made out of real food • bio design and edible garments (made from a derivative of brown algae) by Oonagh O'hagan and Cassandra Quinn	Audio streaming services such as Apple Music, Spotify and SoundCloud regularly release a playlists bringing together the in-store and fashion shows music soundtracks: Examples: • Chanel - ref. [89] • Dion Lee - ref. [90] • & Other Stories - ref. [91] • Dior - ref. [92] etc.

Fig. 6. Overview of brands and principles of sensory simulation

in the sensory system. The use of sensory experiences to design pleasant or unpleasant garments is an important concern. Fashion is an interdisciplinary field, and this review shows some methods of collaboration between psychophysics, textile technology, marketing, and fashion design. However, most of the studies presented in this review have looked at only one factor at a time. This review aimed to explore ways and possibilities of inducing 5 senses and sensory experiences in the field of fashion and point out some relevant examples.

Through this review, we have shown that arousing emotions with different sensory principles is present in the fashion industry. The limitation of our study is that a limited amount of literature has been reviewed but the results indicate that emotions in fashion are composed of many factors, and fashion brands use different techniques and approaches to evoke emotions and associate them with clothing. Some of these factors, shown in this review, are the colour of the fabric, the interior of the store, the scents in the store, the interaction between skin and fabric or touching the textiles, and finally the music in the store.

ACKNOWLEDGEMENTS

This work was supported by the Slovenian Research Agency (Program P2-0213, Textiles and ecology).

REFERENCES

[1] Demir, E., Desmet, P.M.A., Hekkert, P., *Experiential Concepts in Design Research; A (Not Too) Critical Review,* In: Desmet, P.M.A., Karlsson, M.A., van Erp J. (ed.): Design & Emotion. Proceedings of The International Conference on Design and Emotion. Gothenburg, Chalmers University of Technology, 2006, 111–117

[2] Jordan, P.W., *Designing Pleasurable Products: An Introduction to the New Human Factors,* London, Taylor & Francis, 2000

[3] Kodžoman, D., *The psychology of clothing: meaning of Colors, Body Image and Gender Expression in Fashion,* In: Textile & Leather Review, 2019,2,2, 90–103

[4] An, H., Lee, I., *A conceptual framework for Asian women's emotional needs in fashion design,* In: International Journal of Fashion Design, Technology and Education, 2015, 8, 3, 206–213

[5] Xue, Z., Zeng, X., Koehl, L., Shen, L., *Interpretation of fabric tactile perceptions through visual features for textile products,* In: Journal of Sensory Studies, 2015,31,2, 143–162
[6] Ying, B.A., Kwok, Y.L., Li, Y., Zhu, Q.Y., Yeung, C.Y., *Assessing the performance of textiles incorporating phase change materials,* In: Polymer Testing, 2004, 23, 5, 541–549
[7] Samadi, S., *The Effects of Mood and Emotion on Consumer Purchase Behavior of Buying Clothes,* In: International Journal of Innovative Technology and Exploring Engineering, 2019, 8, 12S, 770–774
[8] Colls, R., *'Looking alright, feeling alright': emotions, sizing and the geographies of women's experiences of clothing consumption*, In: Social & Cultural Geography, 2004, 5, 4, 583–596
[9] Oatley, K., Jenkins, J.M., *Understanding Emotions,* Oxford: Blackwell, 1996
[10] Crossley, N., *Emotions and communicative action*, In: Bendelow, G. and Williams, S.J. (eds) Emotions in Social Life: Critical Themes and Contemporary Issues, London: Routledge, 1998, 16–38
[11] Lupton, D., *The Emotional Self,* London: Sage,1998
[12] Illouz, E., *Cold Intimacies: The Making of Emotional Capitalism*, Cambridge, Malden: Polity Press, 2007
[13] Mehrabian, A., Russell, J.A., *An approach to environmental psychology*, Cambridge, MA: MIT Press, 1974
[14] Laros, F., Steenkamp, J., *Emotions in consumer behavior: A hierarchical approach,* In: Journal of Business Research, 2005, 58,10, 1437–1445
[15] Friese, S., *The wedding dress: from use value to sacred object*, In: Guy, A., Green, E. and Banim, M. (eds) Through the Wardrobe: Women's Relationships with Their Clothes, Oxford: Berg, 2001, 53–70
[16] Tseelon, E., *The Masque of Femininity: The Presentation of Women in Everyday Life*, London: Sage, 1995
[17] Negrin, L., *The self as image: a critical appraisal of postmodern theories of fashion,* In: Theory, Culture and Society, 1999,16, 3, 99–118
[18] Sayer, A., *Class, moral worth and recognition,* In: Sociology, 2005, 395, 947–963
[19] Moody, W., Kinderman, P., Sinha P., *An exploratory study relationship between trying on clothing, mood, emotion, personality and clothing preference,* In: Journal of Fashion Marketing and Management, 2009,14, 1, 161–179
[20] Kwon, Y.H., *The influence of the perception of mood and self-consciousness on the selection of clothing,* In: Clothing and Textiles Research Journal, 1991,19, 4, 41–46
[21] Kwon, Y.H., *Feeling toward one's clothing and self-perception of emotion, sociability, and work competency*, In: Journal of Social Behavior and Personality, 1994, 9, 1, 129–139
[22] Asare, TO., Ibrahim, AF., Kwesi, AD., *The Influence of Social and Psychological Factors on the Selection of Clothing among Female Students of Kumasi Polytechnic, Ghana,* In: International Journal of Engineering Research and Reviews, 2016, 4, 4, 20–29
[23] Kim, YK., Sullivan, P., *Emotional branding speaks to consumers' heart: the case of fashion brands,* In: Fashion and Textiles, 2019, 6, 2, 1–16
[24] Akgun, A., Kocoglu, I., Imamoglu, S.Z., *An emerging consumer experience: Emotional branding,* In: Procedia Social and Behavioral Sciences, 2013, 99, 503–508
[25] Fournier, S., *Consumers and their brands: Developing relationship theory in consumer research,* In: Journal of Consumer Research, 1998, 24, 4, 343–353
[26] Otley, P., *Can you feel it? Why brands must focus on emotional connection,* In: Digital Pulse, 2016, Available at: https://www.pwc.com.au/digitalpulse/branded-content-emotional-connection.html [Accessed on April 2022]
[27] Brakus, J.J., Schmitt, B.H., Zarantonello, L., *Brand experience: What is it? How is it measured? Does it affect loyalty?,* In: Journal of Marketing, 2009, 73, 3, 52–68
[28] Schmitt, B., *Experiential marketing,* In: Journal of Marketing Management, 1999, 15,1–3, 53–67
[29] Acharya, M., *The emotional branding process,* In: G. Ruchi, R. Chhikara, K. P. Tapan Kumar, A. Kataria (Eds.), Driving customer appeal through the use of emotional branding, IGI Global: Pennsylvania, 2018, 195–208
[30] Douce, L., Janssens, W., *The presence of a pleasant ambient scent in a fashion store: The moderating role of shopping motivation and affect intensity,* In: Environment and Behavior, 2013, 45, 2, 215–238
[31] Lindstrom, M., *Brand sense: Sensory secrets behind the stuff we buy* (2nd ed.), London: Kogan Page Limited, 2010
[32] Krishna, A., *An integrative review of sensory marketing: Engaging the senses to affect perception, judgment, and behavior,* In: Journal of Consumer Psychology, 2012, 22, 3, 332–351
[33] Orth, U.R., Malkewitz, K., *Holistic package design and consumer brand impressions,* In: Journal of Marketing, 2008, 72, 3, 64–81
[34] Fiore, A., Yah, X., Yoh, E., *Effects of a product display and environmental fragrancing on approach responses and pleasurable experiences,* In: Psychology Marketing, 2000, 17, 1, 27–54
[35] Holbrook, M.B., Hirschman, E.C., *The experiential aspects of consumption: Consumer fantasies, feelings, and fun,* In: Journal of Consumer Research, 1982, 9, 132–140
[36] Eroglu, S.A., Machleit, K.A., Davis, L.M., *Empirical testing of a model of online store atmospherics and shopper responses,* In: Psychology & Marketing, 2003, 20, 139–150
[37] Menon, S., Kahn, B., *Cross-category effects of induced arousal and pleasure on the Internet shopping experience,* In: Journal of Retailing, 2002, 78, 1, 31–40
[38] Fiore, A.M., Jin, H.Y., Kim, J., *For Fun and Profit: Hedonic Value from Image Interactivity and Responses Toward an Online Store,* In: Psychology & Marketing, 2005, 22, 8, 669–694
[39] Mattila, A.S., Wirtz, J., *Congruency of scent and music as a driver of in-store evaluations and behavior,* In: Journal of Retailing, 2001, 77, 2, 273–289

[40] Donovan, R.J., Rossiter, J.R., *Store atmosphere: An environmental psychology approach,* In: Journal of Retailing, 1982, 58, 1, 34–57
[41] Holbrook, M.B., *Emotions in the consumption experience: Toward a new model of consumer behavior,* In: R.A. Peterson, W.D. Hoyer, & W.R. Wilson (Eds.), The role of affect in consumer behavior: Emerging theories and applications, Lexington, MA: Heath, 1986, 17–52
[42] Mehrabian, A., Russell, J.A., *An approach to environmental psychology,* Cambridge, MA: MIT Press, 1974
[43] Delong, M.B., Larntz, K., *Use of schema for evaluating consumer response to an apparel product*, In: Clothing and Textile Research, 1974, 5, 1, 17–26
[44] Strang, E., *Scents and sensibility at Lush cosmetics*, 2015, Available at: https://theregister.co.nz/2015/03/26/scents-and-sensibility-lush-cosmetics/ [Accessed on December 2021]
[45] Karmali, S., *Inside Chanel's new London flagship,* 2017, Available at: https://www.vogue.co.uk/gallery/chanel-london-flagship-new-bond-street-largest-chanel-boutique-store [Accessed on December 2021]
[46] Larocca, A., *Principles of persuasion,* 2013, Available at: nymag.com/nymetro/shopping/features/10345/ [Accessed on December 2021]
[47] Douce, L., Janssens, W., *The Presence of a Pleasant Ambient Scent in a Fashion Store: The Moderating Role of Shopping Motivation and Affect Intensity,* In: Environment and Behavior, 2013, 45, 2, 215–238
[48] Sweeney, J.C., Wyber, F., *The role of cognitions and emotions in the music approach avoidance behavior relationship,* In: Journal of Services Marketing, 2002, 16, 1, 51–69
[49] Crowley, A.E., *The two-dimensional impact of color on shopping,* Marketing Letters, 1993, 4, 59–69
[50] Areni, C.S., Kim, D., *The influence of in-store lighting on consumers' examination of merchandise in a wine store,* In: International Journal of Research in Marketing, 1994, 11, 2, 117–125
[51] Michon, R., Chebat, J.C., Turley, L.W., *Mall atmospherics: The interaction effects of mall environment on shopping behavior,* In: Journal of Business Research, 2005, 58, 5, 576–583
[52] Seo, H.S., Roidl, E., Müller, F., Negoias, S., *Odors enhance visual attention to congruent objects,* In: Appetite, 2010, 54, 3, 544–549
[53] Schmitt, B., *Experiential marketing,* In: Journal of Marketing Management, 1999, 15, 1–3, 53–57
[54] Bäckström, K., Johansson, U., *Creating and consuming experiences in retail store environments: Comparing retailer and consumer perspectives,* In: Journal of Retailing and Consumer Services, 2006, 13, 6, 417–430
[55] Donovan, R.J., Rossiter, J.R., Marcoolyn, G., Nesdale, A., *Store atmosphere and purchasing behavior,* In: Journal of Retailing, 1994, 70, 3, 283–294
[56] Luqman, A., Cao, X., Ali, A., Masood, A., Yu, L., *Empirical investigation of Facebook discontinues usage intentions based on SOR paradigm,* In: Computers in Human Behavior, 2017, 70, 544–555
[57] Orth, U.R., Bourrain, A., *The influence of nostalgic memories on consumer exploratory tendencies: Echoes from scents past,* In: Journal of Retailing and Consumer services, 2008, 15, 4, 277–287
[58] Bruner, G.C., *Music, mood, and marketing,* In: Journal of Marketing, 1990, 54, 4, 94-104
[59] Kodžoman, D., Hladnik, A., Pavko Čuden, A., Čok, V., *Exploring color attractiveness and its relevance to fashion,* In: Color Research and Application, 2021, 47, 182–193
[60] Boland, H., Akram, S., *Age is no barrier to wanting to look good: Women on body image, age and advertising,* In: Qualitative Market Research: An International Journal, 2007,10, 3, 310–333
[61] Nam J., Hamlin R., Gam H.J., Kang J,H., Kim J., Kumphai P., et al., *The fashion-conscious behaviours of mature female consumers,* In: Journal of Consumer Studies, 2007, 31, 1, 102–108
[62] Jantzen, C., Ostergaard, P., Sucena Viera, C.M., *Becoming a 'Woman to the Backbone': Lingerie consumption and the experience of feminine identity,* In: Journal of Consumer Culture, 2006, 6, 2, 177–202
[63] Thesander, M., *The Feminine Ideal*, London: Reaktion Books Ltd., 1997
[64] Tseelon, E., *The Masque of Femininity: The Presentation of Woman in Everyday Life*, London: Sage, 1995
[65] Baker, J., Grewal, D., Parasuraman, A., *The influence of store environment on quality inferences and store image,* In: Journal of the Academy of Marketing Science, 1994, 22, 4, 328–339
[66] Pugh, S.D., *Service with a smile: Emotional contagion in the service encounter,* In: Academy of Management Journal, 2001, 44, 5, 1018–1027
[67] Tsai, W.C., *Determinants and consequences of employee-displayed positive emotions,* In: Journal of Management, 2001, 27, 4, 497–512
[68] Tsai, W.C., Huang, Y.M., *Mechanisms linking employee affective delivery and customer behavioral intentions,* In: Journal of Applied Psychology, 2002, 87, 5, 1001–1008
[69] Söderlund, M., *Employee mere presence and its impact on customer satisfaction,* In: Psychology & Marketing, 2017, 33, 6, 449–464
[70] Otterbring, T., Lu, C., *Clothes, condoms, and customer satisfaction: The effect of employee mere presence on customer satisfaction depends on the shopping situation,* In: Psychology Marketing, 2018, 35, 6, 454–462
[71] Carre, F., Tilly, C., *America's biggest low-wage industry: Continuity and change in retail jobs,* UMass Boston Center for Social Policy Publications, Paper 22, Boston, MA: Center for Social Policy, 2008
[72] Misra, J., Walters, K., *All Fun and Cool Clothes? Youth Workers' Consumer Identity in Clothing Retail,* In: Work and Occupations, 2016, 43, 3, 294–325
[73] Bureau of Labor Statistics, *Clothing and clothing accessories stores: NAICS 448*, 2015, Available at: https://www.bls.gov/iag/tgs/iag448.htm [Accessed on December 2021]

[74] Macdonald, C.L., Merrill, D., *Intersectionality in the emotional proletariat: A new lens on employment discrimination in service work,* In: C.L. Macdonald & M. Korczynski (Eds.), Service work: Critical perspectives, New York, NY: Routledge, 2008, 113–133
[75] Ruetschlin, C., Asante-Muhammad, D., *The retail race divide*, New York, NY: Demos/NAACP, 2015
[76] Williams, C.L., Connell, C., *Looking good and sounding right: Aesthetic labor and social inequality in the retail industry,* In: Work and Occupations, 2010, 37, 3, 349–377
[77] Pettinger, L., *Brand culture and branded workers: Service work and aesthetic labour in fashion retail,* In: Consumption, Markets and Culture, 2004, 7, 2, 165–184
[78] Entwistle, J., *The Fashioned Body,* Blackwell Publishers Inc., Malden, MA., 2000
[79] Kaiser, S.B., *The Social Psychology of Clothing,* 2nd ed., Fairchild Publications, New York, NY., 1997
[80] Sproles, G.B., *Fashion, Consumer Behavior toward Dress*, Burgess Publishing Company, Minneapolis, MN., 1979
[81] Feinberg, R.A., Mataro, L., Burroughs, W.J., *Clothing and social identity*, In: Clothing and Textiles Research Journal, 1992, 11, 1, 18–23
[82] Raunio, A.M., *Favorite clothes – a look at individuals' experience of clothing,* In: Suojanen, U. (Ed.), Clothing and its Social, Psychological, Cultural and Environmental Aspects, Research Report No. 161, Department of Teacher Education, University of Helsinki, 1982, 179–194
[83] Tombs, A.G., *Do Our Feelings Leak Through the Clothes We Wear?,* In: Australian & New Zealand Marketing Academy Conference, Brisbane, Australia. Ed. Ali, Y and van Dessel, M. Brisbane: Australian & New Zealand Marketing Academy Conference, 2006
[84] Woodward, S., *Why Women Wear What They Wear*. Oxford: Berg, 2007
[85] Guy, A., Maura, B., *Personal Collections: Women's Clothing Use and Identity,* In: Journal of Gender Studies, 2000, 9, 3, 313–327
[86] Dubler, M.L.J., Gurel, L.M., *Depression: relationships to clothing and appearance self-concept,* In: Home Economics Research Journal, 1984, 13, 1, 21–26
[87] Ruggerone, L., *The Feeling of Being Dressed: Affect Studies and the Clothed Body*, In: Fashion Theory, 2017, 21, 5, 573–593
[88] Walters, P., Spaulding, M., Catwalk Analytics S/S 22: Print & Colour [trend report]. WGSN, 2021, https://www.wgsn.com/fashion/article/92187 [Accessed on December 2021]
[89] Apple Music, *Chanel,* Playlist, 2022, Available at: https://music.apple.com/us/curator/chanel/1296909420 [Accessed on January 23, 2022]
[90] SoundCloud, *Dion Lee*, Playlist, Available at: https://soundcloud.com/dionleesound [Accessed on January 23, 2022]
[91] Spotify, *& Other Stories*, Playlist, Available at: https://open.spotify.com/playlist/43FKXxc7pzpGK6TozqHGvv [Accessed on January 23, 2022]
[92] Spotify, Dior, Playlist, Available at: https://open.spotify.com/playlist/2R3WIGhCHudzo7WzyZnkZI [Accessed on January 23, 2022]

Authors:

DUJE KODŽOMAN[1], ALENKA PAVKO ČUDEN[1], VANJA ČOK[2]

[1]University of Ljubljana, Faculty of Natural Sciences and Engineering, Department of Textiles, Graphic Arts and Design, 1000 Ljubljana, Slovenia
e-mail: alenka.cuden@ntf.uni-lj.si

[2]University of Ljubljana, Faculty of Mechanical Engineering, Department of Engineering Design and Transportation Systems, 1000 Ljubljana, Slovenia
e-mail: vanja.cok@fs.uni-lj.si

Corresponding author:

DUJE KODŽOMAN
e-mail: dujekodzoman@gmail.com

Quantification and analysis of carbon neutralization in mulberry and silk in China

DOI: 10.35530/IT.074.03.202258

LIU SHUYI
LIU JUNRAN
LI QIZHENG
BAO WEI
XU NUO
WANG XIAOPENG
WANG LAILI

ABSTRACT – REZUMAT

Quantification and analysis of carbon neutralization in mulberry and silk in China

With the concern of global warming, efforts are increasingly focused on understanding and addressing carbon emission in the life cycle of silk products. Whereas, the carbon sequestration effects of mulberry and silk are rarely mentioned in the previous studies on the carbon footprint of silk products. In this regard, this study constructed a biomass method to adequately evaluate the carbon sequestration effects of mulberry and silk produced in China. An application demonstration was conducted in the area of mulberry fields and the cocoon yield of the silk industry in China from 1990 to 2021. The results indicate that mulberry fields in China fixed 875.9608 million tons of CO_2 from 1990 to 2017, while silk in cocoons produced in China fixed a total of 5.9528 million tons of CO_2. These vast quantities of carbon trapped in mulberry leaves enter the silk, the silkworm chrysalis and silkworm droppings, as well as other by-products as silkworms ingest, grow, and spin cocoons. This demonstrates that increased exploitation of sericulture by-products can also contribute to carbon sequestration. Besides, the influence of the silk product's lifespan should be taken into account when quantifying and analysing the carbon neutralization of silk. Therefore, extending the usage life of silk products as long as feasible can also have a great effect on the carbon sequestration of silk products.

Keywords: *carbon storage, carbon neutralization, mulberry, silk, temporary carbon storage effect*

Cuantificarea și analiza neutralizării carbonului la duzi și mătase în China

Cu preocuparea încălzirii globale, eforturile sunt din ce în ce mai concentrate pe înțelegerea și abordarea emisiilor de carbon în ciclul de viață al produselor din mătase, întrucât efectele de captare a carbonului ale dudului și mătăsii sunt rareori menționate în studiile anterioare, privind amprenta de carbon a produselor din mătase. În acest sens, acest studiu a construit metoda biomasei pentru a evalua în mod adecvat efectele de captare a carbonului din duzii și mătasea produsă în China. O demonstrație a aplicației a fost efectuată cu zona câmpurilor de dud și a producției de cocon din industria mătăsii din China din 1990 până în 2021. Rezultatele indică faptul că în general, câmpurile de dud din China au fixat 875,9608 milioane de tone de CO_2 între 1990 și 2017, în timp ce mătasea din coconi a produs în China un total de 5,9528 milioane de tone de CO_2. Aceste cantități uriașe de carbon prinse în frunzele de dud intră în mătase, în crisalida și excrementele de viermi de mătase, precum și în alte produse secundare pe măsură ce viermii de mătase ingerează, cresc și învârt coconii. Acest lucru demonstrează că exploatarea sporită a produselor secundare de sericicultură poate contribui, de asemenea, la captarea carbonului. În plus, influența duratei de viață a produsului de mătase trebuie luată în considerare la cuantificarea și analizarea neutralizării carbonului din mătase. Prin urmare, prelungirea duratei de utilizare a produsului de mătase, atâta timp cât este fezabil, poate avea, de asemenea, un efect semnificativ asupra captării carbonului din produsele din mătase.

Cuvinte-cheie*: depozitarea carbonului, neutralizarea carbonului, dud, mătase, efect de stocare temporară a carbonului*

INTRODUCTION

China is the largest producer and the leading supplier of silk in the world with 53369t/y in 2020 [1]. The production processes, reeling of raw silk, processing of silk yarns into fabrics, dyeing, finishing and manufacturing of products, involve a substantial amount of electricity, steam, fossil fuels, fresh water, chemicals, and packaging materials, and are blamed for producing significant amounts of greenhouse gas (GHG) [2]. According to the comparative research carried out by the Waste & Resources Action Program (WRAP) [3], from cocoon production to the end of life, each ton of silk fibre produced a carbon footprint of 25.425 kg CO_2e. Apart from that, some studies investigated the carbon footprint of silk manufacturing. Barcelos et al. [4] analysed the life cycle assessment (LCA) of the core processes of mulberry and silk cocoon production and evaluated the carbon footprint in the production process. Astudillo et al. [5] conducted the life cycle assessment of raw silk, in which the carbon footprint of mulberry production, silkworm rearing, cocoon drying, and cocoon reeling was evaluated. Ren et al. [6] studied the environmental impact of 100 kg silk textiles and analysed the global warming potential. Jiang et al. [7] introduced the carbon footprint assessment of gambiered canton silk and demonstrated that the total carbon footprint per meter of fabric was 1.88 kg CO_2e. Faragò et al. [8] calculated the environmental impact of yarn-dyed silk fabrics, printed silk fabrics and dyed silk fabrics, and analysed global warming potential (GWP).

In the long production process of silk, mulberry leaves are the raw material and essential components for the front-end process. Over 90% of commercially produced silk is spun by the domesticated silkworm, a monophagous insect whose diet is restricted to the leaves of the mulberry tree [5]. As a fast-growing tree, mulberry starts to produce commercial quantities of leaves for the cultivation of silkworms within one year of planting [9]. Mulberry, as a consequence, has a high capacity for carbon sequestration, which refers to the ability to remove CO_2 from the atmosphere [10]. Due to its high ecological and socioeconomic versatility, and particularly its great potential for carbon sequestration, mulberry has been receiving increasing attention in recent decades. According to research conducted by Giacomin et al. [11], approximately 81.65 tons of CO_2 are fixed in one hectare of mulberry per year, of which 64.80 tons are fixed in mulberry leaves, branches and other above-ground parts, and the remaining 16.80 tons are kept below ground level for quite a long time. In 2020, mulberry orchards occupied 807847 hectares in China, and it can be estimated that Chinese total mulberry fields can fix 65.96 million tonnes of CO_2 annually. Garcia Jr et al. [11, 12] pointed out that mulberry trees have a significant potential for carbon mitigation. Srikantaswamy and Bindroo [13] claimed that the production of mulberry biomass offered appealing properties for carbon sequestration due to its rapid growth and wide adaptability. Research conducted in 2020 found that mulberry cultivation had a negative net carbon emission, suggesting that the carbon emission was less than the photosynthetic carbon sink and that mulberry production had a positive ecological externality [14]. From this perspective, mulberry planting can contribute carbon neutrality to the production of silk [15].

Mulberry synthesizes water and carbon dioxide into carbohydrates by photosynthesis. Some of these carbohydrates are consumed as plant respiration and the other part is converted into branches, leaves, roots, etc. When the silkworm matures and spins cocoons, the carbon trapped in mulberry leaves enters the silk. As a consequence, silk has a carbon sequestration effect and carbon neutralization potential. However, in the previous research, the carbon sequestration effects of mulberry and silk are not thoroughly investigated. Few studies took the carbon mitigation made by mulberry into account to evaluate the carbon footprint of silk. In this regard, this study constructed a biomass method to adequately evaluate the carbon sequestration effects of mulberry and silk from the standpoint of raw materials of silk. In this paper, the carbon sequestration of mulberry and silk was examined from macro and micro perspectives respectively. The carbon sequestration of silk was obtained innovatively by analysing the flow of dry matter sequestered by mulberry leaves during the life cycle of silkworms, and the duration of carbon storage and delayed GHG emissions were considered. These efforts enriched the knowledge of carbon footprint and quantified carbon neutrality in silk.

Besides, an application demonstration was conducted in the area of mulberry fields and the cocoon yield of the silk industry in China from 1990 to 2017 to provide a reference for the carbon sequestration effect assessment of mulberry and silk.

METHODOLOGY AND DATA

Carbon sequestration model of mulberry field

Silk has been regarded as a highly valued textile fibre and is favoured by consumers all over the world. As a result of the demand for silk, mulberry fields flourished. Due to its rapid growth rate and robust yearly regeneration following harvesting, the mulberry field has a significant carbon storage potential. The carbon sequestration coefficient of mulberry fields per hectare has been calculated in previous studies [11, 12, 16]. The total carbon storage of mulberry fields can be obtained by multiplying the total planting areas by the coefficient of carbon sequestration, as shown in equation 1.

$$Q_{CO_2} = \gamma \times S \times 44/12 \tag{1}$$

where, Q_{CO_2} is the total CO_2 storage (t), γ – the coefficient of carbon sequestration, S – the total planting areas (hm^2), 44 – the mole mass of CO_2, 12 – the mole mass of C.

Carbon sequestration model of dry biomass

Mulberry trees synthesize CO_2 into carbohydrates through photosynthesis during their growth process. These carbohydrates are stored in mulberry leaves and support silkworm consumes, growing, and spinning cocoons. The sequestered carbon does not return to the atmosphere before the silk is degraded or burned. The carbon neutralization effect of silk can be quantified using the dry-weight biomass method currently. The dry weight biomass method chiefly calculates CO_2 sequestration based on the changes of biomass indirectly [17]. Biomass multiplied by the carbon coefficient in the dry matter can be converted into carbon storage, as shown in equation 2:

$$Q_{CO_2} = m_{bio} \times (1 - R_{H_2O}) \times R_c \times 44/12 \tag{2}$$

where, Q_{CO_2} is the total CO_2 storage (t), m_{bio} – the weight of biomass consumed (kg), R_{H_2O} – the content of H_2O, R_c – the content of C, 44 – the mole mass of CO_2, 12 – the mole mass of C.

Data sources

China produces more than 80% of the world's cocoon and raw silk in 2019 [18]. The data used for the carbon sequestration accounting were collected from the Silk Yearbook of China (2000–2018), which

Table 1

AREA OF MULBERRY ORCHARDS AND OUTPUT OF SERICULTURE PRODUCTS IN CHINA FROM 1990 TO 2021

Year	Mulberry field area (hm^2)	The output of mulberry Leaf (ten thousand tonnes)	The output of mulberry branch (ten thousand tonnes)	The output of silkworm cocoon (tonne)	The output of cocoon shells (tonne)	The output of silkworm chrysalis (tonne)
1990	484069.09	1452.20	580.88	480179.00	120044.75	360134.25
1991	1026671.80	3080.00	1232.00	511517.00	127879.25	383637.75
1992	1252806.26	3758.40	1503.36	610250.00	152562.50	457687.50
1993	1249739.58	3749.20	1499.68	619800.00	154950.00	464850.00
1994	1244826.22	3734.46	1493.78	673952.00	168488.00	505464.00
1995	1163139.15	3489.40	1395.76	656365.00	164091.25	492273.75
1996	864870.99	2594.60	1037.84	403387.00	100846.75	302540.25
1997	638469.86	1915.40	766.16	404885.00	101221.25	303663.75
1998	626203.13	1878.60	751.44	432821.00	108205.25	324615.75
1999	579602.90	1738.80	695.52	409021.00	102255.25	306765.75
2000	632436.50	1897.30	758.92	454614.30	113653.58	340960.73
2001	721016.94	2163.04	865.22	512707.68	128176.92	384530.76
2002	769083.85	2307.24	922.90	515884.85	128971.21	386913.64
2003	765737.16	2297.20	918.88	481470.15	120367.54	361102.61
2004	781110.57	2343.32	937.33	547091.30	136772.83	410318.48
2005	773643.87	2320.92	928.37	616145.00	154036.25	462108.75
2006	855684.28	2567.04	1026.82	739715.34	184928.84	554786.51
2007	922624.61	2767.86	1107.14	782098.21	195524.55	586573.66
2008	878904.39	2636.70	1054.68	677648.17	169412.04	508236.13
2009	810770.72	2432.30	972.92	649107.06	162276.77	486830.30
2010	802057.34	2406.16	962.46	667239.74	166809.94	500429.81
2011	827450.80	2482.34	992.94	654989.50	163747.38	491242.13
2012	841644.21	2524.92	1009.97	643024.03	160756.01	482268.02
2013	839304.20	2517.90	1007.16	641006.41	160251.60	486225.00
2014	828244.14	2484.72	993.89	641006.40	160251.60	480754.80
2015	821310.77	2465.00	985.57	628210.00	157052.50	478428.75
2016	793110.63	2379.32	951.73	620406.00	155101.50	465304.50
2017	788723.94	2366.16	946.46	643114.00	160778.50	482335.50
2018	789943.95	2369.82	947.93	679038.00	169759.50	509278.50
2019	755277.11	2265.82	906.33	720805.00	180201.25	540603.75
2020	807850.71	2423.54	969.42	687178.00	171794.50	515383.50
2021	796700.00	2390.08	956.04	717200.00	179300.00	537900.00

reported mulberry leaves yields and mulberry field area, as well as the amounts of various sericulture outputs including silkworm cocoons, cocoon shells and silkworm chrysalis in China. The specific data are shown in table 1 [19].

RESULTS AND DISCUSSION

The yearly carbon sequestration of mulberry fields and silk in China was calculated according to equation 1 and equation 2 in the Methodology section respectively. The results are depicted in figure 1 and figure 2.

As shown in figure 1, the carbon sequestration of mulberry fields calculated with γ_1 was the largest, and followed by γ_2. These two coefficients of carbon sequestration were referred to the research of Garcia Jr (γ_1) and National Forestry and Grassland Administration (γ_2). The results calculated using coefficient γ_2 are primarily analysed in this study. The quantity of CO_2 sequestered by mulberry fields increased from 1990 to 1992. It reached 4653.34 million tons in 1992 with an increase of 158.81% compared to the quantity in 1990. Since 1992, the quantity of CO_2 sequestered by mulberry fields showed a slow downward trend until 1995 and began to decline sharply, reaching the lowest point in 1999. The quantity of CO_2 sequestered by mulberry fields increased again from 1999, rising to a peak value of 34.2694 million tons in 2007. Following a slight decline between 2007 and 2010, the quantity of CO_2 sequestered by mulberry fields has been stable since

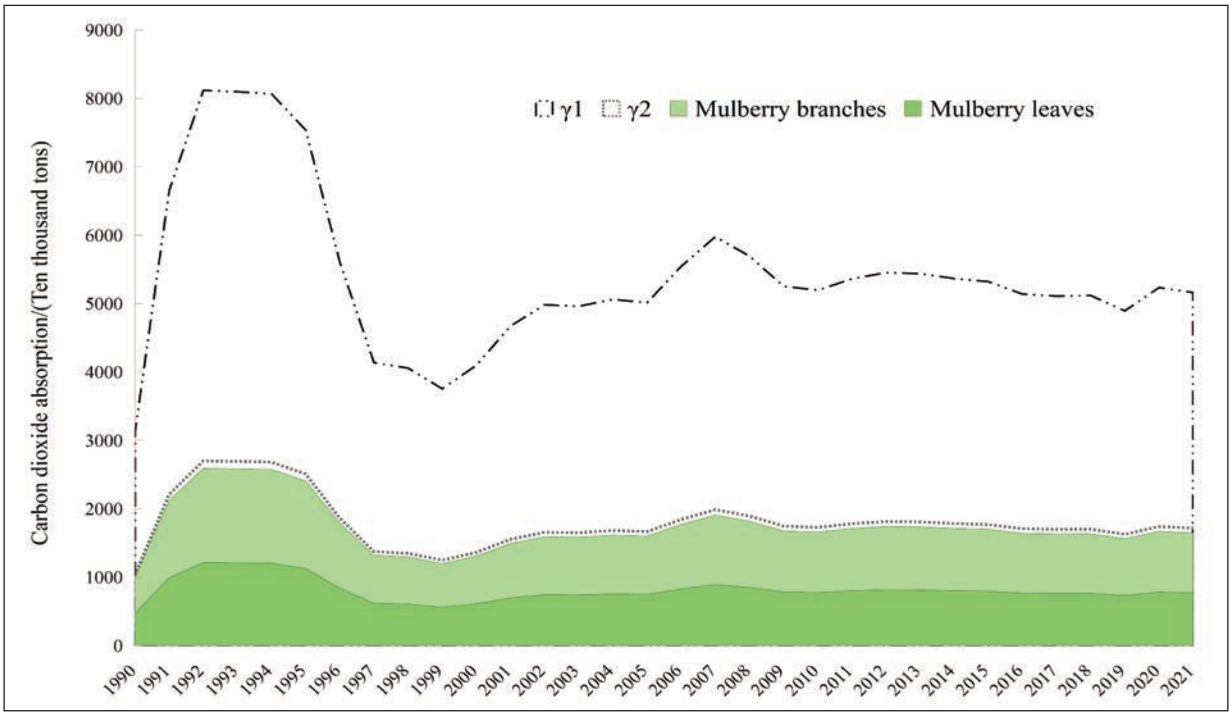

Fig. 1. Carbon sequestration of mulberry fields in China from 1990 to 2021

2010. The amounts of CO_2 immobilized by mulberry leaves and branches sequestered were 26.06% and 29.61% of the total CO_2 sequestered by mulberry fields respectively. They showed the same variation trend as that of CO_2 immobilized by mulberry fields.

Since the economy reformed and opened up, the government has been attaching continuous importance to the restoration and development of sericulture production. In the late 1980s, the popularity of natural fibres under the increasing environmental protection awareness led to a boom in silk consumption, which greatly increased the demand for silk in the international markets. The soaring price of cocoon further stimulated the enthusiasm of sericulture production throughout the country. The area of mulberry fields increased gradually to 1252806 hectares in 1992. However, the demand for silk products all over the world did not increase synchronously with mulberry fields, so the cocoons were overstocked. The cocoon price declined from the second half of 1995. Besides, the enthusiasm of silkworm farmers was severely dampened. Hence, lots of farmers left sericulture for other crops or went to cities to make money, resulting in a substantial decrease in mulberry fields and cocoon production in 1996. The government took measures to regulate the sericulture industries including cocoon production, reeling and weaving from 1996. Therefore, the decline rate of the area of mulberry fields slowed down from 1996 to 1999. After a ten-year adjustment and reform of the mulberry and cocoon industry, sericulture areas shifted from developed regions in eastern China to developing regions in southwestern China. In the developing regions, sericulture areas are expanding because of their low labour costs and stable income. With the increasing demand for silk products in the global market, the area of mulberry fields started to increase from 2000, until the outbreak of the global financial crisis in 2008. The demand for silk products in the global market declined as a result of the financial crisis, and the area of mulberry fields shrunk marginally. The global economy has progressively recovered since 2010, and the area of mulberry garden fields has shown signs of stability.

Figure 2 shows that the quantity of CO_2 sequestered by raw silk also grew at first (1990–1994), then reduced sharply (1994–1996), and then climbed again (1996–2008). Nevertheless, unlike the variation of mulberry orchards, the output of cocoon increased significantly in 2007 compared to the previous peak in 1994 due to the development and application of advanced sericulture technologies.

Meanwhile, the amount of CO_2 immobilized by cocoon shell and silkworm chrysalis accounted for 46.08% and 53.92 % of the total CO_2 sequestered by cocoon respectively (figure 3).

The annual amount of CO_2 sequestered by mulberry fields is significantly larger than that sequestered by silk. Figure 3 depicts the flow of dry matter fixed in mulberry leaves during the silkworm's life cycle. Taking one silkworm as the research unit, the total dry matter of mulberry leaves eaten by a silkworm in its whole life cycle is 5 grams, of which 62% is discharged by the silkworm in the way of silkworm droppings, and the rest is digested by the silkworm. The silkworm consumes 46% of the 1.9 grams of dry matter which it digests for energy consumption during the evolution stage, 7.3% for silk synthesis, 21% for pupae formation and 25.5% for cocoon shell forma-

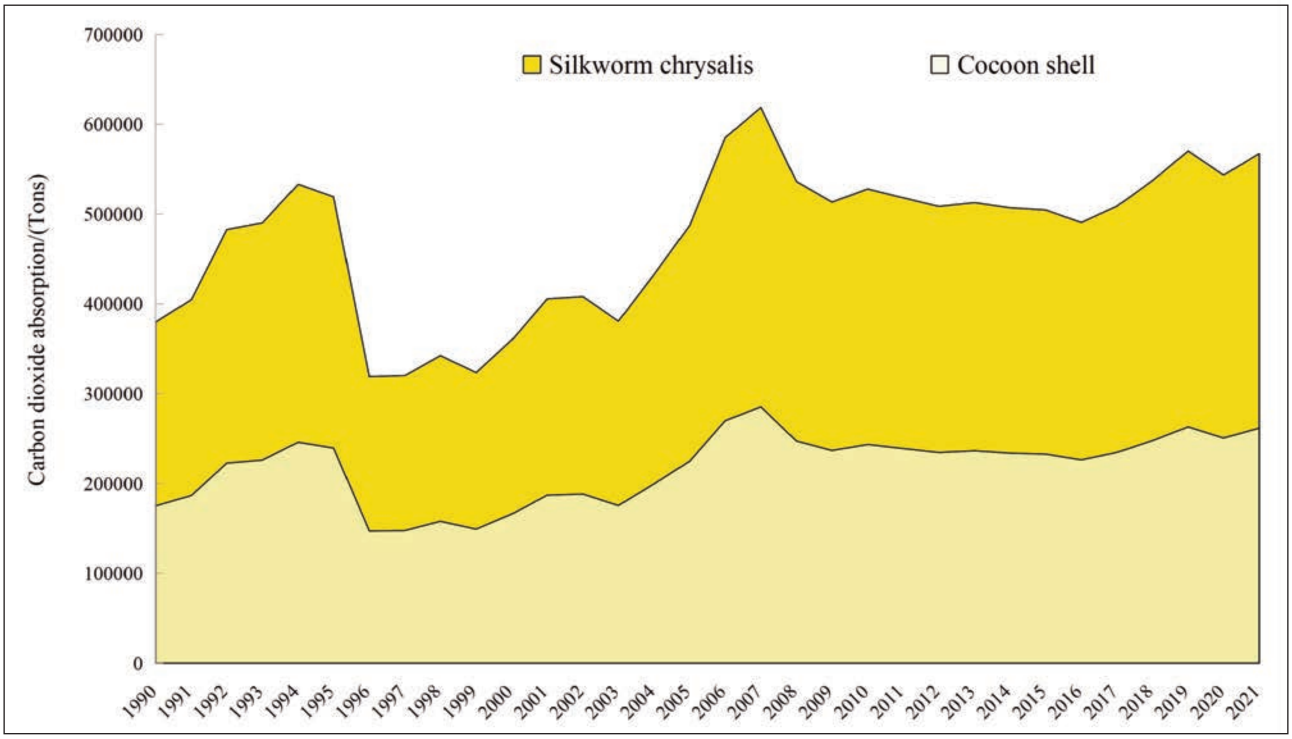

Fig. 2. Carbon sequestration of cocoons in China from 1990 to 2021

tion. It can be seen that in addition to the cocoon shell utilized for silk reeling, a significant quantity of carbon is also fixed in silkworm pupae and silkworm droppings. This demonstrates that using by-products generated from sericulture is also helpful to fix CO_2. The by-products of sericulture such as silk sericin, silkworm droppings and waste silk can be processed and utilized with new and high technologies [20]. For example, after drying at high temperatures, silkworm droppings can be mixed with other therapeutic ingredients to make a pillow conducive to sleep and good for human health. The pillow contains a significant quantity of biological carbon, which helps to offset the carbon produced by the sericulture. When silk by-products are not used and discarded instead, they spontaneously dissolve, releasing the carbon that was trapped in the material. Applications of sericulture by-products could decrease raw material waste and environmental effects, as well as generate employment and income [21].

Once captured and stored by mulberry trees, enters the silk through the consumption of silkworms, and

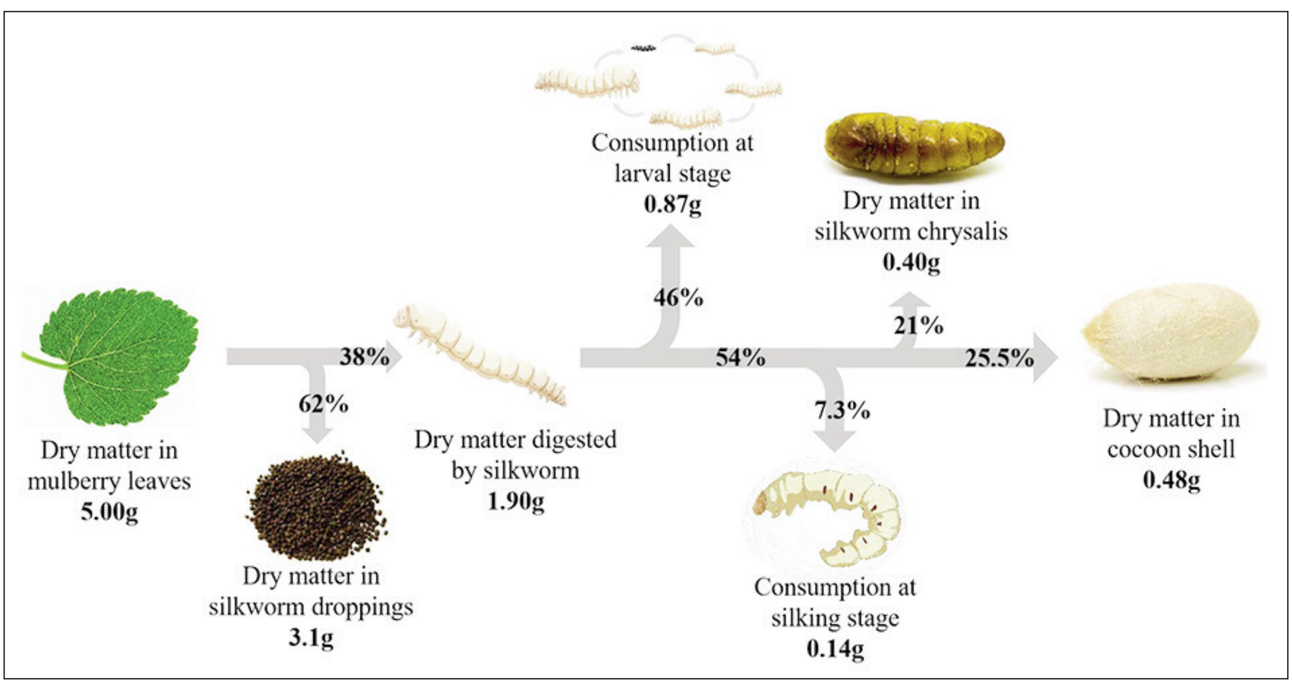

Fig. 3. The flow of dry matter sequestered by mulberry leaves during the life cycle of silkworms

carbon will reenter the atmosphere sooner or later after the use phase of the silk products [22]. As a result, the service cycle of silk products should be considered when quantifying and analysing the carbon neutralization of silk. Carbon sequestration during biomass growth can be accounted for as a negative carbon emission in LCA, but the duration of carbon storage and delayed GHG emissions are usually not taken into account. According to PAS 2050 [23], the later GHG emissions occur, the shorter their residence time in the atmosphere and the smaller their impact on global warming in a 100-year time horizon. It is not until emissions occur after 100 years that their impact will become zero. According to the findings of Giacomin et al. [11], one hectare of mulberry trees fix about 81.65 tons of CO_2 per year, of which 16.80 tons are kept below ground level for a considerable amount of time. The carbon footprint for producing per ton of silk fibre is 25425 kg of CO_2 equivalent from the production of cocoons to the end of life, and silk fibre production per hectare was 111 kg, resulting in a carbon footprint of 2.82 tons/ha. As a result, the amount of CO_2 that is kept below ground level for an extended period per hectare is around six times the amount of CO_2 that will be left by fibre silk produced in the same hectare. From this perspective, mulberry planting can contribute carbon neutrality to the production of silk in a 100-year time horizon. Besides, the effect of carbon sequestration is affected by the duration of silk products. The longer the product is used, the more significant the effect of carbon sequestration will be. Accordingly, when using silk products, consumers should pay attention to reusing and recycling the product to extend the period of carbon storage as long as possible [24].

Abandoned silk products will naturally disintegrate over time and release carbon sequestered inside the products. As a result, proper recycling is a crucial way to carbon neutralization of silk. Obsolete products made from silk can be broken down into smaller units and converted into carpets, bags, accessories, wadding and other recyclable items, thereby extending the service life of products and reducing raw materials consumption and CO_2 emissions [25]. At the same time, once the service life of products made from silk has expired, energy recovery can be carried out, which refers to the incineration process of the products. The energy recovery of products can offer advantageous energy generation [26]. The heat generated by combustion can be utilized to generate electricity, reducing the usage of coal and, on the other hand, minimizing CO_2 emissions.

CONCLUSIONS

As an important material basis for silk production, mulberry trees synthesize CO_2 into carbohydrates through photosynthesis during their growth process, which is a key factor in mitigating increased CO_2 in the atmosphere. Simultaneously, the carbon in mulberry leaves will be fixed in cocoon shells, silkworm chrysalis, silkworm droppings, and other by-products as a result of the life activities of silkworms. In this paper, the carbon neutralization effects of mulberry and silk in China were explored. Given the results found in this study, it would be recommendable to consider the service cycle when quantifying and analysing the carbon neutralization of silk products. The longer the silk product is used, the more significant the effect of carbon sequestration will be.

It is noteworthy that the lifespan of various silk goods varies. From an accurate assessment perspective, specific life cycle models should be constructed to evaluate the carbon sequestration effects of different silk products in future research.

ACKNOWLEDGEMENTS

The authors are grateful to Strategic Research and Consulting Project of Chinese Academy of Engineering (2022-XY-19), the Clothing Engineering Research Centre of Zhejiang Province (2021FZKF01), the Zhejiang Provincial General Scientific Research Projects Fund of China under Grant (Y202148096), Science and Technology Innovation Activities of University Students in Zhejiang Province (2022R406C077).

REFERENCES

[1] International Sericultural Commission (ISC), *Statistics of global silk production*, Available at: https://inserco.org/en/statistics [Accessed on 29 May 2022]

[2] De Saxce, M., Pesnel, S., Perwuelz, A., *LCA of bed sheets – some relevant parameters for lifetime assessment,* In: Journal of Cleaner Production, 2012,37, 221–228, https://doi.org/10.1016/j.jclepro.2012.07.012

[3] Waste and Resources Action Programme (WRAP), *2012 Final Report – A carbon footprint for UK clothing and opportunities for savings*. Available at: https://www.researchgate.net/publication/306145659_A_Carbon_Footprint_for_UK_Clothing_and_Opportunities_for_Savings [Accessed on 29 May 2022]

[4] Barcelos, S.M.B.D, Salvador, R., Guedes, M.G, de Francisco, A.C., *Opportunities for improving the environmental profile of silk cocoon production under Brazilian conditions,* In: Sustainability, 2020, 12, 8, 3214, https://doi.org/10.3390/su12083214

[5] Astudillo, M.F., Thalwitz, G., Vollrath, F., *Life cycle assessment of Indian silk*, In: Journal Of Cleaner Production, 2014, 81, 158–167, https://doi.org/10.1016/j.jclepro.2014.06.007

[6] Ren, Y.E., Yin, J.Y., Wang, X.P., *Life cycle assessment of silk textiles,* In: Consume Guide, 2016, 66, 10, 33–35

[7] Jiang, T., Chen, Z.Y., Yao, T.T., Chen, H., Yang, Z.M., *Product carbon footprint (PCF) assessment of gambiered canton silk,* In: China Dyeing & Finishing, 2012, 38, 8, 39–41

[8] Faragò, S., Sorlini, M., *Silk, History, Processes, Environment*[EB/OL], 2019, Available at: https://www.innovhub-ssi.it/media/pubblicazioni/seta-storia-processi-ambiente.kl [Accessed on 29 May 2022]

[9] Astudillo, M.F., Thalwitz, G., Vollrath, F., *Life cycle assessment of silk production – a case study from India*, In: Subramanian, S.M., editors, Handbook of Life Cycle Assessment (LCA) of Textiles and Clothing, Woodhead Publishing, 2015, 255–274, https://doi.org/10.1016/B978-0-08-100169-1.00011-3

[10] Brandão, M., Levasseur, A., Kirschbaum, M.U.F., Weidema, B.P., Cowie, A.L., Jørgensen, S.V., Hauschild, M.Z., Pennington, M.Z., Chomkhamsri, K., *Key issues and options in accounting for carbon sequestration and temporary storage in life cycle assessment and carbon footprinting,* In: The International Journal of Life Cycle Assessment, 2012, 18, 1, 230–240, https://doi.org/10.1007/s11367-012-0451-6

[11] Giacomin, A.M., Garcia, J.B., Zonatti, W.F., Silva-Santos, M.C., Laktim, M.C., Baruque-Ramos, J., *Silk industry and carbon footprint mitigation,* In: IOP Conference Series: Materials Science and Engineering, IOP Publishing, 2017, 254, 19, 192008

[12] Garcia, Jr. J.B., *Silk Industry and the Millennial Generation "s Desire of Carbon Footprint Mitigation,* In: Proc. 4th International Symposium on Advanced Textile Science and Technology & The International Seminar on Silk Fashion Design and Development Trend, 2016, 35–38

[13] Srikantaswamy, K., Bindroo, B.B., *Organic farming – An option for carbon sequestration technology for the sustainable mulberry leaf production and climate protection*, In: Journal of Innovative Research and Solution, 2014, 196–205

[14] Li, Y., Wang, Y., He, Q., Yang, Y.L., *Calculation and evaluation of carbon footprint in mulberry production: A case of haining in China,* In: International Journal of Environmental Research and Public Health, 2020, 17, 4, 1339, https://doi.org/10.3390/ijerph17041339

[15] Liu, S.Y., Zhu, Z.Y., Qiu, X.X., Wang, X.P., Wang, L.L., *Research progress in the environmental performance assessment of silk product life cycle*, In: Journal of Silk, 2021, 58, 11, 5–9

[16] Wang, X., Deng, Q., Zhou, J., Tang, T., Hu, L.Z., Li, R., Zhang, J.H., *Construction of Carbon Sequestration Estimation Model of Mulberry Garden Based on Statistical Data – A Case Study of Sichuan Province*, In: Chinese Agricultural Science Bulletin, 2022, 38, 2, 31–37

[17] Foley, J.A., *An equilibrium model of the terrestrial carbon budget,* In: Tellus B: Chemical and Physical Meteorology, 1995, 47, 3, 310–319, https://doi.org/10.3402/tellusb.v47i3.16050

[18] Ministry of industry and information technology of the People's Republic of China, *Action plan for high-quality development of silk industry (2021–2025). 2020,* Available at: https://www.miit.gov.cn/jgsj/xfpgys/wjfb/art/2020/art_a57fd110740b49fdb7ad8efa728364f0.html [Accessed on 29 May 2022]

[19] Qian, Y.Q., *Silk yearbook of China (2000-2018)*, Periodicals agency of Zhejiang Sci-Tech University, Hangzhou

[20] Eser, C.O., Yavas, A., *Effect of silk sericin pre-treatment on dyeability of woollen fabric,* In: Industria Textila, 2021, 72, 2, 203–209, https://doi.org/10.35530/IT.072.02.1771

[21] Giacomin, A.M., Garcia, Jr.J.B., Zonatti, W.F., Silva-Santos, M.C., Laktima, M.C., Baruque-Ramos, J., *Brazilian silk production: economic and sustainability aspects*, In: Procedia Engineering, 2017, 200, 89–95, https://doi.org/10.1016/j.proeng.2017.07.014

[22] Vogtländer, J.G., van der Velden, N.M., van der Lugt, P., *Carbon sequestration in LCA, a proposal for a new approach based on the global carbon cycle; cases on wood and on bamboo*, In: The International Journal of Life Cycle Assessment, 2014,19, 1, 13–23, https://doi.org/10.1007/s11367-013-0629-6

[23] BSI (British Standards Institution), *PAS2050:2011 Specification for the assessment of the life cycle greenhouse gas emissions of goods and services*, London, 2011

[24] Yue, W.C., Cai, Y.P., Su, M.R., Tan, Q., Xu, M., *Carbon Footprint of Copying Paper: Considering Temporary Carbon Storage Based on Life Cycle Analysis*, In: Energy Procedia, 2017, 105, 3752-3757, https://doi.org/10.1016/j.egypro.2017.03.870

[25] Nivedita, S., *Recent Developments in Recycling Silk Saris*, In: Nivedita S, Gargi, editors, Functional Textiles and Clothing, Springer, Singapore, 2019, 363–369

[26] Blackburn, R.S., *Sustainable apparel production, processing and recycling*, In: Woodhead Publishing, 2015

Authors:

LIU SHUYI[1,2], LIU JUNRAN[1,2], LI QIZHENG[3,4], BAO WEI[2,5], XU NUO[1,2], WANG XIAOPENG[6], WANG LAILI[2,6]

[1]School of Fashion Design & Engineering of Zhejiang Sci-Tech University, Hangzhou, Zhejiang 310018, China
e-mail: liushuyiiii@163.com (L.S.), junran0911@163.com (L.J.), 1486277686@qq.com (X.N.)

[2]Clothing Engineering Research Center of Zhejiang Province, Zhejiang Sci-Tech University, Hangzhou, Zhejiang 310018, China

[3]International Institute of Silk, Zhejiang Sci-Tech University, Hangzhou 310018, China

[4]International Silk Union, Hangzhou 310018, China

[5]Qingdao University, Collage of Textile & Clothing, Qingdao 266071, China

[6]Silk and Fashion Culture Research Center of Zhejiang Province, Zhejiang Sci-Tech University, Hangzhou 310018, China

Corresponding author:

WANG LAILI
e-mail: wangll@zstu.edu.cn

Anticipating financial distress in monster sectors of Pakistan's economy: an application of logit

DOI: 10.35530/IT.074.03.2022105

EHSANUL HASSAN
MUHAMMAD AWAIS-E-YAZDAN
RAMONA BIRAU
LUCIA PALIU-POPA

ABSTRACT – REZUMAT

Anticipating financial distress in monster sectors of Pakistan's economy: an application of logit

It's always been worthwhile for companies to identify significant predictors of financial distress before its occurrence. This study intends to analyse the scenario of financial distress prediction by focusing on Pakistan. The sample of the study covers companies from the three biggest sectors (textile, sugar and cement)listed on the Pakistan stock exchange for the period of 2005 to 2020. The financial ratios are divided into four main categories of profitability, liquidity, leverage and asset efficiency with a total of 18 financial ratios. The results indicate that the financial ratio produced model accuracy rates of 90.11 percent for the first year prior to bankruptcy, 87.72 percent for the second year prior to bankruptcy, 85.32 percent for the third year prior to bankruptcy, 82.36 percent for the fourth year prior to bankruptcy and 79.57 percent for the fifth year prior to bankruptcy. The results also indicate that profitability, liquidity, leverage, and asset efficiency, are significant predictors of financial distress. The study provides a useful financial distress prediction model for policymakers, company managers, investors, lenders and creditors in the Pakistan stock exchange.

Keywords: *Pakistan stock exchange, financial distress, logistic regression, bankruptcy, non-financial companies, economic sustainability, financial obligations, textile industry*

Anticiparea dificultăților financiare în sectoarele majore ale economiei din Pakistan: un studiu privind aplicarea modelului logit

Întotdeauna a fost util ca firmele să identifice predictori semnificativi privind dificultățile financiare înainte de apariție. Acest studiu își propune să analizeze scenariul de predicție a dificultăților financiare concentrându-se pe economia din Pakistan. Eșantionul studiului acoperă companii din cele mai mari trei sectoare (textil, zahăr și ciment) listate la bursa din Pakistan pentru perioada 2005–2020. Indicatorii financiari sunt împărțiți în patru categorii principale de profitabilitate, lichiditate, efect de levier și eficiență a activelor, cu un total de 18 rate financiare. Rezultatele empirice indică faptul că raportul financiar a produs rate de acuratețe a modelului de 90,11 % pentru primul an anterior falimentului, 87,72 % pentru al doilea an înainte de faliment, 85,32 % pentru al treilea an anterior falimentului, 82,36 % pentru al patrulea an anterior falimentului și de 79,57 % pentru al cincilea an înainte de faliment. Studiul oferă un model util de predicție a dificultăților financiare pentru factorii de decizie, managerii de companii, investitorii și creditorii care vizează piața bursieră din Pakistan.

Cuvinte-cheie: *bursa din Pakistan, dificultăți financiare, regresie logistică, faliment, companii nefinanciare, sustenabilitate economică, obligații financiare, industria textilă*

INTRODUCTION

Financial distress is the failure of the companies to meet their financial obligations. This can be observed from the problems faced by the companies in maintaining their liquid assets and fulfilling their promises regarding credit. the forecast of financial distress of any organization plays a vital role in the decision-making for all stakeholders i.e. creditors, investors, financial institutions, owners (shareholders), suppliers, customers and regulators [1]. It is pertinent that each stakeholder would have different agendas based upon their roles, but the common objective would always be a company's growth. The company's ability to fulfil its obligations is always valuable for the customers [2].

Overall, the major concern of all stakeholders is the prediction for future success and failure of a company [3]. Therefore, it is critical to developing bankruptcy prediction models which help in forecasting business failure and its consequences at micro and macroeconomic levels [4]. These predictive models will help the stakeholders identify future business risks and develop strategies for dealing with risks. Bankruptcy prediction models are also used for the purpose of credit scoring and evaluation of the companies [5]. The models are continuously being enhanced with more prediction accuracy for financial distress [6].

As a developing country, Pakistan is also facing business failures in both small and large companies. A large number of bankruptcies have occurred in the last decade. Sneha [7] reported that the Pakistan Stock Exchange (PSX) is experiencing more delisting than a listing of companies. From 2012 to 2018, 138 companies had been delisted from the PSX under

Liquidation/Winding up under court (PSX, 2018). Pakistan's economy had been affected badly. Therefore, it is necessary to investigate the ratios which are beneficial for the prediction of the instability of companies. Due to the global financial crises of 2008–2009, a sudden shock was faced by the Pakistan stock exchange and companies started struggling for their survival [8]. In 2010 and 2011 there is an increasing trend in the percentage of delisting companies. It is noticed that after the adjustment period of post-financial crises (2010–2011), the percentage of delisted companies increases in 2012 drastically up to 17.89 percent. This increasing trend shows that the Pakistan stock exchange has experienced a high percentage of delisting after the financial crises.

Pakistan's economy has been adversely affected by the financial crises of 2008–2009 and the Pakistan stock exchange has experienced a high rate of bankruptcy following these financial crises. In this situation, it becomes more important to forecast financial distress with maximum accuracy and precision to avoid potential bankruptcy. Even though there is a vast literature on financial distress prediction, most of the studies in the literature have used individual ratios to predict financial distress.

In January 2020, the World Health Organization (WHO) initially declared COVID-19 a health emergency. The economy as a whole is highly unstable on a global level. Many areas and nations may attest to this. The severity, intensity, and long-term economic effects of this pandemic are all quite uncertain. These problems have led to financial market volatility, which has had a significant effect on how businesses make decisions in future years. Companies always try their best to survive in financially distressed markets. The completion of the financial distress cycle may take time and most of the time companies succeed to come out of their financial distress period to the normal business life cycle. Moreover, it is also not necessary for every company that it will be shut down right after any financial distress immediately. Notably, the current study is using the data from 2005 to 2020 and the aftereffects of COVID-19 may be observed or investigated well in the sample after a few years in future. Therefore, it is a limitation of the current study that the impact of COVID-19 in the current sample could not be addressed. Even though this study is an extension of previous studies, this study will strengthen past models through a comprehensive evaluation of financial ratios by focusing on Pakistan. There are very limited studies on predicting financial failure in Pakistan. Only three worth reading studies are found: a study by Rashid and Abbas [9] and a study by Khurshid [10] and a study by Ijaz, Hunjra, Hameed and Maqbool, [11]. Rashid and Abbas [9] conducted the first study in Pakistan in which they used only one model to predict bad financial health and instability. Khurshid [10] conducted a study to investigate the determinants of financial instability of non-financial companies in Pakistan, but the analysis was limited to only two sectors i.e. sugar and textile. As per available literature, no study is found which addressed the need for financial distress prediction model for enormous sectors in Pakistan and if some studies tried to address, they were lacking to address the core contribution of monster sectors independently in the Pakistani economy or cater only a few other sectors using other prediction models.

Moreover, the study comprises various sections. The subsequent section critically reviews the previous literature covering aspects of financial distress models used in past. 3rd section illustrates the methodology. 4th section discusses the results and findings and 5th section elaborates on the detailed discussion and finally 6th section concludes the whole study.

REVIEW OF LITERATURE

The phenomenon of bankruptcy is increasingly likely to happen in modern society, influenced by factors that are within and outside the company [12]. The market is extremely competitive, and it leads the business process by eliminating them unfit. Waqas and Md-Rus [13] conducted a study for the identification of predictors of financial distress in Pakistan. The sample data were obtained for the years 2007 to 2016 with 290 non-financial companies which were listed on the Karachi Stock Exchange of Pakistan. The study used an idiosyncratic sigma of previous returns as a market variable along with the use of financial ratios. However, the results of logistic regression revealed that market variables are not necessary to be significant in the prediction of financial distress in developing countries. On the other hand, financial ratios of profitability, liquidity, asset efficiency, leverage and cashflow indicators were reported as significant predictors of financial distress in Pakistan.

Alifiah and Tahir [14] developed financial distress prediction model in Malaysia. The study used manufacturing and non-manufacturing companies listed on Bursa Malaysia from January 2001 to December 2005. The macroeconomic variable money supply (M2) was also used as an independent variable with individual financial ratios. Logistic regression was used for the analysis. The study concluded that money supply (M2), total asset turnover ratio, net income to total assets and current ratio were the significant predictors of financial distress the for manufacturing sector. However, money supply (M2), net income to total asset ratio, working capital ratio and debt ratio were obtained as significant predictors for non-manufacturing sectors.

Luqman, Hassan, Tabasum, Khakwani and Irshad [15] conducted a study to analyse what role the voluntary adoption of corporate governance systems plays to alleviate financial distress. The study used the data of 52 companies from the non-financial sector listed on the Karachi Stock Exchange from the year 2006 to 2015. The study aimed to analyse the instruments that help the company to mitigate financial distress using logistic regression. The study concluded that the audit committee, block holder ownership and director ownership all are negatively correlated to the probability of financial distress. Moreover, the causal relationship showed that the companies which adopt corporate governance mechanisms face lower financial distress.

Altman et al. [16] conducted research to find out the usefulness of the Z-Score model to predict financial distress and bankruptcy. The focus of the study was on predicting financial distress among banks that operate internationally. The data was gathered from 31 European and three non-European countries. Most of the companies were from the non-financial sector and were primarily private except for the firms in China and the USA. The study concluded that the Z-score model outperformed the results with a prediction accuracy of 75 percent as compared to other market-based and hazard models.

Rashid and Abbas [9] conducted a study in Pakistan focusing only on the textile and sugar sectors. The authors used 24 financial ratios for 52 non-financial companies for the period of 1996 to 2006 and concluded that the most significant financial ratios to predict bankruptcy in Pakistan are earnings before interest and taxes to current liabilities, cash flow ratio and sales to total assets ratio. The model of the study secured a 76.9 percent of accuracy level for bankruptcy prediction.

Research studies compare the ability of such methods to predict bankruptcy and also give attention to building new and more detailed methods that can predict bankruptcy in a better way. After reviewing the above literature, we derive the following hypotheses.

H_1: *Profitability ratios have a significant negative influence on the financial distress prediction of non-financial listed companies in Pakistan.*

H_2: *Liquidity ratios have a significant negative influence on the financial distress prediction of non-financial listed companies in Pakistan.*

H_3: *Leverage ratios have a significant positive influence on the financial distress prediction of non-financial listed companies in Pakistan.*

H_4: *Asset efficiency ratios have a significant negative influence on the financial distress prediction of non-financial listed companies in Pakistan.*

RESEARCH DESIGN

The previous studies have discussed different approaches to measuring corporate insolvency. Enormous researchers have identified more than twenty-five methods (with little variations), widely used. Univariate and multivariate analysis is adopted in the 1960s and 1970s, probit and logit models in the 1980s, models of artificial learning in 1990sand the contingent claim models in the 2000s [17]. The present study has also used logistic regression analysis for obtaining significant financial ratios for non-financial sector companies listed in the PSX.

Selection of financial ratios variables

This study applies extensive ratio analysis of 18 financial ratios as independent variables which are categorized into four indicators of assets efficiency, leverage, profitability and liquidity. These financial ratios are important and selected based on their significance and popularity in the literature to measure financial distress [13, 14]. Each indicator has its group of ratios that will directly assess the significant of the indicator.

Data of the study

The study used the financial data of non-financial companies from three huge sectors namely textile, sugar and cement listed on the Pakistan stock exchange from year 2005 to 2020. Balance sheets of all companies were scanned thoroughly for selecting the companies which fulfilled this criterion of bankruptcy. The final data of 44 companies were selected as bankrupt while the remaining 153 companies were supposed to be non-bankrupt because they showed positive equity. For the selection of non-bankrupt companies' group against the criterion of matched industry and asset size to that of the bankrupt group is used. Meaning that these companies were taken on the basis that the company belonged to the same sector and industry as that of the respective bankrupt company, the company possessed positive equity in all years of the sample period and the company had the same asset size as that of the respective bankrupt company.

Methodology

The logit model is widely used in the literature [18]. Researchers give preference to the logit model because of its unique advantages over the MDA model as it does not assume the normality of predictive variables. Also, it provides a probabilistic output instead of the score which has to be converted to a probabilistic measure that ultimately leads to an additional source of error [19].

Logit model

The Logit model states that for any company, there is a given set of characteristics through which we can measure a definable probability of default. Therefore, the probability of default for a company is based on these conditional sets of characteristics. Statistically, this model can be equated as:

$$P(Y_i = 1) = \frac{1}{1 + \exp(-\alpha - \beta x_i)} \quad (1)$$

where Y_i will be 1 if the company is bankrupt, x_i is vector of the explanatory variable. When the probability of bankruptcy increases the value of $\alpha + \beta x_i$ also increases.

The simplified form of this equation is:

$$P_i = 1/(1 + e^{-Z}) \quad (2)$$

Here,

$$Z = \beta x_i + \mu \quad (3)$$

Equation 1 is showing the cumulative logistic distribution function. To apply the prediction model, we will estimate the weights of the financial ratios with the help of equation 3. Optimal β (weights) can be estimated where the likelihood value is maximized. If the probability of default calculated through the logit model is greater than 0.5 then the company will be considered as financially distressed otherwise it will be considered as a healthy company.

For logit analysis, the econometric model of our study can be written as:

$$P(Y_i = 1) = \alpha + \beta_i NPFA_i + \beta_i SCA_i + \beta_i SFA_i + \\ + \beta_i STA_i + \beta_i TLTA_i + \beta_i LTDTA_i + \beta_i FASE_i + \\ + \beta_i TDSE_i + \beta_i EBITCL_i + \beta_i NPS_i + \beta_i NPSE_i + \\ + \beta_i EBITTA_i + \beta_i RETA_i + \beta_i QR_i + \beta_i CACL_i + \\ + \beta_i CATA_i + \beta_i CCL_i + \beta_i CLTA_i$$

Sample specification for bankruptand non-bankrupt companies

The sample of the study must have the following criteria. For bankrupt companies, the company must belong to the non-financial sector. It is because the financial sector has a different bankruptcy procedure. The company must have at least five years of financial information. A company is considered bankrupt if it shows a negative book value of equity in any one of the years in the sample period. On the other hand, for non-bankrupt companies, the company must belong to the same industry as the other group of non-financial sectors. The company must have the closest asset size matched-with within the bankrupt group. The data for the non-bankrupt company is taken from the corresponding year in which the company went bankrupt in another group. Finally, the company possesses a positive book value of equity in all years of data in the sample period.

RESULTS AND FINDINGS

All ratios are entered using a stepwise logistic regression approach. Before using financial ratios in logistic regression analyses it was necessary to check the multicollinearity problem and whether it exists in the sample data or not. For this purpose, correlation analysis and collinearity diagnostics are done. The results of the correlation analysis are presented in table 1. Moreover, table 2 shows the values of tolerance and variance inflation factor (VIF) for each financial ratio used in the analysis given below.

According to Hair, Black, Babin and Anderson [20] and Waqas and Md-Rus [13] if the value of VIF is greater than 10, it depicts the existence of multicollinearity problem. Moreover, table 1 shows that all the values of VIF are less than 10 which also strengthens the results of correlation and confirms that there is no multicollinearity problem in the data. After multicollinearity diagnostics, the study used all these financial ratios as independent variables in regression analysis for financial distress prediction for each year prior to bankruptcy (YPB) (table 3).

Table 3 shows the results of logistic regression with the coefficient estimates and their significant p-values for the first YPB. P-values of QR and TDSE at alpha one percent, SCA and LTA at alpha 5 percent and NPSE at alpha 10 percent are statistically significant. The model obtained five statistically significant variables or financial ratios which can be developed as below:

$$\text{Logit Score} = 1/\{1 + e^{-[-8.03 + (-0.586 X_1) + (-11.478 X_2) + (-3.168 X_3) + (0.816 X_4) + (0.527 X_5)]}\}$$

or

$$= 1/\{1 + e^{-[-8.03 + (-0.586\, S/CA) + (-11.478\, QR) + (-3.168\, NP/E) + (0.816\, LTA) + (0.527 TD/SE)]}\}$$

where SCA is the ratio of sales to current assets which measures the company's efficiency; (CA-IN)/CL is the ratio of quick assets to current liabilities which measures the company's liquidity; NPSE is the ratio of net profit to shareholders' equity which measures company's profitability and TDSE is the ratio total debt to shareholder equity which measures company's leverage.

The coefficient interpretation of logit estimation is a little bit different because it is a nonlinear estimation. These can be calculated in a spreadsheet and also these are called marginal effects. Marginal effects are calculated as per the suggestion of Brooks (2008). Brooks suggested that for the correct interpretation of coefficients in the logit model the mean value of each explanatory variable should be calculated. So, the mean values here are $\bar{X}_1$, $\bar{X}_2$, $\bar{X}_3$, $\bar{X}_4$ and $\bar{X}_5$ with values of 2.565, 0.726, –2.726, 14.213 and 22.369 respectively. The logit function is calculated as:

$$\hat{P}_{iYPB1} = 1/\{1 + e^{-[-8.03 + (-0.586*2.565) + (-11.478*0.726) + (-3.168*-2.726) + (0.816*14.213) + (0.527*22.369)]}\} = \\ = 1/(1 + e^{-14.137}) = 0.99$$

This shows that with every one-unit increase in the ratio of sales to Current Assets the case's probability to join the bankrupt group will be reduced by $-0.586 \times 0.999 = -0.586$ units. Similarly, one unit increase in quick assets to current liabilities ratio will decrease the probability of financial distress by $-11.478 \times 0.999 = -11.478$ units. The corresponding changes in the probabilities occur for net profit to shareholders equity, natural log of total assets, and total debt to shareholders equity are $-3.168 \times 0.999 = -3.167$ units; $0.816 \times 0.999 = 0.816$ units and $0.527 \times 0.999 = 0.527$ units, respectively. Also, all the coefficients are economically and statistically significant at a 10% level of significance. Furthermore, the same procedure is applied to the results of the second, third, fourth and fifth YPB (table 4).

Table 4 represents the percentages of models' accuracy concerning each year prior to bankruptcy. It is shown that precision percentages of the model are higher in the first YPB with 90.11 percent and 87.72 percent in the second YPB and 85.32, 82.36 and 79.57 in the third, fourth and fifth YPB respectively.

DISCUSSION

The study intents to identify the predictors of financial distress for the non-financial companies listed on the

Table 1

CORRELATION MATRIX

	EBITCL	NPS	NPSE	EBITTA	RETA	QR	CATA	CCL	CLTA	CACL	TLTA	LTDTA	FASE	TDSE	NPFA	SCA	SFA	STA
EBITCL	1																	
NPS	0.579**	1																
NPSE	–0.003	0.003	1															
EBITTA	0.032	0.078*	0.003	1														
RETA	0.001	0.002	0.019	0.444**	1													
QR	0.006	0.006	0.003	0.087**	0.165**	1												
CATA	–0.005	0.009	–0.012	0.143**	0.055	0.044	1											
CCL	0.006	0.001	0.017	0.423**	0.592**	0.308**	0.137**	1										
CLTA	–0.146**	–0.083**	–0.012	–0.006	–0.022	–0.108**	0.237**	–0.098**	1									
CACL	–0.004	–0.003	0.001	–0.002	0.001	0.004	0.029	0.004	0.025	1								
TLTA	–0.064*	–0.032	0.007	–0.051	–0.016	–0.079*	0.081**	–0.072*	0.648**	0.011	1							
LTDTA	0.003	0.002	–0.001	–0.002	0.000	–0.002	0.012	–0.002	–0.004	0.001	–0.001	1						
FASE	–0.002	–0.002	0.011	0.006	0.001	0.001	0.037	0.002	–0.020	–0.003	–0.012	–0.005	1					
TDSE	0.015	0.010	0.004	–0.001	–0.006	–0.007	0.037	–0.005	0.006	0.013	0.010	0.024	–0.002	1				
NPFA	0.002	0.002	–0.016	0.697**	0.001	–0.003	0.069*	0.000	0.180**	0.001	0.081**	–0.001	0.000	–0.005	1			
SCA	0.048	0.052	–0.018	0.007	–0.015	–0.062*	–0.041	–0.030	–0.123**	–0.034	–0.081**	–0.007	0.031	0.016	–0.026	1		
SFA	0.010	0.008	–0.001	–0.011	–0.010	0.002	0.097**	–0.001	–0.010	0.004	–0.013	0.000	0.000	0.021	0.001	0.034	1	
STA	0.048	0.044	–0.010	0.052	–0.013	–0.040	0.322**	–0.014	–0.064*	–0.001	–0.087**	–0.002	0.019	0.024	–0.019	0.701**	0.091**	1

Note: Dependent variable: Financial Distress Proxy (Binary); Independent variables: EBITCL is earnings before interest and taxes to current liabilities, NPS is net profit to sales, NPSE is net profit to shareholders equity, EBITTA is earnings before interest and taxes to total assets, RETA is retained earnings to total assets, QR is quick ratio, CATA is current assets to total assets, CCL is cash to current liabilities, CLTA is current liabilities to total assets, CACL is current assets to current liabilities, TLTA is total liabilities to total assets, LTDTA is the long-term debt to total assets, FASE is fixed assets to shareholders equity, TDSE is total debt to shareholders equity, NPFA is net profit to fixed assets, SCA is sales to current assets, SFA is sales to fixed assets, STA is sales to total assets.

Table 2

MULTICOLLINEARITY ANALYSIS		
Financial ratios	**Collinearity statistics**	
	Tolerance	**VIF**
EBITCL	0.613	2.560
NPS	0.620	1.516
NPSE	0.913	4.033
EBITTA	0.216	4.060
RETA	0.558	1.930
QR	0.292	1.187
CATA	0.570	1.119
CCL	0.429	3.047
CLTA	0.180	2.082
CACL	0.488	1.127
TLTA	0.746	3.832
LTDTA	0.756	1.646
FASE	0.189	1.111
TDSE	0.921	1.086
NPFA	0.216	3.186
SCA	0.162	2.764
SFA	0.732	2.018
STA	0.370	2.019

Table 3

COEFFICIENT ESTIMATES FOR INDIVIDUAL FINANCIAL RATIOS MODELS				
Years prior to bankruptcy (YPB)	**Variables**	**Coefficient**	**ME**	**Prob.**
First YPB	C	–8.03	-	0.085
	SCA	–0.586	–0.586	0.040
	QR	–11.478	–11.478	0.002
	NPSE	–3.168	–3.168	0.080
	TDSE	0.527	0.527	0.003
Second YPB	C	–6.658	-	0.019
	FASE	0.273	0.236	0.026
	EBITCL	–4.485	–3.862	0.019
	QR	–2.073	–1.786	0.030
Third YPB	C	–2.496	-	0.265
	TDSE	0.625	0.323	0.000
	CATA	–4.465	–2.302	0.006
	SCA	–0.479	–0.247	0.038
Fourth YPB	C	–4.998	-	0.082
	LTDTA	5.319	2.293	0.090
	RETA	–1.207	–0.52	0.033
	CACL	–0.897	–0.387	0.048
Fifth YPB	C	–1.584	-	0.155
	EBITTA	–10.661	–5.245	0.031
	TLTA	2.931	1.442	0.087

Note: SCA is sales to current assets, QR is quick ratio, NPSE is net profit to shareholders equity, TDSE is total debt to shareholders equity, FASE is fixed assets to shareholders equity, EBITCL is earnings before interest and taxes to current liabilities, CATA is current assets to total assets, LTDTA is the long-term debt to total assets, RETA is retained earnings to total assets, CACL is current assets to current liabilities, EBITTA is earnings before interest and taxes to total assets, TLTA is total liabilities to total assets.

Table 4

MODEL ACCURACY	
Years prior to bankruptcy (YPB)	**Percentages of model accuracy (%)**
First YPB	90.11
Second YPB	87.72
Third YPB	85.32
Fourth YPB	82.36
Fifth YPB	79.57

PSX. The data analysis is done using logistic regression with 18 individual financial ratios. However, results of individual financial ratios show that EBITCL, NPSE, EBITTA and RETA are significant profitability ratios. The profitability ratios possess negative sign of coefficients which means that the higher the value of profitability ratios lesser will be the probability of financial distress. The results of profitability ratios align with previous studies like Cederburg and O'Doherty [21], Hu and Sathye [22], Altman et al. [16], Rashid and Abbas [9], Campbell et al. [23], Choe and Her [24] and Hotchkiss, Smith, and Stromberg [25].

In addition, liquidity ratios analysis is also worth important for a company. Basically, it is the ability of a company to fulfil its short-term liabilities. The ratios QR, CACL and CATA are significant liquidity ratios with the negative sign of coefficient values obtained for this study. The negative sign of coefficient estimates shows that an increase in a company's liquidity decreases the probability of financial distress. Past studies which articulated the same results for liquidity ratios are Chiaramonte and Casu [26], Ijaz et al. [11], Rashid and Abbas [9], Yap et al. [27], Campbell et al [23], Allayannis et al. [28], Ugurlu and Aksoy [29].

The rational introduction of debt in a company's capital structure is very important. The logistic regression results for leverage ratios show LTDTA, FASE, TDSE and TLTA are statistically significant. Leverage ratios exhibit positive sign of coefficient estimates which indicates the inverse relationship between leverage ratios and the probability of financial distress. The lower the unnecessary debt in capital structure, the lesser will be the probability of financial distress. Past studies like Agarwal and Bauer [30], Tinoco and Wilson [31], Abdullah et al. [32], Jones and Hensher [33], and Eljelly and Mansour [34].

The proper and efficient utilization of company assets is an important aspect of a running business. The findings of the study suggest only one asset efficiency ratio which is SCA. The ratio is statistically significant with a negative sign to predict financial distress. The inverse relationship shows that efficient utilization of assets reduces the probability of financial distress. Furthermore, the asset efficiency ratios' results are similar to the previous study like Ugurlu and Aksoy [29] and Eljelly and Mansour [34]. Spulbar et al. [35] have conducted a research study on the effects of tax revenue on the evolution of Gross domestic product (GDP) in the case of European Union member states. On the other hand, Sumera et al. [36] examined the implications of education on the dynamics of economic growth. Spulbar et al. [37] investigated the impact of digitalization on poverty alleviation and economic growth due to the COVID-19 pandemic.

CONCLUSION

The empirical findings of the study fulfil all the research objectives and answer all the research questions of the present study. The study reveals that significant profitability ratios are earnings before interest and taxes to current liabilities (EBITCL), net profit to shareholder's equity (NPSE), earnings before interest and taxes to total assets (EBITTA) and retained earnings to total assets (RETA). Additionally, the liquidity ratios which show significant results are quick ratio (QR), current assets to current liabilities (CACL) and current assets to total assets (CATA). The significant leverage ratios for financial distress prediction are a long-term debt to total assets (LTDTA), fixed assets to shareholders equity (FASE), total debt to shareholders equity (TDSE) and total liabilities to total assets (TLTA). Furthermore, the findings reveal that sales to current assets (SCA) are the only significant individual financial ratio as an asset efficiency ratio. Lastly, the highest precision rate of model accuracy produced in the study is 90.11 percent for the first YPB.

REFERENCES

[1] Garcia, C.J., Herrero, B., *Female directors, capital structure, and financial distress,* In: Journal of Business Research, 2021, 136, 592–601

[2] Macerinskiene, I., Mendelsonas, T., *Macroeconomic determinants of corporate insolvency*, In: KSI Transactions on Knowledge Society, 2013, 6, 3, 35–40

[3] Reinhart, C.M., *From health crisis to financial distress*, In: IMF Economic Review, 2022, 70, 1, 4–31

[4] Jardim, P.C., Pereira, T.E., *Corporate Bankruptcy of Portuguese Firms*, In: Zagreb International Review of Economics and Business, 2013, 16, 2, 39–56

[5] Altman, E.I., *An emerging market credit scoring system for corporate bonds,* In: Emerging Markets Review, 2005, 6, 4, 311–323

[6] Bharath, T., Shumway, T., *Forecasting Default with the Kmv-Merton Model*, AFA 2006 Boston Meetings Paper, 2004, Available at: https://ssrn.com/abstract=637342 [Accessed on September 2022]

[7] Sneha, P., *More delisting than new listings on bourses,* Business Standard, 2015, Available at: http://www.business-standard.com/article/markets/more-delisting-than-new-listings-on-bourses-115012000905_1.html [Accessed on September 2022]

[8] Liahmad, K.R., Utami, Y.P., Sitompul, S., *Financial Factors and Non-Financial to Financial Distress Insurance Companies That Listed in Indonesia Stock Exchange*, In: Humanities and Social Sciences, 2021, 4, 1, 1305–1312

[9] Rashid, A., Abbas, Q., *Predicting Bankruptcy in Pakistan*, In: Theoretical and Applied Economics, 2011, 18, 9, 103–128

[10] Khurshid, M.R., *Determinants of Financial Distress Evidence from KSE 100 Index*, In: Research Journal of The Institute of Business Administration Karachi-Pakistan, 2013, 8, 1, 7

[11] Ijaz, M.S., Hunjra, A.I., Hameed, Z., Maqbool, A., *Assessing the financial failure using z-score and current ratio: A case of sugar sector listed companies of Karachi stock exchange*, In: World Applied Sciences Journal, 2013, 23, 6, 863–870

[12] Alaminos, D., del Castillo, A., Fernandez, M.A., *A global model for bankruptcy prediction*, In: PloS one, 2016, 11, 11, 1–18

[13] Waqas, H., Md-Rus, R., *Predicting financial distress: Importance of accounting and firm-specific market variables for Pakistan's listed firms*, In: Cogent Economics & Finance, 2018, 6, 1, 1545739

[14] Alifiah, M.N., Tahir, M., *Predicting financial distress companies in the manufacturing and non-manufacturing sectors in Malaysia using macroeconomic variables,* In: Management Science Letters, 2018, 8, 6, 593–604

[15] Luqman, R., Hassan, U.M., Tabasum, S., Khakwani, M.S., Irshad, S., *Probability of financial distress and proposed adoption of corporate governance structures: Evidence from Pakistan,* In: Cogent Business & Management, 2018, 5, 1, 1–14

[16] Altman, E.I., Iwanicz-Drozdowska, M., Laitinen, E.K., Suvas, A., *Financial distress prediction in an international context: A review and empirical analysis of Altman's Z-score model*, In: Journal of International Financial Management & Accounting, 2017, 28, 2, 131–171

[17] Jackson, R.H., Wood, A., *The performance of insolvency prediction and credit risk models in the UK: A comparative study,* In: The British Accounting Review, 2013, 45, 3, 183–202

[18] Aziz, A.M., Dar, H.A., *Predicting corporate bankruptcy: where we stand?*, In: Corporate Governance: The International Journal of Business in Society, 2006, 6, 1, 18–33

[19] Ohlson, J.A., *Financial ratios and the probabilistic prediction of bankruptcy*, In: Journal of Accounting Research, 1980, 18, 1, 109–131

[20] Hair, J.F., Black, W.C., Babin, B.J., Anderson, R.E., *Multivariate data analysis,* (7th ed). Prentice Hall, 2010

[21] Cederburg, S., O'Doherty, M.S., *Asset-pricing anomalies at the firm level*, In: Journal of Econometrics, 2015, 186, 1, 113–128

[22] Hu, H., Sathye, M., *Predicting financial distress in the Hong Kong growth enterprises market from the perspective of financial sustainability*, In: Sustainability, 2015, 7, 2, 1186–1200

[23] Campbell, J.Y., Hilscher, J., Szilagyi, J., *In search of distress risk*, In: The Journal of Finance, 2008, 63, 6, 2899–2939

[24] Choe, C., Her, Y.W., *A Comparative Study of Australian and Korean Accounting Data in Business Failure Prediction Models*, In: Journal of Accounting and Finance, 2002, 1, 41–68

[25] Hotchkiss, E.S., Smith, D.C., Stromberg, P., *Private equity and the resolution of financial distress*, In: The Review of Corporate Finance Studies, 2021, 10, 4, 694–747

[26] Chiaramonte, L., Casu, B., *Capital and liquidity ratios and financial distress. Evidence from the European banking industry*, In: The British Accounting Review, 2017, 49, 2, 138–161

[27] Yap, B.C.F., Yong, D.G.F., Poon, W.C., *How well do financial ratios and multiple discriminant analysis predict company failure in Malaysia,* In: International Research Journal of Finance and Economics, 2010, 54, 166–175

[28] Allayannis, G., Brown, G.W., Klapper, L.F., *Capital structure and financial risk: Evidence from foreign debt use in East Asia,* In: The Journal of Finance, 2003, 58, 6, 2667–2710

[29] Ugurlu, M., Aksoy, H., *Prediction of corporate financial distress in an emerging market: the case of Turkey,* In: Cross Cultural Management: An International Journal, 2006, 13, 4, 277–295

[30] Agarwal, V., Bauer, J., *Distress Risk and Stock Returns: The neglected Profitability Effect,* In: FMA Annual Meeting, Nashville, TN, 2014, 15–18

[31] Tinoco, M.H., Wilson, N., *Financial distress and bankruptcy prediction among listed companies using accounting, market and macroeconomic variables,* In: International Review of Financial Analysis, 2013, 30, 394–419

[32] Abdullah, N.A.H., Halim, A., Ahmad, H., Rus, R.M., *Predicting corporate failure of Malaysia's listed companies: Comparing multiple discriminant analysis, logistic regression and the hazard model*, In: International Research Journal of Finance and Economics, 2008, 15, 201–217

[33] Jones, S., Hensher, D.A., *Predicting firm financial distress: A mixed logit model*, In: The Accounting Review, 2004, 79, 4, 1011–1038

[34] Eljelly, A.M., Mansour, I.H.F., *Predicting private companies' failure in the Sudan*, In: Journal of African Business, 2001, 2, 2, 23–43

[35] Spulbar, C., Ehsanifar, M., Birau, R., Babaie, A., Doagă, D.I., *Advanced empirical research based on structural equation modeling (SEM) regarding the impact of tax revenue on GDP dynamics at EU-28 level*, In: Scientific Annals of Economics and Business, 2021, 68, 3, 285–307, https://doi.org/10.47743/saeb-2021-0017

[36] Sumera, A., Zahid Naeem, M., Spulbar, C., Birau, R., Ninulescu, P.V., *Impact of Education and Income Inequality on Per Capita Income Amid COVID-19 pandemic*, In: Revista de Științe Politice. Revue des Sciences Politiques, 2022, 76, 18–33

[37] Spulbar, C., Anghel, L.C., Birau, R., Ermiș, S.I., Treapăt, L.-M., Mitroi, A.T., *Digitalization as a Factor in Reducing Poverty and Its Implications in the Context of the COVID-19 Pandemic*, In: Sustainability, 2022, 14, 17, 10667, https://doi.org/10.3390/su 141710667

Authors:

EHSANUL HASSAN[1], MUHAMMAD AWAIS-E-YAZDAN[2], RAMONA BIRAU[3], LUCIA PALIU-POPA[3]

[1]National University of Sciences and Technology (NUST), Sector H-12, Islamabad, Pakistan
e-mail: ehsanul.hassan@seecs.edu.pk

[2]Faculty of Business and Management Sciences, The Superior University Lahore, Lahore, Pakistan
e-mail: awais.yazdan@gmail.com

[3]Faculty of Economic Science, University Constantin Brancusi, Tg-Jiu, Romania
e-mail: univers_cont@yahoo.com

Corresponding author:

RAMONA BIRAU
e-mail: ramona.f.birau@gmail.com

Antimicrobial treatment for textiles based on flavonoid-mediated silver nanoparticles dispersions

DOI: 10.35530/IT.074.03.202333

MIHAELA-CRISTINA LITE
RODICA ROXANA CONSTANTINESCU
NICOLETA BADEA
ELENA-CORNELIA TĂNĂSESCU
IRINA-MARIANA SĂNDULACHE
OVIDIU GEORGE IORDACHE

ABSTRACT – REZUMAT

Antimicrobial treatment for textiles based on flavonoid-mediated silver nanoparticles dispersions

*The use of "green" reagents for silver nanoparticles (AgNPs) synthesis represents an attractive alternative to conventional methods, due to the abundance of available biomass with reducing properties. Herein, a flavonoid compound, hesperidin, was used to produce AgNPs, and the resulting dispersion was applied to textile fabrics and tested for its antimicrobial properties. Different ratios of flavonoid to the silver precursor (v:v) were prepared. The formation of the nanoparticles was indicated by the presence of the SPR specific band in the UV–Vis spectra. For the synthesis optimization, the DLS technique was used to determine the size and polydispersity of the AgNPs, while zeta potential measurements were performed to assess their physical stability. For the dispersion with the optimal ratio, particles with the average size (Z_{av}) of 93.55±3.51 nm were obtained, with a polydispersity index (PdI) of 0.259. For this ratio, the value of the zeta potential (ξ.) was –28.80±1.54 mV, indicating that the dispersion is physically stable. The nanoparticles were further characterized using SEM-EDS techniques to confirm the particles' nature and evaluate their morphology. The AgNPs were deposited on textile samples, by direct soaking into the dispersion. The distribution of the AgNPs on the textile samples fibres was evaluated by SEM and the chromatic parameters L*a*b* were determined compared to the untreated samples. Antimicrobial tests were conducted against Escherichia coli, Staphylococcus aureus, and Bacillus subtilis strains, according to the ISO 20743:2013 standard, and percentages of bacterial reduction up to 99.99% were obtained.*

Keywords: *silver nanoparticles, flavonoids, hesperidin, dispersions, antimicrobial textiles*

Tratament antimicrobian pentru textile pe bază de dispersii de nanoparticule de argint mediate de flavonoizi

*Utilizarea de reactivi „verzi" pentru sinteza nanoparticulelor de argint (AgNPs) reprezintă o alternativă atractivă la metodele convenționale, datorită abundenței biomasei disponibile cu proprietăți reducătoare. În lucrarea de față, un compus flavonoid, hesperidina, a fost folosit pentru a produce AgNPs, iar dispersia rezultată a fost aplicată pe țesături textile și testată pentru proprietățile sale antimicrobiene. Au fost preparate diferite rapoarte de flavonoid la precursor de argint (v:v). Formarea nanoparticulelor a fost indicată de prezența benzii specifice SPR în spectrele UV-Vis. Pentru optimizarea sintezei, tehnica DLS a fost utilizată pentru a determina dimensiunea și polidispersitatea AgNPs, în timp ce măsurătorile potențialului zeta au fost efectuate pentru a evalua stabilitatea lor fizică. Pentru dispersia cu raportul optim, s-a obţinut AgNPS cu dimensiunea medie de particule (Z_{av}) de 93,55±3,51 nm, cu un indice de polidispersitate (PdI) de 0,259. Pentru acest raport, valoarea potențialului zeta (ξ.) a fost de –28,80±1,54 mV, ceea ce indică faptul că dispersia este stabilă din punct de vedere fizic. Nanoparticulele au fost caracterizate în continuare, folosind tehnicile SEM-EDS, pentru a confirma natura particulelor și pentru a evalua morfologia lor. AgNPs au fost depuse pe probele textile, prin îmbibarea directă în dispersia de AgNPs. Distribuția AgNPs pe fibrele din probele textile a fost evaluată prin SEM și au fost determinați parametrii cromatici L*a*b* comparativ cu probele netratate. Au fost efectuate teste antimicrobiene pe tulpini de Escherichia coli, Staphylococcus aureus și Bacillus subtilis, conform standardului ISO 20743:2013 și s-au obținut procente de reducere bacteriană de până la 99,99%.*

Cuvinte-cheie: *nanoparticule de argint, flavonoizi, hesperidină, dispersii, textile antimicrobiene*

INTRODUCTION

Textile fabrics represent an excellent media for the growth of microorganisms, such as fungi, moulds, and bacteria. The metabolism products of these pathogens lead to the degradation of the fibres, the generation of unwanted odour, and an increased risk of contamination [1, 2]. Even though if the research of antimicrobial textiles is not a new topic, the context of the SARS-CoV-2 pandemic brought attention to the continuous need for developing innovative treatments for textiles disinfection [3]. The current antimicrobial reagents include quaternary ammonium salts, polyhexamethylene biguanide, regenerable N-halamines and peroxyacids, chitosan and chitosan derivatives etc. [1, 4]. Apart from chemicals, there are reports about achieving the manufacturing of antimicrobial textiles by using natural compounds, such as curcumin, chitosan, or essential oils [3]. The field of nanomaterials gained the attention of the research community for its remarkable properties and applications [4, 5]. Ag, ZnO, MgO, CaO, CuO, and TiO_2 nanoparticles are among the nanomaterials assessed for exhibiting antimicrobial properties [6–10]. Silver nanoparticles (AgNPs) present the capacity to inactivate bacteria due to the interaction with the sulfur contained in the constituent amino acids of the proteins from the bacterial cell membranes. Moreover, the interaction of the silver ion with the DNA phosphoric groups leads to the inhibition of the enzyme's activities [11]. The advantage of using AgNPs consists of the ease to produce them, at low costs, and by environment-friendly methods when using green synthesis [12]. Otávio Augusto L. dos Santos investigated the antimicrobial potential of AgNPs applied on cotton gauze. The AgNPs treatment led to microbial growth inhibition from 50% to 90% against *E. coli*, *S. epidermidis*, *S. aureus* and the fungal strain of *C. albicans* [13]. In another study, published by Fatma A., the antimicrobial effect of AgNPs on linen textile samples was investigated. The antibacterial tests against *E. Coli* and *S. aureus* demonstrated that the treated samples maintained their antibacterial properties even after 20 washing cycles [14].

In this study silver nanoparticles (AgNPs) have been synthesized using hesperidin as a reducing agent. Hesperidin is a flavonoid compound present in many plant parts. Its potential as a reducing agent arises from the phenolic groups in its structure [15]. Different ratios of hesperidin to silver ions were tested and the formation of the AgNPs was revealed by recording the UV-Vis absorption spectrum, due to the presence of the specific absorption band called the surface-plasmon resonance (SPR) band. Synthesis optimization consisted of determining the average size, polydispersity, and physical stability of the nanoparticles, by performing dynamic light scattering (DLS) measurements and by determining the zeta potential, respectively. The size and nature of the particles were confirmed by scanning electron microscopy (SEM) coupled with an X-ray detector (energy dispersive X-ray spectroscopy – EDS). The optimal dispersion of AgNPs was tested on textile samples (cotton and wool) for its antimicrobial effect against *Escherichia coli, Staphylococcus aureus, and Bacillus subtilis strains.* The distribution of AgNPs on the textile fibres was assessed by SEM and their nature was confirmed by EDS. Moreover, the chromatic parameters of the treated and untreated samples were determined and compared, and a total colour change was quantified.

EXPERIMENTAL

Material and methods

The source of silver ions consisted of silver nitrate, which was purchased from Anal-R NORMAPUR. The rest of the substances were purchased from Merck. The cotton and wool textile samples were provided by the National R&D Institute for Textiles and Leather (INCDTP, Bucharest, Romania). The antibacterial tests were conducted using *Escherichia coli* ATCC 10536, *Staphylococcus aureus* ATCC 6538, and *Bacillus subtilis* ATCC 6633 strains. The culture media consisted of: TSA (Casein Soya Bean), TSB (Tryptic Soy Broth), NB (Nutrient broth), EA (Enumeration Agar), Digest Agar, and SCDLP (Casein Soya Bean Digest).

The pretreatment of the samples for performing the DLS tests consisted of adding 300 µl of AgNPs dispersion to 20 ml of distilled water. For the zeta potential measurements, an increase in the conductivity of the samples was necessary. Hence, 50 µl of NaCl 0.9% solution was added to the 20 mL of water and 300 µl of AgNPs dispersion.

Before the AgNPs morphology evaluation, 300 µl of dispersion was deposited, by pipetting, on a SiO_2 slide. After the evaporation of the liquid, the SiO2 slide was subjected to analysis

Synthesis and optimization

Aqueous solutions of hesperidin 1 mM were prepared, while adjusting the pH to 11.80 with NaOH, for completing the dissolution of flavonoid compounds. For the pH monitorization, the Crison GLP 21+ pH meter (Barcelona, Spain) was used.

For optimization, different ratios flavon:$AgNO_3$, were used - 1:1, 1:3, 1:5 and 1:9 (v:v). The first indicator of the AgNPs formation consisted of the dark colour of the reaction mixtures, after adding the silver precursor to the flavonoid solutions. After two hours, the reaction mixtures were centrifuged at 5000 rpm for 30 minutes. The supernatant was collected for characterization and used in further experiments.

A Lambda 950 UV-Vis spectrophotometer, from Perkin Elmer, was used to record the absorption spectra of the AgNPs dispersion. The presence of the AgNPs was confirmed by the characteristic SPR (surface plasmon resonance) absorption band [16, 17].

The size, polydispersity, and physical stability of the dispersions were evaluated using a Zetasizer Nano ZS instrument from Malvern Instruments Ltd. (Worcestershire, UK). Dynamic Light Scattering (DLS) technique was conducted for determining the average size (Z_{av}) and polydispersity index (PdI), which indicates the distribution of the particles size populations. The physical stability of the AgNPs dispersions was determined by performing zeta potential (ξ) measurements, which is an indicator of physical stability. A dispersion is considered stable when the absolute value of its zeta potential exceeds 25 mV [18].

Characterization of produced AgNPs

Scanning Electron Microscopy (SEM) was performed to evaluate the morphology of the produced AgNPs. For this purpose, a FEI Quanta 200 microscope was used, which was provided with an Everhart-Thornley (ET) detector. Moreover, the nature of the nanoparticles was confirmed by performing X-ray dispersive spectroscopy (EDS), using an EDAX-AMETEK X-ray detector coupled to the electron microscope instrument. The dispersion with the optimal ratio was deposited on a SiO_2 slide and, after evaporation of the liquid, the sample was subjected to the SEM-EDS characterization.

Effect of AgNPs dispersions on textile samples

The treatment of the textile samples (10 × 10 cm) consisted of directly soaking the cotton and wool samples into the silver nanoparticles dispersions. The samples were left to dry at room temperature, then they were characterized by SEM, to evaluate how the AgNPs were distributed on the textile fibres. Their nature was confirmed by performing EDS measurements.

The chromatic parameters, expressed in the CIE L*a*b* system of colours, of the treated and untreated textile samples (the reference fabrics) were measured, using the Datacolor spectrophotometer, from DKSH Holding Ltd. (Zurich, Switzerland), equipped with a D65/10 lamp).

The antibacterial tests were conducted according to the ISO 20743:2013 standard, which involves quantitative test methods to determine the antimicrobial activity of finished antimicrobial samples. The absorption method was used, which involved the direct inoculation of the test bacteriological inoculum directly onto the treated samples.

RESULTS AND DISCUSSION

Characterization of the AgNPs dispersions

Spectral characterization

The reduction of the silver is firstly indicated by the brownish colour of the reaction mixture. The UV-Vis spectra recorded for the hesperidin solution and the AgNPs dispersions prepared in different ratios of hesperidin solution to silver ions are presented in figure 1. The bands present at 280 nm and 350 nm correspond to hesperidin, while the bands at 430 nm are attributed to the reduced silver and appear due to the specific surface plasmon resonance (SPR) of AgNPs [19–21]. The width of the bands is an indicator of the size and polydispersity of the AgNPs.

Size, polydispersity, and physical stability of the AgNPs dispersions

The average particle size (Z_{av}) determined by DLS measurements (figure 2, *a*) of the AgNPs varied from 65 to 155 nm (from the ratio 1:1 to the ratio 1:9).

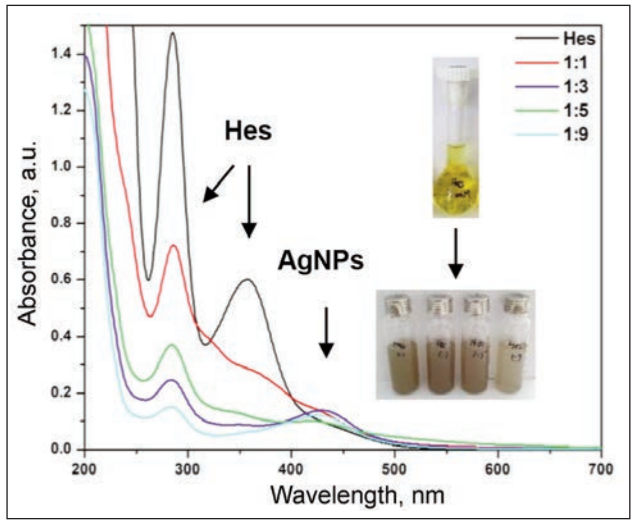

Fig. 1. UV-Vis spectra of hesperidin solution and AgNPs dispersions

While the average particle size underwent a linear growth, the polydispersity index was constant for the first three ratios, and, at values 0.255–0.271, and had the value 0.378 when the ratio was 1:9. Moreover, while for the ratios 1:1 and 1:3 the particle size is situated in the nanoscale, the size of the particles produced using 1:5 and 1:9 ratios exceed this scale (the particle size exceed 100 nm).

The absolute values of the zeta potential (figure 2, *b*) exceeded 25 mV, when the ratio was 1:3, 1:5, and 1:9, indicating that this dispersion is physically stable. When correlating the variation of the size, polydisperisy and physical stability of the dispersions, it is observed that large and polydisperse silverpartiles lead to the stabilization of the dispersions.

The optimal ratio selected for further characterization is 1:3.

Morphological characterization of AgNPs

The SEM-EDS results are illustrated in figure 3. The DLS values are confirmed by the SEM measurements. The silver nanoparticles agglomerate into clusters of different sizes and shapes. The nature of the particles was confirmed by the EDS spectrum.

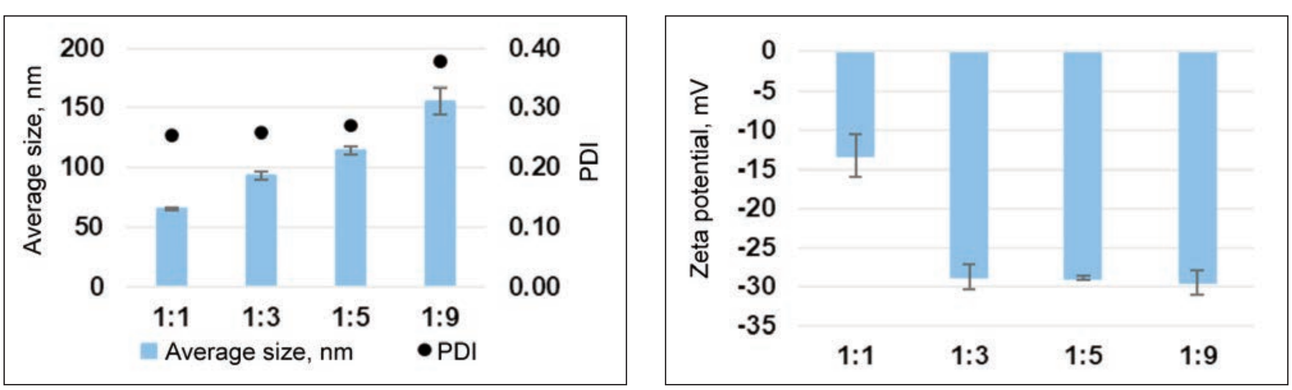

a *b*

Fig. 2. Graphical representations of: *a* – the average size (Z_{ave}) and polydispersity index (PdI) of AgNPs, evaluated using the Dynamic Light Scattering (DLS) technique; *b* – zeta potential measurements of the AgNPs dispersions

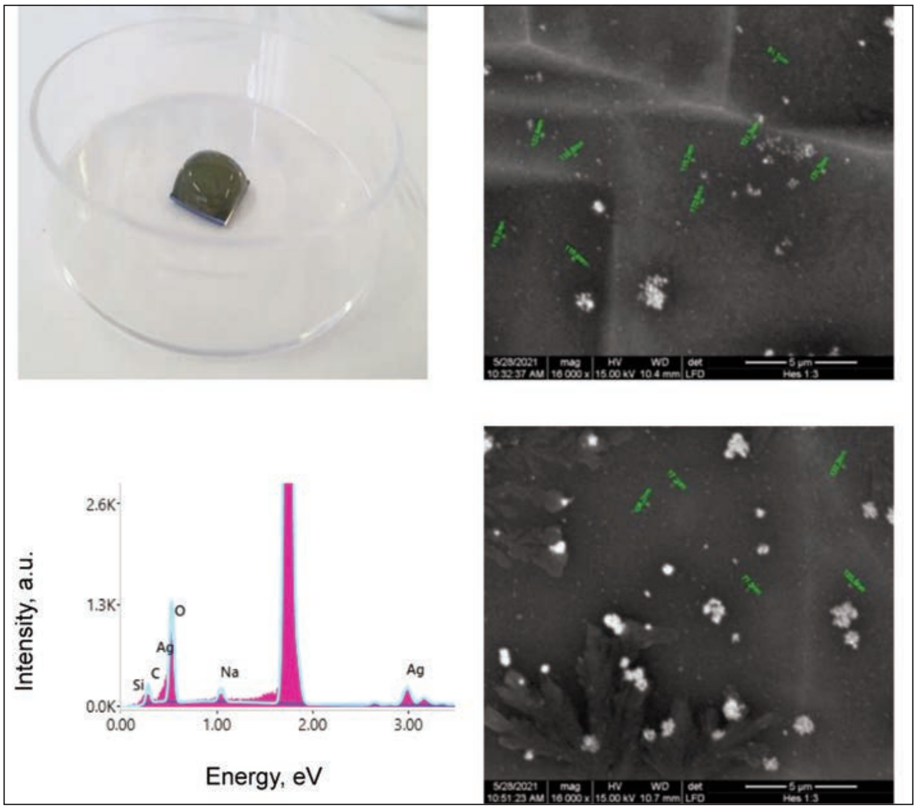

Fig. 3. SEM-EDS results of the AgNPs fabricated using the ratio Hes:$AgNO_3$ of 1:3

Characterization of textile samples treated with AgNPs dispersions

Morphological evaluation and nature confirmation of the AgNPs deposited on textile

The morphology of the treated textile fibres is presented in figure 4 and the EDS spectra in figure 5. The results suggest a uniform distribution of the silver nanoparticles on the surface of the fibres.

Chromatic evaluation

The values of the chromatic parameters L* a* b* are listed in table 1. The total colour change is quantified through the value of ΔE*.

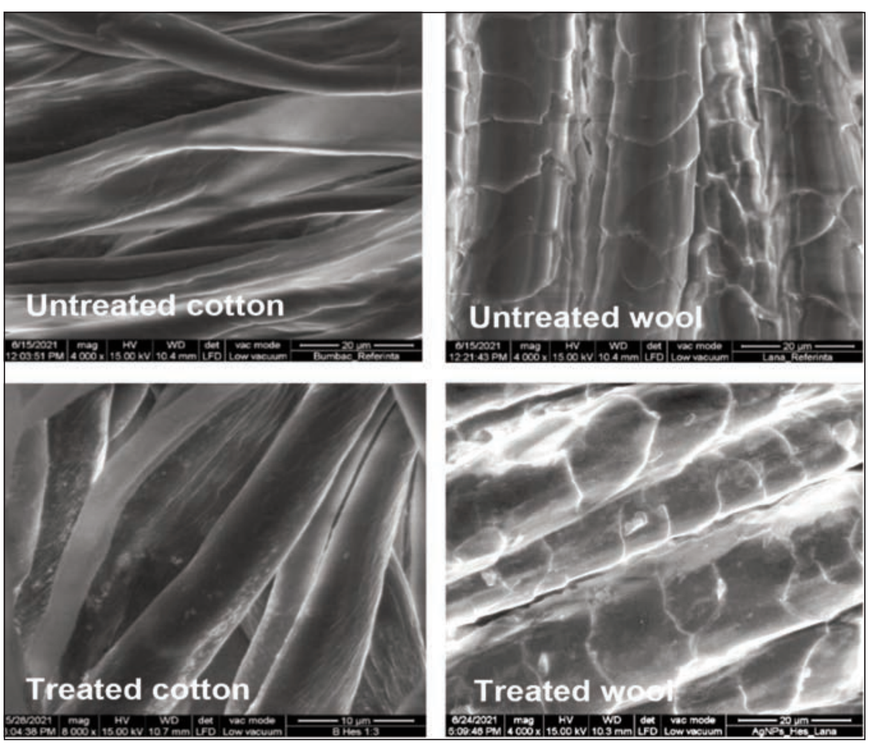

Fig. 4. SEM micrographs of textile fibres before and after applying the AgNPs dispersions

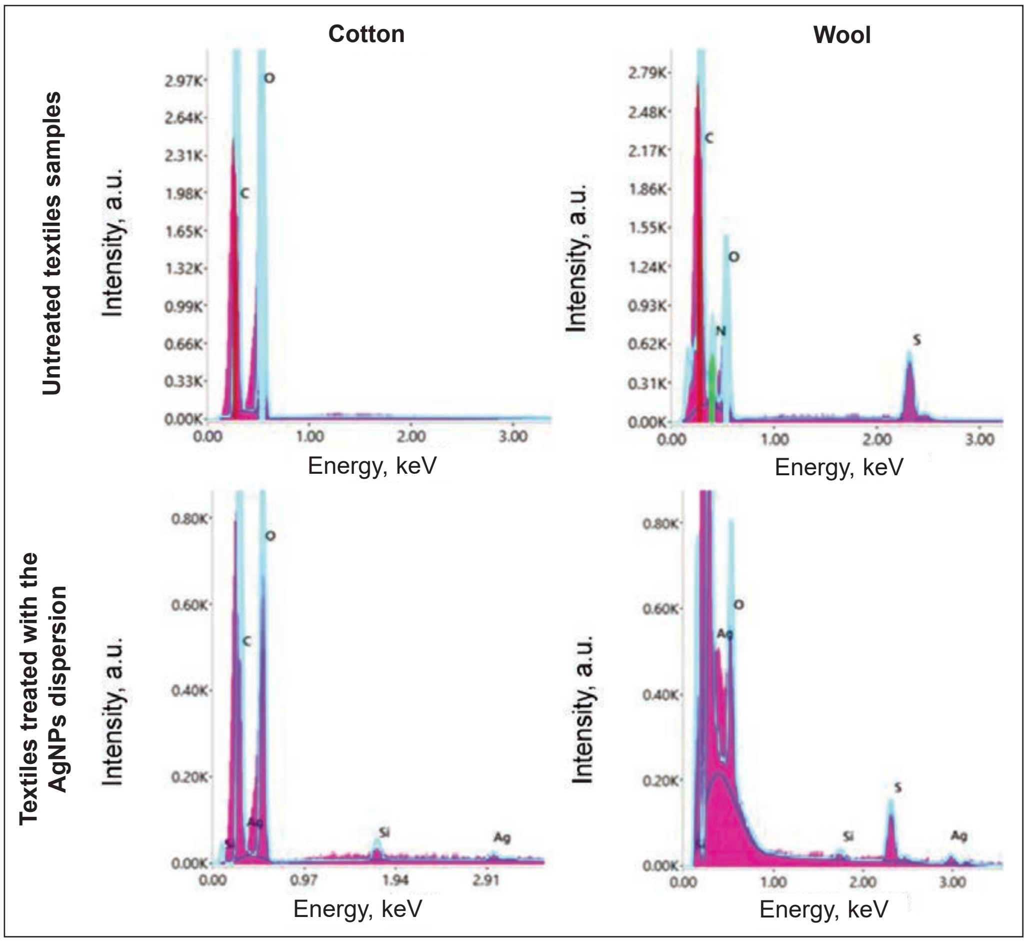

Fig. 5. EDS spectra of textile fibres before and after applying the AgNPs dispersions

While the colour of the cotton sample is visibly affected by the AgNPs dispersion, having a colour difference ΔE* of 6.18, the wool sample is not chromatically affected by the treatment (ΔE* = 0.83). Compared to our previous study where the cotton sample colour was affected in terms of luminosity, the current treatment produces an increase of the b* parameter, from 3.19 to 9.07, meaning that the sample becomes more yellow [22].

Antimicrobial activity

The percentage of bacterial reduction exceeded 99% in all cases (table 2). The treatment has been effective against the tested bacteria strains for both cotton and wool samples.

Table 1

CHROMATIC PARAMETERS OF THE TEXTILE SAMPLES BEFORE AND AFTER APPLYING THE AGNPS DISPERSIONS

Textile sample	**Cotton**							**Wool**						
Chromatic parameter	**L***	**a***	**b***	**ΔL***	**Δa***	**Δb***	**ΔE***	**L***	**a***	**b***	**ΔL***	**Δa***	**Δb***	**ΔE***
Untreated textile samples	93.58	–0.01	3.19	-	-	-	-	85.32	–0.04	12.07	-	-	-	-
Textile samples treated with AgNPs	91.86	–0.82	9.07	–1.73	–0.81	5.88	**6.18**	84.51	–0.24	12.18	–0.80	–0.20	0.11	**0.83**

Table 2

PERCENTAGES OF BACTERIA REDUCTION OF THE TEXTILE SAMPLES (COTTON AND WOOL) TREATED WITH AGNPS SYNTHESIZED WITH HESPERIDIN

Bacteria strains	***Escherichia coli***	***Staphylococcus aureus***	***Bacillus subtilis***
Cotton	99.99%	99.99%	100.00%
Wool	99.99%	99.99%	100.00%

CONCLUSIONS

The present study demonstrated the effectiveness of green synthesized AgNPs for antibacterial textile application. Hesperidin, a flavonoid compound, was used in the synthesis as a reducing agent of the silver ions. Stable nanoparticles (ξ = –28.80±1.54 mV), with an average diameter of 93.55±3.51 nm and a polydisperse index of 0.259 were obtained for the optimal ratio used for the synthesis (1:3). The average size was confirmed by SEM characterization and the nature was confirmed by EDS technique. The textile samples (cotton and wool) treated with the dispersion with the optimal ratio (1:3), Hes: $AgNO_3$ (v:v), were characterized by SEM-EDS and by determining the colour change and the antibacterial effectiveness. ΔE* was 0.83 for the wool sample and 6.18 for the cotton sample, with b* as the main parameter affected, leading to the acquirement of a yellow colour. The treatment has been proven to be effective against the *Escherichia coli, Staphylococcus aureus,* and *Bacillus subtilis* bacteria strains for both cotton and wool samples, with the percentage of bacterial reduction exceeding 99%.

The present study demonstrated both the effectiveness of the AgNPs synthesis using hesperidin as a reducing agent and the superior antibacterial performances of the resulting dispersion for obtaining antimicrobial textiles.

ACKNOWLEDGEMENTS

This work was supported by the Ministry of Research and Innovation within Program 1–Development of the national RD system, Subprogram 1.2 – Institutional Performance – RDI Excellence Funding Projects, contract no. 4PFE/2021, with contribution from the European Social Fund from the Sectoral Operational Programme Human Capital 2014-2020, through the financial agreement with the title “Training of PhD students and post-doctoral researchers in order to acquire applied research skills–Smart”, contract no. 13530/16.06.2022–SMIS code: 153734 and through the Core programme within the National Research Development and Innovation Plan 2022-2027, carried out with the support of MCID, project no. 6N/2023, PN 23 26 01 03, project title “Advanced functional textile materials for protection and improving the quality of life – TEX4AGE”.

REFERENCES

[1] Ibrahim, A., Laquerre, J.-É., Forcier, P., Deregnaucourt, V., Decaens, J., Vermeersch, O., *Antimicrobial Agents for Textiles: Types, Mechanisms and Analysis Standards*, In: Textiles for Functional Applications, IntechOpen, 2021

[3] Bou-Belda, E., Indrie, L., Ilieș, D.C., Hodor, N., Berdenov, Z., Herman, G., Caciora, T., *Chitosan – a Non-Invasive Approach for the Preservation of Historical Textiles*, In: Industria Textila 2020, 71, 576–579, https:/doi.org/10.35530/IT.071.06.1756

[3] Gulati, R., Sharma, S., Sharma, R.K., *Antimicrobial Textile: Recent Developments and Functional Perspective*, In: Polymer Bulletin, 2022, 79, 5747–5771, https:/doi.org/10.1007/s00289-021-03826-3

[4] Khan, I., Saeed, K., Khan, I., *Nanoparticles: Properties, Applications and Toxicities*, In: Arabian Journal of Chemistry 2019, 12, 908–931, https:/doi.org/10.1016/j.arabjc.2017.05.011

[5] Lite, M.C., Constantinescu, R.R., Tanasescu, E.C., Iordache, O.G., Badea, N., *Textile Artefacts Conservation Using Nanomaterials – Review*, In: Industria Textila, 2022, 73, 607–613, https:/doi.org/10.35530/IT.073.06.202263

[6] Imani, M.M., Safaei, M., *Optimized Synthesis of Magnesium Oxide Nanoparticles as Bactericidal Agents*, In: J. Nanotechnol., 2019, 1–6, https:/doi.org/10.1155/2019/6063832

[7] Roy, A., Gauri, S.S., Bhattacharya, M., Bhattacharya, J., *Antimicrobial Activity of CaO Nanoparticles*, In: J. Biomed. Nanotechnol., 2013, 9, 1570–1578, https:/doi.org/10.1166/jbn.2013.1681

[8] Román, L.E., Gomez, E.D., Solís, J.L., Gómez, M.M., *Antibacterial Cotton Fabric Functionalized with Copper Oxide Nanoparticles*, In: Molecules 2020, 25, 5802, https:/doi.org/10.3390/molecules25245802

[9] Veselova, V.O., Plyuta, V.A., Kostrov, A.N., Vtyurina, D.N., Abramov, V.O., Abramova, A. V., Voitov, Y.I., Padiy, D.A., Thu, V.T.H., Hue, L.T., et al., *Long-Term Antimicrobial Performance of Textiles Coated with ZnO and TiO2 Nanoparticles in a Tropical Climate*, In: J. Funct. Biomater., 2022, 13, 233, https:/doi.org/10.3390/jfb13040233

[10] Barbinta-Patrascu, M.E., Ungureanu, C., Badea, N., Bacalum, M., Lazea-Stoyanova, A., Zgura, I., Negrila, C., Enculescu, M., Burnei, C., *Novel Ecogenic Plasmonic Biohybrids as Multifunctional Bioactive Coatings*, In: Coatings 2020, 10, 1–23, https:/doi.org/10.3390/coatings10070659

[11] Deshmukh, S.P., Patil, S.M., Mullani, S.B., Delekar, S.D., *Silver Nanoparticles as an Effective Disinfectant: A Review*, In: Materials Science and Engineering: C 2019, 97, 954–965, https:/doi.org/10.1016/j.msec.2018.12.102

[12] Lite, M.C., Constantinescu, R.R., Tănăsescu, E.C., Kuncser, A., Romanițan, C., Mihaiescu, D.E., Lăcătuşu, I., Badea, N., *Phytochemical Synthesis of Silver Nanoparticles and Their Antimicrobial Investigation on Cotton and Wool Textiles*, In: Materials, 2023, 16, 3924, https:/doi.org/10.3390/ma16113924

[13] dos Santos, O.A.L., de Araujo, I., Dias da Silva, F., Sales, M.N., Christoffolete, M.A., Backx, B.P., *Surface Modification of Textiles by Green Nanotechnology against Pathogenic Microorganisms*, In: Current Research in Green and Sustainable Chemistry, 2021, 4, 100206, https:/doi.org/10.1016/j.crgsc.2021.100206

[14] Abdelghaffar, F., Mahmoud, M.G., Asker, M.S., Mohamed, S.S., *Facile Green Silver Nanoparticles Synthesis to Promote the Antibacterial Activity of Cellulosic Fabric*, In: Journal of Industrial and Engineering Chemistry, 2021, 99, 224–234, https:/doi.org/10.1016/j.jiec.2021.04.030

[15] Pyrzynska, K., *Hesperidin: A Review on Extraction Methods, Stability and Biological Activities*, In: Nutrients 2022, 14, 2387, https:/doi.org/10.3390/nu14122387

[16] Smitha, S.L., Nissamudeen, K.M., Philip, D., Gopchandran, K.G., *Studies on Surface Plasmon Resonance and Photoluminescence of Silver Nanoparticles*, In: Spectrochim Acta A Mol Biomol Spectrosc, 2008, 71, 186–190, https:/doi.org/10.1016/j.saa.2007.12.002

[17] Barbinta-Patrascu, M.-E., Gorshkova, Y., Ungureanu, C., Badea, N., Bokuchava, G., Lazea-Stoyanova, A., Bacalum, M., Zhigunov, A., Petrovic, S., *Characterization and Antitumoral Activity of Biohybrids Based on Turmeric and Silver/Silver Chloride Nanoparticles*, In: Materials, 2021, 14, 4726, https:/doi.org/10.3390/ma14164726

[18] Shnoudeh, A.J., Hamad, I., Abdo, R.W., Qadumii, L., Jaber, A.Y., Surchi, H.S., Alkelany, S.Z., Synthesis, *Characterization, and Applications of Metal Nanoparticles*, In: Biomaterials and Bionanotechnology; Elsevier, 2019, 527–612

[19] Barbinta-Patrascu, M.E., Nichita, C., Badea, N., Ungureanu, C., Bacalum, M., Zgura, I., Iosif, L., Antohe, S., *Biophysical aspects of bio-nanosilver generated from urtica dioica leaves and vitis vinifera fruits' extracts*, In: Romanian Reports in Physics, 2021, 73, 601

[20] Barbinta-Patrascu, M.E., Badea, N., Ungureanu, C., Constantin, M., Pirvu, C., Rau, I., *Silver-Based Biohybrids "Green" Synthesized from Chelidonium Majus L.*, In: Opt Mater (Amst) 2016, 56, 94–99, https:/doi.org/10.1016/j.optmat.2015.10.021

[21] Barbinta-Patrascu, M.E., Badea, N., Bacalum, M., Ungureanu, C., Nadejde, P.L., Ion, C., Rau, I.*, Multifunctional soft hybrid bio-platforms based on nano-silver and natural compounds*, In: Materials Science and Engineering C, 2019, 69, 922–932, https:/doi.org/10.1016/j.msec.2016.07.077

[22] Lite, M.C., Constantinescu, R.R., Tănăsescu, E.C., Kuncser, A., Romanițan, C., Lăcătuşu, I., Badea, N., *Design of Green Silver Nanoparticles Based on Primula Officinalis Extract for Textile Preservation*, In: Materials, 2022, 15, 7695, https:/doi.org/10.3390/ma15217695

Authors:

MIHAELA-CRISTINA LITE[1,2], RODICA ROXANA CONSTANTINESCU[1], NICOLETA BADEA[2], ELENA-CORNELIA TĂNĂSESCU[1,2], IRINA-MARIANA SĂNDULACHE[1], OVIDIU GEORGE IORDACHE[1]

[1]National Research and Development Institute for Textiles and Leather – INCDTP,
Lucretiu Patrascanu, 16, 030508 Bucharest, Romania
e-mail: office@incdtp.ro

[2]Politehnica University of Bucharest, 1-7 Gheorghe Polizu Street, 011061, Bucharest, Romania
e-mail: secretariat@chimie.upb.ro

Corresponding author:

MIHAELA CRISTINA LITE
e-mail: cristina.lite@incdtp.ro

INFORMATION FOR AUTHORS

Industria Textila magazine is an international peer-reviewed journal published by the National Research & Development Institute for Textiles and Leather – Bucharest, in print editions.

Aims and Scope: Industria Textila journal is addressed to university and research specialists, to companies active in the textiles and clothing sector and to the related sectors users of textile products with a technical purpose.

Submission of Manuscripts

Please read the guidelines below then visit the Journal's submission site **manuscriptmanager.net/it** or the button **Submit manuscript** to upload your manuscript. Please note that manuscripts not conforming to these guidelines may be returned.

Copyright Transfer Agreement must be signed and returned to our Editorial Office by mail, as soon as possible, after the preliminary acceptance of the manuscript. By signing this agreement, the authors warrant that the entire work is original and unpublished, it is submitted only to this Journal and all the text, data, Figures and Tables included in this work are original and unpublished, and have not been previously published or submitted elsewhere in any form. Please note that the reviewing process begins as soon as we receive this document. In the case when the paper has already been presented at a conference, it can be published in our journal only if it has not been published in a generally available conference materials; in such case, it is necessary to give an appropriate statement placed in Editorial Notes at the end of the article.

Manuscripts submitted are check against plagiarism with **Anti-plagiarims System**. Manuscripts of the following types are accepted:

Research Papers – An original research document which reports results of major value to the Textile Community

Book Reviews – A brief critical and unbiased evaluation of the current book, normally invited by the Editor.

Manuscripts shall be submitted in English in single-spaced typing, A4 paper, Arial, margins 2 cm on all sides, under electronic version in Word for Windows format.

The volume of the submitted papers shall not exceed 8 pages (including the bibliography, abstract and key words), typescript pages including tables, figures and photographs.

All articles received are reviewed by minimum two reviewers, renowned scientist and considered expert in the subject the article concerns, which is appointed by the editorial board. After the article has been accepted, with the completions and the modifications required by the reviewers or by the editorial staff, it will be published.

The submission of the above-mentioned papers is by all means the proof that the manuscript has not been published previously and is not currently under consideration for publication elsewhere in the country or abroad.

There may also be published papers that have been presented at national or international scientific events, which have not been published in volume, including the specification related to the respective event.

The articles assessed as inappropriate by the reviewer or by the editorial staff, concerning the subject matter or level, shall not be published.

The manuscript shall be headed by a concise title, which should represent in an exact, definite and complete way the paper content.

The manuscript shall also be headed by complete information about the author(s): titles, name and forename(s), the full name of their affiliation (university, institute, company), department, city and state, as well as the complete mailing address (street, number, postal code, city, country, e-mail, fax, telephone).

Tables and figures (diagrams, schemes, and photographs) shall be clear and color, where possible.

The photographs shall be sent in original format (their soft), or in JPEG or TIF format, having a resolution of at least **300 dpi**.

All tables and figures shall have a title and shall be numbered with Arabic numerals, consecutively throughout the paper and referred by the number in the text.

Generally, symbols and abbreviations shall be used according to ISO 31: Specifications for quantities, units and symbols. SI units must be used, or at least given comprehensive explanations or their equivalent.

Cited references shall be listed at the end of the paper in order of quotation and contain: **for a paper in a periodical** – the initials and surname of the author(s), title of journal and of the article, year and number of issue, number of volume and page numbers; **for a book** – the initial and surname of the author(s), full name of the book, publisher, issue, place and year of publishing, and the pages cited; **for patents** – the initial and surname of the author(s), the title, the country, patent number and year. It is preferable not to use sites as references.

[1] Hong, Y., Bruniaux, P., Zhang, J., Liu, K., Dong, M., Chen, Y., *Application of 3D-to-2D garment design for atypical morphology: a design case for physically disabled people with scoliosis*, In: Industria Textila, 2018, 69, 1, 59–64, http://doi.org/10.35530/IT.069.01.1377

Authors are requested to send an abstract of the paper, preferably no longer than 250 words and a list of 5–6 key words (preferably simple, not compound words, in alphabetical order).